NOUVELLE APPROCHES POUR LA RESTAURATION D'UN RESEAU ELECTRIQUE APRES UN INCIDENT GENERALISE

Abbas Ketabi

New Approaches for Bulk Power System Restoration

by

Abbas KETABI

M.Sc in Electrical Engineering, Sharif University of Technology, Tehran, Iran, 1996.

A THESIS SUBMITTED IN PARTIAL FULFILLMENT OF

THE REQUIREMENTS FOR THE DEGREE OF

DOCTOR OF PHILOSOPHY

with the collaboration of:

Institut National Polytechnique De Grenoble Laboratoire d'Electrotechnique de Grenoble, Grenoble, France

and

Sharif University of Technology Department of Electrical Engineering, Teheran, Iran

Supervisors:

SHARIF Professor: ***Ali M. RANJBAR***

INPG Professor: ***René FEUILLET***

December 2001

Abstract

The problem of restoring power systems after a complete or partial blackout is as old as the power industry itself. In recent years, due to economic competition and deregulation, power systems are operated closer and closer to their limits. At the same time, power systems have increased in size and complexity. Both factors increase the risk of major power outages. After a blackout, power needs to be restored as quickly and reliably as possible, and consequently, detailed restoration plans are necessary.

In recent years, there has also been an increasing demand in the power industry for the automation and integration of tools for power system planning and operation. This is particularly true for studies in power system restoration where a great number of simulations, taking into account different system configurations, have to be carried out. In the past, these simulations were mostly performed using power flow analysis, in order to find a suitable restoration sequence. However, several problems encountered during practical restoration procedures were found to be related to dynamic effects. On the one hand, suitable approaches that help to quickly assess these problems are needed. On the other hand, accurate modeling techniques are necessary in order to carry out time-domain simulations of restoration studies.

In this work, new approaches for bulk power system restoration are presented. Theirs purpose is to quickly evaluate the feasibility of restoration steps, and if necessary, to suggest remedial actions. This limits the number of time-consuming time-domain simulations, based on the trial and error principle, and helps to efficiently find feasible restoration paths. The approach's principle is to subdivide the problem of assessing the multitude of different phenomena encountered during a restoration procedure into sub-problems.

This thesis concentrates on the initial stages of restoration where four major problem areas are identified. A method to determine optimal units start-up sequence during power plants re-start up is presented. The system frequency behavior after the energization of loads is assessed using a novel approach. An approach to standing phase angle reduction is explained. The occurrence of overvoltages is assessed in the frequency domain. Sensitivity analysis is used in order to find the most efficient network change that can be applied to limit overvoltages. In case time-domain simulations need to be carried out, a method based on Short-Time Fourier Transform helps to limit the overall calculation time. All the proposed approaches are validated using time-domain simulations based on IEEE test systems data.

Also a blockset in MATLAB/SIMULINK environment has been developed for long term dynamics simulation to study frequency and voltage responses due to load and generation mismatches for analysis power system restoration scenarios.

Contents

LIST OF TABLES

LIST OF FIGURES

Acknowledgement

I wish to express my sincere gratitude to all the people who have assisted me in the accomplishment of this thesis works:

I would like to express my deepest gratitude to my thesis supervisors: Dr. Ali Mohammad Ranjbar, professor of Sharif University of Technology (SUT), and Dr. Rene Feuillet, professor of Institut National Polytechnique de Grenoble (INPG), whom I respect and admire tremendously. In particular, I would like to thank Dr. Ali Mohammad Ranjbar for the great opportunity to carry out a part of my work at Niroo Research Institute (NRI). Thank you both very much for your encouragement and support.

Many thanks to the faculty members of SUT for introducing me to the principle of the electrical engineering in their outstanding courses at the Electrical Engineering Department. Their expertise and background in the area of power systems not only made this work possible but also tremendously enriched my professional life. Special thank to Dr. Mehdi Valilian, my M.Sc thesis supervisor and director of Electrical Engineering Department, for his encouragement and support.

I am much indebted to Dr. J.P Rognon, director of Laboratoire d'Electrotechnique de Grenoble (LEG), for accepting me in the LEG to pursue a Ph.D. program.

Many thanks to all the jury member of my thesis for reading the report and participating in the defense of my thesis, especially Dr. Forouhar Farzaneh for translating my presentation to the French language for the French delegates. The proof-reading of the English report by Dr. Nouredine Hadjsaid and the French resume by Khaled Laouamri are also appreciated.

The financial support of Superior Education Ministry of Iran is gratefully acknowledged. I thank to the people of Office of International and Scientific Cooperation of SUT.

I also thank the Foreign Ministry of France and people of the Center Cultural of France in Iran who has financed my research in France.

Finally, I would like to express my deepest appreciation and sincere gratitude to my parents for their encouragement and genuine care taken towards my life from the very beginning, to my wife for her unlimited understanding, support and sacrifices during these

years of my graduate studies, and to my daughter, Zeinab, who missed many hours of fun since " Baba has to go to university", all of which made this thesis possible.

December 10, 2001 Abbas KETABI

CHAPTER 1

INTRODUCTION

CHAPTER 1

INTRODUCTION

1.1 GENERAL BACKGROUND

The operating condition of a given power system can be mathematically described in terms of two set of equations: the equality (or load flow) constraints, **E**, and the inequality (or limit) constraints, **I**. The load flow constraints impose requirement on customer load demand that should be met at any time, while the limit constraints reflect the fact that the system variables such as voltage magnitudes or transmission line flow, must always be kept within limits representing the physical limitations of power system equipments. Power system operations can be described by five operating "states*": normal, alert, emergency, in extremis*, and *restorative* (see Figure 1.1) [57, 120].

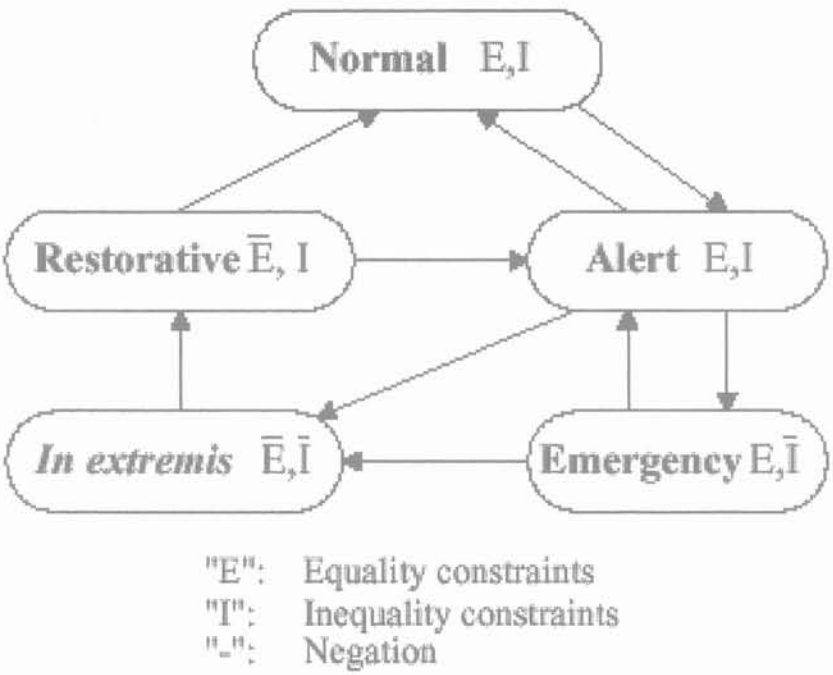

Figure 1.1: Power System Operating States

In the normal operating state, all system variables are within the normal range and no equipment is being overloaded. The system can withstand a contingency without threatening its security limits, and both equality and inequality constraints are satisfied. In the alert operating state, the system's security level is reduced, but the equality and

inequality constraints are still satisfied. Even though the system is still operated within allowable limits, a contingency might lead to an emergency state, or, in case of a severe disturbance, to an in extremis state. In the emergency state, the inequality constraints are violated when the system operates at a lower frequency with abnormal voltages, or with a portion of the equipment overloaded. After the system has entered an emergency state, as a consequence of a severe disturbance, it may led back to an alert state by applying appreciable emergency control actions. If these measures are not applied successfully, the system may enter an in extremis state where both inequality and equality constraints are violated. Cascading outages might lead to partial or complete blackout of the system [120].

The system condition where control actions are being taken to reconnect all the facilities to restore system load and to eventually bring the system back to its normal state, is called the restorative state. In this state the set of limit constraints is satisfied but the set of load flow equation is not completely satisfied. In other words, the restorative state is characterized by feasible operations of power system equipment but with portion or total of load not being served and /or with loss of system integrity. Power system restoration following a complete or a partial system collapse, is the process of restoring power plants, re-energizing the transmission network, restoring customer loads and accomplishing this process as rapidly as possible without causing any further failure or equipment damage.

Due to the deregulation of the power industry worldwide, and the almost revolutionary changes in the industry structure, power systems are operated closer and closer to their limits. Furthermore, in recent years, they have grown considerably in size and complexity. This has led to an increasing number of major blackouts, such as the large power outages on the West Coast of North America in 1996, the Brazilian blackout in 1999, or the Iranian blackout in 2001.

Disturbances that can cause such power blackouts are natural disasters, line overloads, system instabilities, etc. Furthermore, temporary faults such as lightning, even if cleared immediately, can initiate a "cascading effect" that might lead to a partial or complete outage, involving network separation into several subsystems, and load shedding. After power black-outs, the system has to be restored as quickly and efficiently as possible. In this restoration, the initial cause of the outage is of secondary importance and it might be futile to investigate it [2].

Power system restoration is a very complex process which typically involve all of the components of the power system, including generation, transmission, and distribution. However, it is customary in electric power utility operating practice to develop distinct strategies for restoring the bulk transmission system and the distribution system. This thesis deals with the bulk transmission and generation systems.

Although power outages differ in cause and scale, virtually every utility has experienced blackouts and gone through restoration procedures. As a consequence, there is an increasing interest in systematic restoration procedures, tools, and models for on line restoration, as well as for restoration planning. A speedy, effective, and orderly restoration process reduces the impact of a power outage on the public and the economy, while reducing the probability of equipment damage [2].

1.2 Goals and Steps in Restoration

Even though each power blackout and restoration scenario is a unique event, there are certain goals and steps that are common in all restoration procedures. The goals in restoration, as generally defined in [59, 128, 130], are shown in Figure 1.2. They involve almost all aspects of power system operations and planning.

Each restoration procedure that follows a complete or partial blackout of a power system can be subdivided into the following steps [2, 33]:

1. *Determination of System Status.* In this stage, the boundaries of energized areas are identified, and frequencies and voltages within these areas are assessed. Furthermore, in cases where no connections to neighboring systems exist, black start (or cranking) sources are identified in each subsystem and critical loads are located.

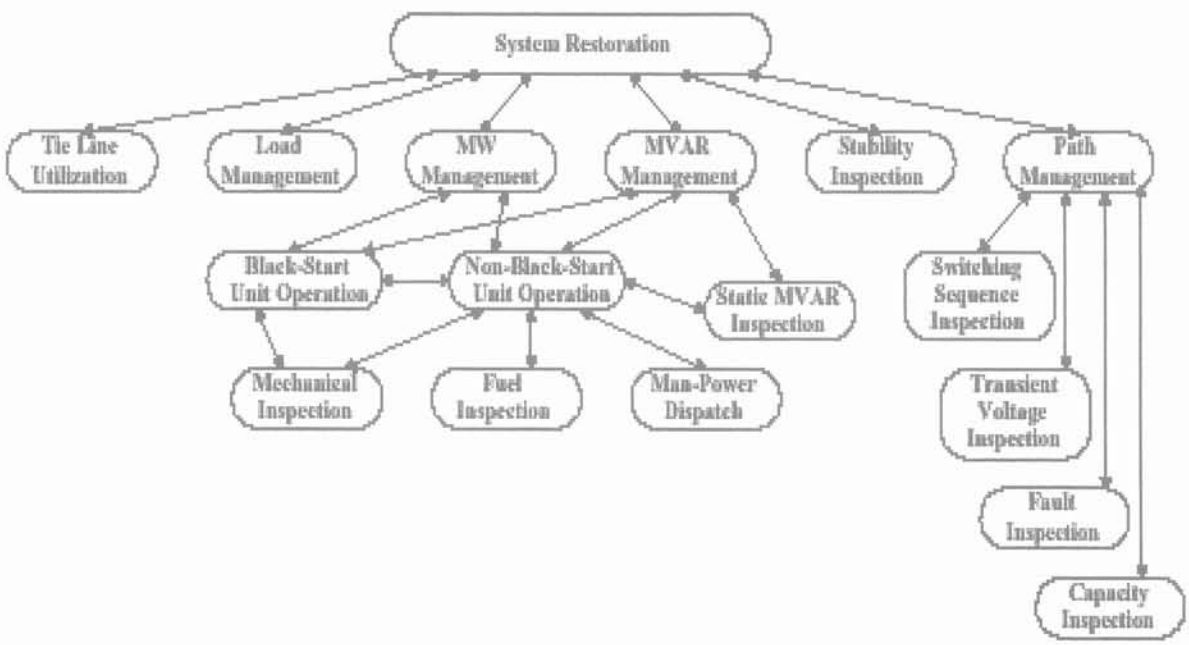

Figure 1.2: Power system restoration goals

2. *Starting of Large Thermal Power Plants.* Large thermal power plants have to be restarted within a certain period of time. For example, hot restart of drum type boilers is

only possible within thirty minutes. If it cannot be accomplished and the boiler is not available for four to six hours, a cold restart has then to be performed. Thermal power plants can be restarted by means of smaller units with black start capability, i. e. power plants that can be started and brought online without external help and within a short period of time. Power plants with black start capability are hydro, gas, or diesel power plants. After such a power plant has been brought to full operation, a high voltage path to a large thermal power station is built and the thermal unit's auxiliaries which are driven by large induction motors are started. Along the path, "ballast" loads have to be supplied to maintain the voltage profile within acceptable limits and to prepare a load base for the thermal units. Additional smaller units can also be brought on line through the path to improve system stability [40].

3. *Energization of Subsystems.* In case of a large power blackout, it is advantageous in most cases to split the power system into subsystems in order to allow parallel restoration of islands, and to reduce the overall restoration time. Within each sub-system, starting from a large thermal power station, the skeleton of the bulk power system is energized. Paths to other power plants and to the major load centers are built, and loads are energized to firm up the transmission system. At the end of this step, the network has sufficient power and stability to withstand transients as a result of further load pick-up and addition of large generating units.

4. *Interconnection of Subsystems.* In this stage of the power system restoration process, the subsystems are interconnected. Eventually, remaining loads are picked up and the system performs its transition to the alert or normal state.

Among the above four general steps of the restoration process, the second and third step are the most critical ones. Mistakes in these stages can lead to unwanted tripping of generators and load shedding due to extensive frequency and voltage deviations, and consequently to a recurrence of the system outage. Because of time-critical boiler-turbine start-up characteristics and possible further equipment damage, extensively prolonged restoration times may occur, resulting in a much higher impact on the public and industry, and an increased damage to the economy.

1.3 Problems in Restoration

During power system restoration, a multitude of different phenomena and abnormal conditions may occur. The problems encountered during restoration can be subdivided into three general areas [2, 33, 69, 70, 75]:

1. *Active Power Balance and Frequency Response.* During the restoration process, two different aspects of this type of problem can be identified. The first one is the start of large thermal power plants, where large auxiliary motor loads are picked up, using relatively small hydro generators, diesel, or gas turbines. This can result in large frequency excursions and consequently in an activation of under-frequency load shedding relays and, in the worst case, in the loss of already restored load and a recurrence of the blackout [33]. Due to the importance of this problem, it is defined as a problem area in its own, as discussed further below.

   The second aspect is the pick-up of cold loads. When the network is extended, power plants are added to the generation, and loads are picked up, it is necessary to preserve a balance between active load and generation. In case of this balance is disturbed, frequency deviations are resulted. If these deviations are extensive, an unwanted activation of load- shedding schemes can occur, and newly connected loads can be lost again. In the worst case, the frequency decline may reach levels that can lead to the tripping of steam turbine generating units as a consequence of the operation of under-frequency protective relays. This is due to the fact that the operation of steam turbines below a frequency of 58.8 Hz (for 60Hz system) is severely restricted as a result of vibratory stress on the long low-pressure turbine blades [120].

   As an example for an islanded system, Table 1.1 shows typical load shedding frequency limits for the (50 Hz) Cyprus power system [36]. The table indicates that at a frequency decline of 3 Hz almost all of the load will be disconnected.

Table 1.1: Frequency thresholds for Cyprus power system

Frequency (Hz)	49.0	48.8	48.4	47.8	47.0
Load shedding (%)	15	20	25	10	10
Delay (s)	0.2	0.2	0.35	0.35	0.35
Cumulative shed (%)	15	35	60	70	80

Thus, in order to keep the frequency deviations within allowable limits, the load increments should not exceed a certain level. However, if the load increments are too small, the overall restoration time will be unnecessarily prolonged [5, 40, 69].

2. *Reactive Power Balance and Voltage Response.* Analogous to the active power balance it is necessary to maintain a balance in reactive power. High charging currents, originating from lightly loaded transmission lines, can lead to the violation of generator reactive capability limits and to the occurrence of sustained (power frequency) over-voltages. These may cause underexciation, selfexcitation, and instability. Sustained overvoltages can also cause saturation of transformers and generation of harmonic distortions. Transient overvoltages are a consequence of switching operations on long transmission lines, or of capacitive devices switching, and may result in arrester failures.

Harmonic resonance overvoltages are a result of system resonance frequencies close to multiples of the fundamental frequency in combination with the injection of harmonics, mainly caused by transformer switching. They may lead to long-lasting overvoltages, resulting in arrester failures and system faults. Due to the small amount of load connected to the system, especially at the beginning of a restoration process, the voltage oscillations are lightly damped and can last for a long time, reaching very high amplitudes. This effect can be aggravated by transformer saturation as a result of sustained overvoltages, and power electronics [69].

As an example, the tolerable voltage deviations during restoration for the Hydro Quebec power system are shown in Table 1.2 [143]. It shows that in the case of temporary overvoltages, the overvoltage duration has to be taken into account in addition to the amplitude.

Table 1.2: Voltage limits during restoration for Hydro-Quebec power system

Steady-state voltages (p.u.)	$0.9 \leq V \leq 1.05$
Switching overvoltages (p.u.)	$V \leq 1.8$
Temporary overvoltages (p.u.)	$V \leq 1.5$ (8 cycles)

3. *Standing Phase Angle (SPA) Reduction.* In re-integrating a power system, operators sometimes encounter an excessive SPA difference across a line. Closing a power circuit breaker on a large SPA difference can shock the system, causing equipment damage and

possible recurrence of the system outage. In order to avoid inadvertent closing with a large phase angle difference, breakers are equipped with synchrocheck relays, which prevent their closure for angle greater than a preset value. Under such conditions, system operators may attempt to reduce the SPA difference by changing the real power generation in a few power plants by trial and error. This is a time consuming process and result in prolonging the restoration time [6].

1.4 Thesis Motivation and Objective

We can conclude from the previous sections, that a number of complex and serious problems need to be resolved during power system restoration. Detailed analysis during system planning stage as well as during on-line restoration is therefore necessary. As will be shown in the literature survey in Chapter 2, most of the research work that has been done so far in the area of power system restoration focuses on the application of artificial intelligence techniques in restoration path development. However expert systems or similar approaches are not always easily generalized since circumstances and philosophies are different for each utility.

The evaluation of the feasibility of restoration steps has been mainly assessed by means of steady-state analysis while ignoring dynamic effects. However, there is a trend in industry to include dynamic effects in power system restoration planning. In order to take these effects into consideration, a number of additional analytical tools, such as long-term dynamics stability and electromagnetic transient programs have to be utilized, and new models and modeling techniques need to be developed to allow for the simulation of extreme off-nominal frequency and voltage conditions [32, 33].

The multitude of different phenomena and abnormal conditions during restoration makes it impractical to solve all problems at once, and the combinatorial nature of restoration problems makes it difficult or even impossible to investigate the feasibility of every restoration step combination. Applying the above mentioned simulation tools results in a large amount of time necessary to build suitable sequences during restoration planning, and makes their application for on-line restoration almost infeasible due to time limitations.

The objective of this thesis is to give simple and approximate rules to assess the feasibility of restoration steps, and to provide modeling techniques for the simulation of abnormal voltage and frequency conditions. The rules provide operators with a simple and speedy methodology during on-line restoration, and limit the number of time-consuming simulations based on the trial and error principle during restoration planning.

In Chapter 2, a comprehensive overview of the literature published in the area of restoration during the last two decades is given. Chapter 3 introduces the simulation of long-term dynamics for power system restoration. Chapter 4 presents a method to determine optimal units start-up sequence during power plants re-start up. Chapter 5 describes methods for estimating of frequency responses of prime movers after load pickup. Chapter 6 explains an approach to standing phase angle reduction. Chapter 7 describes methods that help to estimate and control overvoltages, and to shorten calculation times during time-domain simulations. Chapter 8 finally summarizes the contributions of this thesis and gives an outlook on future work to be done.

CHAPTER 2

LITERATURE OVERVIEW

CHAPTER 2

LITERATURE OVERVIEW

This chapter gives a literature survey that provides an overview of the relevant areas in restoration. It is subdivided into ten different topics. The first topic provides a general overview of the restoration process. It is followed by a discussion of active and reactive power system characteristics, and control of frequency and voltages during restoration. Then, topics covering the basic restoration switching strategies are explained, and protective system and local control problems are discussed. After an overview of power system restoration planning and of case studies, the training of operators in restoration is reviewed. The final two topics cover the applications of analytical tools and expert systems in power system restoration. The restoration of distribution systems is not specifically addressed in this survey.

2.1 OVERVIEW OF RESTORATION PROCESS

This section covers publications that give a general introduction to the restoration process, as well as technical committees reports dealing with system restoration.

In a typical restoration procedure, the stages of the restoration process are summarized as follows [2, 3, 15, 33, 57, 92, 100, 155]: in the first stage, the system status is assessed, initial cranking sources are identified, and critical loads are located. In the following stage, restoration paths are identified and subsystems are energized. These subsystems are then interconnected to provide a more stable system. In the final stage, the bulk of unserved loads is restored.

In 1986 the Power System Restoration Task Force was established by the IEEE PES System Operations Subcommittee in order to review current operating practices, and to promote information exchange. Its first two reports [69, 70] give a general overview and a comprehensive introduction to power system restoration. Restoration plans, active and reactive power system characteristics, and various restoration strategies are reviewed. Furthermore, a survey on selected power disturbances and their restoration issues are given. These restoration issues are further discussed by the same authors in [3].

An international survey by CIGRE Study Committee 38.02.02 (modeling of abnormal conditions) on black start and power system restoration in 1990 [32], and a paper based on this survey in 1993 [33], identified the needs of the power industry for system restoration planning. These papers give an overview of black start and restoration methods. In addition, a number of examples based on actual operating experiences are given, and requirements for modeling and simulation are recommended. Another CIGRE Task Force 38.06.04 investigated expert system applications for power system restoration [34].
Other publications that provide a general overview of power system restoration can be found in [2, 15, 71, 73, 75].

2.2 Active Power System Characteristics and Frequency Control

An overview of different types of generating units, and their characteristics relevant to restoration is provided in [69]. Special emphasis is placed on the treatment of steam units in [39], whereas [79] focuses on nuclear power plants and provision for off-site power during restoration.
Depending on the available cranking power, thermal units are either restarted hot or cold. Hot restarts allow for start-up with hot turbine metal temperature, whereas cold restarts require a slow start-up in order to keep the turbine metal temperature changes within given limits [75]. These characteristics result in different start-up times for different types of generating units that have to be estimated and taken into account during restoration [2, 7, 42, 69, 75].
The black start of generating units and subsequent cranking of other large thermal units is an important topic in restoration [32, 33], since mistakes in this early stage can lead to prolonged start-up times of thermal power plants, and consequently to a significant delay in the restoration process. A number of publications deal with this topic: a method for the identification of black start sources is described in [130], and the proper start-up sequence of power plants is discussed in [3, 75, 126, 130]. Several case studies show how gas turbines [82, 133, 170] or hydro units [40, 62, 124, 125, 133] were utilized as black start sources. In addition, a number of papers deal with the treatment of nuclear power plants after a blackout, using on-site diesel engines [58, 60, 193] or combustion turbines [82, 147] as emergency supply sources.
The pick-up of cold loads is discussed in a recently published doctoral thesis [12], and in a number of other papers [24, 28, 75, 87, 172, 194]. Picking up heavy loads during the initial stages of restoration can lead to large frequency dips beyond a point of no return. The prediction of frequency dips and the optimal distribution of generator reserves are

discussed in [5, 42, 113]. Load shedding schemes that can be utilized during restoration are introduced in [4, 36, 126, 127, 165, 188].

2.3 Reactive Power System Characteristics and Voltage Control

The overvoltages of concern during power system restoration are classified as: sustained power frequency overvoltages, switching transients, and harmonic resonance overvoltages. They may lead to failure of equipment, such as transformers, breakers, arresters, etc. [74], and thus need to be analyzed. Systematic procedures dealing with the control of sustained overvoltages by means of optimal power flow programs can be found in [67, 68, 96, 143], and methods that deal with harmonic overvoltages in [143, 146]. Simple and approximate methods that deal with the evaluation of transient and sustained overvoltages, and asymmetry issues during transmission line energization are discussed in [1, 9].

The preparation of the network for re-energization and the energization of high voltage transmission lines during restoration are discussed in [2, 3, 62], and the special treatment of cables in underground transmission systems in [75]. The application of shunt reactors for overvoltage control, particularly in the cases of lightly loaded transmission lines in the beginning of the restoration procedures, is treated in [11, 12, 13, 62, 143].

Another issue of importance, especially in the early stages of the restoration process, is the lead and lag reactive power capability limits of synchronous machines. These limits are important for high charging current requirements of lightly loaded transmission lines, or for the high reactive currents drawn by the start-up of power plant auxiliary motors [6, 8, 42, 82]. The generator reactive power resources must therefore be optimized in such cases [10, 130].

2.4 Switching Strategies

Two different switching strategies can be applied during restoration. For the "all open" strategy, all breakers are opened immediately after the loss of voltage, whereas for the "controlled operation" strategy only selected breakers are opened [3, 75].

A large amount of research work that has been done in power system restoration concentrates on finding suitable restoration paths. Most of these approaches are based on artificial intelligence techniques that try to capture an operator's knowledge [52, 61, 66, 89, 103, 110, 111, 132, 151, 161]. They are mostly restricted to specific systems and restoration philosophies. A general approach to this problem that subdivides each

restoration process into generic restoration actions common to all utilities is proposed in [51, 126, 190].

Restoration paths have to be validated with respect to different phenomena. An overview of steady-state and time-domain based tools that can be utilized for this purpose can be found in [2, 15, 77, 189]. Cases where simulation tools were actually applied to the validation of restoration paths can be found in [141].

2.5 Protective Systems and Local Control

The continuing change in power system configurations and their operating conditions during restoration might lead to undesired operation of relays, since their settings are optimized for normal operating conditions. An overview of resulting delays, possible modifications of relays, and other protective system issues is provided in [81].

Relay schemes that allow for low frequency isolation, whereby local generation and local load are matched in order to avoid extensive delays due to the otherwise necessary complete generator shutdowns, and controlled islanding schemes are treated in [3, 69]. A network protection scheme that focuses on stability issues is introduced in [160].

In cases where a dramatic decline in frequency occurs during the restoration process, it is necessary to reduce the amount of load that is connected, which can be accomplished by the application of under-frequency load shedding schemes [36, 114]. In closing network loops, e.g., reconnecting two subsystems, sometimes a significant standing phase angle difference appears across the circuit breakers. This difference has to be reduced in order to close the circuit breaker without causing instability of the system [64, 77, 192].

2.6 Power System Restoration Planning

The organization and implementation of a restoration plan will substantially determine its success. Reports that deal with the actual deployment of restoration plans can be found in [57, 152]. An overview of how restoration tasks can be shared most efficiently between operator and supporting computer systems is given in [73, 195]. Telecommunication issues during restoration are discussed in [50, 75, 152], and alarm issues in [71, 75].

One can distinguish between two different restoration approaches: the "bottom-up", and the "top-down" restoration strategies [2, 69]. For the "top-down" approach, the bulk power transmission system is established first, using interconnection assistance or hydro plants with large reactive absorbing capability. Subsequently, transmission stations and the

required substations are energized, generators are resynchronized, and loads are picked up [2, 52, 67, 68, 69, 100, 143, 171]. For the " bottom-up" strategy, the system is first divided into subsystems, each with black-start capability. Then, each subsystem is stabilized, and eventually the subsystems are interconnected [2, 57, 68, 92, 93, 133].

The verification of steady-state models used for power system restoration planning is discussed in [93]. A number of publications describe the modeling of boilers, turbines, generators, controls, motors, etc. for black start studies in the time-domain, using stability programs [40, 58, 147, 170], or the Electromagnetic Transients Program (EMTP) [60, 193]. Special emphasis on the modeling of transmission lines for black start studies is given in [21], and the modeling of steam plants is treated in [39]. More information on analytical tools for restoration planning is given in Section 2.9.

2.7 Power System Restoration Training

In order to provide operators with the necessary experience to confidently deal with time-critical restoration problems, thorough training is essential. A general overview of operator training techniques for power system restoration is given in [71, 76], and methods showing how restoration drills can be conducted and evaluated in practice are described in [186, 187].

Interactive and realistic operator training can be accomplished by means of an operator training simulator (OTS) [3, 46, 73, 139, 157, 173, 174, 183, 197]. OTS can also be used to verify restoration plans [104], or in combination with knowledge-based systems for power system restoration planning [59, 112, 155]. Information on simulator-expert-system combinations that are specifically designed to train operators at utilities and to replace human instructors, can be found in [29, 30, 31, 72, 95, 106, 117, 159].

2.8 Power System Restoration Case Studies

Most of the published case studies come from North America. A number of black start studies can be found in [58, 60, 125, 170, 193]. The restoration of large power systems in North America for Pacific Northwest, Ontario-Hydro and Hydro-Quebec is covered in [17, 67, 68, 143, 163, 171], and a report dealing with the restoration of a metropolitan electrical system in [92]. A Mexican study of restoration policies and their application is treated in [57].

European case studies describe restoration experiences in French, Greek, and Swedish Systems [12, 37, 53, 100], Italy [46, 133], Slovenia [147], and Germany [182].

2.9 Analytical Tools

An overview of analytical tools and their application for solutions of power system restoration problems is given in [33, 77]. The analytical tools can be subdivided into different categories depending on the frequency range of their application. The first type of tool is based on steady-state analysis: (optimal) power flow programs [67, 68, 96, 105] are the most basic tools used in system restoration. An overview of how they can be applied to different types of restoration problems is provided in [189], and applications to the control of sustained overvoltages can be found in [74, 143]. Other tools, based on steady-state models, allow frequency scans that can be used to investigate and control resonance conditions during power system restoration [74, 143].

Operator training simulators (OTS) can be regarded as quasi steady-state tools, since in addition to analyzing the power system's electrical behavior using power flow methods, they allow taking into account long-term dynamics, i.e. the electromechanical and mechanical aspects of power systems. Analytical tools that are applied to study frequency transients of short-, mid-, and long-term range are introduced in [53]. Electromagnetic transients during restoration are investigated using the EMTP [21, 74] or similar programs [141].

Methods that apply stability and security methods to restoration can be found in [50, 153]. Other analytical tools that are of importance in restoration are short-circuit programs [77], or tools that help to identify system islands [122].

There is an increasing demand in the power industry to integrate existing tools and to develop combination tools that allow studying different phenomena over a broad range of frequency [33, 77]. Attempts in integration or combination of analytical tools, and their applications to practical problems, are described in [53, 59].

2.10 Expert Systems

Power system restoration problems are of a combinatorial nature, and their solution is often based on the operator's knowledge and experience. Consequently, it is not surprising that most of the research that has been done in the area of system restoration has been concentrated on artificial intelligence applications.

A general bibliographical survey on the application of expert systems to electric power systems can be found in [196]. References [164, 199] give an overview of expert system applications in power system operation. An international survey among utilities that investigated restoration expert systems and their application is presented in [34]. A number

of publications address the requirements for knowledge-based systems, and give an overview of how expert systems can be applied during different stages of power system restoration [73, 78, 136].

The development of expert systems for restoration requires the transfer of operator knowledge into heuristic rules. That process has been the topic of a great number of publications: [20, 29, 38, 41, 43, 51, 54, 55, 56, 88, 89, 90, 91, 94, 95, 96, 97, 98, 99, 101, 102, 103, 104, 106, 107, 108, 109, 110, 111, 116, 117, 118, 119, 127, 129, 130, 132, 137, 138, 144, 145, 150, 151, 154, 161, 165, 166, 177, 179, 180, 184, 185, 188, 189, 199]. Practical implementations of prototype knowledge-based systems in energy management systems can be found in [34, 42, 47, 48, 59, 66, 102, 103, 108, 112, 123, 131, 132, 140, 142, 155, 169].

To reduce the number of rules of an expert system, mathematical programming [111, 145, 167] or other analytical optimization methods [144, 150, 151, 167, 168] can be applied in combination with knowledge-based systems. The verification of restoration solutions provided by expert systems is accomplished using an integration with time-domain simulators [41, 59, 104, 112, 155].

Other artificial intelligence methods that are applied to black start and power system restoration problems are the use of petri nets [52, 61, 190], the utilization of genetic algorithms for load restoration [113], the generation of switching sequences [115, 149], or as a hybrid approach of an expert system and the application of neural networks [90, 199].

CHAPTER 3

LONG TERM DYNAMICS SIMULATION DURING SYSTEM RESTORATION

LONG TERM DYNAMICS SIMULATION DURING SYSTEM RESTORATION

3.1 INTRODUCTION

Instability in a power system may be manifested in many different ways depending on the system configuration and operating mode. *Power system stability* may be broadly defined as that property of a power system that enables it to remain in a state of operating equilibrium under normal operating conditions and to regain an acceptable state of equilibrium after being subjected to a disturbance [120]:

A. Rotor Angle Stability

Instability in a power system can occur in a variety of ways depending on the system configuration and operating conditions. Traditionally, the stability problem has been associated with maintaining synchronous operation. In the evaluation of stability, the concern is the behavior of the power system when subjected to a disturbance. The disturbance may be small or large.

A.1 Small-signal (small-disturbance) stability

Small-signal (small-disturbance) stability is the ability of the power system to maintain synchronism under small disturbances. Instability can result in the form of 1) steady increase in rotor angle due to lack of sufficient synchronizing forces, or 2) rotor oscillations due to lack of sufficient damping forces. In today's power systems, small-signal stability is largely a problem of insufficient damping of oscillations.

A.2 Transient stability

Transient stability is the ability of the power system to maintain synchronism when subjected to large disturbances. The system equations for a transient stability study are usually nonlinear.

B. Voltage Stability

Instability may also be encountered without loss of synchronism. A system could become unstable because of the collapse of voltages at certain buses in the system. In this instance, the concern is stability and control of voltage. The analysis in this case deals with the ability of the power system to maintain steady acceptable voltages at all buses in the system under normal operating conditions and after being subjected to disturbances. The

main factor causing instability is the inability of the power system to meet the demand for reactive power.

C. Long-Term Stability

Long-Term Stability analysis assumes that inter-machine synchronizing power oscillations have damped out, the result being uniform system frequency. The analysis focuses on the slower and longer-duration phenomena accompanying large system upsets and on the resulting large, sustained mismatches between generation and load [44, 49, 53, 65, 158]. The modeling requirements for this analysis include boiler dynamics of thermal units, penstock and conduit dynamics of hydro units, automatic generation control, power plant and transmission system protection and controls, transformer saturation, and off-nominal frequency effects on load and the transmission network.

The focus of long term dynamics is to analyze the effects of wide excursions of voltage and frequency for extended periods of time on the bulk power system. The emphasis on modeling the sequence of event that follows a major disturbance distinguishes long term dynamics from transient and midterm stability analysis where the effects of inter-machine oscillations on synchronous machines are the primary focus. The assumption of uniform system frequency makes it possible to use a numerical step-size of one or more seconds for long term studies, as opposed to a fraction of a cycle for transient-midterm stability, and to simulate the voltage and frequency effects of such system events as automatic load shedding and unit tripping for periods up to twenty minutes. **LTD** (**L**ong **T**erm **D**ynamics) analytical studies address system performance under large-scale upsets which invoke the action of slow processes, protective system and controls not present in conventional transient stability programs. A typical range of long –term time period can exceed several tens of minutes. The LTD simulation program should include, in addition to the models used in conventional transient stability simulations, adequate representation of the prime mover and energy supply systems. It should also include appropriate models for the wide range of protection and control systems that are invoked when the system is in the emergency and in extremes states.

Some intended uses for a long term dynamics program are to evaluate [49, 53, 155, 158]:

- Studying frequency and voltage responses due to load and generation mismatches in isolated systems or during extension of the existing system in the restoration phase.
- Load shedding practices and policies.
- The effects of boiler control alternatives and sizing power plant auxiliaries on the ability of generating units to ride through major upsets.
- The effectiveness of emergency reactive power supplies.

- The effects of manual load dropping for relief of low voltage on the bulk transmission network.
- Emergency procedure for operator training.
- The allocation and distribution of spinning and non-spinning reserves.
- Alternative strategies for automatic generation control.

In this thesis, long term dynamics simulation is used for studying frequency and voltage responses due to load and generation mismatches to the analysis power system restoration scenarios.

3.2 POWER SYSTEM MODELING FOR LTD SIMULATION

Long term dynamics simulation requires a detailed representation of the power system being modeled, including the transmission network, system loads, protective relays, area generation control, generators, exciters and the prime movers. One of the most important requirements for LTD simulation is to choose models of these power system components, which are appropriate to the long term dynamics time frame. One approach to choosing the components models for LTD simulation is by considering the relative time frame of the dynamics of individual components. As a starting point to determine which sub-components are needed, open-loop time constants of the sub-components should be considered. A sample of such available data is given as Figure 3.1. The dashed lines separating the sub-component categories have been added for clarity. As pointed out in the Discussion of [25] some closed loop response time constant may vary from that shown.
The extracted and converted models for the long term dynamics are:

I. Prime Movers
   1. Fossil steam turbine and controls
   2. Gas turbine and controls
   3. Hydro turbine and controls
   4. Boiling Water Reactor (BWR) and controls
   5. Pressured Water Reactor(PWR) and controls

II. System frequency

III. Electric generation
   1. Synchronous machine

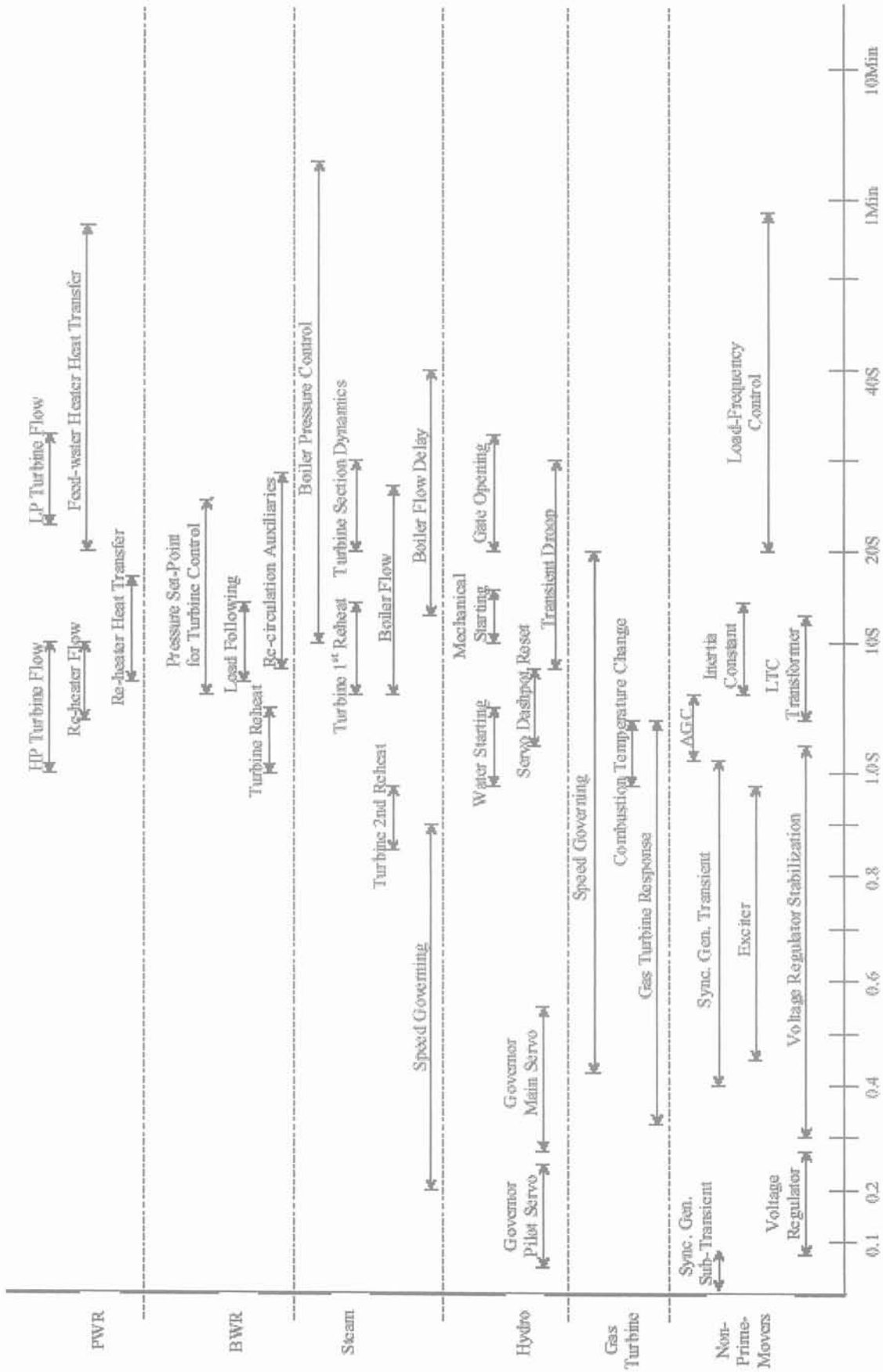

Figure 3.1. Sub-components time constants

Figure 3.1: sub-components time constants

2. Excitation system and automatic voltage regulator

IV. Automatic Generation Control (AGC)

V. Network components

1. Ac Transmission lines
2. Transformers
3. Loads
4. Shunt reactors and capacitors
5. SVC

VI. Relays

1. Under frequency load shedding relay
2. Under voltage relay (generator and load)
3. Generator under frequency relay
4. Transformer Volt per Hertz (V/Hz) relay

The choice of mathematical models for power plant prime movers, generation control and protection systems, load representation, under frequency control and other type of automation are discussed in the following section.

3.2.1 Prime Movers

The prime sources of electrical energy supplied by utilities are the kinetic energy of water and the thermal energy derived from fossil fuels and nuclear fission. The prime mover convert these sources of energy into mechanical energy that is, in turn, converted to electrical energy by synchronous generators. Figure 3.2 shows the functional relationship between the basic elements associated with power generation and control [120].

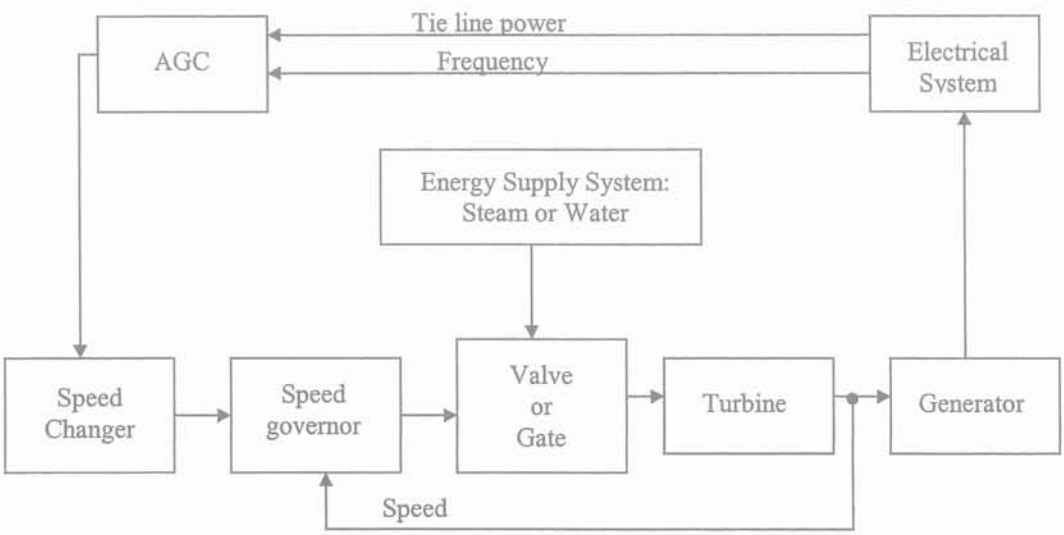

Figure 3.2: Functional block diagram of power generation and control system

A. Hydro Turbine and Controls

The extracted Hydro turbine model is divided into three parts [49]: the input, governor, and turbine sections. A description of the model structure is given in Figure 3.3 [49].

In the input section, both the manual and automatic modes are allowed. The governor of hydraulic unit requires transient droop compensation for stable speed control performance. Because a change in the position of the gate at the foot of the penstock produces an initial short-term turbine power change, which is opposite to that sought, hydro turbine governors are designed to have relatively large transient droop, with long resetting time. This ensures stable frequency regulation under isolated operating conditions (islanding). Consequently, the response of a hydraulic unit to speed change or to changes in speed changer setting is relatively slow. The governor includes transient droop and gate rate limit. The water column effect is also represented by a lead-lag block.

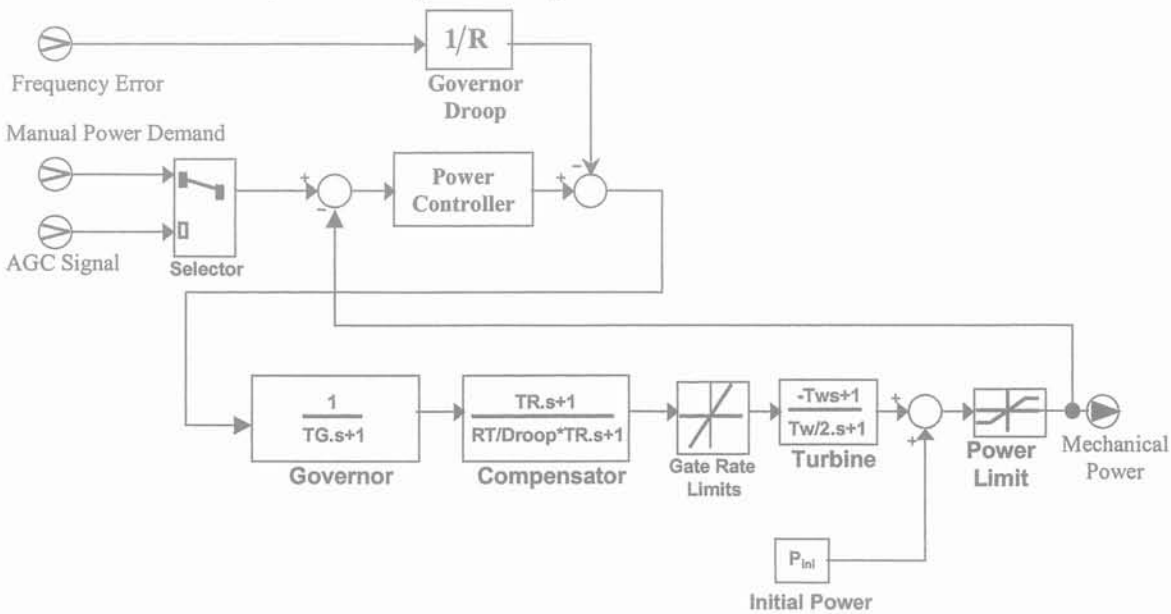

Figure 3.3: Block diagram of hydro unit model

B. Combustion Gas Turbine and Controls

The extracted gas turbine model consists of a representation of the input section and turbine section of a gas unit. Figure 3.4 shows block diagram of gas unit model [49]. In the input section, it models the manual and automatic modes of power demand. The turbine dynamics are represented by a simple lag with non-windup limits. In this case, the upper limit is temperature dependent. The temperature value is presently taken from input data and not automatically changed within a simulation. This can model the situation of a gas turbine having a higher value of the upper limit in winter and a lower value of the upper on a hot summer day.

An area that can use further development, especially for longer-term application such as in a dispatcher training simulator, is a mechanism to simulate the initial response of a gas unit to a start up command. Such an initial response, after a start-up command is sent and before any loading is resulted, may take between 5 to15 minutes. This lies within the long-term simulation time frame. The function performed during this time period include:

Starting (take approximately 4 to 14 minutes): Induction motor rolling turbine to speed; Ignition transformer firing; Flame detection; Software guided acceleration of turbine.

Synchronizing (takes approximately 1 to 4 minutes): Adjusting field voltage; Fine tuning speed; Closing main breaker.

Loading to minimum load (10%)

As a start, an appropriate length of time delay to represent this time period may be considered for inclusion in the model.

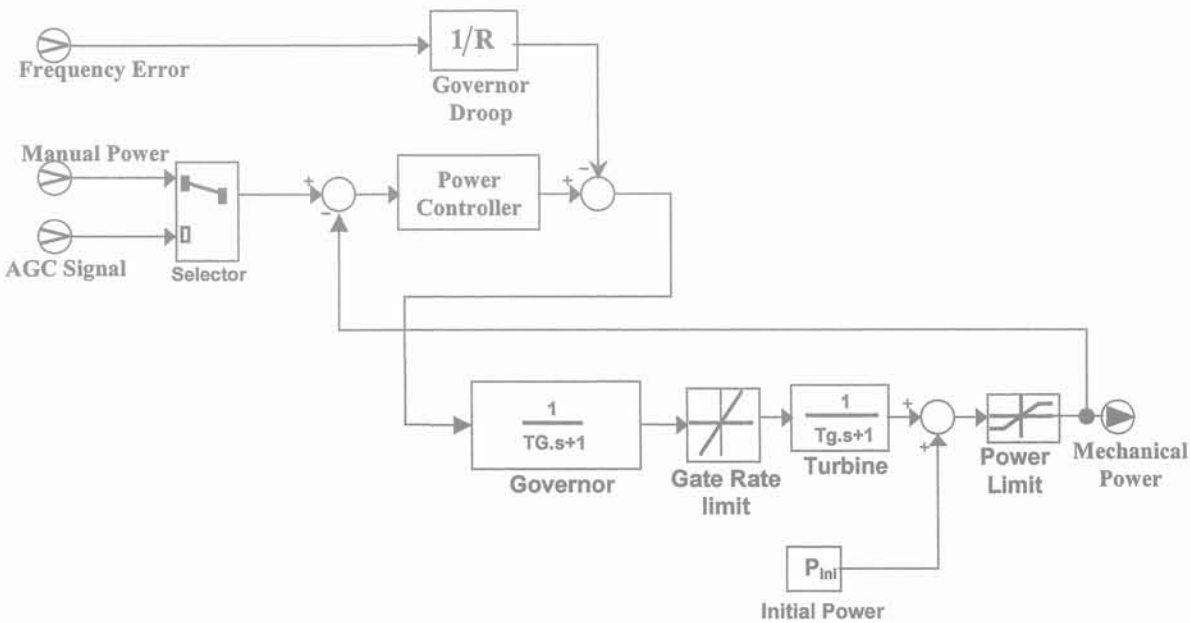

Figure 3.4: Block diagram of Combustion Gas unit model

C. *Fossil-Fueled Steam Turbine and Controls*

The extracted fossil-fueled steam turbine model consists of a representation of a fossil-fueled plant in five sections: coordinated control, turbine control, turbine dynamics, boiler pressure controller and boiler dynamics [49, 86]. The model can represent once-through sub-critical, once-through supercritical, and drum boiler units. This model was developed by the Philarerfia Electric Co. and validated against field tests of their units to be within 2% accuracy [49]. A similar model has been used by the General Electric Co.[49]

Figure 3.5 shows an overview of the fossil-fueled prime mover model structure where a detailed description for each section is given as Figures 3.6 through 3.10. The input signals to the model consist of power demand signals (AGC and Manual), the real power (MW) feedback, electrical frequency error. The reference values for the model include the pressure set point. The 'limit' type of input to the model is numerous; these inputs include: limit values for AGC input signal, for AGC output signal, for frequency bias signal, initial pressure limit, load limit, for LRM (Load Reference Motor) drive error, for LRM position

error, for pressure valve, for boiler demand signal, for the throttle pressure error dead band, and for feed-water controller output.

A functional description of the model starts with Figure 3.6, which describes the input section. Operating in the manual mode, the manual power demand signal is enhanced by a gain factor to directly become the LRM drive error signal. In AGC mode, the AGC signal passed through the demand accumulator and combine with the frequency bias signal to produce MW demand. The MW demand less the MW feedback (the value being generated) produces MW demand error. The typical data for the model is given in [49].

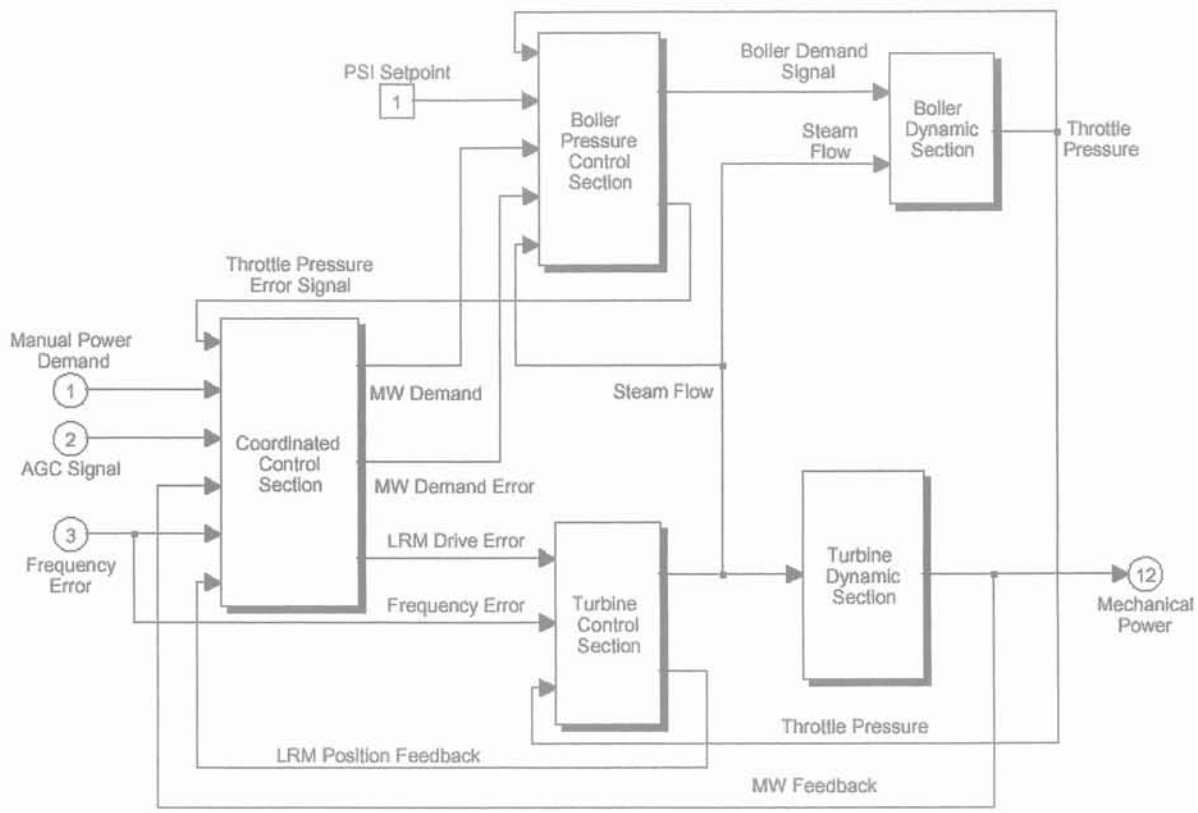

Figure 3.5: Different sections of the fossil-fueled prime mover model

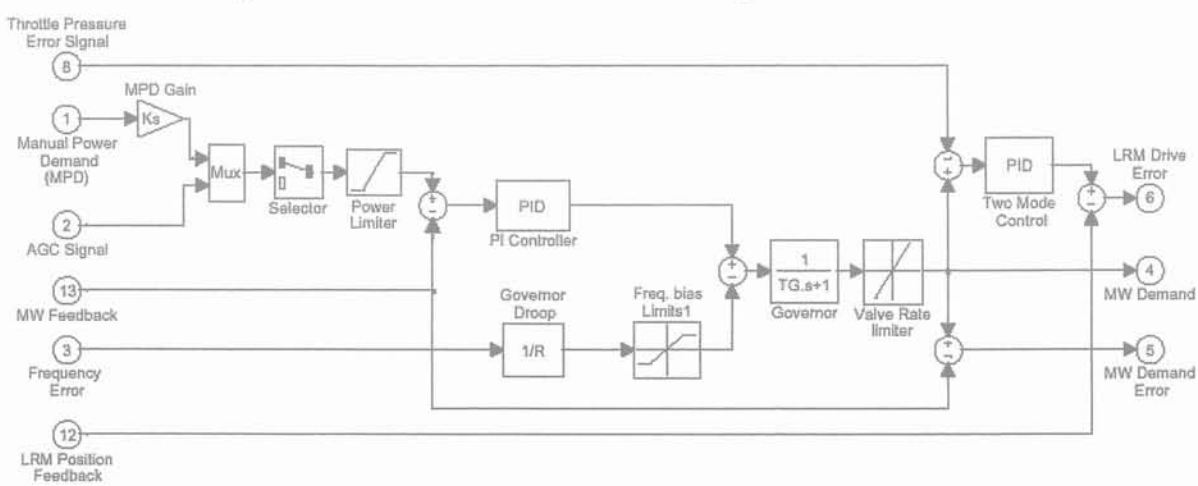

Figure 3.6: Coordination control section

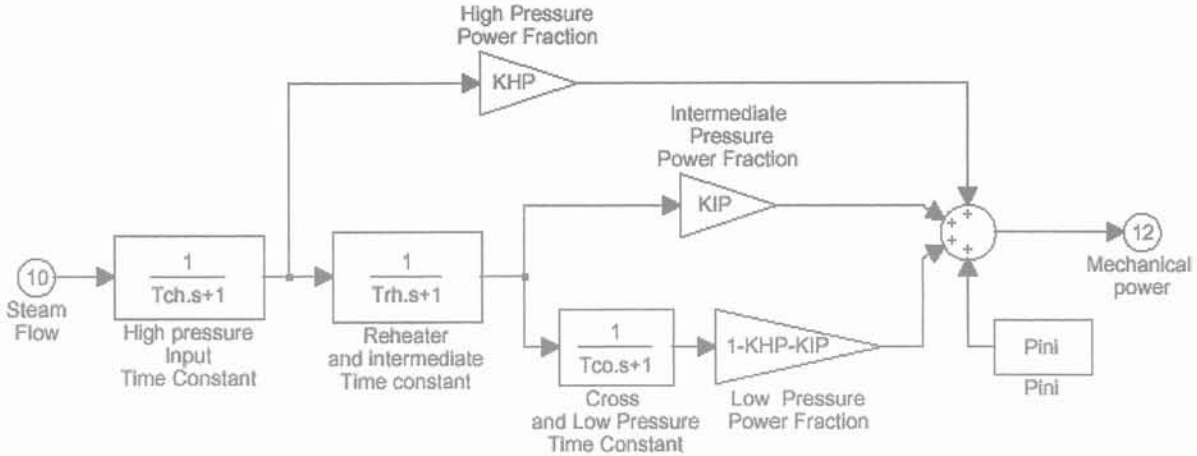

Figure 3.7: Turbine dynamic section

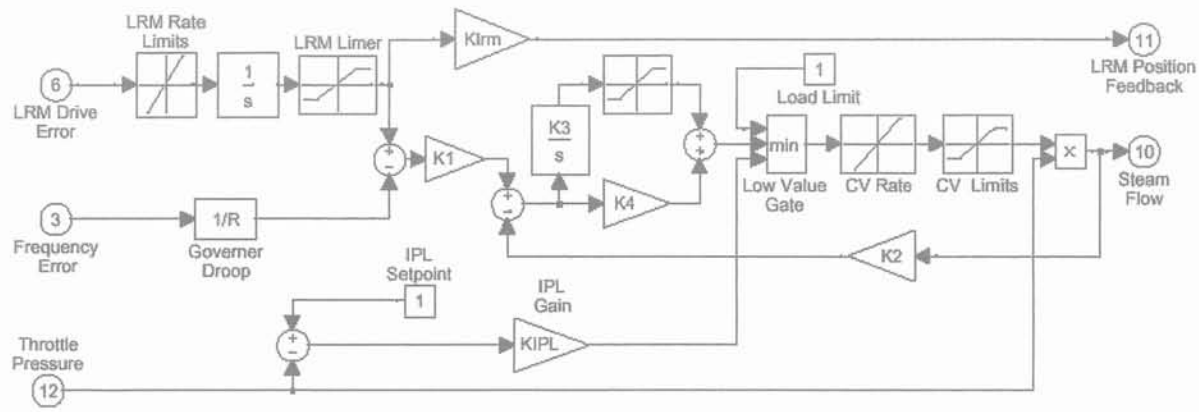

Figure 3.8: Turbine control section

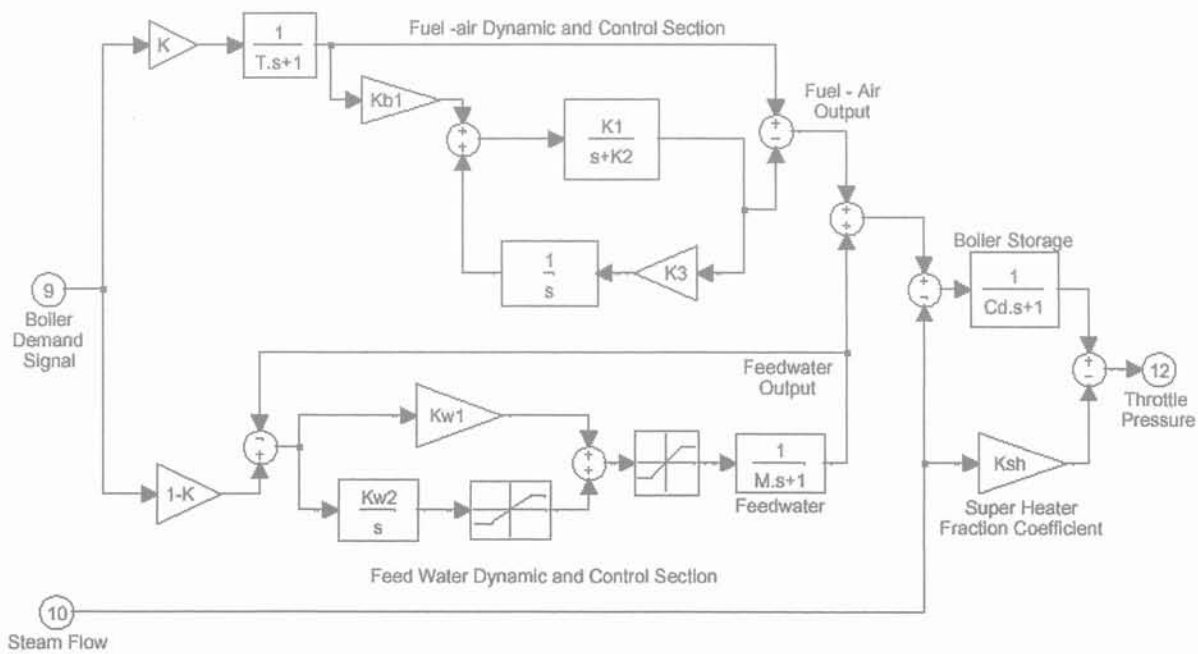

Figure 3.9: Boiler dynamic section

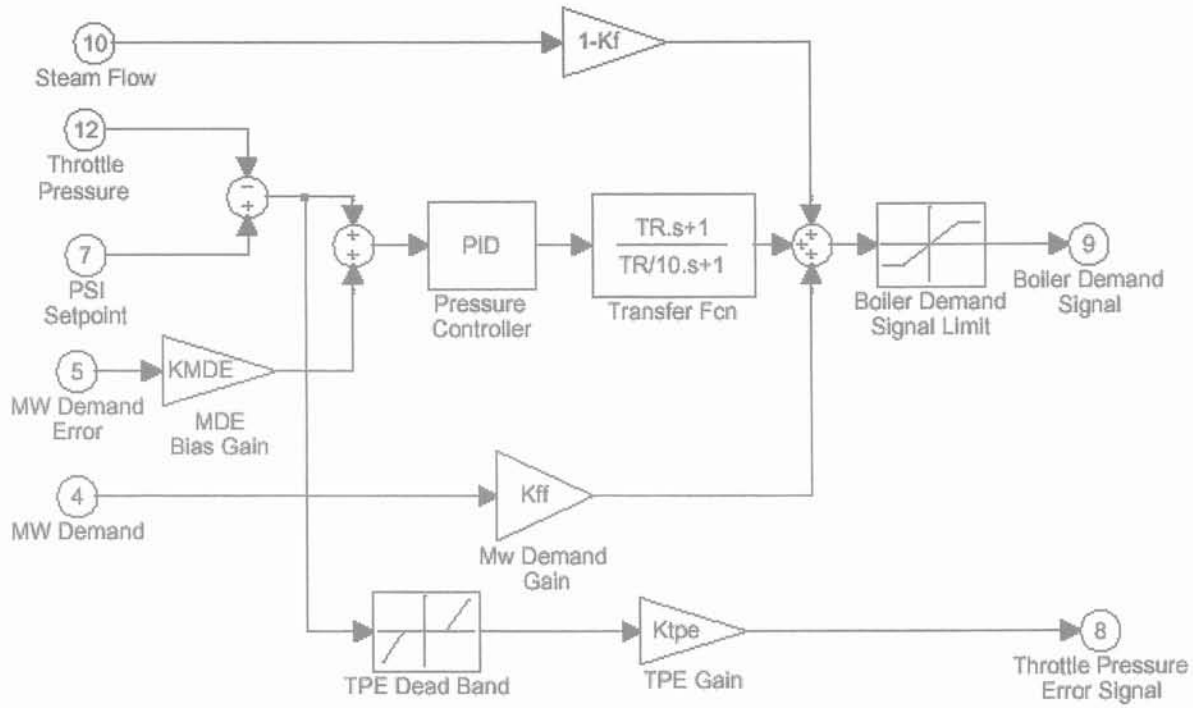

Figure 3.10: Boiler pressure control section

D. Boiling Water Reactor and Controls

Figure 3.11 shows the extracted boiling water reactor (BWR) model witch consists of a representation of the input, controls, and auxiliary effect sections [49, 86]. The turbine model of fossil fuel unit is used in the nuclear unit model [86].

The control and auxiliary effects section models the allowed load-following response characteristic of the BWR. The allowed limits (lower and upper limit) are calculated

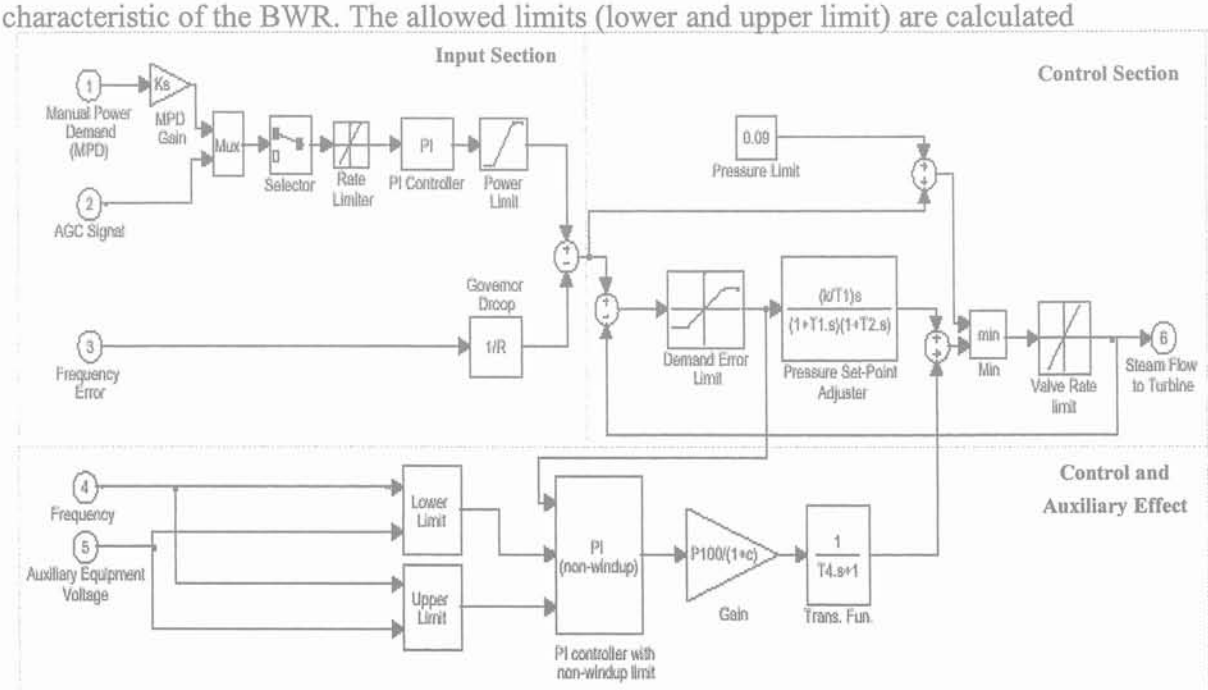

Figure 3.11: Boiling Water Reactor (BWR) Model

according to the make-type of the BWR. Simplified representation of steam pressure and steam flow controls is also included.

Overall, the BWR model is a generic model for BWR plant designs BWR/3 through BWR/6. It represents the control of the plant by two mechanisms: reactor reticulation flow changes and transient changes in the pressure regulator set point. Effects of frequency and voltage perturbations are also included, in a lumped manner. This model is specifically designed for simulation time steps of about 1 second. Power demand change is accommodated by a change in the recalculation flow.

3.2.2 System Frequency

The principal assumption made in this long term dynamics simulation is that the system has a uniform frequency. The implication of this assumption is that the accelerating power (the sum of turbine mechanical powers less the sum of generator active powers) must be scheduled to the generator buses in some manner. An allocation method using relative proportioning of their inertias was considered and is carried forward in this thesis [49]. The usual Newton-Raphson power flow method is modified to compute the remaining generator active powers when the controlled unit active powers are known and the accelerating power is distributed in proportion to the generator inertias. A dynamic model is required to simulate the change of system frequency in response to the accelerating power. Figure 3.12 shows the structure of the model.

This is a model that has been accepted for representing system frequency in long term dynamic simulation [49, 86, 158]. Although the system frequency is simple, it is one of the key pieces that interacts with electrical network solution of the simulation. The system frequency from this model affects the impedance elements in the electrical network, for the particular area or island.

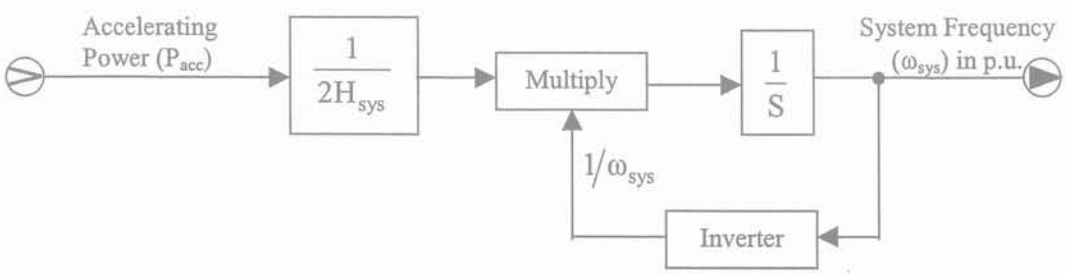

Figure 3.12: System frequency baseline dynamic model

3.2.3 ELECTRIC GENERATION

A. Synchronous Machine Modeling

In long term stability studies, synchronous generators are model using the electromotive force magnitude E behind the transient impedance X, but, it is important to consider their reactive capability limits [158].

A.1. Reactive Capability Limits

In voltage stability and long-term stability studies, it is important to consider the reactive capability limits of synchronous machines. The capability curves identify these limitations. Synchronous generators are rated in terms of the maximum MVA output at a specified voltage and power factor (usually 0.85 or 0.9 lagging) which they can carry continuously without overheating [6, 10]. The active power output is limited by the prime mover capability to a value within the MVA rating. The continuos reactive power output capability is limited by three considerations: armature limit, field current limit, and end region heating limit.

Figure 3.13 shows the generator reactive capability curves for rated machine reactive limits for a 460 MVA, 23 kV generator [6]. This curve that furnished by manufactures are strictly a function of the generator's design parameters at the rated terminal voltage and hydrogen pressure and can be used for modeling of reactive power limitation of generator. However these curves do not consider power plant and power system operating conditions as the limiting factors which superimposed on the rated reactive capability curves [6].

The reactive power generation is given as [158]:

$$Q_g = -\frac{V_t^2}{X} + \sqrt{\frac{E^2 . V_t^2}{X^2} - P_g^2} \tag{3.1}$$

In the above equation the effect of generator resistance is neglected. Using operational limits of reactive capabilities, when a generator reaches limits, E is calculated by following equation:

$$E = \frac{X}{V_t}\sqrt{\left(Q_g + \frac{V_t^2}{X}\right)^2 + P_g^2} \tag{3.2}$$

Figure 3.14 shows block diagram for reactive power limitation modeling.

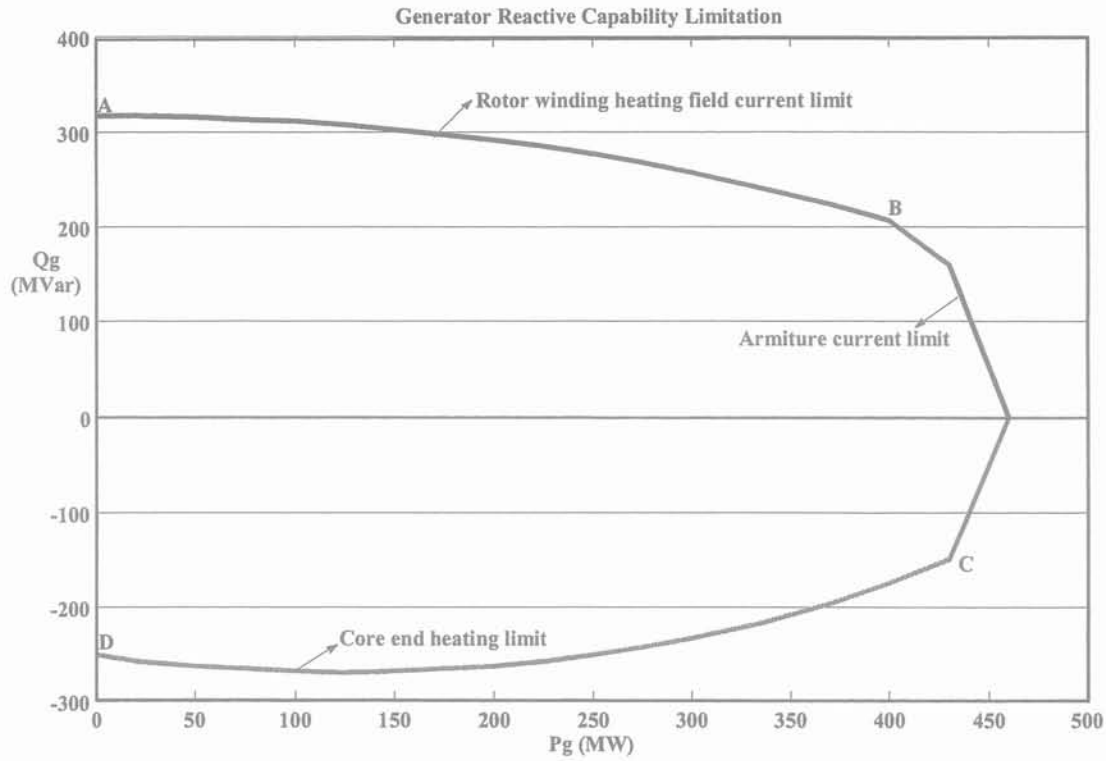

Figure 3.13: Generator Reactive Capability Limitation

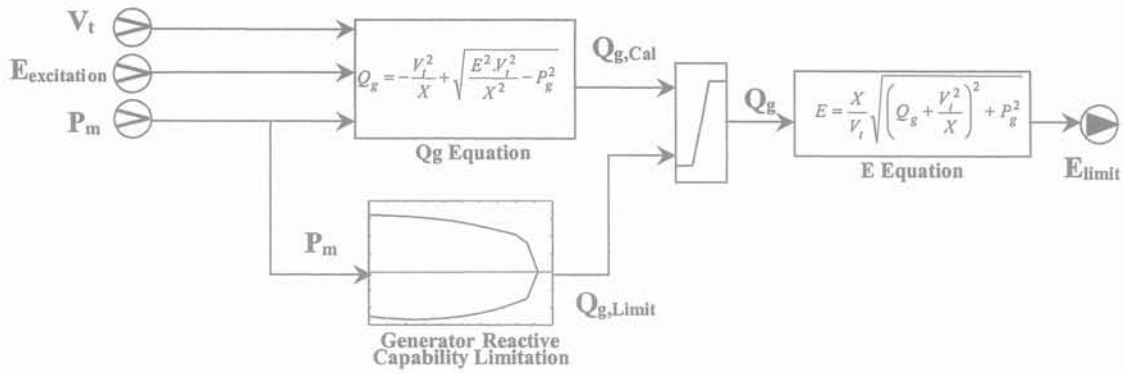

Figure 3.14: Block diagram for reactive power limitation modeling

B. Excitation system and automatic voltage regulator

The appreciate structure for the excitation system depends on the type of excitation system. The IEEE has standardized 12 model structure in block diagram form for representing the wide variety of excitation systems currently in use [83]. Figure 3.15 shows IEEE type DC1A excitation system model [83]. This type exciter model represents field-controlled dc commutator exciters, with continuously acting voltage regulators. The exciter may be separately excited or self-excited, the latter type being more common. When self-excited, K_E is selected so that initially V_R=0, representing operator action of tracking the voltage regulator by periodically trimming the shunt field rheostat set-point.

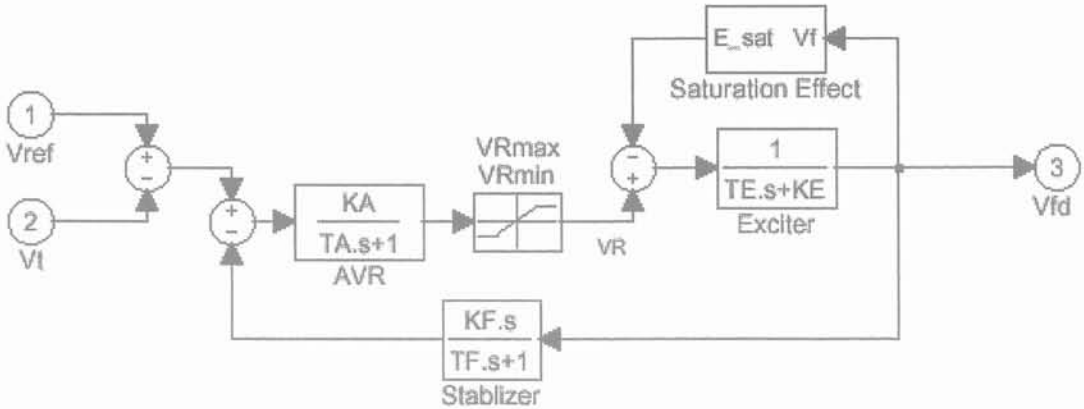

Figure 3.15: IEEE type DC1A excitation system model

3.2.4 Automatic Generation Control

In an isolated power system, maintenance of interchange power is not an issue. Therefore, the function of AGC is to restore frequency to the specific nominal value. This is accomplished by adding a reset or integral control which acts as the load reference setting of the governors of units on AGC, as shown in Figure 3.16 [120]. The integral control action ensures zero frequency error in the steady state. The supplementary generation control action is much slower than the primary speed control action. As such it takes effect after the primary speed control (which acts on all units on regulation) has stabilized the system frequency. Thus, AGC adjusts load reference setting of selected units, and hence their output power, to override the effects of the composite frequency regulation characteristics of the power system. In so doing, it restores the generation of all other units not on AGC to scheduled values. In this simulator we do not consider behavior of AGC in interconnected power system [157].

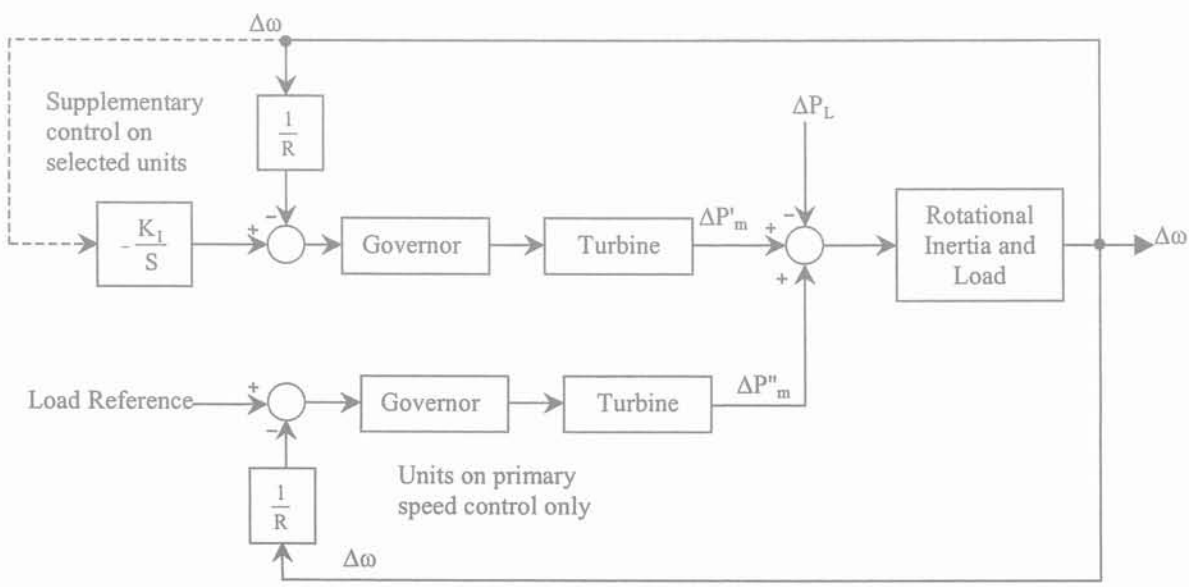

Figure 3.16: Addition of integral control on generating units selected for AGC

3.2.5 NETWORK COMPONENTS

A. Transmission Lines

Transmission lines are represented with the standard lumped parameter π-circuit line model. For long term dynamics simulation, the line impedance is a function of system frequency and thus the admittance matrix representing the network should be updated during a simulation when frequency deviation is substantial.

B. Transformers

Transformers are represented with the standard parameter model. The model represents the effects of series reactance, off nominal turns ratio, and saturation.
A transformer with phase-shifting can be represented by the equivalent circuit shown in Figure 3.17. It consists of an admittance in series with an ideal transformer having a complex turn ratio. The admittance matrix for the transformer can be written as [120]:

$$Y = \begin{bmatrix} y_t/|a|^2 & -y_t/a^* \\ -y_t/a & y_t \end{bmatrix} \tag{3.3}$$

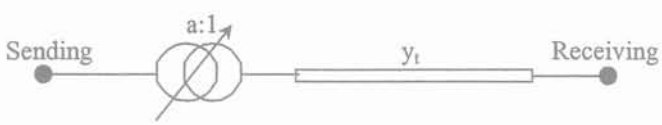

Figure 3.17: Transformer representation with tap-changing and Phase-shifting

B.1 Modeling of transformer Under-Load Tap-Changer (ULTC) control systems

Figure 3.18 shows the block diagram of the control system used for automatically changing transformer taps under load, which is suitable for long-term dynamics simulation [120]. In the input section current voltage of transformer bus compare with reference value. The PI controller and standard tap step show the motor drive unit and tap-changer mechanism. The limitter shows minimum and maximum limit of the tap changer.

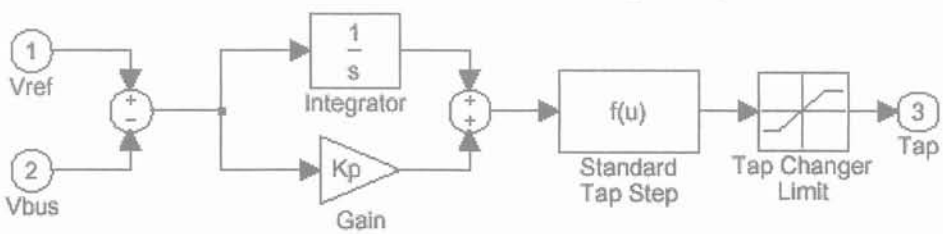

Figure 3.18: Block diagram of ULTC control system

C. Loads

C.1. Load Modeling for Restored Loads

The load powers are functions of bus voltage and frequency. In LTD simulation program, loads have modeled using a static model, which consisting of ZIP (impedance, current and power constant load model) terms plus two voltage-frequency dependent terms [80]:

- Active component :

$$\begin{aligned} P = P_0 [\, & K_{pz}.(V/V_0)^2 + K_{pi}.(V/V_0) + K_{pc} \\ & + K_{p1}.(V/V_0)^{n_{pv1}}.(1 + n_{pf1}.\Delta f) \\ & + K_{p2}.(V/V_0)^{n_{pv2}}.(1 + n_{pf2}.\Delta f)] \end{aligned} \tag{3.4}$$

- Reactive component:

$$\begin{aligned} Q = Q_0 [\, & K_{qz}.(V/V_0)^2 + K_{qi}.(V/V_0) + K_{qc} \\ & + K_{q1}.(V/V_0)^{n_{qv1}}.(1 + n_{qf1}.\Delta f) \\ & + K_{q2}.(V/V_0)^{n_{qv2}}.(1 + n_{qf2}.\Delta f)] \end{aligned} \tag{3.5}$$

Where P_0 and Q_0 are the initial active and reactive load powers from the power flow base case. This model provides the flexibility to model various types of load. For instance, the frequency dependent term could be used for static representation of two types of motors. Alternatively, the frequency dependent terms could be used to represent a motor and also fluorescent lighting.

C.2. Cold Load Pick up Modeling

Representation of reconnected loads plays significant role in the safe evolution of the restoration plan, with particular reference to island frequency behavior. In fact, there is a close relationship between the duration of the outage and the power demand profile. In [40] experimental data are used to model equivalent load demands after cold load pick-up with linear (active power) and exponential (reactive power) fitting. Load real and reactive powers are therefore as [40]:

$$P(t) = \begin{cases} 0 & , \quad t < t_0 \\ P_{init} - \dfrac{P_{init} - P_{fin}}{T_d}.(t - t_0) & , \; t_0 \le t < t_0 + T_d \\ P_{fin} & , \quad t > t_0 + T_d \end{cases} \tag{3.6}$$

$$Q(t)=\begin{cases} 0 & , t<t_0 \\ Q_{init}-(Q_{init}-Q_{fin}).(1-e^{\frac{t-t_0}{\tau}}) & , t\geq t_0 \end{cases} \quad (3.7)$$

Where:

t_0: instant of insertion of the cold load;

T_d : time interval of the real power linear decay;

τ : time constant of the reactive exponential decay;

P_{init}, Q_{init} : peak value at cold load pick-up;

P_{fin} , Q_{fin} : final steady state values of the cold load. Active power component has a decreasing linear form until T_d seconds after load pick up, where T_d is dependent to duration of load outage.

D. Shunt Reactors And Capacitors

The shunt elements are modeled as constant admittance and are included in Y_{bus} matrix.

E. SVC

Static VAR Compensator (SVC) is modeled as a variable admittance for long-term dynamics simulation [198]. Figure 3.19 shows the proposed block diagram of SVC. The SVC limit shows limitation of maximum and minimum admittance of SVC.

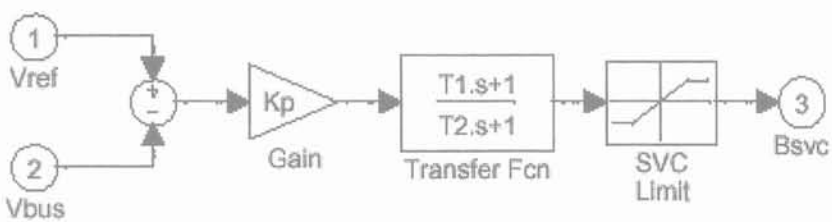

Figure 3.19: Block diagram of SVC's model

3.2.6 RELAYS

For long-term dynamics simulation, the relays which operate on the long term time scale must be represented by appropriate models [120, 65]. The extracted relay models are pertinent to the long time frame simulation.

Under frequency load shedding relay: to prevent extended operation of separated areas at lower than normal frequency, load-shedding schemes are used to reduce the connected load to a level that can be safely supplied by available generation. A load shedding scheme is modeled using relay action. Three stages of under frequency load shedding are used. The uniform frequency of the system is used to trigger the relays.

Under voltage relay (generator and load): under-voltage relays may be modeled for a load bus, or a generator bus. For a load bus, if the magnitude of the bus voltage remain below the voltage set point for a length of time greater than the relay time delay, then the load (both P and Q) at the bus is disconnected. Different voltage set points and time delay may be specified for each bus.

Generator under frequency relay: under-frequency relays may be modeled for a generator bus. If the system frequency drops below the limit specified for the relay then the unit at the bus is tripped off-line. A time delay can be included for the relay.

Volt per Hertz (V/Hz) relay: These are used to protect the generator and set-up transformer from damage due to excessive magnetic flux resulting from low frequency and/or overvoltage. Excessive magnetic flux, if sustained can cause serious overheating and may result in damage to the unit transformer and to the generator core. The ratio of per unit voltage to per unit frequency, referred to as volts per hertz (V/Hz), is a readily measurable quantity that is proportional to magnetic flux.

3.3 DYNAMIC LOAD FLOW

In this section dynamic load flow is explained that is used for analysis of network equations to perform long-term dynamics simulation [65, 156]. The conventional load flow (or power flow) analysis assumes a balanced operation. That is total generation satisfies total load plus total transmission loss in the system. However , transmission loss is not known prior to the load flow solution. For example, consider a system of N_G generators, N_L loads that have N bus. By specifying the generation at (N_G -1) of m generators, all the degrees of freedom of the problem are set. Hence the active real power at all the generator buses cannot be specified, and one of the available voltage controlled buses is chosen as slack or swing bus. The normal load flow formulation utilizes this fictitious concept of slack bus. The concept is somewhat mathematical, and has reduced relation to the physical system. The slack bus active and reactive power are assumed unknown and the bus voltage magnitude and angle are usually assigned as the system complex phase reference. The unspecified unknown real generation is then obtained by the solution of the load flow calculations. In the long-term dynamics simulation, the power balance condition is usually not satisfied. These usually will by a net accelerating or decelerating power in the system. Also, all N_G generators mechanical power outputs are independent variables. Where as the

normal load flow utilizes only (N_G -1) bus injections as independent variables. For these reasons a normal power flow without any modifications may give erroneous result.

To overcome these difficulties the regular load flow equations are extended in to dynamic load flow. Dynamic load flow based on the uniform frequency power system model is a special type of power flow. The main differences between the dynamic load flow and static load flow are:

1. Active power of slack generator is determined in dynamic load flow;
2. Transient impedance , Z, is considered as a series element of electrical network for all generators ;
3. In dynamic load flow an additional variable is known, which is named acceleration power and shows mismatch between generation and consumption;

The accelerating power, P_a, is included as an additional variable and the allocation of the accelerating power is added as another equation:

$$PG_i - PE_i = F_i . P_a \quad , \quad i=1,2,\ldots,N_G \tag{3.8}$$

where:

$$F_i = H_i / H_{sys} \; , \; H_{sys} = \sum_{i=1}^{N_G} H_i \tag{3.9}$$

with the vectors $\mathbf{P}_a$, $\mathbf{P}_E$, and $\mathbf{P}_G$ respectively representing accelerating, scheduled generation and generated real powers as used in Figure 3.20, while H is vector of generator inertia constant. The generator electric power vector, $\mathbf{P}_E$, is treated as an output of the power flow solution rather than an input value.

The complex bus power injections are defined as follow:

$$S_i = P_i + jQ_i = V_i . I_i^* \tag{3.10}$$

Using bus admittance matrix the current can be written as:

$$I_i = \sum_{k=1}^{N} Y_{ik} . V_k \tag{3.11}$$

Thus:

$$P_i + jQ_i = V_i . \sum_{k=1}^{N} Y_{ik}^* . V_k^* = \sum_{k=1}^{N} |Y_{ik}| . |V_i| . |V_k| . e^{j(\theta_i - \theta_k - \delta_{ik})} \tag{3.12}$$

Where:

$$Y_{ik} = |Y_{ik}| . e^{j\delta_{ik}} \; , \; V_k = |V_k| . e^{j\theta_k} \tag{3.13}$$

One of the basic method for solving the power flow equation is Newton-Raphson algorithm. The following correction and mismatch variables are defined for the interface variables V_L, θ_L, P_L, Q_L, θ_E and P_E:

$\Delta |V_L|$: load bus voltage magnitude correction;

$\Delta\theta_L$: load bus voltage angle correction;

ΔP_L: load bus active power mismatch;

ΔQ_L: load bus reactive power mismatch;

$\Delta\theta_E$: Generator bus voltage angle correction;

ΔP_E: Generator bus active power mismatch;

and the following notations will be used for presenting the linearized power flow equations:

$$\Delta\theta = [\Delta\theta_k \quad : k = 1,...,N-1] = \begin{bmatrix} \Delta\theta_L \\ \Delta\theta_E \end{bmatrix} \tag{3.14}$$

$$\Delta|V| = [\Delta|V_{L_k}| \quad : k = 1,...,N_L] \tag{3.15}$$

$$\Delta P = [\Delta P_k \quad : k = 1,...,N-1] = \begin{bmatrix} \Delta P_L \\ \Delta P_E \end{bmatrix} \tag{3.16}$$

$$\Delta Q = [\Delta Q_{L_k} \quad : k = 1,...,N_L] \tag{3.17}$$

Since V_E and $Q_{E,slack}$ are scheduled variables for the static power flow equations, correction terms are not included for them in ΔV or $\Delta\theta$. Similarly, mismatch terms for Q_E and $P_{E,slack}$ are not included in ΔQ and ΔP, because the equations for Q_E and $P_{E,slack}$ are eliminated in the static power flow equations.

With this notation , the linearized power flow equations take the form:

$$\begin{bmatrix} \Delta P \\ \Delta Q \end{bmatrix} = \begin{bmatrix} H & N \\ J & L \end{bmatrix} \cdot \begin{bmatrix} \Delta\theta \\ \Delta|V| \end{bmatrix} \tag{3.18}$$

Where:

$$H = [H_{km}] = \left[\frac{\partial P_k}{\partial \theta_m}\right] = [|Y_{km}|.|V_k|.|V_m|.\sin(\theta_k - \theta_m - \delta_{km})] \tag{3.19}$$

$$N = [N_{km}] = \left[\frac{\partial P_k}{\partial |V_m|}\right] = [|Y_{km}|.|V_k|.\cos(\theta_k - \theta_m - \delta_{km})] \tag{3.20}$$

$$J = [J_{km}] = \left[\frac{\partial Q_k}{\partial \theta_m}\right] = [-|Y_{km}|.|V_k|.|V_m|.\cos(\theta_k - \theta_m - \delta_{km})] \tag{3.21}$$

$$L = [L_{km}] = \left[\frac{\partial Q_k}{\partial |V_m|}\right] = [|Y_{km}|.|V_k|.\sin(\theta_k - \theta_m - \delta_{km})] \tag{3.22}$$

are Jacobian sub-matrices.

For the application of Newton-Raphson' method for the solution of the dynamic load flow equations, the following additional correction and mismatch terms are defined for the variable P_a and $P_{E,slack}$:

ΔP_a: Accelerating power correction;

ΔP_R: Slack bus active power mismatch;

The mismatch term ΔP_R is required for the $P_{E,slack}$ equations and ΔP_a is the correction term for the variable P_a associated with the equation for $P_{E,slack}$.

With this extended notation, the linearized dynamic load flow equations take the form:

$$\begin{bmatrix} \Delta P \\ \Delta P_R \\ \Delta Q \end{bmatrix} = \begin{bmatrix} H & F & N \\ H_R & F_R & N_R \\ J & 0 & L \end{bmatrix} \cdot \begin{bmatrix} \Delta\theta \\ \Delta P_a \\ \Delta|V| \end{bmatrix} \tag{3.23}$$

Where H,N,J and L are the matrices defined above and :

$$H_R = [H_{km} : \mathrm{k} = \mathrm{N}_{\mathrm{slack}}] = \left[\frac{\partial P_k}{\partial \theta_m} : \mathrm{k} = \mathrm{N}_{\mathrm{slack}} \right] \tag{3.24}$$

$$= [|Y_{km}| \cdot |V_k| \cdot |V_m| \cdot \sin(\theta_k - \theta_m - \delta_{km}) : \mathrm{k} = \mathrm{N}_{\mathrm{slack}}]$$

$$N_R = [N_{km} : \mathrm{k} = \mathrm{N}_{\mathrm{slack}}] = \left[\frac{\partial P_k}{\partial |V_m|} : \mathrm{k} = \mathrm{N}_{\mathrm{slack}} \right] = [|Y_{km}| \cdot |V_k| \cdot \cos(\theta_k - \theta_m - \delta_{km}) : \mathrm{k} = \mathrm{N}_{\mathrm{slack}}] \tag{3.25}$$

$$F = \left[\begin{cases} 0 & , \text{for load buses} \\ F_i & , \text{for generator buses} \end{cases} \right] \tag{3.26}$$

$$F_R = [F_{slack}] \tag{3.27}$$

Where F_i was defined for the generator buses in equation (3.9).

For considering voltage dependent loads, the diagonal elements of Jacobean matrices change as:

$$N_{kk} = \frac{\partial P_k}{\partial |V_k|} = 2G_{kk} \cdot |V_k| + \frac{\partial P_{Lk}}{\partial |V_k|} \tag{3.28}$$

$$L_{kk} = \frac{\partial Q_k}{\partial |V_k|} = -2B_{kk} \cdot |V_k| + \frac{\partial Q_{Lk}}{\partial |V_k|} \tag{3.29}$$

This modification improve the convergence of the load flow iterations during voltage dependent loads process.

The application of Newton-Raphson method for the solution of the dynamic load flow equations is illustrated in Figure 3.20 and briefly outlined as follow:

- Initial Data: Scheduled values for the interface variables:

  $P_{Li} : i=1,2,\ldots,N_L$,

  $Q_{Li} : i=1,2,\ldots,N_L$,

  P_{Gi} and $V_{Gi} : i=1,2,\ldots,N_G$,

  $\theta_{G,slack}$

  are defined and remain fixed for the solution procedure. In addition, initial (predicted) values of the interface variables:

  $V_{Li} : i=1,2,\ldots,N_L$,

  $\theta_{Li} : i=1,2,\ldots,N_L$,

  $\theta_{Gi} : i=1,2,\ldots,N_L$,

  P_a

are defined.

- Mismatch Calculation: the mismatch for the dynamic load flow equations are computed as follows:
  - Load (PQ) buses:

$$\Delta P_{Li} = -P_{Li} - \sum_j |Y_{ij}|.|V_i|.|V_j|.\cos(\theta_i - \theta_j - \delta_{ij}) \quad (3.30)$$

$$\Delta Q_{Li} = -Q_{Li} - \sum_j |Y_{ij}|.|V_i|.|V_j|.\sin(\theta_i - \theta_j - \delta_{ij}) \quad (3.31)$$

  - Generator (PV) buses:

$$\Delta P_{Gi} = -P_{Gi} - F_i.P_a - \sum_j |Y_{ij}|.|V_i|.|V_j|.\cos(\theta_i - \theta_j - \delta_{ij}) \quad (3.32)$$

  - Slack Bus:

$$\Delta P_R = -P_{Gi} - F_i.P_a - \sum_j |Y_{ij}|.|V_i|.|V_j|.\cos(\theta_i - \theta_j - \delta_{ij}) \quad (3.33)$$

- Correction Calculation: The correction variables:

  ΔV_{Li},

  $\Delta\theta_{Li}$: i=1,2,…,N_L,

  $\Delta\theta_{Gi}$: i=1,2,…,N_L-1,

  ΔP_a

  are computed by solving the linearized equations and the corresponding interface variables are updated:

$$V_{Li}^{(new)} = V_{Li}^{(old)} + \Delta V_{Li} \quad , \ i = 1,2,...,N_L \quad (3.33)$$

$$\theta_{Li}^{(new)} = \theta_{Li}^{(old)} + \Delta\theta_{Li} \quad , \ i = 1,2,...,N_L \quad (3.34)$$

$$\theta_{Ei}^{(new)} = \theta_{Ei}^{(old)} + \Delta\theta_{Ei} \quad , \ i = 1,2,...,N_G - 1 \quad (3.35)$$

$$P_a^{(new)} = P_a^{(old)} + \Delta P_a \quad (3.36)$$

- Iteration: The mismatch and correction calculations are alternatively repeated until the corrected values of the interface variables converge.

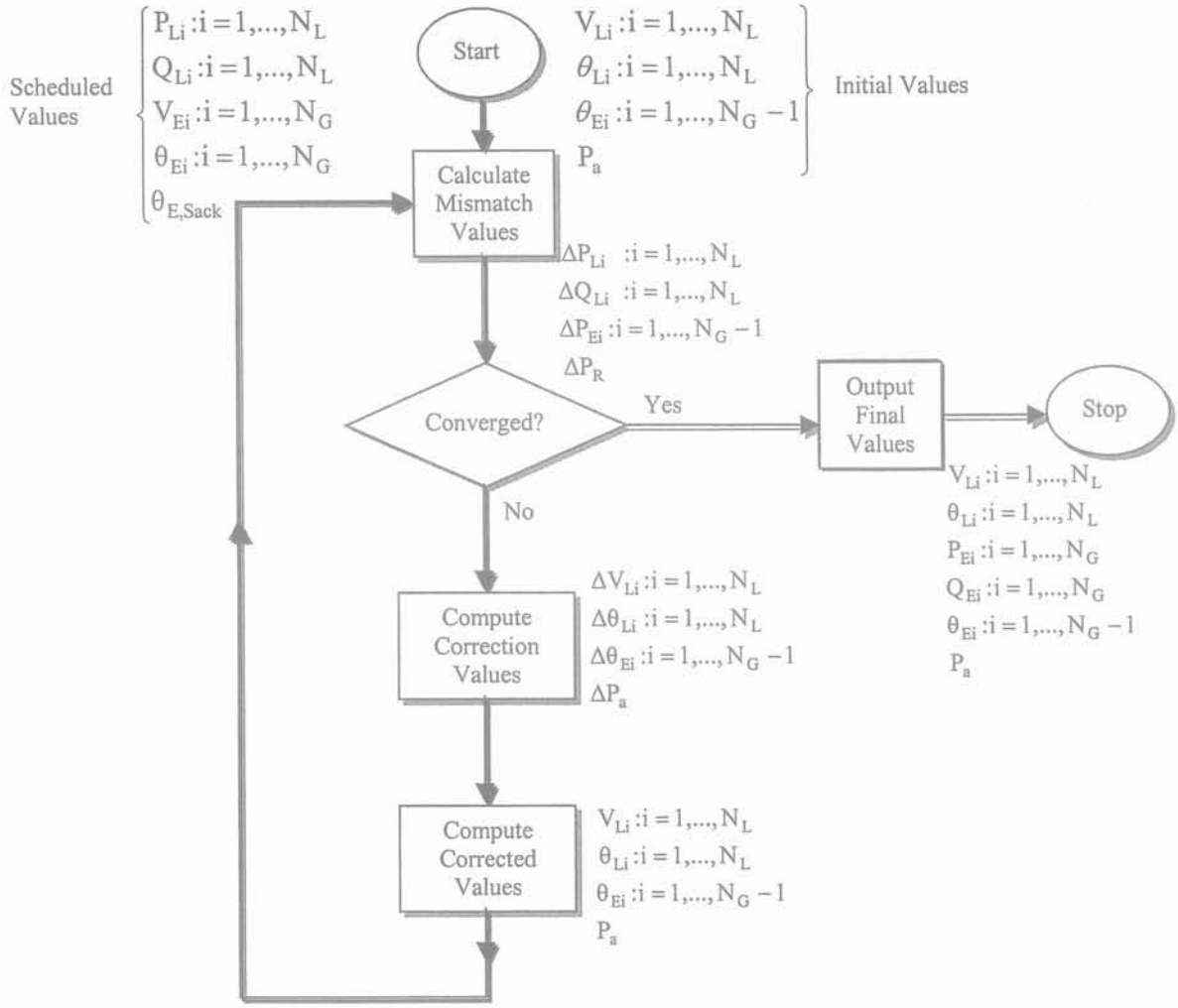

Figure 3.20: Newton-Raphson algorithm for dynamic load flow equations

In order to speed up the calculation process we use the following aspect of the MATLAB program [134]:

- Sparse matrix technique
- Vectorization
- Variable step time integration

Vectorization refers to the notion that loops over indexes should be avoided and replaced, whenever possible, with high level construct that operate on entire vectors, arrays, or sets of data. Vectorized coding in MALAB has a dramatic impact on execution speed.

Solution of differential equations is accomplished using the state-space approach with variable-step integration algorithms. The formula that is used for the numerical solution of the system equations is *ode23tb* [135]. Ode23tb is an implementation of TR-BDF2, an implicit Runge-Kutta formula with a first stage that is a Trapezoidal Rule (TR) step and a second stage that is a Backward Differentiation Formula (BDF) (also known as Gear's method) of order two that is A-stable (the stability region includes the entire left half complex plane). By construction, the same iteration matrix is used in evaluating both

stages. This method is one of the most efficient solver for stiff problems. The time step varies automatically and continuously, which guarantees the accuracy of simulation results and robustness.

3.4 Graphical User Interface for LTD Simulation

Figure 3.21 illustrate the main components of the integrated long-term dynamics simulation program developed in this thesis. These are, the electrical network, generation units, island frequency calculation, protection relays, and restoration scenario and network data updating.

This blockset is a graphic tool that allows building schematics and simulation of power systems in the SIMULINK environment. The blockset uses the SIMULINK environment

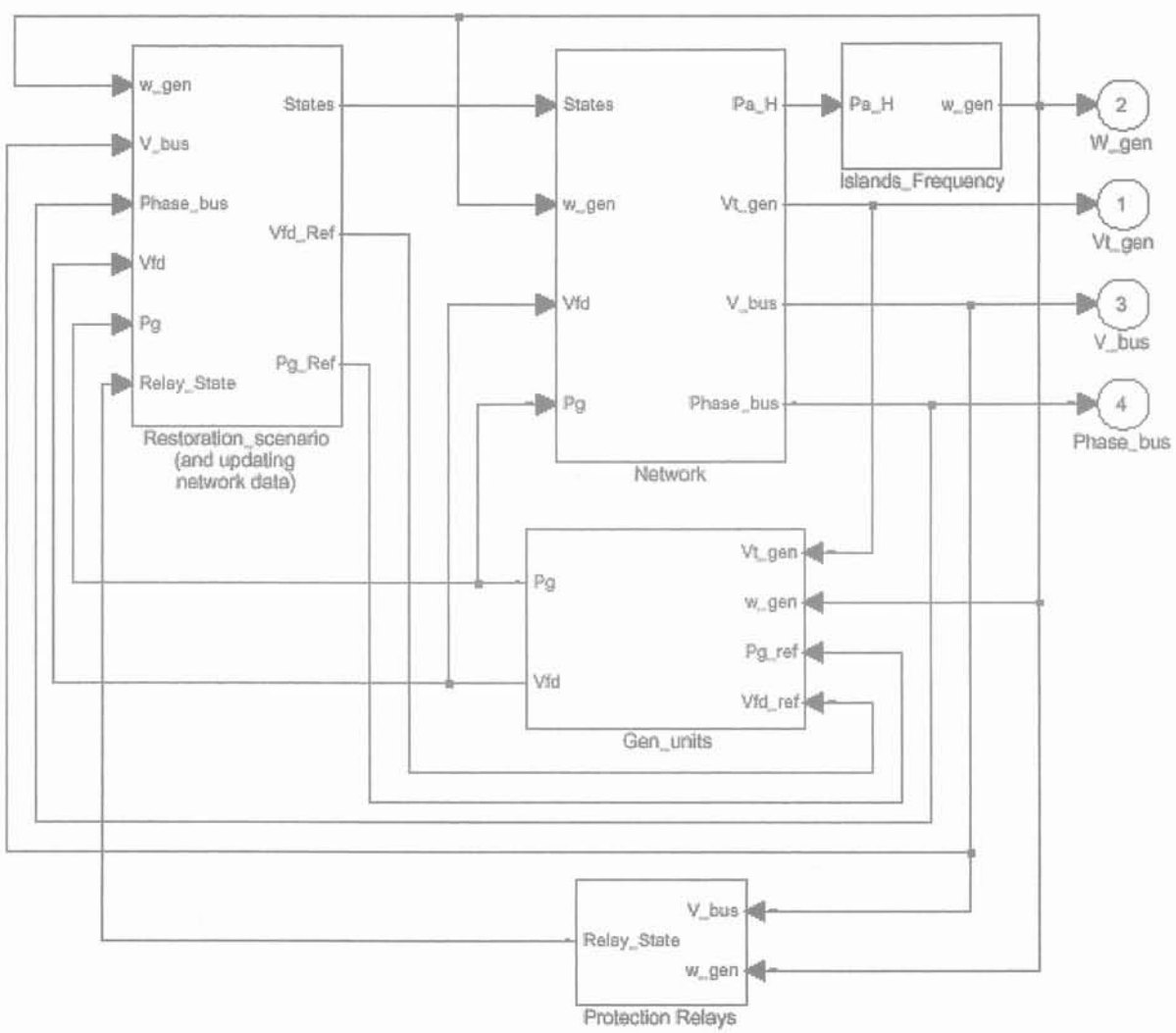

Figure 3.21: Partitioned system formulation

to represent common components and devices found in electrical power network. It consists of a element library that includes transmission line, transformer, load, shunt reactor, shunt capacitor, SVC, electrical bus, and generation units (hydro, combustion gas, steam and BWR type). Figure 3.22 shows the LTD simulation library.

Diagrams can be assembled by using click and drag procedures into SIMULINK windows. The power system simulator uses the same drawing and interactive dialogue boxes to enter parameters as in standard simulink blocks. Figure 3.23 shows the Dialog Box for different elements.

The program is developed in the graphical Simulink environment of the general-purpose Matlab software. This block-set inherits a number of advantages from its development environment, namely, an open architecture and a powerful graphical user interface.

The capability of using interactive graphics greatly facilitates tasks such as restoration planning in data input, modification of network data, simulation and analysis of the results. Simulation results can be visualized with SIMULINK scopes connected to output ports of the simulator.

Figure 3.24 shows a portion of IEEE 39-Bus system that has been prepared for simulation during system restoration the results are described in Chapter 5.

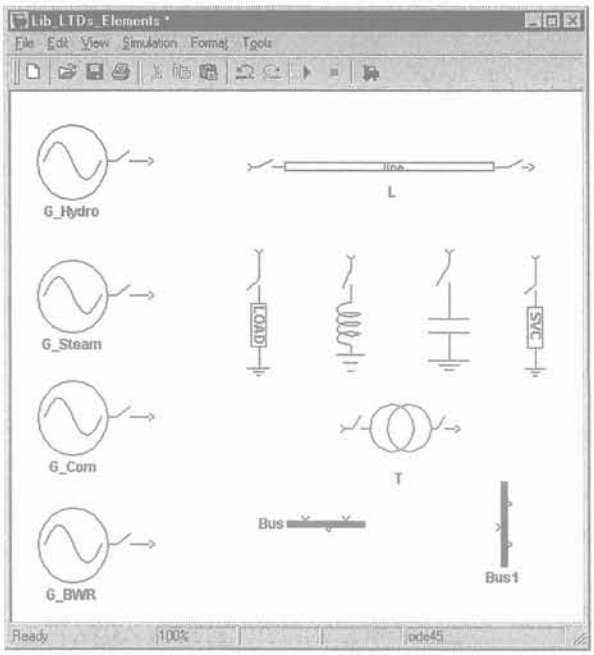

Figure 3.22: The LTD simulation library

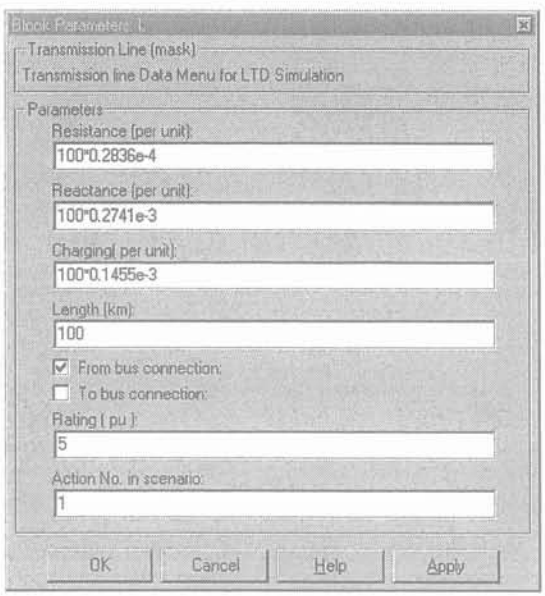

a)

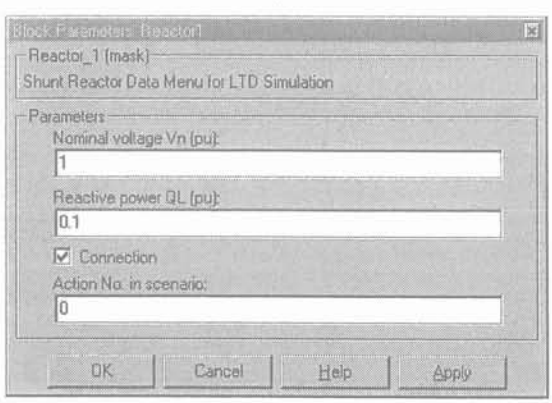

b)

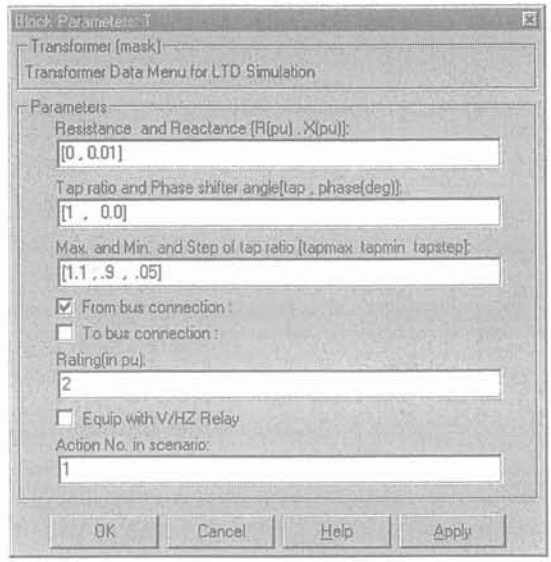

c)

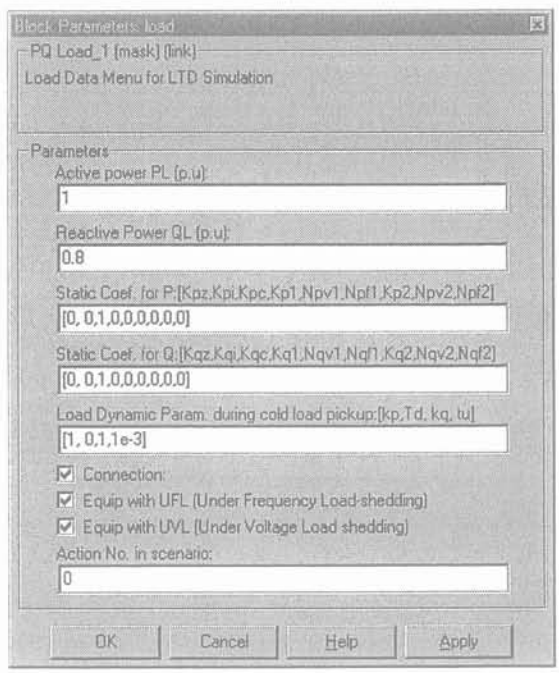

d)

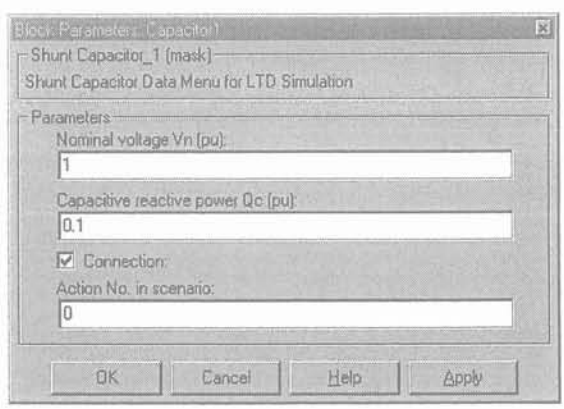

e)

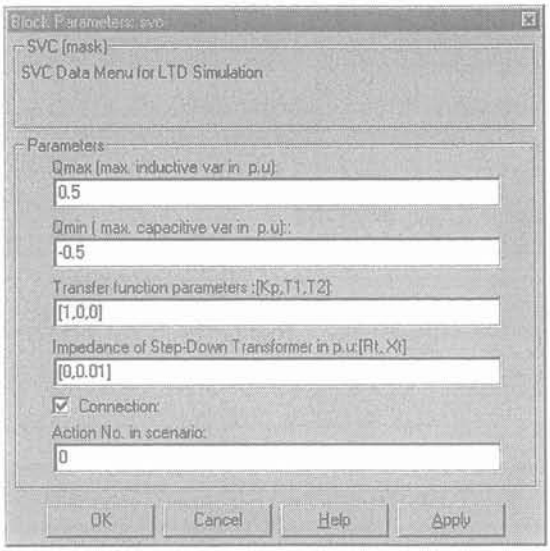

f)

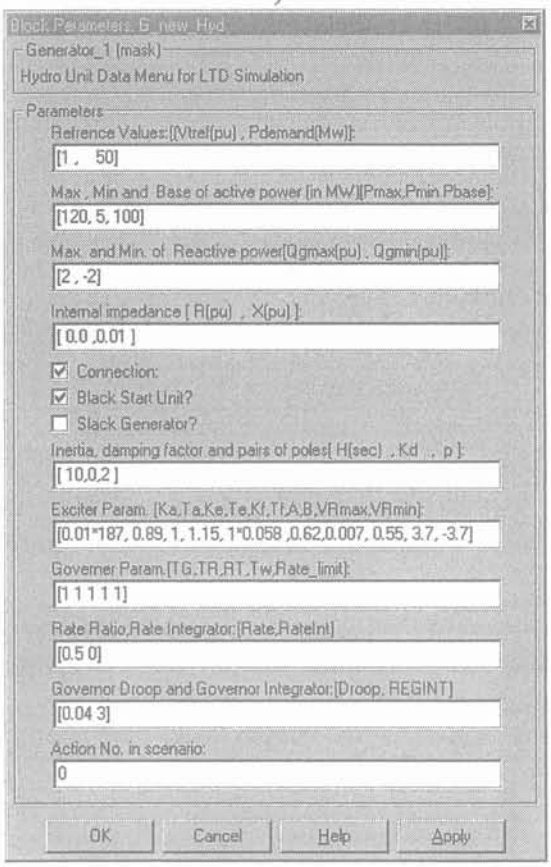

g)

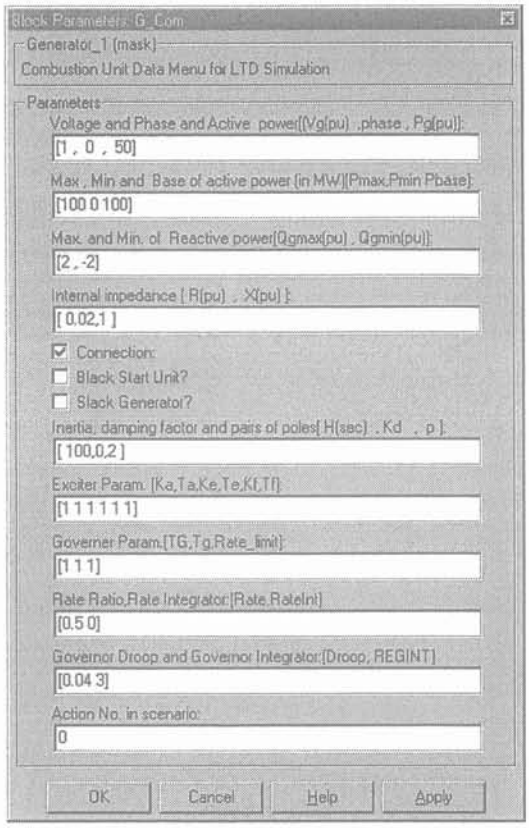

h)

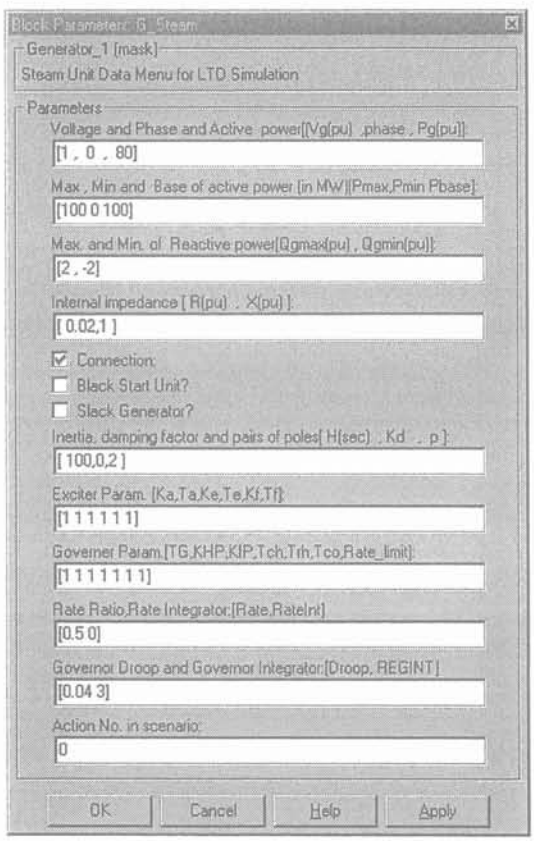

k)

Figure 3.23: Dialog box for the elements:

a) Transmission line b) Shunt reactor
c) Transformer d) Load
e) Shunt capacitor f) SVC
g) Hydro unit h) Combustion unit
k) Steam unit

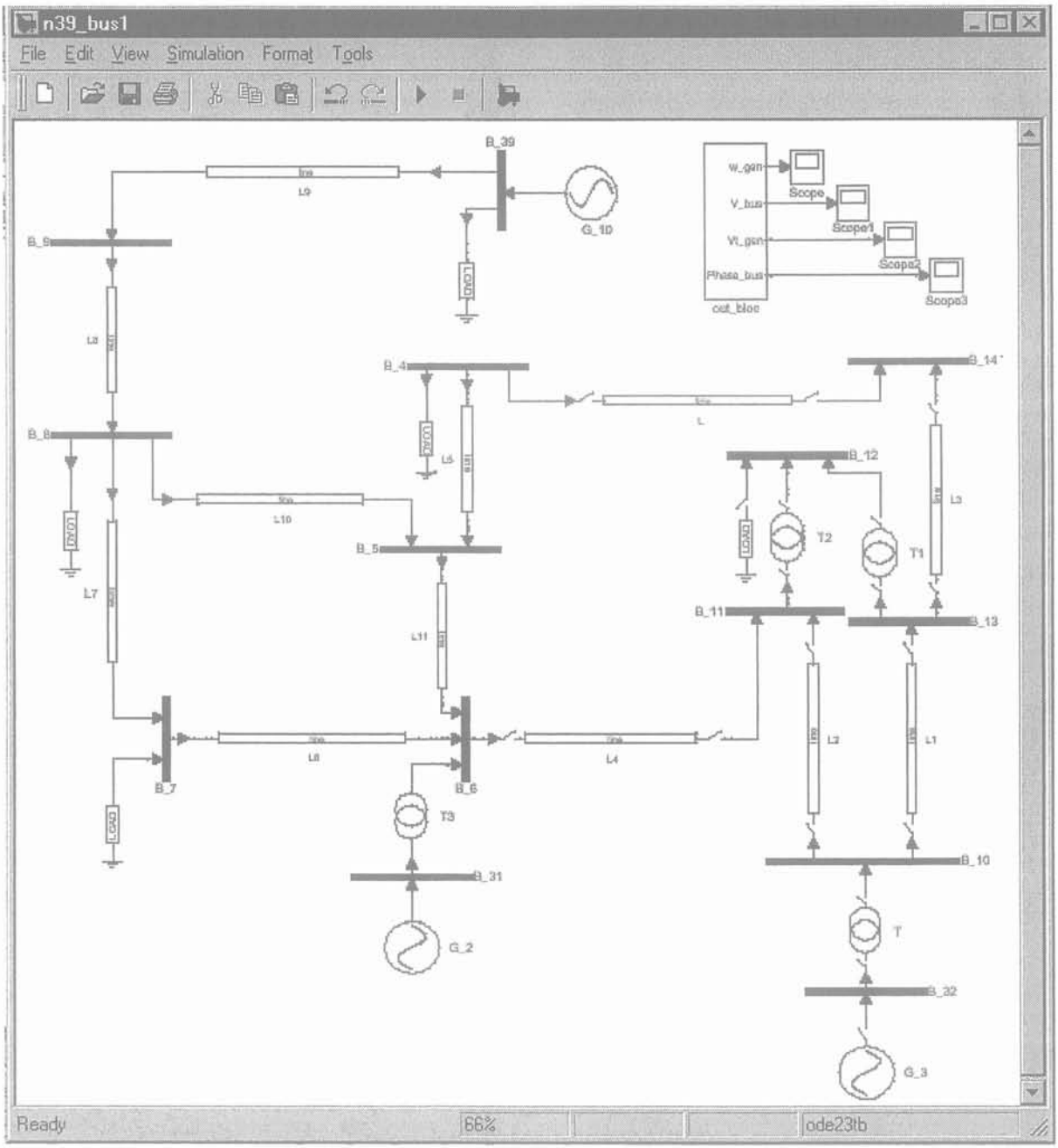

Figure 3.24: A portion of IEEE 39-Bus system in the simulator for LTD simulation

3.5 SUMMARY

In This chapter, Long-Term Dynamics (LTD) simulation is explained as follow:

- Suitable power system modeling for long-term dynamics analysis is described. The important elements are: Prime movers, system frequency, electric generation, AGC, network components, and relays. The proposed modeling considers the dynamics of system components as well as their non-linearity and limitations.

- Dynamic load flow is explained for analysis of electrical network equations during long-term dynamics simulation. Using of sparse matrix technique and vectorization technique can speed up the simulation.

- A blockset in MATLAB/SIMULINK environment is developed for LTD simulation during system restoration. It consists of an element library and has a powerful graphical user interface.

This blockset has been tested on the restoration planning problem the results are described in Chapter 5.

This simulator can also be used for operator training purposes.

CHAPTER 4

DETERMINATION OF UNITS START-UP SEQUENCE DURING UNITS RESTARTING

CHAPTER 4

DETERMINATION OF UNITS START-UP SEQUENCE DURING UNITS RESTARTING

4.1 INTRODUCTION

System restoration after total blackout requires coordination among generating units, load characteristics and transmission system. To restore the whole system successfully, it is necessary to know the characteristics of all the system components and network structure in details. Furthermore, various constraints imposed in generating restoration plans must be taken into consideration. Constraints considered can be physical constraints and scheduling constraints. Physical constraints appear in the form of minimum or maximum time to restart various types of generators. In this case, generator maximum MW output, ramp rate, and response of the prime mover to sudden loss of generation must be taken into account. Scheduling constraints refer to the availability of personnel in a power station. An obvious example is that it is unlikely to have enough plant operators to start two or more units simultaneously within one power station. After considering various coordination constraints, the modeling of the bulk power system is divided into generating system, load pick-up characteristic, system frequency response and transmission network.

In the past, a number of researchers investigated the problem related to the determination of generators start-up sequence [107, 126]. However, these methods are mostly heuristic and do not guarantee optimality of the start up sequence.

This chapter describes a method for unit start-up sequence determination during system restoration. This method is based on backtracking search method, which determines the generating starting times to maximize the MWH generated over a restoration period. The dynamic characteristics of different types of units and system constraints have to be considered.

The shortest path, i.e., the path that requires the minimum number of switching action, between the supplying unit and load is selected unless it is not feasible.

4.2 PROBLEM FORMULATION

Generating units have different physical characteristics and requirements. For start-up sequence planning, units' constraints must be considered. Table 4.1 shows start up characteristics of different types of units [75, 126]. The units which, after a certain period, will become cold and require a longer time to restart are defined as units with *critical maximum intervals*. If a unit with a critical maximum interval is not started within the interval, there may be a delay of hours before the unit becomes available again. The units that require minimum off-line periods due to turbine thermal stress or vibration limits prior to restart are defined as *critical minimum intervals* units. A unit with a critical minimum interval can not be started until the interval ends.

Figure 4.1 shows start up timing for a typical unit [23], where:

t_0: time of unit restart up;

t_1: time of synchronization;

t_2- t_1: time to reach minimum load;

t_3- t_2: time to reach maximum load;

Table 4.1: Start up Characteristics of Different Types of Units

Unit Type	Crank power	Critical Maximum Interval	Critical Minimum Interval
Black start (CT or Hydro)	no	no	no
Drum	Yes	Yes	no
SCOT	Yes	No	Yes

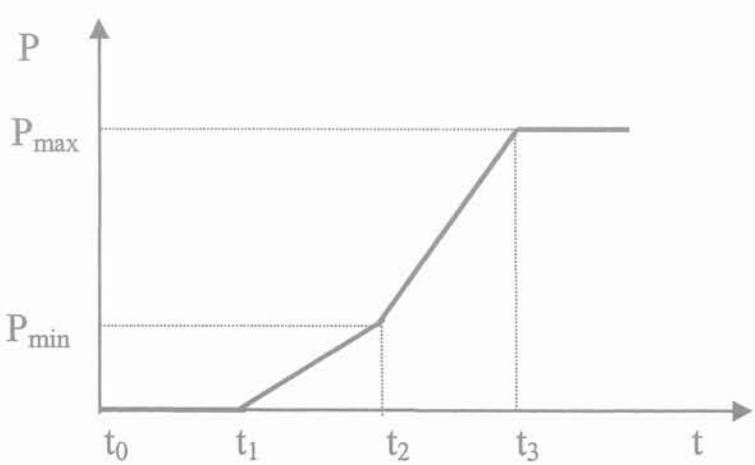

Figure 4.1: Start up timing for a typical unit

During total blackout, we must find the initial power source to crank non black-start generators. The initial source of power is provided by quickly starting black-start generator. For non-black-start generators, we have to consider different physical

characteristics and the starting requirements in each power station. Different types of boilers have different start-up requirements. In addition, we must consider the maximum and minimum starting interval after the total system blackout. Finding a proper start-up sequence of generator can avoid violation of constraints while increasing the system MW output.

The goal is to maximize the total MWH that can be served during the restoration period [151]:

$$G = \sum_{i=1}^{n} \int_{t_i}^{T} P_i(t - t_i)dt \tag{4.1}$$

where:

t_i is the start time for the i^{th} generating unit whose generating capability is $P_i(t\text{-}t_i)$;

T is the planning ending time.

System constraints are:

1. Max MW output of units;
2. Reactive power over and under excitation limits (from generator capability curve);
3. Start-up times;
4. Start-up and house-load requirement;
5. Ramping rates.

4.3 Backtracking Search Method

Many problems, which deal with searching for a set of solution satisfying some constraints, can be solved using the backtracking formulation [63].

In order to apply the backtrack method, the desired solution must be expressible as a n-level $(x_1, x_2, \ldots, x_n)$, where x_i are chosen from some finite set S_i . Often the problem to be solved consists of finding one vector which maximizes (or minimizes or satisfies) a *criterion function* $P(x_1, x_2, \ldots, x_n)$. Sometimes it seeks all such vectors which satisfy P. Suppose m_i is the size of set S_i . Then there are $m = m_1 . m_2 . \ldots m_n$ n-levels which are possible candidates for satisfying the function P. The *brute force approach* would be to form all of these n-levels and evaluate each one with P, saving those which yield the optimum. The backtracking algorithm has as its virtue the ability to yield the same answer with far fewer than m trials. Its basic idea is to build up the same vector one component at a time and to use modified criterion functions $P_i(x_1, x_2, \ldots, x_n)$ (sometimes called bounding functions) to test whether the vector being formed has any chance of success.

The major advantage of this method is this: if it is realized that the partial vector $(x_1, x_2, \ldots, x_i)$ can in no way lead to an optimal solution, then $m_{i+1} \ldots m_n$ possible test vectors may be ignored entirely.

Backtracking algorithms determine problem solutions by systematically searching the solution space for the given problem instance. This search is facilitated using a *tree organization* for the solution space. For a given solution space many tree organizations may be possible.

All paths from the root to other nodes define the *state space* of the problem. *Solution states* are those problem states S for which the path from the root to S defines a level in the solution space.

Once a state space tree has been conceived for any problem, this problem may be solved by systematically generating the problem states, determining which of these are solution states and finally determining which solution states correspond to answer states. There are two fundamentally different ways in generating the problem states. Both of these begin with the root node and generate other nodes. A node which has been generated and all of whose children have not yet been generated is called a *live node*. The live node, whose children are currently being generated, is called the E-node (node being expended). A *dead node* is a generated node that is either not to be expanded further or if all of its children have been generated. In both methods of generating problem states a list of live nodes will be obtained. In the first of these two methods as soon as a new child, C, of the current E-node, R, is generated, this child will become the new E-node. R will become the E-node again when the sub-tree C has been fully explored. This corresponds to a depth first generation of the problem states. In the second state generation method, the E-node remains the E-node until it is dead. In both methods, bounding functions will be used to kill live nodes without generating all their children. This will be done carefully so that at the conclusion of the process at least one answer node is always generated, or all answer nodes are generated if the problem requires finding all solutions. Depth first node generation with bounding function is called backtracking. State generation methods in which the E-node remains the E-node until it is dead lead to *branch-and-bound* methods.

Let $(x_1, x_2, \ldots, x_i)$ be a path from the root to a node in a state space tree and $T(x_1, x_2, \ldots, x_i)$ be the set of all possible values for x_{i+1} such that $(x_1, x_2, \ldots, x_{i+1})$ is also a path to a problem state. We shall assume the existence of bounding function B_{i+1} (expressed as predicates) such that $B_{i+1}(x_1, x_2, \ldots, x_{i+1})$ is false for a path $(x_1, x_2, \ldots, x_{i+1})$ from the root node to a problem state only if the path can not be extended to reach an answer node. Thus the candidates for position $i+1$ of the solution vector $X(1:n)$ are those values which are generated by T and satisfy B_{i+1}. Figure 4.2 shows the general backtracking schema. This is a program scheme which describes the backtracking process. All solutions are

```
Procedure BACKTRACK

Integer k; n; local X(1:n)
```

```
k← 1
while k > 0 do
    if there remains an untried X(k) such that
      X(k) ∈ T(X(1), …, X(k-1)) and Bk(X(1),…, X(k)) = true
    then if (X(1),…, X(k)) is a path to an answer node
            then print (X(1),…, X(k)) endif
            k← k+1 //consider the next set//
    else    k← k-1 //backtrack to pervious set//
    endif
repeat

end BACKTRACK
```

Figure 4.2: General backtracking algorithm

generated in *X(1:n)* and printed as soon as they are determined. Vector *T(X(1),...,X(k-1))* gives all possible values of *X(k)* given that *X(1),...,X(k-1)* have already been chosen. The predicates $B_k(X(1),...X(k))$ determine those elements *X(k)* which satisfy the implicit constraints.

Note that *T*( ) will yield the set of all possible values which can be placed as the first component, *X*(1), of the solution vector. *X*(1) will take on those values for which the bounding function $B_1(X(1))$ is true. Also note how the elements are generated in a depth first manner. K is continually incremented and a solution vector is grown until either a solution is found or no untried value of X(k) remains. When k is decremented, the algorithm must resume the generation of possible elements for the k^{th} position which have not yet been tried.

The efficiency of backtracking algorithm depends strongly on 4 factors: (i) the time to generate the next *X(k)*; (ii) the number of *X(k)* satisfying the explicit constraints; (iii) the time for the bounding functions B_i; and (iv) the number of *X(k)* satisfying the B_i for all *i*.

4.3.1 Application to Generators Start-up Sequence Determination

In order to find optimal start-up sequence using backtracking method, the state space tree is defined such that the state in each path has the following data structure:

$$State = \{ t, f, s_1, s_2, ..., s_n, cu_1, cu_2, ..., cu_n, p_1, p_2, ..., p_n, pd_1, pd_2, ..., pd_n, u_1, u_2, ..., u_n \}$$

where :

t is the time at the level of state; *f* is equal to 2 if all units are started-up, else *f* is equal to 1 if there isn't any state for search; s_i is the starting time of i^{th} unit; cu_i is the unit number that

provides cranking power for i^{th} unit; p_i is the generating capability of i^{th} unit; pd_i is the provided power by the i^{th} unit to crank the other units; u_i is equal to 0 if i^{th} unit don't start-up,1 if it starts-up but it has not reached the maximum capability, 2 if it starts-up and has reached the maximum capability. State space tree is determined on the basis of the number of black-start and non-black-start units and their's time characteristics. Figure 4.3 shows the algorithm flow chart for finding optimal start-up sequence. Where *k*: level of state space tree, *Try_plant_start*: function searches for units that they can be restarted up at the k^{th} state. *Create*: a function that creates another level in the data structure. *Delete:* a function that deletes a path of states that already are examined.

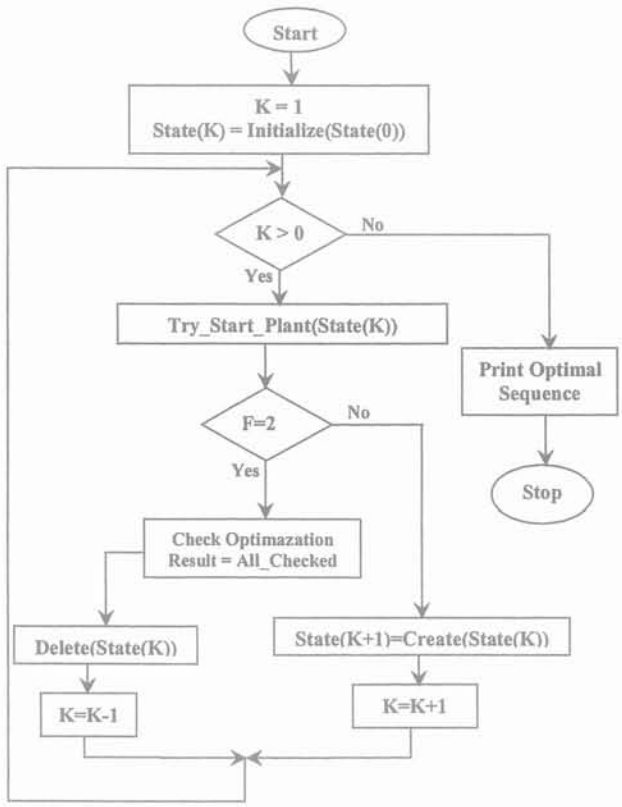

Figure 4.3: Flow chart of the backtracking search method for generators start-up sequence determination

As an example we consider three units *A, B,* and *C* where unit A is a black-start unit. Figure 4.4 shows the state space tree for this case, where (A) shows that unit A is started at the k^{th} level and (0) shows that any unit can't be started at the k^{th} level .

For the acceleration of state space creation , the flowing rules are used:

1. First, the black-start units are started. The units with critical maximum intervals have high priority to receive cranking power.

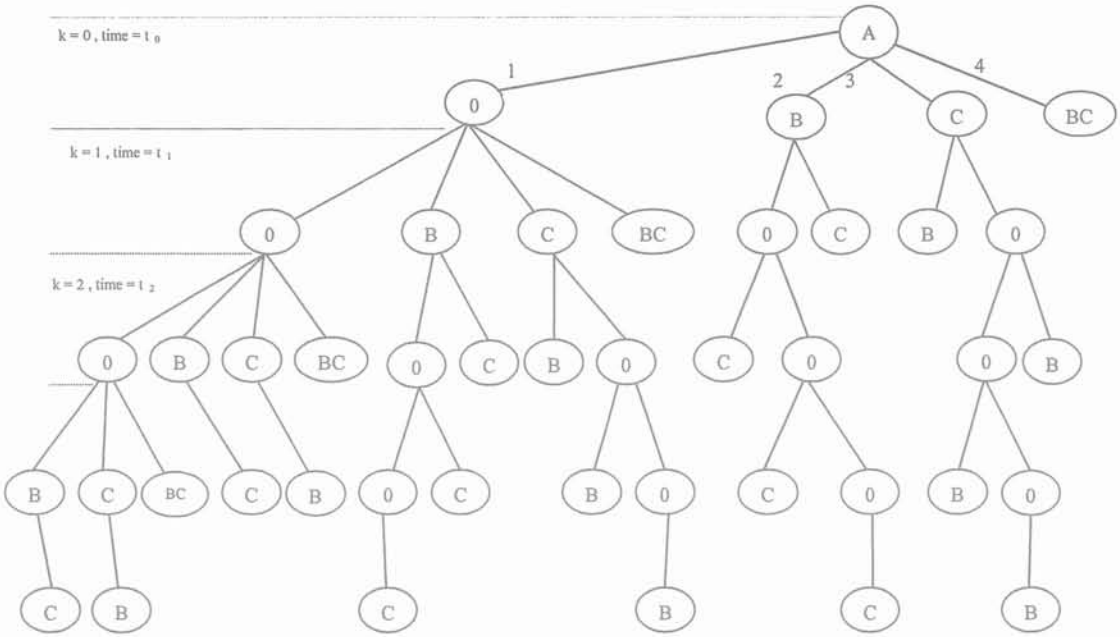

Figure 4.4: Portion of state space tree for 3 units

2. If the cranking power is insufficient, the critical maximum interval unit with the most urgent time constraint is cranked first.

3. If two or more units are equally urgent, the one with lower MW rating is cranked first.

4. If all units with critical maximum intervals are started, then the unit which can generates the highest MWH within the restoration period is given a higher priority.

5. If any critical maximum interval unit is not started, say, due to insufficient cranking power, starting a different unit can be considered.

For finding the optimal start-up sequence, the total MWH that can be served during the restoration period is measured for all the feasible sequences.

To deliver cranking power to non-black-start units, it is necessary to build transmission paths between black-start and other non-black-start units. Two important subject for path selection are MVAR capabilities limits of generating units and the number of required switching.

The shortest path, i.e., the path which requires the minimal number of switching actions between the supplying and receiving unit is desirable unless it is not feasible.

We use A^* search which is a heuristic algorithm for the identification of the shortest path between given nodes in a network [178]. This algorithm identifies a path and calculates the sum of theirs line charging. It must be smaller than the limit MVAR absorbing capabilities of generating units.

4.4 CASE STUDY

4.4.1 CASE 1

In this case study we have applied the proposed approach to provide optimal start-up sequence for the unit given by [75]. The characteristic of these units are shown in Table 4.2.

The backtracking method start-up sequence and the heuristic method start-up sequence are given in Table 4.3 and Table 4.4, respectively. The two methods suggest to start the only black-start unit, Unit 1, first. Once unit 1 is able to supply sufficient cranking power, unit 3 and unit 7 are started. Then, unit 7 supplies power to crank units 6, 8, and 9. Units 2 and 5 have critical minimum intervals of 4 hours and Unit 4 has an interval of 6 hours. They will start after the expiration of the intervals and when sufficient cranking power can be provided.

Table 4.2: Unit Characteristics

Unit No.	Type	MW Cap. (MW)	Min. load (MW)	Start-up Req. (MW)	Crank to Paral. (min)	Paral. To Min. load (min)	Min. To Full Load (min)	Crit. Min. Int. (min)
1	CT	20	5	0	6	2	6	N/A
2	SCOT	92	25	3	120	42	66	240
3	Drum	110	25	3	90	6	90	N/A
4	SCOT	235	50	7	360	60	120	360
5	SCOT	275	30	8	90	42	60	240
6	Drum	550	180	17	240	60	90	N/A
7	Drum	500	150	15	54	30	120	N/A
8	Drum	600	200	18	240	30	120	N/A
9	Drum	800	420	24	240	90	90	N/A

Table 4.3: Unit Start-up Sequence with Backtracking Method

Unit No.	Cranking Unit	Start Time
1	(Black-start)	0:00
3	1	0:10
7	1	0:20
9	7	1:20
6	7	1:30
8	7	1:30
2	3	4:10
5	3	4:10
4	9	6:10

* For this sequence the total MWH is 32381 at the 1000 min.

Table 4.4: Unit Start-up Sequence with Heuristic Method

Unit No.	Cranking Unit	Start Time
1	(Black-start)	0:00
3	1	0:10
7	1	0:20
6	7	1:20
8	7	1:30
9	7	1:30
2	7	4:10
5	7	4:10
4	9	6:10

* For this sequence the total MWH is 32339 at the 1000 min

At 1:20, the output of Unit 7 has ramped up to 30 MW which is sufficient to crank either Unit 6, Unit 8, or Unit 9. Under this situation, heuristic method gives priority to the Unit 6, but backtracking method selects Unit 9 and thus the system generation capability curve is slightly better and reaches the maximum capacity 10 minutes sooner.

The two generation capability curves for the two start-up sequences are shown in Figure 4.5. This figure provides a good projection of available generation during the restoration period.

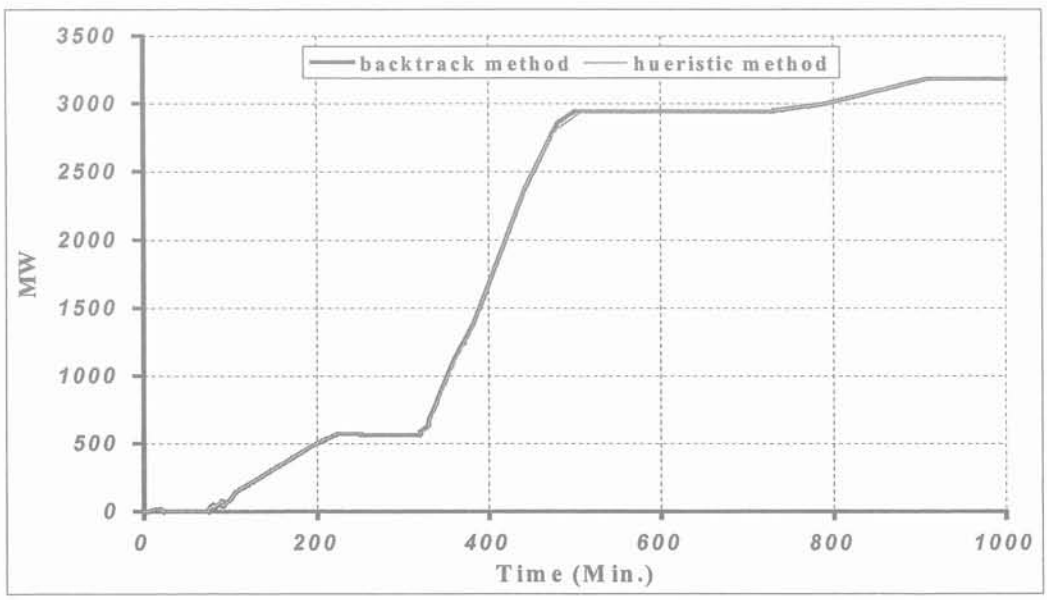

Figure 4.5: System Generation Capability Curves

4.4.2 Case 2

In this section, the proposed method is used for the determination of units start-up sequence for the New England system (39 bus). The results are compared with those of P/t method. The system includes 39 buses, 10 generators, 35 lines and 12 transformers. It is also divided into 2 subsystems (islands) for simultaneous restoration. The first island includes generators in buses 30, 33, 34, 35, 36, 37, 38 and the second island includes generators in buses 31, 32, 39. Lines between buses 1 and 39, 3 and 4, 15 and 16, are out of service. The characteristic of these units are given in Appendix.

In P/t method the priority for generators start-up are determined in the basis of the ratio of MW capability and the time required for the plants to be synchronized with the system, i.e., the generator that its P/t is greater than the others, has the most priority to start-up [107].

Table 4.5 and 4.6 show the results of generators start-up sequence using backtracking search method and P/t method, respectively.

Figure 4.6 shows generation capability of the system after system restoration for the

backtracking search method and P/t method.

During the first 800 minutes of system restoration, the energy generated by units for the two sequence are 48535 and 46946 MWH, respectively. It shows that determination of optimal sequence to start-up can increase generation capability of the system during system restoration.

These simulation results and other test case show the effectiveness and accuracy of the proposed method.

Table 4.5: Generator Start-up Sequence and Selected Path with Backtracking Method

Unit No.	Bus No.	Cranking Unit	Start Time	Selected Path for Energization
1	30	Black-start	0:00	———
6	35	Black-start	0:00	———
4	33	6	0:10	(35-22), (22-21), (21-16), (16-19), (19-33)
7	36	6	0:20	(35-22), (22-23), (23-36)
8	37	1	0:20	(30-2), (2-25), (25-37)
5	34	4	0:40	(19-20), (20-34)
3	32	4	0:50	(16-15), (15-14), (14-13), (13-10), (10-32)
2	31	4	0:50	(10-11), (11-6), (6-31)
10	39	8	1:40	(2-1), (1-39)
9	38	8	3:30	(25-26), (26-29), (29-38)

Table 4.6: Generator Start-up Sequence and Selected Path with P/T Method

Unit No.	Bus No.	Cranking Unit	Start Time	Selected Path for Energization
1	30	Black-start	0:00	———
6	35	Black-start	0:00	———
7	36	6	0:20	(35-22), (22-23), (23-36)
8	37	1	0:20	(30-2), (2-25), (25-37)
5	34	6	0:30	(22-21), (21-16), (16-19), (19-20), (20-34)
4	33	7	1:10	(19-33)
2	31	7	1:10	(16-15), (15-14), (14-4), (4-5), (5-6), (6-32)
3	32	7	1:20	(14-13), (13-10), (10-32)
10	39	8	1:40	(2-1), (1-39)
9	38	8	3:30	(25-26), (26-29), (29-38)

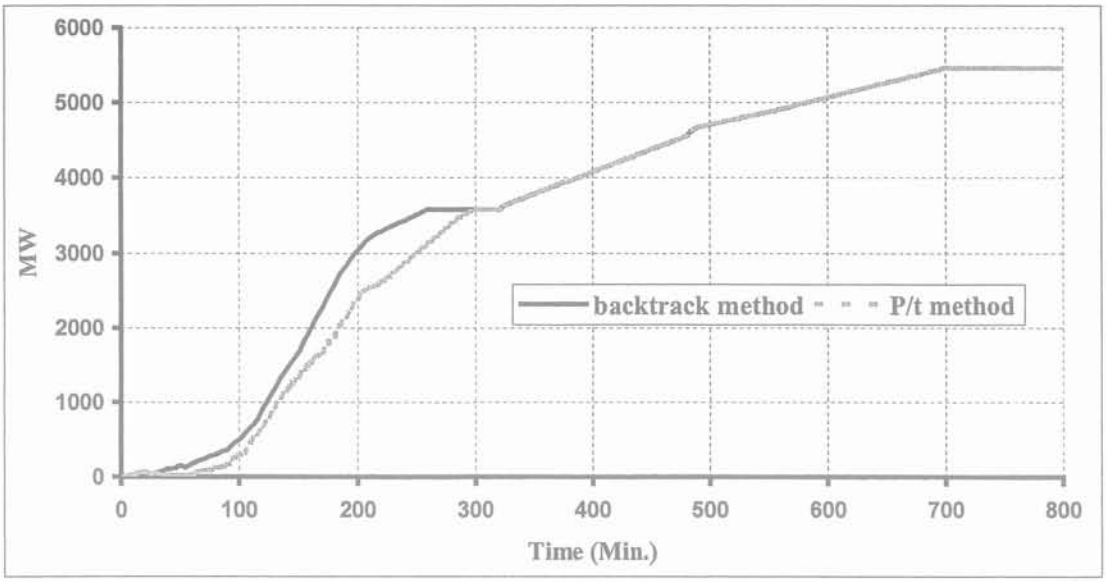

Figure 4.6: Generation capability of 39 bus New England system

4.5 SUMMARY

This chapter describes an approach for unit start-up sequence determination during system restoration. This approach is based on backtracking search method, which determines the generating starting times to maximize the MWH generated over a restoration period and guarantees optimality of the start up sequence. The dynamic characteristics of different types of units and system constraints have to be considered. The shortest path, i.e., the path that requires the minimum number of switching action, between the supplying unit and load is selected unless it is not feasible. The proposed method has been compared with heuristic and *P/t* approaches. Simulation tests, carried out on the 39-bus New England test system, have shown the effectiveness of the proposed method.

CHAPTER 5

PRIME MOVERS FREQUENCY RESPONSE DURING RESTORATION

CHAPTER 5

PRIME MOVERS FREQUENCY RESPONSE DURING RESTORATION

5.1 INTRODUCTION

During power system restoration, it is desirable to reconnect loads as quickly and reliably as possible. At the beginning of a restoration process, the loads that help to maintain a reasonable voltage profile in the transmission system, and help to stabilize the generating units, and the induction motors that drive the auxiliary systems of thermal power plants, are energized first. Power plants that are in operation at this stage are small generating units with black start capability.

This chapter concentrates on the initial stages of restoration where operators are often searching for the size of load, which can safely be picked-up, and the effectiveness of the generation reserve [3, 5, 82, 124]. Load pick-up in small increments prolongs the restoration duration. If an attempt be made to pick-up a larger load block than can be accommodated by the response capability of generators on line, then block of load already restored that are subject to under- frequency load shedding will be lost. If the frequency swing is severe, one or more generators may trip, precipitating another shutdown [3, 5, 82]. Hence it is desirable to determine the magnitude of load blocks, which can be restored, as a guideline for operators. An assessment of the maximum load that can be picked up safely at each time shortens the time during on-line restoration as well as during restoration planning [2].

In the past, the minimum frequency during load pick-up has been mostly determined by means of time-domain simulations using stability programs. This strategy, however, can lead to long overall simulation times, particularly in cases where a multitude of scenarios has to be studied. Hence, there is a need to find the minimum frequency by simpler rules that are not based on time-domain simulations.

A general overview of relevant publications in the area of frequency response analysis in power system restoration was given in Chapter 2. Simple guidelines for the estimation of the frequency response of prime movers during restoration are listed in [5]. They are based on look-up tables that relate frequency dips to sudden load increases and that are produced based on a number of time-domain simulations. Other methods, outlined in [45, 113], are

based on neural networks that are trained by running a large number of time-domain simulations.

An alternative to above methods is the application of the Laplace transform. All methods, based on Laplace-domain calculations, are average frequency models, i. e. oscillations between generators are filtered out and only an average system frequency is retained. This means that in case of more than one generator is in operation, the generators are lumped into one dynamic equivalent. An approach that belongs to this group of methods and that is based on strongly simplified governor and turbine models is presented in [19]. It gives a simple function for the system's frequency behavior after a load pick-up. A low-order system frequency response model and the analysis of the frequency-response behavior of steam reheat turbines in an islanded condition is described in [16].

Other similar methods that are based on dynamic equivalents, and extended application of the Laplace transform are outlined in [26]. An extended analytical analysis of frequency decay rates can be found in [18].

In the pervious works [5, 124] dynamics of loads and limitations of prime mover are not considered, thus the evaluation of frequency behavior is not complete and exact, especially for calculation of the minimum frequency point during load pick-up. Operation of under frequency load shedding relays and generators protective relays depends on the minimum frequency point. In this chapter a new method for calculation of load steps is presented which determines the maximum load pick-up within the allowable system frequency dip for each bus and each stage of load restoration. This method considers dynamics of frequency response of prime mover and load. Also a suitable form is used for behavior of frequency during load reconnection, which transforms differential equations of the system into algebraic equations to find the minimum frequency. The proposed method is suitable for on-line guiding the operator to select load steps, and/or to compute the minimal frequency for a given load step during system restoration.

To analyze the frequency behavior after load pick-up, long term dynamics simulation program, that described in chapter 3, is used.

5.2 Cold Load Pick up Modelling

Restoring customer load to service, which has been disconnected for some time, presents important challenges. The disconnected load will probably be much higher than its value at the time of interruption. The simultaneous starting of motors, compressors, etc., will cause high peak demands for power. These higher than usual load requirements are commonly referred to as cold load pickup. Cold load pickup can involve inrush currents of ten or more times the normal load current depending on the nature of the load being picked up

[12]. This will generally decay to about two times normal load current in two to four seconds and remain at a level of 150% to 200% of pre-shutdown levels for as long as 30 minutes [103]. When restoring load, sufficient time must be allowed between switching operations to permit stabilizing the generation.

Representation of reconnected loads plays significant role in safe evolution of the restoration plan, with particular reference to island frequency behavior. In fact, there is a close relationship between the duration of the outage and the power demand profile. In [40] experimental data are used to model equivalent load demands after cold load pick-up with linear (for active power) and exponential (for reactive power) fitting. Load real and reactive powers are therefore as:

$$P(t)=\begin{cases} 0 & , \quad t<t_0 \\ P_{ini}-\dfrac{P_{ini}-P_{fin}}{T_d}.(t-t_0) & , \quad t_0 \le t < t_0+T_d \\ P_{fin} & , \quad t>t_0+T_d \end{cases} \tag{5.1}$$

$$Q(t)=\begin{cases} 0 & , t<t_0 \\ Q_{ini}-(Q_{ini}-Q_{fin}).(1-e^{\frac{t-t_0}{\tau}}) & , t \ge t_0 \end{cases} \tag{5.2}$$

Where:

t_0: instant of insertion of the cold load; T_d : time interval of the real power linear decay; τ : time constant of the reactive exponential decay; P_{ini}, Q_{ini} : peak value at cold load pick-up; P_{fin}, Q_{fin} : final steady state values of the cold load. The Active power component has a decreasing linear form for T_d seconds after load pick up, where T_d is dependent of the duration of load outage.

5.3 Frequency Response of Prime Movers after Load Pick-up

System frequency can exhibit large excursions due to load pick-up. Generators usually have protective relays or other protections to trip them off line if the frequency exceeds 110 percent or drops below 95 percent [51]. While both frequency limits are important, it is the lower one that causes greater concern [51]. Frequency decline is due to inadequate system response, following loss of generation or picking up a larger load than can be handled by the generators on line. When a load is restored or a generator trips, the magnitude of the frequency excursion is determined by response reserve of the power system. This reserve largely comes from 3 sources: generation reserve of prime movers, load shedding, and demand relief. Prime movers of generating units will respond to a fall in frequency by increasing their power output, within 2 to 10 seconds interval after the

contingency. Customer loads already restored that subject to under-frequency load shedding will be lost, if the frequency swing is severe [51]. The frequency sensitivity of the system demand can provide substantial amounts of reserve immediately following a contingency due to the nature and characteristics of the load.

The minimum frequency, after load pick up, determines activation of under frequency load shedding relays and generators protective relays. Thus, it is important to correctly calculate the minimum frequency, as a dynamic constraint, during load pick up. In this section, the approach for finding minimum frequency after load reconnection is presented. Then, load step calculation algorithm is denoted.

After load pick up, power consumption increases and system frequency decreases. Swing equation for the power system, based on a uniform frequency, determines the frequency variation [49]:

$$P_{acc} = 2H_{sys}.\omega.\frac{d\omega}{dt} \tag{5.3}$$

Where:

$$P_{acc} = \sum_{i=1}^{ng} P_{g,i} - \sum_{i=1}^{nl} P_{l,i} - P_{loss} \tag{5.4}$$

$$P_{g,i} = P_{g0,i} + P_{gov,i} \tag{5.5}$$

$$P_{l,i} = \begin{cases} P_{l0,i} & , for\ i \neq j \\ P_{l0,j} + \Delta P_{l,j} & , for\ i = j \end{cases} \tag{5.6}$$

H_{sys} : Total Inertia Constant of power system; ng: number of on-line generators; nl: number of bus loads; $P_{g0,i}$: active power generation of i^{th} unit, before load pick up; $P_{gov,i}$: increment of active power generation of i^{th} unit, after load pick-up, due to its governor response; $P_{l0,i}$: load power of bus no. i, before load pick up; $\Delta P_{l,j}$: load power that is picked up at j^{th} bus as it is expressed in (5.1); P_{loss}: active power loss of electrical network.

Equation (5.3) shows system frequency response, after load pick-up. For a static load, $\Delta P_{l,j}$ is not function of time after load pick-up. However for a dynamic load, as it is stated in (5.1), it has a linear form until the final's value after load pick-up. Also $P_{l0,i}$ is a function of bus voltage and frequency during load pick-up. In order to simplify the calculation, bus voltage variations are neglected.

A quadratic form until minimum point is fitted for system frequency changes after switching a load as follows (Figure 5.1):

$$\omega - \omega_0 = a.t^2 + b.t \quad , 0 \leq t \leq t_{min} \tag{5.7}$$

Where:

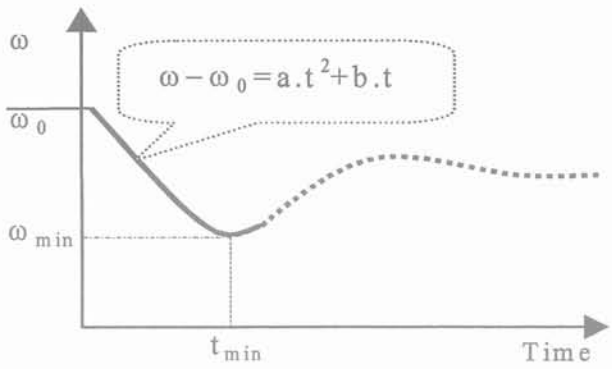

Figure 5.1: Quadratic form of frequency change

ω_0 : initial frequency of power system; ω_{min}: system minimum frequency after load pick-up; t_{min} : time to reach minimum frequency.

With this assumption, the minimum frequency point can be calculated with no need to solve the differential equations of the system, and hence speeding up the calculation increases significantly. Considering the condition at the minimum frequency point, it yields:

$$\omega(t=t_{min})=\omega_{min} \quad , \quad \left.\frac{d\omega}{dt}\right|_{t=t_{min}}=0 \tag{5.8}$$

According to (5.7) and (5.8), t_{min} and a can be derived as follows:

$$t_{\min}=\frac{2(\omega_{\min}-\omega_0)}{b} \tag{5.9}$$

$$a=-\frac{b^2}{4(\omega_{min}-\omega_0)} \tag{5.10}$$

Employing (5.7) at the initial time, initial rate of system frequency can be obtained from the following equation:

$$\left.\frac{d\omega}{dt}\right|_{t=0^+}=b \tag{5.11}$$

With substituting the above equation in (5.3) to (5.6), b is calculated as follows:

$$b=\frac{1}{2\omega_0 H_{sys}}.\left(\sum_{i=1}^{ng}P_{g0,i}-\sum_{i=1}^{nl}P_{l0,i}(\omega_0)-\Delta P_{l,j}(\omega_0)-P_{loss}(\omega_0)\right) \tag{5.12}$$

Assuming steady state ω, before load pick-up, and using (5.4), power loss at the initial time is expressed as:

$$P_{loss}(\omega_0)=\sum_{i=1}^{ng}P_{g0,i}-\sum_{i=1}^{nl}P_{l0,i}(\omega_0) \tag{5.13}$$

Replacing power loss from the above equation in (5.12), b can be derived as:

$$b=\frac{1}{2\omega_0 H_{sys}}.\left[-\Delta P_{l,j}(\omega_0)\right]=\frac{-1}{2\omega_0 H_{sys}}.P_{ini} \tag{5.14}$$

Employing (5.4) to (5.6), load pick-up value at the minimum frequency point can be expressed as:

$$\Delta P_{l,j}(\omega_{min}) = \sum_{i=1}^{ng} P_{g0,i} + \sum_{i=1}^{ng} P_{gov,i}(\omega_{min}) - \sum_{i=1}^{nl} P_{l0,i}(\omega_{min}) - P_{loss}(\omega_{min}) \quad (5.15)$$

In Section 5.4, using (5.7), P_{gov} is expressed in terms of t_{min} in the minimum frequency point as:

$$P_{gov}(t = t_{\min}) = \sum_i K_i . e^{S_i . t_{\min}} + A.t^2{}_{\min} + B.t_{\min} + C \quad (5.16)$$

If the governor reaches its rate limit, then the governor's response at a minimum point can be expressed as:

$$P_{gov}(t = t_{\min}) = \sum_i \hat{K}_i . e^{\hat{S}_i . t_{\min}} + \hat{A}.t_{\min} + \hat{B} \quad (5.17)$$

In (5.15), P_{loss} is needed at the minimum frequency (ω_{min}), but with a good approximation, it can be calculated at the initial frequency (ω_0) by (5.13), since the effect of frequency changes can be neglected in power loss of the electrical network.

Therefore, load pick-up value at the minimum frequency can be written as follows:

$$\Delta P_{l,j}(\omega_{\min}) = \sum_{i=1}^{ng} P_{gov,i} - \sum_{i=1}^{nl} P_{l0,i}(\omega_{\min}) + \sum_{i=1}^{nl} P_{l0,i}(\omega_0) \quad (5.18)$$

There are two expressions for the value of picked up load at the minimum frequency that depend on the relation between T_d and t_{min}. Employing (5.1), relation between initial load value and load value at minimum point, where t_{min} is smaller than T_d, can be expressed as follows:

$$P_{ini} = \Delta P_{l,j}(\omega_0) = \frac{k_p}{k_p + (1 - k_p).t_{\min}/T_d} . \Delta P_{l,j}(\omega_{\min}) \quad : \quad if \ t_{\min} \le T_d \quad (5.19)$$

Or:

$$\Delta P_{l,j}(\omega_{\min}) = (k_p + (1 - k_p).t_{\min}/T_d).P_{fin} \quad (5.20)$$

Where k_p is the ratio of initial to final active power of load at j^{th} bus after load pick-up.

In the proposed method for frequency response calculation, as shown in Figure 5.2, where t_{min} is greater than T_d, we use a linear relationship between initial power value and final power value in place of original relationship, such that energy consumption until the minimum frequency point have the same value for the two forms. Thus:

$$\hat{P}_{ini} = \hat{k}_p . \Delta P_{l,j}(\omega_{\min}) \quad : \quad if \ t_{\min} > T_d \quad (5.21)$$

$$\Delta P_{l,j}(\omega_{\min}) = P_{fin} \quad (5.22)$$

$$b = -\hat{k}_p . \Delta P_{l,j}(\omega_{\min}) / (2\omega_0 H_{sys}) \quad (5.23)$$

Where:

$$\hat{k}_p = 1 + (k_p - 1).T_d / \hat{t}_{\min} \quad (5.24)$$

We apply this modification in order to consider active power variations of load before the minimum frequency point.

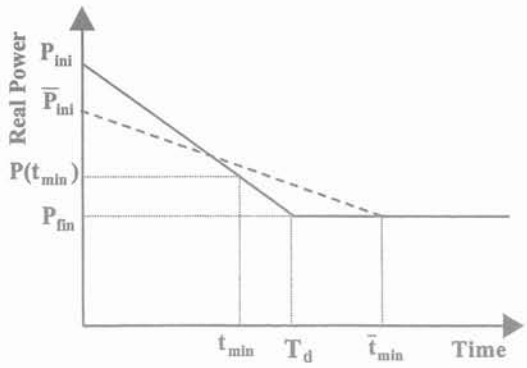

Figure 5.2: Real power changes after load pick-up

There are two problems during load pick-up: (a) calculation of maximum load pick-up for a given frequency decline, (b) computing the minimum frequency for picking up an estimated low voltage AC network load. The proposed algorithms for the calculation of load step size and minimum frequency are presented in Section 5.5.

The initial guess value of load step for a given frequency decline is selected equal to steady state value as follows:

$$P_{fin}^{(0)} = P_{ini}^{(0)} / k_p = -(\omega_{min} - \omega_0).(\sum_{i=1}^{ng} 1/R_i) \tag{5.25}$$

Where R_i is permanent droop coefficient of i^{th} unit.

Similarly, the initial guess value of minimum frequency for an estimated load step, is computed as follows:

$$\omega_{\min}^{(0)} = \omega_0 - P_{fin} \Big/ \sum_{i=1}^{ng} 1/R_i \tag{5.26}$$

5.4 Governor Response after Load Pick-up

The frequency behavior of an islanded system, such as the one shown in Figure 5.3, is controlled by the governors [120]. In case of a load pick-up they detect the decline of frequency and as a consequence, increase the gate or valve position in order to bring up the mechanical output power of the turbine, until a new equilibrium point with an acceptable system frequency.

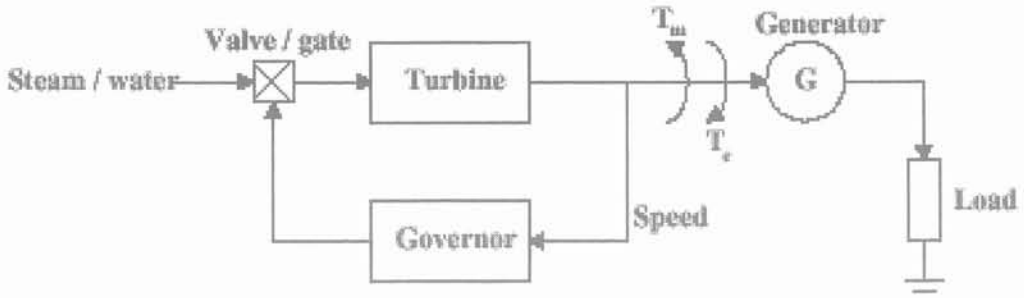

Figure 5.3:Generator supplying isolated load

The initially available prime movers during power system restoration consist of:

- Black-start Combustion Turbines (CT)
- Low-head short-conduit Hydro Electric (HE)
- Gas or oil-fired drum-type boiler-turbine Steam Electric (SE)

The subsequently available prime movers consist of large CTs, high-head long-conduit HEs, and combined cycle units. The finally available prime movers consist of large drum-type coal-fired SEs, super-critical once-through units and nuclear plants.

For load step calculation, a general turbine and governor system model as shown in Figure 5.4, is used [120]. The model includes governor and turbine dynamics and a gate rate limit.

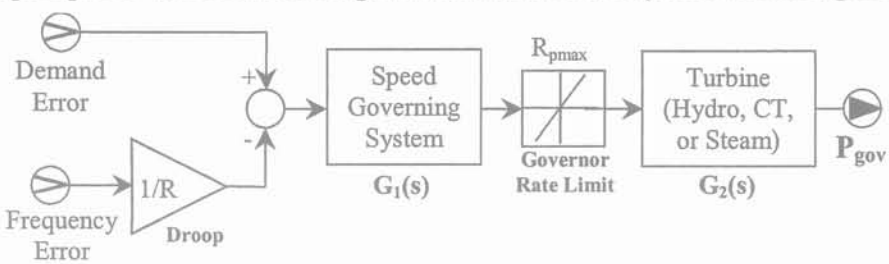

Figure 5.4: Governor and turbine model for load Step calculation

In the following sections, the calculation of a governor's response of the initially available prime movers are presented, where the frequency error has been expressed in (5.7).

5.4.1 Combustion Turbine Units

The transfer functions for a typical back-start CT are as follows [5]:

$$G_1(s) = 1/(1 + s.T_G) \quad ; \quad G_2(s) = 1/(1 + s.T_T) \tag{5.27}$$

Where:

R: governor's speed regulation ; R_{pmax}: governor's rate limit ; T_G: governor time constant; T_T: turbine time constant ; H: Inertia constant;

Using the block diagram of Figure 5.4 and (5.27), the differential equation of governor system for Combustion turbine units can be found in the following form:

$$P_{gov} + T'.\frac{dP_{gov}}{dt} + T''.\frac{d^2P_{gov}}{dt^2} = K(\omega - \omega_0) = K(a.t^2 + b.t) \tag{5.28}$$

Where:

$$T' = T_T + T_G \quad , \quad T'' = T_T.T_G \quad , \quad K = -\frac{1}{R} \tag{5.29}$$

Employing (5.28), governor's response at the minimum frequency point is derived as:

$$P_{gov}(t = t_{min}) = K_1.e^{S_1.t_{min}} + K_2.e^{S_2.t_{min}} + A.t^2{}_{min} + B.t_{min} + C \tag{5.30}$$

Where:

$$A = K.a \ , \ B = K.b - 2K.a.T_1 \ , \ C = -K.T_1.b + 2K.a.T_1^2 - 2K.a.T_2 \tag{5.31}$$

$$\begin{bmatrix} K_1 \\ K_2 \end{bmatrix} = \begin{bmatrix} 1 & 1 \\ S_1 & S_2 \end{bmatrix}^{-1} . \begin{bmatrix} -C \\ -B \end{bmatrix} \tag{5.32}$$

S_1 and S_2 are roots of the following equation:

$$1 + T'.S + T''.S^2 = 0 \tag{5.33}$$

5.4.2 Steam Electric Units

The transfer function for a typical tandem compound, single reheat SE unit are as follow [5]:

$$G_1(s) = 1/(1 + s.T_G); \ G_2(s) = (1 + s.F_{hp}.T_{rh})/((1 + s.T_{ch}).(1 + s.T_{rh})) \tag{5.34}$$

Where:

T_G: governor time constant ; T_{ch}: crossover (IP-LP) time constant ; T_{rh}: reheater time constant; F_{hp}: HP turbine power fraction; H: Inertia constant; R_{pmax}: governor's rate limit; R: governor's speed regulation;

Using the block diagram of Figure 5.4 and (5.34), the differential equation of the governor system for Steam Electric units can be expressed as follows:

$$P_{gov} + T'.\frac{dP_{gov}}{dt} + T''.\frac{d^2P_{gov}}{dt^2} + T'''.\frac{d^3P_{gov}}{dt^3} = K(\omega - \omega_0 + F_{hp}.T_{rh}.\frac{d(\omega - \omega_0)}{dt}) = a_1.t^2 + \ b_1.t + c_1 \tag{5.35}$$

Where:

$$T' = T_G + T_{ch} + T_{rh} \quad , \quad T'' = T_{ch}.T_{rh} + T_G.(T_{ch} + T_{rh}) \ , T''' = T_{ch}.T_{rh}.T_G, \quad K = -\frac{1}{R} \tag{5.36}$$

$$a_1 = K.a \ , \ b_1 = K.(b + 2a.F_{hp}.T_{rh}) \quad , \quad c_1 = K.(b.F_{hp}.T_{rh}) \tag{5.37}$$

Employing (5.35), governor's response at the minimum frequency point can be derived as:

$$P_{gov}(t = t_{min}) = K_1.e^{S_1.t_{min}} + K_2.e^{S_2.t_{min}} + K_3.e^{S_3.t_{min}} + A.t^2{}_{min} + B.t_{min} + C \tag{5.38}$$

Where:

$$A = a_1 \ , \ B = b_1 - 2a_1.T_1 \ , \ C = c_1 - T_1.b_1 + 2a_1.T_1^2 - 2a_1.T_2 \tag{5.39}$$

$$\begin{bmatrix} K_1 \\ K_2 \\ K_3 \end{bmatrix} = \begin{bmatrix} 1 & 1 & 1 \\ S_1 & S_2 & S_3 \\ S_1^2 & S_2^2 & S_3^2 \end{bmatrix}^{-1} . \begin{bmatrix} -C \\ -B \\ -2A \end{bmatrix} \tag{5.40}$$

S_1, S_2, and S_3 are roots of the following equation:

$$1 + T'.S + T''.S^2 + T'''.S^3 = 0 \tag{5.41}$$

5.4.3 Hydro Electric Units

The transfer functions for a typical run-of-the-river Kaplan turbine are as follows [5]:

$$G_1(s)=1/(1+s.T_G)\ ;\ G_2(s)=(1+s.T_r).(1-s.T_w)/((1+s.T_r.(R_t/R)).(1+0.5T_w.s)) \quad (5.42)$$

Where:

T_G: governor time constant; T_r: dashpot time constant; T_w: water starting time penstock; R_t: transient speed droop coefficient; R: permanent speed droop coefficient; H: Inertia constant; R_{pmax}: governor's rate limit;

Using the block diagram of Figure 5.4 and (5.42), the differential equation of governor system for Hydro Electric units can be derived as follows:

$$P_{gov}+T'.\frac{dP_{gov}}{dt}+T''.\frac{d^2P_{gov}}{dt^2}+T'''.\frac{d^3P_{gov}}{dt^3}=K(\omega-\omega_0+(T_r-T_w).\frac{d(\omega-\omega_0)}{dt}-(T_r.T_w).\frac{d^2(\omega-\omega_0)}{dt^2})$$
$$=a_1.t^2+\ b_1.t+c_1+d_1.\delta(t) \quad (5.43)$$

Where:

$$T'=T_G+(R_t/R).T_r+0.5T_w\ ,\quad T''=T_G.T_r.R_t/R+0.5T_w.(T_G+(R_t/R).T_r),$$

$$T'''=0.5T_w.T_G.T_r.(R_t/R),\quad K=-\frac{1}{R} \quad (5.44)$$

$$a_1=K.a\ ,\ b_1=K.(b+2a.(T_r-T_w))\ ,\ c_1=K.(-2a.T_r.T_w+b.(T_r-T_w))\ ,\ d_1=-K.b.T_r.T_w \quad (5.45)$$

Employing (5.43), governor's response at the minimum frequency point can be expressed as:

$$P_{gov}(t=t_{min})=K_1.e^{S_1.t_{min}}+K_2.e^{S_2.t_{min}}+K_3.e^{S_3.t_{min}}+A.t^2{}_{min}+B.t_{min}+C \quad (5.46)$$

Where:

$$A=a_1\ ,\ B=b_1-2a_1.T_1\ ,\ C=c_1-T_1.b_1+2a_1.T_1^2-2a_1.T_2 \quad (5.47)$$

$$\begin{bmatrix}K_1\\K_2\\K_3\end{bmatrix}=\begin{bmatrix}1&1&1\\S_1&S_2&S_3\\S_1^2&S_2^2&S_3^2\end{bmatrix}^{-1}.\begin{bmatrix}-C\\-B\\-2A+(d_1/T_3)\end{bmatrix} \quad (5.48)$$

S_1, S_2, and S_3 are roots of the following equation:

$$1+T'.S+T''.S^2+T'''.S^3=0 \quad (5.49)$$

If the governor reaches its rate limits, then its response at the minimum frequency point can be written as:

$$P_{gov}(t=t_{\min})=\sum_i \hat{K}_i.e^{\hat{S}_i.t_{\min}}+\hat{A}.t_{\min}+\hat{B} \quad (5.50)$$

Where the parameter values are determined with a similar method.

5.5 PROPOSED ALGORITHMS FOR CALCULATION OF FREQUENCY RESPONSE

There are two problems during load pick-up: (a) calculation of maximum load pick-up for a given frequency decline, (b) computing the minimum frequency for picking up an estimated low voltage AC network load. In the following sections the proposed algorithms for load step size and minimum frequency calculation are presented.

5.5.1 LOAD STEP CALCULATION

An iterative algorithm is used for finding load step size for a given frequency decline. Figure 5.5 shows flow chart of the proposed algorithm. The solution steps for the algorithm are listed below:

1) Get load flow data before load pick-up and load parameter (k_p and T_d). Get initial frequency (ω_0) and acceptable minimum frequency (ω_{min})

2) Initialize P_{ini} using (5.25) and set N=0

3) Compute sum of load powers ($\sum_{i=1}^{nl} P_{l0,i}$) at the initial frequency and the minimum frequency

4) Compute $\Delta P_{l,j}(\omega_{\min})$ at N^{th} step using (5.18)

5) Calculate b and a at N^{th} step using (5.14) and (5.10), respectively

6) Compute t_{min} at N^{th} step using (5.9)

7) Calculate governor's response at the minimum frequency point for all connected unit using (5.30), (5.38), and (5.46) for CT, HE, and SE unit, respectively

8) Compute governor's rate for all connected units. If the governor's rate has reached the rate limit, then calculate governor's response for the rate limit state

9) If t_{min} is smaller than T_d ,then compute the new P_{ini} using (5.19); else compute the new P_{ini} using (5.21)

10) If the algorithm is converged then print load step size , else N=N+1 and go to step 4

11) Stop

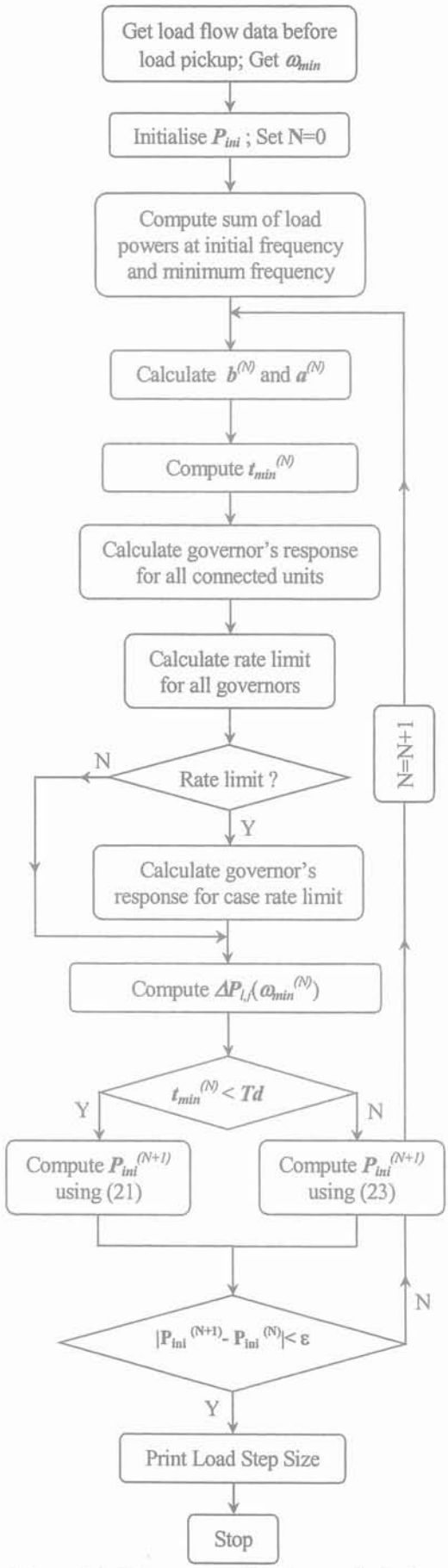

Figure 5.5: Flow chart of load step calculation

5.5.2 Minimum Frequency Calculation

A similar iterative algorithm is used for calculating the minimum frequency for a given load step. The solution steps for the algorithm are listed below:

1) Get load flow data before load pick-up and load parameter (k_p and T_d) and load step size

2) Initialize ω_{min} using (5.26) and set N=0

3) Compute sum of load powers ($\sum_{i=1}^{nl} P_{l0,i}$) at the initial frequency; Calculate b using (5.14)

4) Compute sum of load powers ($\sum_{i=1}^{nl} P_{l0,i}$) at the minimum frequency

5) Calculate t_{min} and a at N^{th} step using (5.9) and (5.10), respectively

6) Compute governor's rate for all connected units

7) If governor's rate has reached its rate limit , then set governor's rate to rate limit state

8) If t_{min} is smaller than T_d ,then compute $\Delta P_{l,j}(\omega_{\min})$ and b using (5.20) and (5.14), respectively; else compute them using (5.22) and (5.23), respectively

9) Calculate new t_{min} using the following Equation:

$$t_{\min}^{(new)} = \frac{\Delta P_{l,j}(\omega_{\min}) - \sum_{k=1}^{ng1} C_k - \sum_{k=1}^{ng1}\sum_{i} K_i.e^{S_i.t_{\min}^{(old)}} - \sum_{k=1}^{ng2} \hat{A}_k - \sum_{k=1}^{ng2}\sum_{i} \hat{K}_i.e^{\hat{S}_i.t_{\min}^{(old)}}}{(\sum_{k=1}^{ng1} A_k).t_{\min}^{(old)} + (\sum_{k=1}^{ng1} B_k) + (\sum_{k=1}^{ng2} \hat{A}_k)} \quad (5.51)$$

Where: ng1 is the number of units that governor's rate have not reached their rate limits; ng2 is the number of units which governor's rate reached their rate limits. This equation is derived by employing (5.16), (5.17), and (5.18). Then compute new ω_{min} using the following Equation:

$$\omega_{min}^{(new)} = \omega_0 + 0.5b.t_{min}^{(new)} \quad (5.52)$$

This equation is derived by employing (5.9)

10) If the algorithm is converged then print minimum frequency value, else N=N+1 and go to step 4

11) Stop

Figure 5.6 shows flow chart of the proposed algorithm.

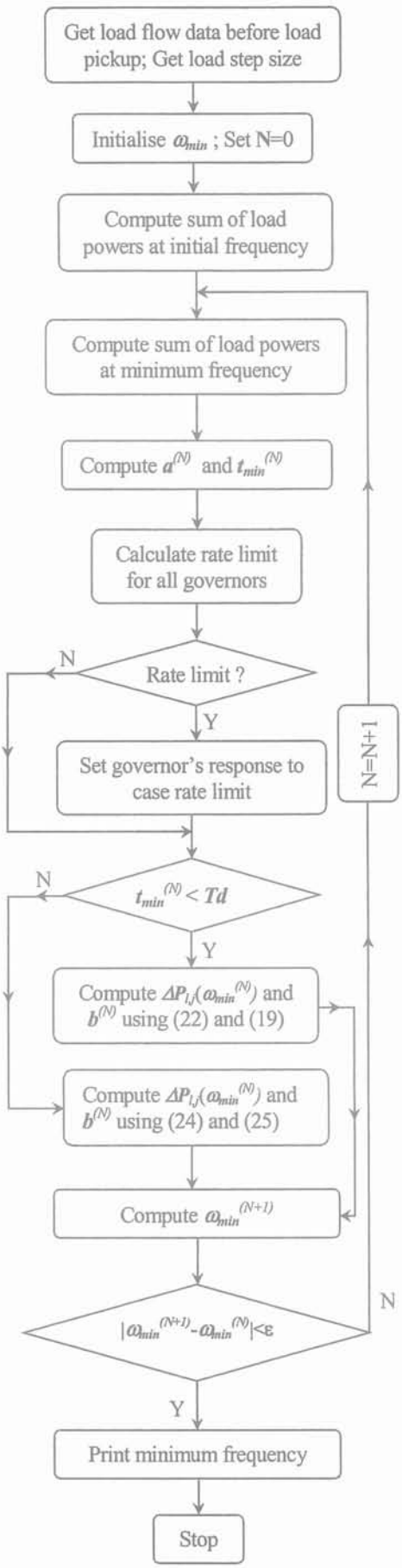

Figure 5.6: Flow chart of minimum frequency calculation

5.6 SIMULATION RESULTS AND DISCUSSION

5.6.1 CASE 1

In this section, the new method is employed for the calculation of load step and minimum frequency for each initially available prime movers, i.e. CT, HE, and SE. The results are compared with the results of simulation program that described in chapter 3.

5.6.1.1 Minimum frequency calculation

I. CT Unit

The proposed method is used to calculate the minimum frequency after picking-up a load connected to the CT unit. Unit data is listed in Table 5.1 .

Table 5.1:Governor data for the CT Unit

T_t (Sec.)	T_G (Sec.)	R (p.u.)	H (Sec.)	R_{pmax} (p.u./Sec.)	D (p.u.)
0.5	0.15	0.05	5	0.15	0.75

A. Static load

Result of Minimum frequency calculation for static load pick-up is listed in Table 5.2, where governor's rate limit is equal to 0.2 p.u./sec, and $\Delta\omega_{min}$ is calculated as follow:

$$\Delta\omega_{\min} = \omega_{\min} - \omega_0 \tag{5.53}$$

The Number of iterations for finding the minimum frequency where using the proposed method is 5.

The Error (%) in the table is calculated as follow:

$$Error\,(\%) = \frac{\Delta\omega^{*}_{\min} - \Delta\omega^{**}_{\min}}{\Delta\omega^{**}_{\min}} \times 100 \tag{5.54}$$

Where $\Delta\omega_{min}{}^{*}$ and $\Delta\omega_{min}{}^{**}$ are frequency dip that have been calculated by the proposed method and the simulation, respectively.

Figure 5.7 illustrates comparison of the frequency deviation after load pick-up between the quadratic form and the simulation, which shows good agreement between them.

Table 5.2: Minimum frequency Calculation for Static Load (CT unit)

	Load step (p.u.)	$\Delta\omega_{min}$ (p.u.)	t_{min}(sec)	Error %
Calculation	0.22	-0.02008	1.53379	0.25
Simulation	0.22	-0.02013	1.54260	

Figure 5.8 shows frequency deviation without and with governor's rate limit, respectively. Figure 5.9 shows calculated minimum frequency for various values of load step size, without and with governor's rate limit.

B. Dynamic load

Result of Minimum frequency Calculation for dynamic load pick-up is listed in Table 5.3 where governor's rate limit is equal to 0.2 p.u./sec, k_p=2, and T_d=1.2 Sec. The number of iterations necessary for finding the minimum frequency where using the proposed method is 6. Figure 5.10 to Figure 5.12 illustrate the calculated minimum frequency for various values of T_d and k_p.

Table 5.3: Results of minimum frequency Calculation for Dynamic Load (CT unit)

	$\Delta\omega_{min}$ (p.u.)	Load step (p.u.)	t_{min}(sec)	Error %
Calculation	-0.01950	0.15	1.17035	0.93
Simulation	-0.01933	0.15	1.18130	

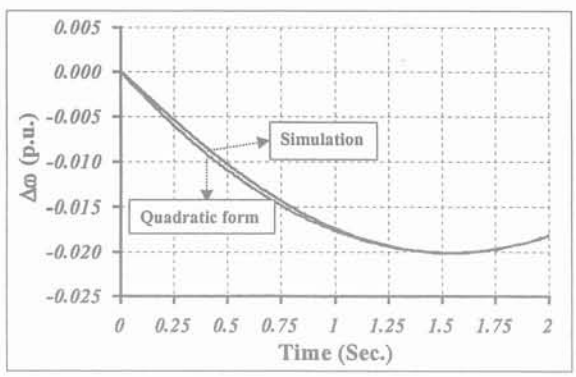

Figure 5.7: Comparison of frequency deviation after load pick-up between quadratic form and the simulation

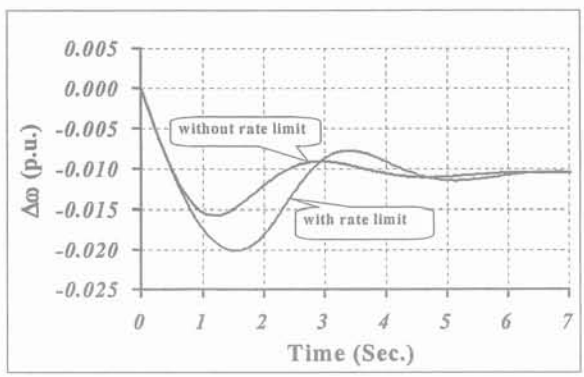

Figure 5.8: Frequency deviation after static load pick-up: without and with rate limit=0.2 p.u./sec

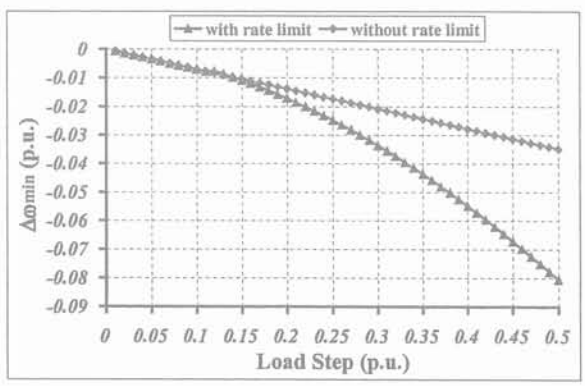

Figure 5.9: Calculated minimum frequency vs. static load step size: without and with rate limit=0.2 p.u./sec

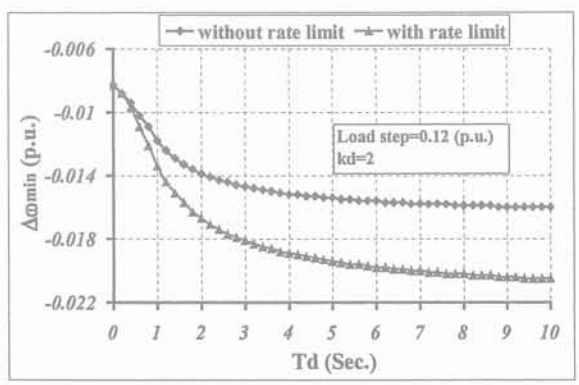

Figure 5.10: Calculated minimum frequency vs. Td: without and with rate limit=0.2 p.u./sec

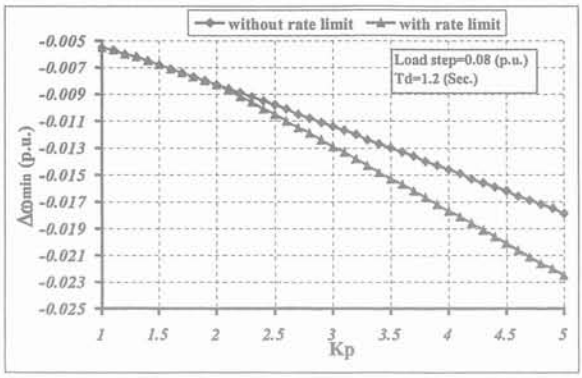

Figure 5.11: Calculated minimum frequency vs. K_p : without and with rate limit

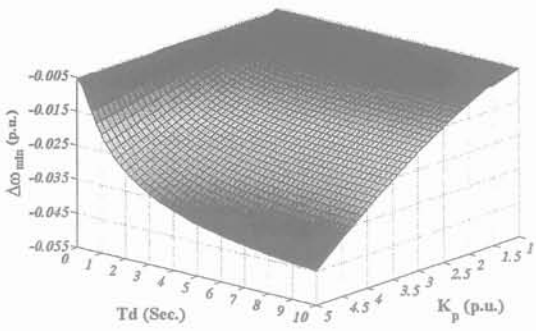

Figure 5.12: Calculated minimum frequency vs. Td and K_p (for load step =0.08 p.u. and rate limit=0.2 p.u./sec)

II. Hydro Unit

The proposed method is used to calculate the minimum frequency after picking-up a load connected to the Hydro unit. Unit data is listed in Table 5.4.

Table 5.4:Governor data for the hydro unit

T_r (Sec.)	T_w (Sec.)	T_G (Sec.)	R_t (p.u.)	R (p.u.)	H (Sec.)	R_{pmax} (p.u./Sec.)	D (p.u.)
5.0	7.0	0.2	0.38	0.05	6	0.01	1.0

A. Static load

Result of Minimum frequency calculation for static load pick-up is listed in Table 5.5 where the governor's rate limit is equal to 0.01 p.u./sec. The number of iterations necessary for finding the minimum frequency where using the proposed method is 6. Figure 5.13 shows frequency deviation without and with governor's rate limit, respectively. Figure 5.14 shows calculated minimum frequency vs. static load step size for various values of governor's rate limit.

Table 5.5: Results of minimum frequency calculation for static load (HE unit)

	Load step (p.u.)	$\Delta\omega_{min}$ (p.u.)	t_{min}(sec)	Error %
Calculation	0.07	-0.02006	6.55986	2.8
Simulation	0.07	-0.02065	6.54656	

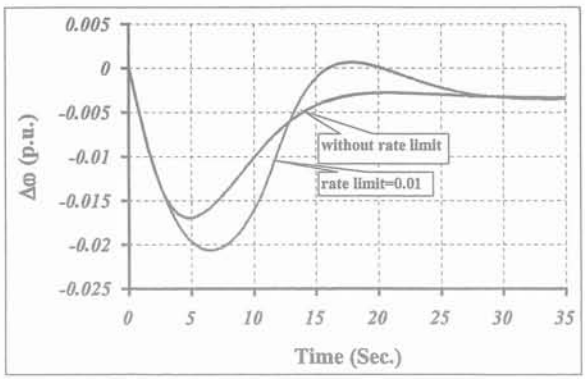

Figure 5.13: Frequency deviation after static load pick-up: without and with rate limit=0.01

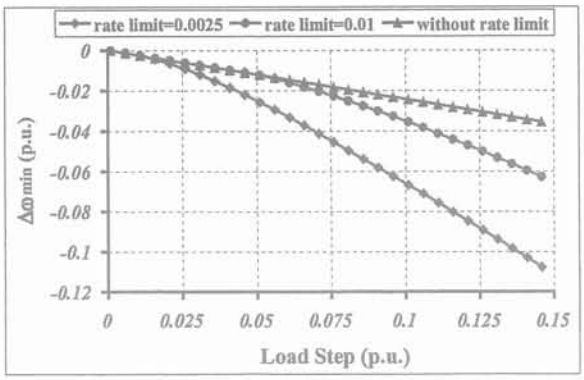

Figure 5.14: Calculated minimum frequency vs. static load step size for various values of rate limit

B. Dynamic load

Result of minimum frequency calculation for dynamic load pick-up is listed in Table 5.6, where governor's rate limit is equal to 0.01 p.u./sec, k_p=2, and T_d=3.5 (sec). The number of iterations for finding the minimum frequency where using the proposed method is 6. Figures 5.15 to 5.17 show calculated minimum frequency for various values of T_d and k_p.

Table 5.6: Results of minimum frequency Calculation for Dynamic Load (HE unit)

	$\Delta\omega_{min}$ (p.u.)	Load step (p.u.)	t_{min}(sec)	Error %
Calculation	-0.02068	0.05	4.73409	0.23
Simulation	-0.02073	0.05	4.74819	

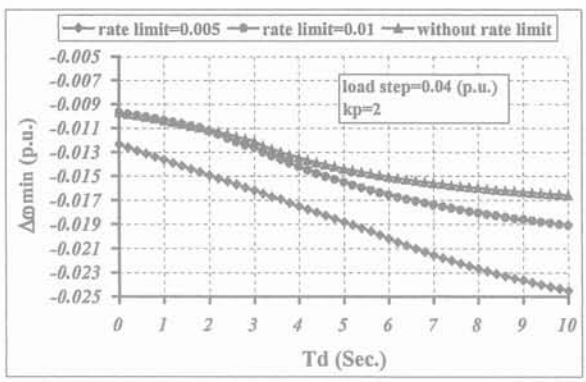

Figure 5.15: Calculated minimum frequency vs. Td for various values of rate limit

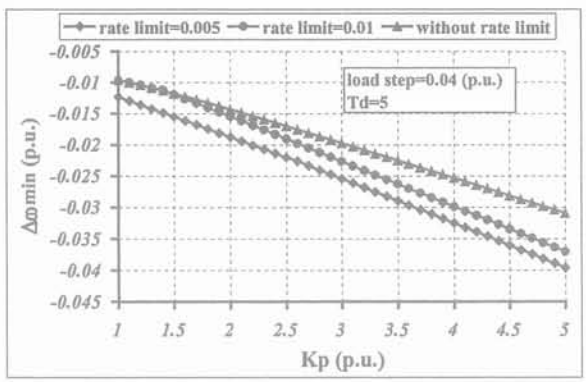

Figure 5.16: Calculated minimum frequency vs. K_p for various values of rate limit

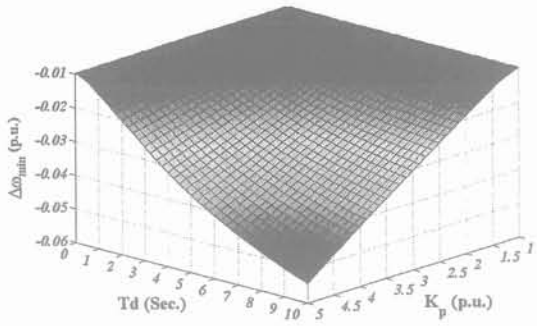

Figure 5.17: Calculated minimum frequency vs. Td and K_p (for load step=0.04 p.u. and rate limit=0.01)

III.SE Unit

The proposed method is used to calculate minimum frequency after picking-up a load connected to the SE unit. Its data is listed in Table 5.7.

Table 5.7:Governor data for the SE Unit

T_{ch} (Sec.)	T_{rh} (Sec.)	T_G (Sec.)	F_{hp} (p.u.)	R (p.u.)	H (Sec.)	R_{pmax} (p.u./Sec.)	D (p.u.)
0.3	7.0	0.2	0.3	0.05	5.0	1.0	1.0

A. Static load

Result of Minimum frequency calculation for static load pick-up is listed in Table 5.8 where the governor's rate limit is equal to 0.15 p.u/sec. The number of iterations necessary for finding the minimum frequency where using the proposed method is 6. Figure 5.18 shows frequency deviation without and with governor's rate limit, respectively. Figure 5.19 shows calculated minimum vs. static load step size for various values of governor's rate limit.

Table 5.8: Results of minimum frequency Calculation for Static Load (SE unit)

	$\Delta\omega_{min}$ (p.u.)	Load step (p.u.)	t_{min}(sec)	Error %
Calculation	-0.020527	0.15	2.51804	3
Simulation	-0.021161	0.15	2.49147	

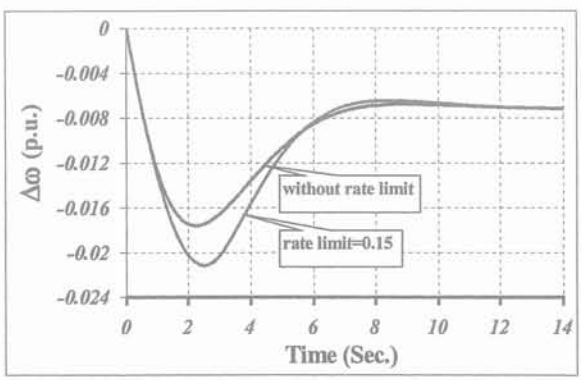

Figure 5.18: Frequency deviation after static load pick-up: without and with rate limit=0.15 p.u./sec

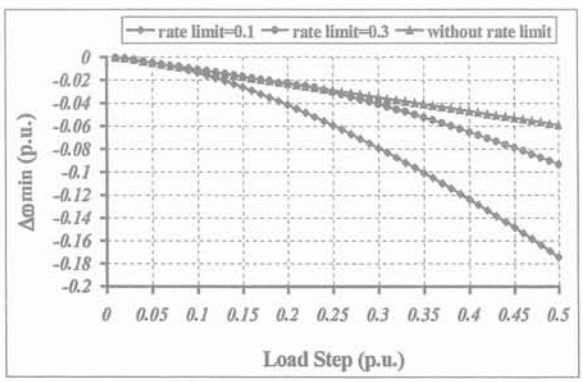

Figure 5.19: Calculated minimum frequency vs. static load step size for various values of rate limit

B. Dynamic load

Result of Minimum frequency Calculation for dynamic load pick-up is shown in Table 5.9 where governor's rate limit equal to 0.15 p.u./sec, k_p=2, and T_d=2 Sec. The number of iterations necessary for finding the minimum frequency where using the proposed method is 5. Calculated minimum frequency vs. Td and Kp are demonstrated in Figure 5.20 and Figure 5.21, respectively, for various values of rate limit. Figure 5.22 illustrates calculated minimum frequency for various values of T_d and k_p. Figure 5.23 shows calculated minimum frequency for various values of load step size and governor's rate limit.

Table 5.9: Results of minimum frequency Calculation for Dynamic Load (SE unit)

	$\Delta\omega_{min}$ (p.u.)	Load step (p.u.)	t_{min}(sec)	Error %
Calculation	-0.033945	0.15	2.29696	1.63
Simulation	-0.033400	0.15	2.29696	

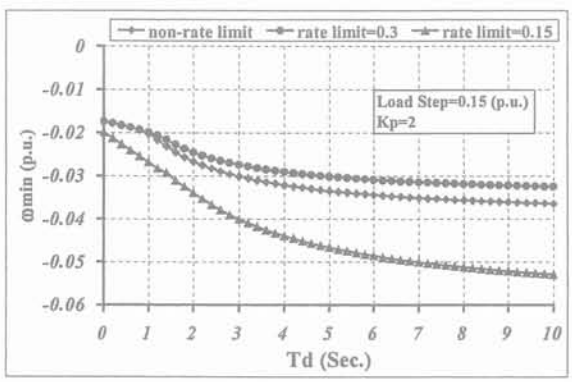

Figure 5.20: Calculated minimum frequency vs. Td for various values of rate limit

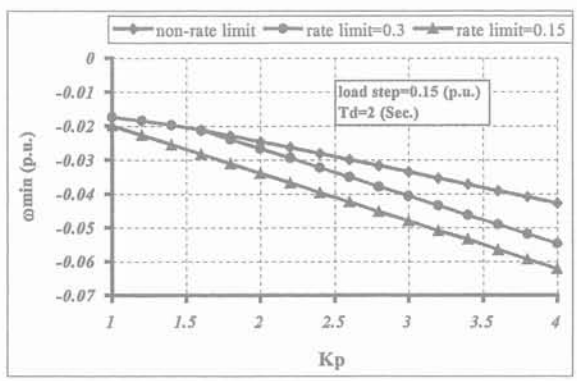

Figure 5.21: Calculated minimum frequency vs. K_p for various values of rate limit

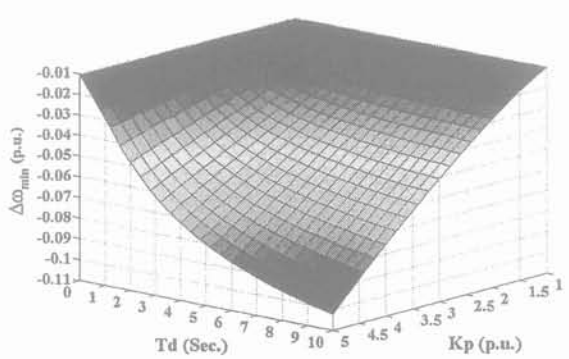

Figure 5.22: Calculated minimum frequency vs. Td and K_p (for load step =0.1 p.u. and rate limit=0.15 p.u./sec)

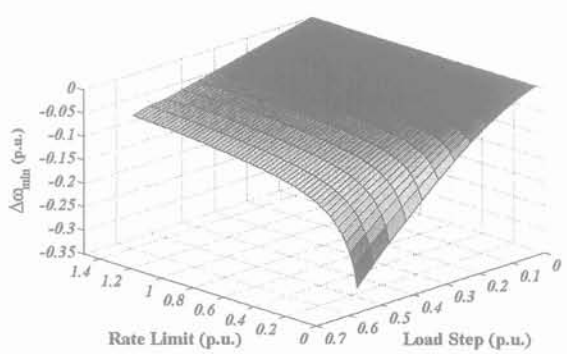

Figure 5.23: Calculated minimum frequency vs. Load step size and rate limit (for Td=2 (Sec.) and K_p=2)

5.6.1.2 Load step calculation

I. CT Unit

The proposed method is used to calculate load step size after picking-up a load connected to the CT unit.

A. Static load

Result of static load step calculation is listed in Table 5.10 where the governor's rate limit is equal to 0.2 p.u./sec. The number of iterations necessary for finding the load step size where using the proposed method is 6.

Figure 5.24 shows load step size vs. minimum frequency for various values of governor's rate limit.

Table 5.10: Results of static load step calculation (CT unit)

	$\Delta\omega_{min}$ (p.u.)	Load step (p.u.)	t_{min} (Sec.)	Error %
Calculation	-0.0200	0.2202	1.5266	0.8
Simulation	-0.0202	0.2202	1.5424	

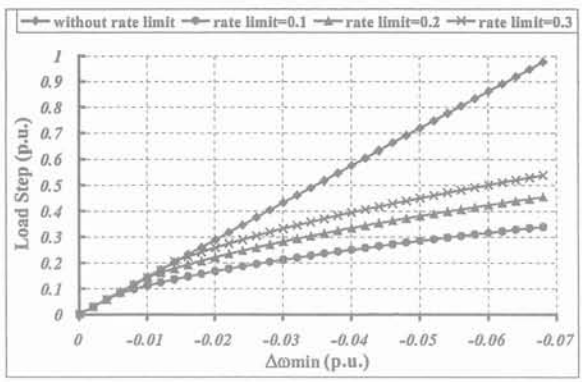

Figure 5.24: Calculated load step size vs. minimum frequency for various values of rate limit

B. Dynamic load

Result of dynamic load step calculation for dynamic load pick-up is mentioned in Table 5.11 where governor's rate limit is equal to 0.2 p.u./sec, k_p=2, and T_d=1.2 (sec). The number of iterations for finding the load step size where using the proposed method is 6. Figure 5.25 illustrates calculated load step size vs. Td for various values of rate limit. Figure 5.26 shows calculated load step size vs. K_p for various values of rate limit.

Table 5.11: Result of dynamic load step calculation (CT unit)

	$\Delta\omega_{min}$ (p.u.)	Load step (p.u.)	t_{min}(sec)	Error %
Calculation	-0.0200	0.1507	1.16767	2.8
Simulation	-0.0194	0.1507	1.1692	

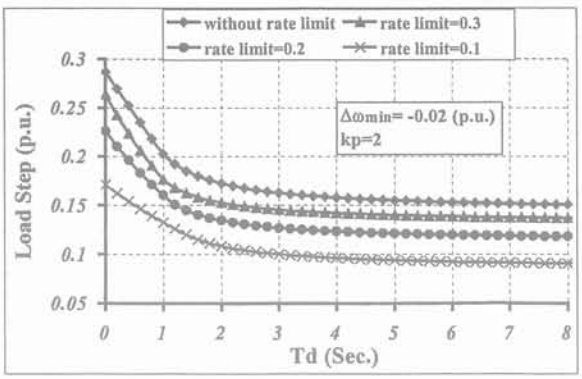

Figure 5.25: Calculated load step size vs. Td for various values of rate limit

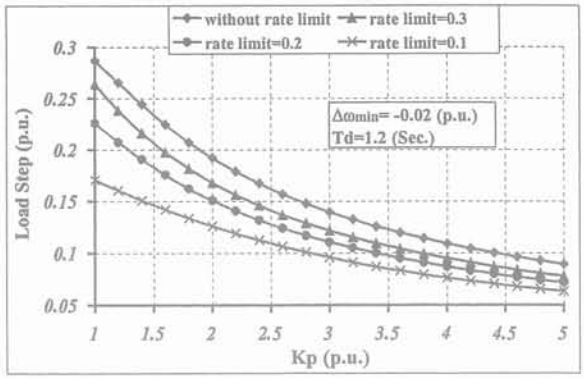

Figure 5.26: Calculated load step size vs. K_p for various values of rate limit

II. Hydro Unit

The proposed method is used to calculate load step size after picking-up a load connected to the hydro unit.

A. Static load

Result of Static Load Step Calculation is listed in Table 5.12 where governor's rate limit is equal to 0.01 p.u./sec. The number of iterations necessary for finding the load step size where using the proposed method is 6.

Figure 5.27 shows load step size vs. the minimum frequency for various values of governor's rate limit.

Table 5.12: Results of Static Load Step Calculation (HE unit)

	$\Delta\omega_{min}$ (p.u.)	Load step (p.u.)	t_{min}(sec)	Error %
Calculation	-0.02000	0.06970	6.54064	2.6
Simulation	-0.02052	0.06970	6.57747	

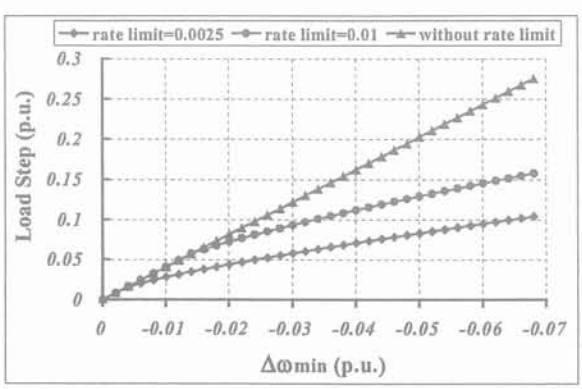

Figure 5.27: Calculated load step size vs. the minimum frequency for various values of rate limit

B. Dynamic load

Result of dynamic load step calculation for dynamic load pick-up is listed in Table 5.13 where governor's rate limit equal to 0.01 p.u./sec, k_p=2, and T_d=3.5 (Sec.). The number of iterations necessary for finding the load step size where using the proposed method is 6. Figure 5.28 and Figure 5.29 shows calculated load step size vs. Td for various values of K_p and governor's rate limit, respectively. Figure 5.30 and Figure 5.31show calculated load step size vs. k_p for various values of Td and governor's rate limit, respectively.

Table 5.13: Results of dynamic Load Step Calculation (HE unit)

	$\Delta\omega_{min}$ (p.u.)	Load step (p.u.)	t_{min}(sec)	Error %
Calculation	-0.02000	0.05397	4.93462	0.88
Simulation	-0.01982	0.05397	4.93739	

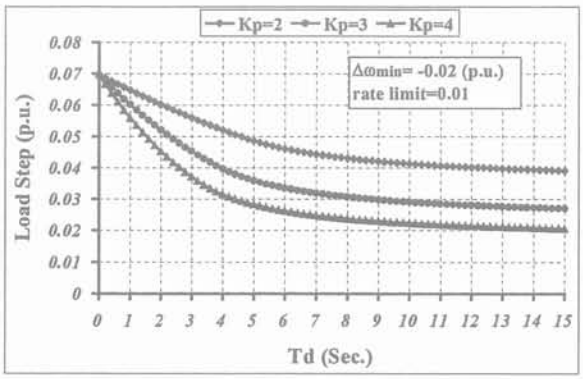

Figure 5.28: Calculated load step size vs. Td for various values of K_p

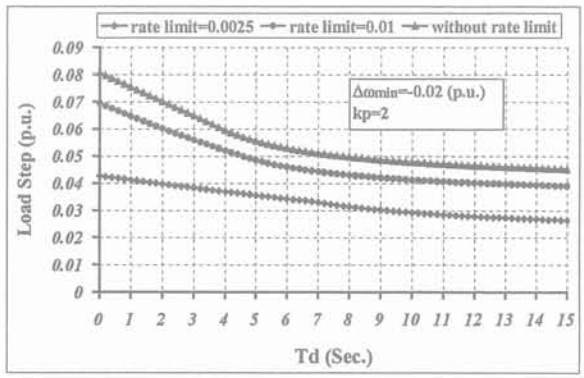

Figure 5.29: Calculated load step size vs. Td for various values of rate limit

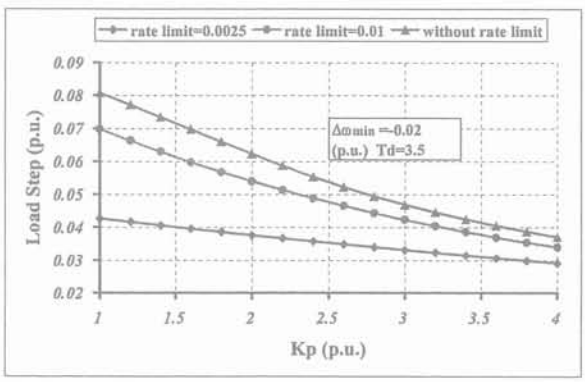

Figure 5.30: Calculated load step size vs. K_p for various values of rate limit

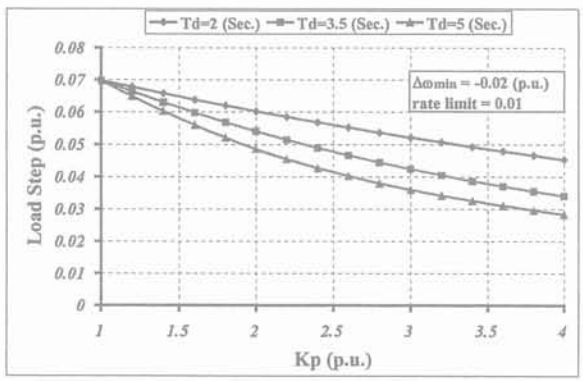

Figure 5.31: Calculated load step size vs. K_p for various values of Td

III. SE Unit

The proposed method is used to calculate load step size after picking-up a load connected to the SE unit.

A. Static load

Result of static load step calculation is listed in Table 5.14 where governor's rate limit is equal to 0.15 p.u./sec. The number of iterations necessary for finding the load step size where using the proposed method is 6.

Figure 5.32 shows load step size vs. the minimum frequency for various values of governor's rate limit.

Table 5.14: Results of Static Load Step Calculation (SE unit)

	$\Delta\omega_{min}$ (p.u.)	Load step (p.u.)	t_{min}(sec)	Error %
Calculation	-0.02000	0.14822	2.51456	3.9
Simulation	-0.02078	0.14822	2.49558	

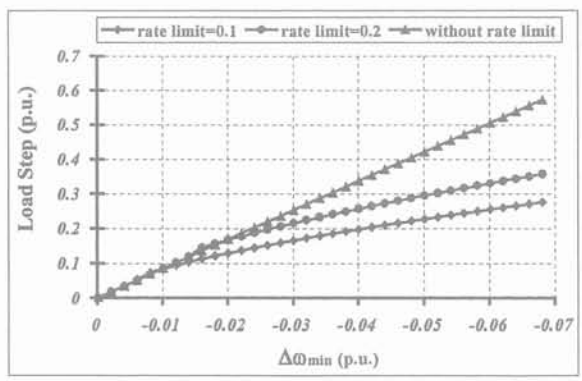

Figure 5.32: Calculated load step size vs. the minimum frequency for various values of rate limit

B. Dynamic load

Result of dynamic load step calculation for dynamic load pick-up is listed in Table 5.15 where governor's rate limit is equal to 0.15 p.u./sec, k_p=2, and T_d=2 (sec). The number of iterations necessary for finding the load step size where using the proposed method is 5. Figure 5.33 shows calculated load step size vs. T_d for various values of governor's rate limit. Figure 5.34 shows calculated load step size vs. k_p for various values of governor's rate limit.

Table 5.15: Results of Static Load Step Calculation (SE unit)

	$\Delta\omega_{min}$ (p.u.)	Load step (p.u.)	t_{min}(sec)	Error %
Calculation	-0.02000	0.10027	1.87459	0.48
Simulation	-0.01990	0.10027	1.85074	

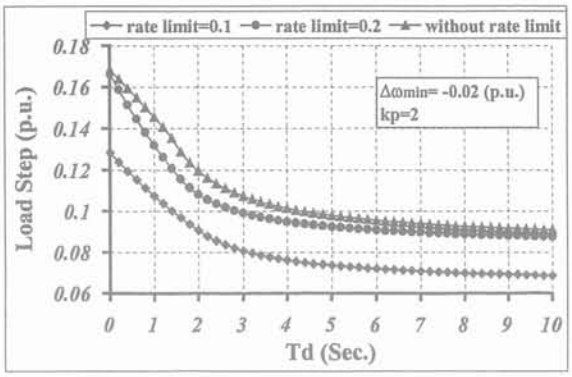

Figure 5.33: Calculated load step size vs. Td for various values of rate limit

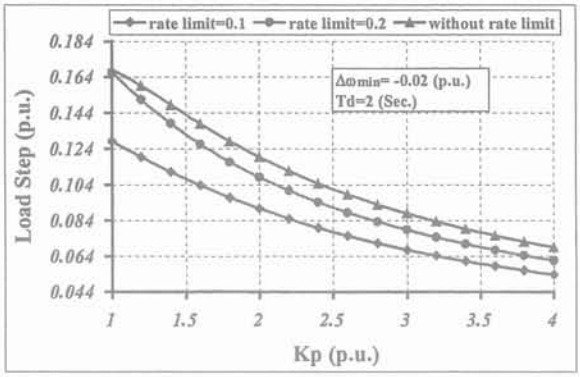

Figure 5.34: Calculated load step size vs. K_p for various values of rate limit

These results shows that the load step size for a given dip frequency depends on:

- Load characteristics (type of load, T_d, K_p),
- Parameters of the governor system, especially the governor rate limit.

5.6.2 Case 2

In this section, the proposed methods are tested on the well known 39-bus, New England test system (Figure 5.35), and the results obtained are compared with the results of long-term dynamics simulation program that described in chapter 3. The system includes 39 buses, 10 generators, 35 lines and 12 transformers, and is divided into 2 subsystems (islands) for simultaneous restoration. The first island includes generators in buses 30,33,34,35,36,37,38 and the second island includes generators in buses 31,32,39. Lines between buses 1 and 39, 3 and 4, 15 and 16, are out of service and hence divide the system into 2 islands. The line data, bus data, and parameters of prime mover models are listed in Appendix-A. Note that the inertia constant of generator of bus 39, which plays the role of equivalent for the neighboring system, is set equal to 42 p.u. seconds (ten times less than in original data). This value enables the system to be more sensitive to load pick-up.

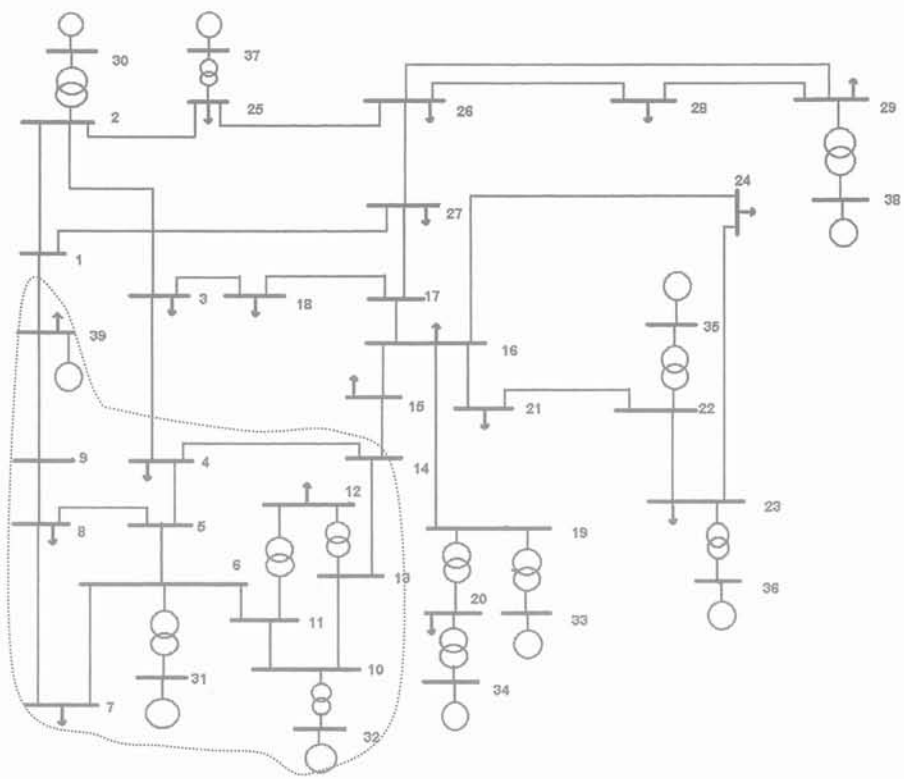

Figure 5.35: One line diagram of 39 bus New England test system

5.6.2.1 Minimum Frequency Calculation

In this case, the load step is selected equal to one per unit and the minimum frequency is calculated by the proposed method in each island.

Table 5.16 shows the results of calculations and simulation where buses are selected according to restoration scenario for this system. The third and fourth columns of this table show the result of the minimum frequency calculation by the proposed method and the

result of long-term dynamics simulation, respectively, for the load step equal to one per unit. The Error (%) in the table is calculated using Equations (5.31) and (5.32), where f_0 is equal to 60 HZ.

Table 5.16: Minimum Frequency Calculation Results

Bus No.	No. of Island	f_{min}* (Hz)	f_{min}** (Hz)	Error (%)
3	1	59.78	59.77	4.3
8	2	59.51	59.47	7.5
15	2	59.50	59.46	7.4
18	1	59.78	59.76	8.3
27	1	59.77	59.76	4.2
39	2	59.55	59.52	6.2

* Minimum frequency calculation for load step=1 p.u

**Long-term dynamics simulation results for f_{min} after load pick up with load step=1 p.u

5.6.2.2 Load Step Calculation

For calculating load steps, the minimum allowable frequency is selected according to power system characteristics (inertia constant of generators, settings of under frequency load shedding relays and generators protective relays,...). The minimum frequency is selected equal to 59.64Hz (or –0.6%) for 39-bus test system and then load step is calculated for a number of load buses during system restoration. Table 5.17 shows the results of load step calculation by the proposed method and the results of minimum frequency from long-term dynamics simulation for these load steps. Figure 5.36 shows frequency response of the system after load pick up in load bus no. 39 at t=13 (sec).

The results of these cases and other test cases show the effectiveness and accuracy of the proposed method.

Table 5.17: Load Step Calculation Results

Bus No.	No. of Island	Load Step* (p.u)	f_{min}**(Hz)	Error (%)
3	1	1.5842	59.652	3.3
7	2	0.6530	59.670	8.33
8	2	0.6532	59.670	8.33
15	2	0.6547	59.667	7.5
18	1	1.5302	59.664	6.6
27	1	1.5037	59.652	3.3
28	1	1.5317	59.664	6.6
39	2	0.7266	59.667	7.5

*Load Step calculation for f_{min}=59.64 Hz

**Long-term dynamics simulation results for f_{min} after load pick up with the calculated load step

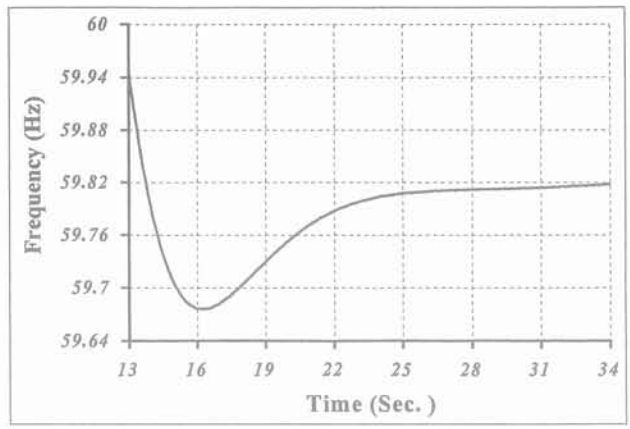

Figure 5.36: Frequency response after load picks up in load bus No. 39

5.7 SUMMARY

In this chapter a new method for calculating prime movers frequency response during restoration is presented. There are two problems during load pick-up:

- Calculation of the maximum load pick-up for a given frequency decline,
- Computation of the minimum frequency for picking up an estimated low voltage AC network loads.

This method is suitable for on-line operator guide to select appropriate load steps and to calculate the minimum frequency after reconnection of a given load, since it requires less computations time than full simulation. Simulation tests on CT unit, HE unit, SE unit, and on the 39-bus New England system show the effectiveness of the proposed methods.

In addition, this method can be used for dynamic security assessment during a forced outage of a generating unit by predicting the operation of an under-frequency load shedding system.

CHAPTER 6

STANDING PHASE ANGLE REDUCTION DURING RESTORATION

CHAPTER 6

STANDING PHASE ANGLE REDUCTION DURING RESTORATION

6.1 INTRODUCTION

In re-integrating a power system, operators sometimes encounter an excessive SPA difference across a line (Figure 6.1).

Figure 6.1: SPA difference across the line before closing the circuit breaker ($|\theta_i-\theta_j|$)

Closing a power circuit breaker on a large SPA difference can shock the system, causing equipment damage and possible recurrence of the system outage [3]. In order to avoid inadvertent closing with a large phase angle difference, breakers are equipped with synchrocheck relays, which prevent their closure for angle greater than a preset value. The ranges of SPA differences that a system can withstand depends on voltage level, operating condition, and location of its circuit breakers. Typical settings for synchrocheck relays in a normal practice is [192]:

- 20° for EHV (400KV and above) lines,
- 30° to 40° for 230KV lines,
- 50° to 60° for 132KV and low voltage lines.

In the restorative state the phase angle should be reduced to ten degrees or less before starting interconnection [163]. Under such conditions, system operators may attempt to reduce the SPA difference by changing the real power generation in a few power plants by

trial and error. This is a time consuming process and may result in prolonging the restoration time [77].

In the past, a number of researchers have investigated standing phase angle reduction and uses DC load flow [192], which may not be exact in some cases, and load shedding wasn't considered as a solution. Since power system is weakly linked in the first steps of restoration process, active and reactive power are not decoupled. Thus we use accurate model of load flow instead of DC load flow.

In this chapter a new and fast method for reducing SPA is presented. The proposed algorithm reduces the excessive SPA difference between two buses via generators rescheduling, such that the changes in the power generations value and the number of rescheduling generators are minimum and subject to the:

- Generators MW and MVAR limits
- Transmission line limits

SPA difference between two specified buses is expressed in terms of change in real power generations and based on the sensitivity of the generating buses, the optimal set of generating units is selected for reducing SPA. If all generators attain their limits, then regulation of real power at load buses is allowed by load shedding. In this case, load shedding value and number of bus load that participate in load shedding must be minimum.

6.2 SPA DIFFERENCE IN TERMS OF CHANGE IN REAL POWER INJECTION

In this section, SPA difference and change of reactive power generation are expressed in terms of active power change. Using accurate models, the change in active and reactive power injection and consumption at buses can be expressed as [191]:

$$\begin{bmatrix} \Delta P_{g,slack} \\ \Delta P_g \\ \Delta P_l \\ \Delta Q_g \\ \Delta Q_l \end{bmatrix} = \begin{bmatrix} J_{slack,\theta l} & J_{slack,\theta l} & J_{slack,ul} \\ J_{pg\theta g} & J_{pg\theta l} & J_{pgul} \\ J_{pl\theta l} & J_{pl\theta l} & J_{plul} \\ J_{qg\theta g} & J_{qg\theta l} & J_{qgul} \\ J_{pl\theta l} & J_{pl\theta l} & J_{plul} \end{bmatrix} \cdot \begin{bmatrix} \Delta\theta_g \\ \Delta\theta_l \\ \Delta U_l \end{bmatrix} \tag{6.1}$$

Where:

$\Delta\theta$: vector of voltage phase angle changes;

ΔU: vector of changes of bus voltages;

ΔP: vector of changes of active power;

ΔQ: vector of changes of reactive power;

J: Jacobean sub-matrix;

g : index of generating buses;

l : index of load buses;

slack: index of slack bus;

In Equation (6.1) $\Delta\theta_{g,slack}=0$, because phase angle of slack generator is fix and reference for others generators. Also, change in active power of slack is separated from other generators, since we can not change it directly and independently. This generator balance active power generation and consumption for keeping frequency. Of course, in practice, active power changes of slack generator is limited and must be considered as a constraint during SPA difference reduction.

For generation rescheduling, load shedding is not considered and we have:

$$\Delta P_l = 0 \quad , \quad \Delta Q_l = 0 \tag{6.2}$$

Substituting Equation (6.2) in Equation (6.1), we have:

$$\begin{bmatrix} J_{pl\theta l} & J_{plul} \\ J_{ql\theta l} & J_{qlul} \end{bmatrix} \cdot \begin{bmatrix} \Delta\theta_l \\ \Delta U_l \end{bmatrix} = -\begin{bmatrix} J_{pl\theta l} \\ J_{ql\theta l} \end{bmatrix} \cdot \Delta\theta_g \tag{6.3}$$

Equation (6.3) can be rearranged as given below:

$$\begin{bmatrix} \Delta\theta_l \\ \Delta U_l \end{bmatrix} = \begin{bmatrix} J_{\theta\theta} \\ J_{u\theta} \end{bmatrix} \cdot \Delta\theta_g \tag{6.4}$$

Where:

$$\begin{bmatrix} J_{\theta\theta} \\ J_{u\theta} \end{bmatrix} = -\begin{bmatrix} J_{pl\theta l} & J_{plul} \\ J_{ql\theta l} & J_{qlul} \end{bmatrix}^{-1} \cdot \begin{bmatrix} J_{pl\theta l} \\ J_{ql\theta l} \end{bmatrix} \tag{6.5}$$

Now from Equation (6.1) and Equation (6.4) we have:

$$\begin{aligned} \Delta P_{g,slack} &= \tilde{J}_{\theta g,slack} \cdot \Delta\theta_g \\ \Delta P_g &= \tilde{J}_{pg\theta g} \cdot \Delta\theta_g \\ \Delta Q_g &= \tilde{J}_{qg\theta g} \cdot \Delta\theta_g \end{aligned} \tag{6.6}$$

Or:

$$\Delta\theta_g = X_{\theta gpg} \cdot \Delta P_g \tag{6.7}$$

Where:

$$\begin{aligned} \tilde{J}_{\theta g,slack} &= J_{\theta g,slack} + J_{\theta l,slack} \cdot J_{\theta\theta} + J_{ul,slack} \cdot J_{u\theta} \\ \tilde{J}_{pg\theta g} &= J_{pg\theta g} + J_{pg\theta l} \cdot J_{\theta\theta} + J_{pgul} \cdot J_{u\theta} \\ \tilde{J}_{qg\theta g} &= J_{qg\theta g} + J_{qg\theta l} \cdot J_{\theta\theta} + J_{qgul} \cdot J_{u\theta} \\ X_{\theta gpg} &= \tilde{J}_{pg\theta g}^{-1} \end{aligned} \tag{6.8}$$

For expressing all variables in terms of change in active power generation, we replace Equation (6.7) in Equation (6.4) and Equation (6.6) as follow:

$$\Delta\boldsymbol{\theta} = \begin{bmatrix} \Delta\boldsymbol{\theta}_g \\ \Delta\boldsymbol{\theta}_l \end{bmatrix} = \boldsymbol{X}.\,\Delta\boldsymbol{P}_g \tag{6.9}$$

$$\Delta P_{g,slack} = \mathbf{J}_{pg,slack}.\Delta\mathbf{P}_g = \sum_{k\neq slack}^{ng} PF_k\,.\Delta P_{g,k} \tag{6.10}$$

$$\Delta\boldsymbol{Q}_g = \boldsymbol{J}_{qpg}.\Delta\boldsymbol{P}_g \tag{6.11}$$

Where:

$$\boldsymbol{X} = \begin{bmatrix} \boldsymbol{X}_{\theta gpg} \\ \boldsymbol{J}_{\theta\theta}\boldsymbol{X}_{\theta gpg} \end{bmatrix} \quad , \quad \boldsymbol{J}_{pg,slack} = \tilde{\boldsymbol{J}}_{\theta g,slack}.\boldsymbol{X}_{\theta gpg} \quad , \quad \boldsymbol{J}_{qpg} = \tilde{\boldsymbol{J}}_{qg\theta g}.\boldsymbol{X}_{\theta gpg} \tag{6.12}$$

Equation (6.9) indicates linear relation between change of voltage phase angle of all buses in terms of change in vector of power generation. Thus for bus i and bus j , the change in voltage phase angle can be written as:

$$\Delta\theta_{ij} = \mathbf{X}_{ij}\,.\Delta\mathbf{P}_g = \sum_{k\neq slack}^{ng} SF_k.\Delta P_{g,k} \tag{6.13}$$

Where:

$$\Delta\theta_i = \boldsymbol{X}_i.\Delta\boldsymbol{P}_g \quad , \quad \Delta\theta_j = \boldsymbol{X}_j.\Delta\boldsymbol{P}_g \quad , \quad \boldsymbol{X}_{ij} = \boldsymbol{X}_i - \boldsymbol{X}_j$$

Equation (6.13) gives the change in SPA difference between two buses (i.e. between bus i and bus j) in terms of Sensitivity Factor SF_k and change in active generation $\Delta\boldsymbol{P}_g$. Sensitivity factors depend on the value of vector $\boldsymbol{\theta}$ and $\boldsymbol{U}$ along with the network parameters of the system. Also in Equation (6.10), PF_k indicates Participation Factor (P.F) of K^{th} generator for change in $P_{g,slack}$. When slack generator reaches its active power limitation, the participation factors is used to select a generator to be add in the participating generator list.

In (6.13) *Xij* is a vector. Therefore $\Delta\boldsymbol{Pg}$ value, based on minimization of $\Sigma(\Delta P_{gk})^2$, are to be calculated using pseudo inverse technique, i.e. :

$$\Delta\boldsymbol{P}_g = \boldsymbol{X}_{ij}^{\,t}.\left(\boldsymbol{X}_{ij}\,.\boldsymbol{X}_{ij}^{\,t}\right)^{-1}.\Delta\theta_{ij} \tag{6.14}$$

Where:

$$\Delta\theta_{ij} = \theta_{ij,actual} - \theta_{ij,limit}$$

For reducing θ_{ij}, Equation (6.14) determines the rescheduling values for all generation units. During system restoration, Automatic Generation Control (AGC) may not be practically realizable and a solution, which identifies a minimum number of generators to be rescheduled, is preferred. In section (6.5), we will explain the proposed algorithm within the constraints of limits on active and reactive power generations and limits on transmission line flows.

6.3 SPA DIFFERENCE IN CASE OF LOAD SHEDDING

If all generators reach their limits, then regulation of real power at load buses is allowed by load shedding at selected buses. These load buses are selected based on the minimum of load shedding value and minimum number of buses.

For load shedding, generation rescheduling is not considered. Also power factors of loads are constant. Thus we have:

$$\Delta P_g = 0 \quad , \quad \frac{\Delta Q_{lk}}{\Delta P_{lk}} = tan\varphi_k = \text{constant} \quad , \quad k = 1,..,nl \tag{6.15}$$

Or:

$$\Delta Q_l = T_g . \Delta P_l \qquad \text{where:} \qquad T_g = diag([\, tan\varphi_1 \, , tan\varphi_2 \, ,..., tan\varphi_{nl}\,]) \tag{6.16}$$

In this case a relationship between $\Delta\theta$ and ΔP_l is investigated, and then all variable is expressed in terms of ΔP_l. By substituting Equation (6.15) and Equation (6.16) in Equation (6.1), we have:

$$\begin{bmatrix} J_{pg\theta g} & J_{pgul} \\ J_1 & J_2 \end{bmatrix} \cdot \begin{bmatrix} \Delta\theta_g \\ \Delta U_l \end{bmatrix} = -\begin{bmatrix} J_{pg\theta g} \\ J_3 \end{bmatrix} . \Delta\theta_l \tag{6.17}$$

Where:

$$\begin{aligned} J_1 &= J_{ql\theta g} - T_g . J_{pl\theta g} \\ J_2 &= J_{qlul} - T_g . J_{plul} \\ J_3 &= J_{ql\theta l} - T_g . J_{pl\theta l} \end{aligned} \tag{6.18}$$

In Equation (6.17) the matrix of left-hand side is full rank. After inversion of the matrix, we have:

$$\begin{bmatrix} \Delta\theta_g \\ \Delta U_l \end{bmatrix} = \begin{bmatrix} \tilde{J}_{\theta\theta} \\ \tilde{J}_{u\theta} \end{bmatrix} . \Delta\theta_l \tag{6.19}$$

Where:

$$\begin{bmatrix} \tilde{J}_{\theta\theta} \\ \tilde{J}_{u\theta} \end{bmatrix} = -\begin{bmatrix} J_{pg\theta g} & J_{pgul} \\ J_1 & J_2 \end{bmatrix}^{-1} \cdot \begin{bmatrix} J_{pg\theta g} \\ J_3 \end{bmatrix} \tag{6.20}$$

If Equation (6.19) is replaced in Equation (6.1), then we have:

$$\Delta P_l = \tilde{J}_{pl\theta l} . \Delta\theta_l \tag{6.21}$$

$$\Delta P_{g,slack} = \tilde{J}_{\theta l,slack} . \Delta\theta_l \tag{6.22}$$

$$\Delta Q_g = \tilde{J}_{qg\theta g} . \Delta\theta_l \tag{6.23}$$

Or:

$$\Delta\theta_l = X_{\theta lpl} . \Delta P_l \tag{6.24}$$

Where:

$$\begin{aligned}
\tilde{J}_{\theta l,slack} &= J_{\theta l,slack} + J_{\theta g,slack}.\tilde{J}_{\theta\theta} + J_{ul,slack}.\tilde{J}_{u\theta} \\
\tilde{J}_{pl\theta l} &= J_{pl\theta l} + J_{pl\theta l}.\tilde{J}_{\theta\theta} + J_{plul}.\tilde{J}_{u\theta} \\
\tilde{J}_{qg\theta g} &= J_{qg\theta g} + J_{qg\theta l}.\tilde{J}_{\theta\theta} + J_{qgul}.\tilde{J}_{u\theta} \\
X_{pl\theta l} &= \tilde{J}_{pl\theta l}^{-1}
\end{aligned} \tag{6.25}$$

For expressing all variables in terms of change in active power consumption, we replace Equation (6.24) in Equation (6.19) and Equation (6.22) as follows:

$$\Delta\theta = \begin{bmatrix} \Delta\theta_g \\ \Delta\theta_l \end{bmatrix} = X.\ \Delta P_l \tag{6.26}$$

$$\Delta P_{g,slack} = J_{pl,slack}.\ \Delta P_l \tag{6.27}$$

$$\Delta Q_g = J_{qpl}.\ \Delta P_l \tag{6.28}$$

Where:

$$\tilde{X} = \begin{bmatrix} \tilde{J}_{\theta\theta}.X_{\theta lpl} \\ X_{\theta lpl} \end{bmatrix}, \qquad J_{pl,slack} = \tilde{J}_{\theta l,slack}.X_{\theta lpl}\ , \qquad J_{qpl} = \tilde{J}_{qg\theta g}.\ X_{\theta lpl} \tag{6.29}$$

Using Equation (6.26), change of voltage phase angle for bus i and j can be written as given below:

$$\Delta\theta_i = \tilde{X}_i.\ \Delta P_l \qquad , \qquad \Delta\theta_j = \tilde{X}_j.\Delta P_l$$

Or:

$$\Delta\theta_{ij} = \tilde{\mathbf{X}}_{ij}.\Delta\mathbf{P}_l = \sum_{k=1}^{nl} SF'_k.\ \Delta P_{lk} \tag{6.30}$$

where : $\tilde{\mathbf{X}}_{ij} = \tilde{\mathbf{X}}_i - \tilde{\mathbf{X}}_j$

Equation (6.30) gives the change in SPA difference between two buses (i.e. between bus i and bus j) in terms of Sensitivity Factor SF'_k and load shedding ΔP_l.

In (6.30) X_{ij} is a vector therefore ΔP_l value, based on minimization of $\Sigma(\Delta P_{lk})^2$, are to be calculated using pseudo inverse technique, i.e. :

$$\Delta P_l = \tilde{X}_{ij}^{\ t}.\left(\tilde{X}_{ij}.\tilde{X}_{ij}^{\ t}\right)^{-1}.\ \Delta\theta_{ij} \tag{6.31}$$

For reducing θ_{ij}, Equation (6.31) determines the optimum load shedding where all load buses are participated in the process. However minimum number of load buses must be selected for load shedding and the limits on active power consumption and transmission lines limits should be also respected in this process. In section (6.5), we will explain complete procedure for finding solution.

6.4 TRANSMISSION LINE LIMIT IN TERMS OF CHANGE IN ACTIVE POWER

In this section, we express transmission line flow limit in terms of change in active power generation. Current flowing in line m-k (from m to k) can be written as:

$$\underline{I}_{mk} = \underline{y}_{mk}.(\underline{U}_m - \underline{U}_k) \tag{6.32}$$

Where:

$\underline{y}_{mk}$: admittance of line m-k

$\underline{U}_m$: Voltage of bus m

$\underline{U}_k$: Voltage of bus k

Absolute value of the line current can be written as:

$$|I_{mk}|^2 = G_{mk}^2.[U_m^2 + U_k^2 - 2.U_m.U_k.\cos(\theta_m - \theta_k)] + B_{mk}^2.[U_m^2 + U_k^2 - 2.U_m.U_k.\cos(\theta_m - \theta_k)] \tag{6.33}$$

Where:

$\underline{y}_{mk} = G_{mk} + jB_{mk}$, $\underline{U}_m = U_m.\exp(j\theta_m)$, $\underline{U}_k = U_k.\exp(j\theta_k)$

Changing in the current absolute value of the line m-k with respect to changes of voltage phase angles can be expressed as:

$$\Delta|I_{mk}|^2 = \begin{bmatrix} J_{Imk} & -J_{Imk} \end{bmatrix}.\begin{bmatrix} \Delta\theta_m \\ \Delta\theta_k \end{bmatrix} \tag{6.34}$$

Where:

$$J_{Imk} = 2.U_m.U_k(G_{mk}^2 + B_{mk}^2).\sin(\theta_m - \theta_k) \tag{6.35}$$

From Equations (6.13) and (6.34) the following equation can be obtained:

$$\Delta|I_{mk}|^2 = \boldsymbol{X}_{line,mk}. \ \boldsymbol{\Delta P}_g \tag{6.36}$$

Where:

$$\boldsymbol{X}_{line,mk} = J_{Imk}.(\boldsymbol{X}_m - \boldsymbol{X}_k) \tag{6.37}$$

Equation (6.36) gives the change in current absolute value in terms of change in active power generation $\boldsymbol{\Delta P_g}$ during excessive SPA difference reduction.

In general form, for all lines, changes in the current absolute value in terms of change in power generations can be written as given below:

$$\Delta|\boldsymbol{I}|^2 = \boldsymbol{X}_{line}. \ \boldsymbol{\Delta P}_g \tag{6.38}$$

6.5 SOLUTION STEPS FOR SPA DIFFERENCE REDUCTION

For SPA difference reduction helping rescheduling generation, it can be formulated as an optimization problem with minimum change in power generation and minimum number of participating generators with constraints as described below :

$$
\begin{aligned}
&\boldsymbol{X}_{ij} \cdot \Delta \boldsymbol{P}_g = \Delta\theta_{ij} \\
&\Delta \boldsymbol{P}_{g,min} \le \Delta \boldsymbol{P}_g \le \Delta \boldsymbol{P}_{g,max} \\
&\Delta P_{g,slack,min} \le \Delta P_{g,slack} = \boldsymbol{J}_{pg,slack} \cdot \Delta \boldsymbol{P}_g \le \Delta P_{g,slack,max} \\
&\Delta \boldsymbol{Q}_{g,min} \le \Delta \boldsymbol{Q}_g = \boldsymbol{J}_{qpg} \cdot \Delta \boldsymbol{P}_g \le \Delta \boldsymbol{Q}_{g,max} \\
&\Delta |\boldsymbol{I}|^2_{line,min} \le \Delta |\boldsymbol{I}|^2_{line} = \boldsymbol{X}_{line} \cdot \Delta \boldsymbol{P}_g \le \Delta |\boldsymbol{I}|^2_{line,max}
\end{aligned}
\tag{6.39}
$$

Where:

$$\Delta P_{g,slack,min} = P_{g,slack} - P_{g,slack,min}$$

$$\Delta P_{g,slack,max} = P_{g,slack,max} - P_{g,slack}$$

$$\Delta \boldsymbol{P}_{g,max} = \boldsymbol{P}_{g,max} - \boldsymbol{P}_g \quad , \quad \Delta \boldsymbol{P}_{g,min} = \boldsymbol{P}_g - \boldsymbol{P}_{g,min}$$

$$\Delta \boldsymbol{Q}_{g,max} = \boldsymbol{Q}_{g,max} - \boldsymbol{Q}_g \quad , \quad \Delta \boldsymbol{Q}_{g,min} = \boldsymbol{Q}_g - \boldsymbol{Q}_{g,min}$$

$$\Delta |\boldsymbol{I}|^2_{line,max} = |\boldsymbol{I}|^2_{line,max} - |\boldsymbol{I}|^2_{line}$$

$\boldsymbol{P}_{g,min}$: vector of minimum active power generation ;

$\boldsymbol{P}_{g,max}$: vector of maximum active power generation;

$\boldsymbol{Q}_{g,min}$: vector of minimum reactive power generation;

$\boldsymbol{Q}_{g,max}$: vector of maximum reactive power generation;

$|\boldsymbol{I}|^2_{line,max}$: vector of maximum lines current;

If all generators reach their limits, then we use load shedding. In this case we must solve an optimization problem. The cost functions in this optimization problem are minimum load shedding value and minimum number of load buses that selected for load shedding. The problem constraints are:

$$
\begin{aligned}
&\tilde{\boldsymbol{X}}_{ij} \cdot \Delta \boldsymbol{P}_l = \Delta\theta_{ij} \\
&\Delta \boldsymbol{P}_{l,min} \le \Delta \boldsymbol{P}_l \le \Delta \boldsymbol{P}_{l,max} \\
&\Delta P_{g,slack,min} \le \Delta P_{g,slack} = \boldsymbol{J}_{pl,slack} \cdot \Delta \boldsymbol{P}_l \\
&\Delta \boldsymbol{Q}_{g,min} \le \Delta \boldsymbol{Q}_g = \boldsymbol{J}_{qpl} \cdot \Delta \boldsymbol{P}_l \le \Delta \boldsymbol{Q}_{g,max}
\end{aligned}
\tag{6.40}
$$

The solution steps for SPA reduction between two buses, are listed below:

1) Perform load flow for the network with present topology;
2) Compute Sensitivity Factor for generation buses
3) Calculate $\Delta\theta_{dij}$ (desired phase angle difference)
4) Adding generator which has the highest S.F to the list of participating generators
5) Solving optimization problem with current list of generators
6) If solution is found, then go to (10)
7) If solution is not found and slack generator has reached its active power limit, then add a generator, which has the highest Participation factor (P.F) to the list and go to (5)
8) Else if solution is not found and one of generators in list reaches its active power limit, then add a generator which has the highest S.F to the list and go to (5)
9) Else (case load shedding), use similar method for load shedding
10) Stop

Figure 6.2 shows flow chart of these steps.

6.6 Simulation Results and Discussion

In this section the proposed approach is tested on IEEE 118 bus system and the results are mentioned. The bus and line data of the system are reported in Appendix. Removing existing lines from the system created situations for excessive SPA difference between two buses. In case 1, line between buses 23 and 25 and line between buses 25 and 27 are removed from the system.

In case 2, line between buses 26 and 30 and line between buses 25 and 27 are removed and in case 3, line between buses 23 and 24 is removed from the system. Generation rescheduling is used for case 1 and 2, where load shedding is used for case 3 for SPA reduction.

We set a maximum limit for the slack bus generation to 3.5 p.u. The maximum and minimum limits on a generating bus are taken as 1.5 times and 0.2 times the current generation, respectively. For load shedding, we assume that there are five feeders in each load bus and load at targeted load-bus can be reduced up to 40% of its old value.

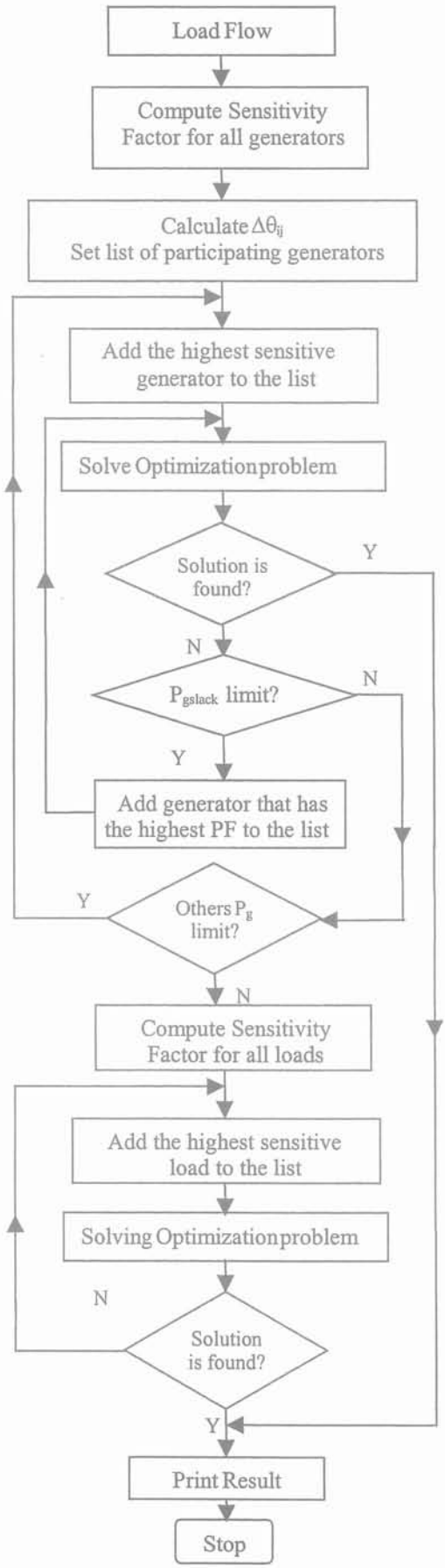

Figure 6.2: Flowchart of SPA reduction

In each case in the first step, a load flow is carried out for the modified topology of the system with all generators and load remaining fixed. SPA limit between two buses, before connecting the corresponding line, is set to 20°.

6.6.1 Case 1

In this case SPA between buses 23 and 25 before connecting their interconnection line is 44.45°. In order to reduce this excessive phase angle, we use the proposed method. Table 6.1 shows order of generator buses, in terms of SF (Sensitivity Factor) and PF (Participation Factor), used for reducing excessive SPA difference between buses 23-25.
Table 6.2 shows the optimal rescheduling for the selected generators, where generator buses 25 and 26 have the highest S.F and generator buses 27 and 31 have the highest P.F that keep slack bus generation within 3.5 (pu.). In this table, active power generation before and after SPA reduction are denoted by $P_g(0)$ and $P_g(1)$, respectively.
Table 6.3 shows voltage phase angles during the SPA reduction, where $\Delta\theta(0)$ and $\Delta\theta(1)$ are standing phase angle difference across lines before and after SPA reduction process, respectively. After the SPA reduction for the buses 23-25, line 23 –25 can be closed and then line 25 – 27 will be closed without excessive SPA difference problem.

Table 6.1: Order of generator buses in terms of SF and PF for case 1

Order of S.F*	25	26	24	72	4	12	10	8
Order of P.F**	27	31	54	24	113	59	40	42

* Sensitivity factor for change in SPA
** Participation factor for change in slack generation

Table 6.2: The optimal generation rescheduling for case 1

Bus No.	**U** (p.u.)	**$P_g(0)$** (p.u.)	**$P_g(1)$** (p.u.)	**ΔP_g** (p.u.)
25	1.02	1.9	0.38	-1.52
26	1.02	3.0	1.85	-1.15
27	1.02	1.0	1.50	0.50
31	1.02	1.0	1.41	0.41
69 (Slack)	1	1.72	3.37	1.65

Table 6.3: SPA difference between two buses for case 1

Line No.	From Bus	To Bus	Δθ (0) (deg.)	Δθ (1) (deg.)	Δθ (after closing line23-25) (deg.)	Δθ (after closing line25-27) (deg.)
1	25	23	44.4	19.9	4.6	3.1
2	25	27	47.4	21.8	10.1	5.2

6.6.2 Case 2

In this case SPA between buses 26 and 30 before connecting their interconnection line is 49.7°. In order to reduce this excessive phase angle, we use the proposed method.

Table 6.4 shows order of generator buses in terms of SF (Sensitivity Factor) and PF (Participation Factor) selected for reducing excessive SPA difference between buses 26-30. Table 6.5 shows the optimal rescheduling for the selected generators, where generator buses 26 and 25 have the highest S.F and generator buses 12 and 113 have the highest P.F that keep slack bus generation within 3.5 pu.

Table 6.6 shows voltage phase angles during the SPA reduction process, where $\Delta\theta(0)$ and $\Delta\theta(1)$ are standing phase angle difference across lines before and after SPA reduction, respectively. After the SPA reduction for the buses 26-30, line 26 –30 can be closed and then line 25 – 27 will be closed without excessive SPA difference problem.

6.6.3 Case 3

In this case SPA between buses 23 and 24 before connecting their interconnection line is 53.8°. In order to reduce this excessive phase angle, we use the proposed method that it proposed load shedding in the selected buses.

Tables 6.7, 6.8 and 6.9 show the results of optimal load shedding obtained for this case. The priority order of load buses for participating in SPA reduction is bus number: 22, 20 and 23, respectively. Although it is expected that load bus 23 would be the high sensitive bus for this case, however load bus 22 has the highest priority. After load shedding, phase angle difference between buses 23 and 24 is reduced to 19.7 ° and hence this line can be closed. In Table 6.8 active power consumption before and after SPA reduction is denoted by $P_L(0)$ and $P_L(1)$, respectively.

Table 6.4: Order of generator buses in terms of SF and PF for case 2

Order of S.F	26	25	24	72	8	4	12	10
Order of P.F	12	113	54	40	27	31	8	4

Table 6.5: The optimal reschedule for case 2

Bus No.	U (p.u.)	$P_g(0)$ (p.u.)	$P_g(1)$ (p.u.)	ΔP_g (p.u.)
12	1.02	0.9	1.35	0.45
25	1.02	1.9	0.72	-1.18
26	1.02	3	1.55	-1.45
113	1.02	1	1.41	0.41
69 (slack)	1	2.19	3.49	1.3

Table 6.6: SPA difference between two buses for case 2

Line No.	From bus	To bus	$\Delta\theta$ (0) (deg.)	$\Delta\theta$ (1) (deg.)	$\Delta\theta$ (after closing line26-30) (deg.)	$\Delta\theta$ (after closing line25-27) (deg.)
1	26	30	49.7	19.9	4.9	3.4
2	25	27	43.3	22.7	14.2	7.3

Table 6.7: Order of the load buses in terms of SF for case 3

Order of S.F	22	20	23	115	114	29	17	16

Table 6.8: The optimal load shedding for case 3

Bus No.	P_L (0) (p.u.)	$P_L(1)$ (p.u.)	ΔP_L (p.u.)
20	2.00	1.20	-0.80
22	2.40	1.44	-0.96
23	1.7	1.02	-0.68

Table 6.9: SPA difference between two buses for case 3

Line No.	From bus	To bus	$\Delta\theta$ (0) (deg.)	$\Delta\theta$ (1) (deg.)
1	24	23	53.8	19.7

These simulation results and other test case show the effectiveness and accuracy of the proposed method.

6.7 SUMMARY

This chapter describes a new approach for the reduction of Standing Phase Angle (SPA) difference between two buses of a power system during system restoration. SPA difference must be within limit before an attempt is made to close breakers to firm up the bulk power transmission network. The method proposed in this chapter, offers a fast algorithm that considers all operational constraint.

SPA difference is reduced with rescheduling of power generation of units. This operation can be expressed as a special optimization problem that minimizes generation changes value and number of participating generators in the rescheduling process. Generators MW and MVAR limits, transmission lines limits and slack generator MW and MVAR limits are problem's constraints. If SPA isn't reduced to a desired value by generation rescheduling, then SPA difference is reduced by load shedding.

Simulation tests were carried out on IEEE 118 bus system has shown the effectiveness of the proposed method. This method is a direct basis type and is suitable for real time applications.

CHAPTER 7

ANALYSIS AND CONTROL OF HARMONICS OVERVOLTAGES

CHAPTER 7

ANALYSIS AND CONTROL OF HARMONICS OVERVOLTAGES

7.1 INTRODUCTION

7.1.1 OVERVIEW OF OVERVOLTAGES

One of the major concerns in power system restoration is the occurrence of overvoltages as a result of switching procedures [77]. These can be classified as transient overvoltages, sustained overvoltages, harmonic resonance overvoltages and overvoltages resulting from ferro-resonance [74]. Steady-state overvoltages occur at the receiving end of lightly loaded transmission lines as a consequence of line charging currents (reactive power balance). Excessive sustained overvoltages may lead to damage of transformers and other power system equipment. Transient overvoltages are a consequence of switching operations on long transmission lines, or of switching of capacitive devices, and may result in arrester failures. Harmonic resonance overvoltages are a result of system resonance frequencies close to multiples of the fundamental frequency. They may lead to long lasting overvoltages resulting in arrester failures and system faults. Ferro-resonance is a non-harmonic resonance characterized by overvoltages whose waveforms are highly distorted and which can cause catastrophic equipment damages [74].

7.1.2 HARMONIC OVERVOLTAGES

During the early stages of the restoration procedures following a partial or complete blackout of the power system, the system is lightly loaded and resonance conditions are different from the ones at normal operations.

If the frequency characteristic shows resonance peaks around multiples of the fundamental frequency, high overvoltages of long duration may occur when the system is excited by a harmonic disturbance. Such a disturbance can originate from the saturation of transformers, from power electronics, etc.

The major cause of harmonic resonance overvoltage problems is the switching of lightly loaded transformers at the end of transmission lines. Thereby inrush currents with significant harmonic content up to frequencies around $f = 10f_0$ are created. They can be represented by a harmonic current source I(h) connected to the transformer bus [143]. The relationship between nodal voltages, network matrix and current injections can be represented by:

$$V(h) = Z(h).\ I(h) \qquad (7.1)$$

where h represent the harmonic frequency $h = 2f_0, 3f_0, \ldots$. The harmonic current components of the same frequency as the system resonance frequencies are amplified in case of parallel resonance, thereby creating higher voltages at the transformer terminals. This leads to a higher level of saturation resulting in higher harmonic components of the inrush current which again results in increased voltages. This can happen particularly in lightly damped systems, common at the beginning of a restoration procedure when a path from a black-start source to a large power plant is being established and only a few loads are restored yet [74, 143].

Whereas the control of steady state overvoltages can be dealt with thoroughly using conventional load flow programs, a systematic method to deal with resonant overvoltages has not yet been developed. Therefore, this chapter focuses on the analysis and control of harmonic overvoltages during power system restoration.

This phenomenon is usually investigated with the electromagnetic transients programs [74, 176]. In order to study a large number of possible system configurations, it is necessary to run many time-domain simulations resulting in a large amount of simulation time. A way to limit the overall calculation time is to reduce the number of simulations by applying analytical or knowledge-based rules to discard a number of system configurations before an actual time-domain simulation is carried out.

This chapter describes an approach to power system restoration planning using the Power System Blockset (PSB), a MATLAB/Simulink-based simulation tool [176], in combination with analytical calculations. The procedure is based on harmonic analysis of the system and sensitivity analysis. Examples are presented on how the optimum system configuration for controlling harmonic resonance can be calculated in a fast and efficient way, and how the number of time-consuming PSB time-domain simulations based on the common trial-and-error method can be reduced significantly.

However, a number of simulations will still have to be performed to find the optimum system configuration for each restoration step. In this case we concentrate on the aspect of a minimum calculation time and investigate conditions for the early termination of PSB runs using Short-Time Fourier Transform.

7.2 Modeling Issues

7.2.1 PSB

Simulations presented in this chapter are performed using the Power System Blockset (PSB). The simulation tool has been developed using state-variable approach and runs in MATLAB/Simulink environment. This program has been compared with other popular simulation packages (EMTP and Pspice) in [176]. The user friendly graphical interfaces of PSB allow faster development for power system transient analysis.

7.2.2 Transmission Line Model

Transmission lines are described by PI cells, the R, L and C parameters being derived from distributed line models. The number of PI cells has been chosen 10 in order to represent correctly its exact impedance under the tenth harmonic. This model is also accurate enough for frequency dependent parameters, because the positive sequence resistance and inductance are fairly constant up to approximately 1 KHz [21] which cover the frequency range of phenomena this chapter deals with.

7.2.3 Generator Model

In [21] generators have been modeled by the generalized Park's model where both electrical and mechanical part are thoroughly modeled. However, it has been shown the dynamic behavior of generators does not influence the temporary overvoltages. Thus in this work, generators are represented by a sinusoidal voltage source behind their sub-transient reactances X''_d. Phases of voltage sources are determined by the load flow results.

7.2.4 Load and Shunt Devices Model

All the loads and shunt devices such as capacitors and reactors are modeled as constant impedances.

7.2.5 Transformer Model

The model takes into account the winding resistances (R_1, R_2), the leakage inductances (L_1, L_2) as well as the magnetizing characteristics of the core, which is modeled by a resistance, R_c, simulating the core active losses and a saturable inductance, L_{sat}. The saturation characteristic is specified as a piece-wise linear characteristic [175].

7.2.6 Harmonic Characteristic of Transformers

For an assessment of harmonic overvoltages during transformer switching, the harmonic characteristic, i. e. the harmonics of the inrush current as a function of the voltage of the

transformer that is energized, is needed. In case the harmonic characteristic is not given by the manufacturer, it can be determined from the saturation characteristic and the transformer terminal voltage. In the following section, analytical equations are introduced to determine the harmonic content of the transformer inrush current.

A. Analytical Calculation of Transformer Inrush Current

The development of the equations for the calculation of transformer inrush currents is described in detail in [22, 175] and, is therefore omitted from this section.

When applying a sinusoidal voltage:

$$v(t) = V_m . cos(\omega t) \tag{7.2}$$

directly to a saturated inductance, the harmonics of the transformer inrush current can be calculated as [22]:

$$I_0 = \frac{1}{2\pi}.[2\cos(\alpha) + (2\alpha - \pi)].\frac{V_{max}}{\omega L_s} \tag{7.3}$$

$$I_1 = \frac{1}{2\pi}.[\pi - 2\alpha - \sin(2\alpha)].\frac{V_{max}}{\omega L_s} \tag{7.4}$$

$$I_k = \frac{1}{k\pi}.\left[\frac{\sin(k-1)(\alpha+\pi/2)}{k-1} - \frac{\sin(k+1)(\alpha+\pi/2)}{k+1}\right].\frac{V_{max}}{\omega L_s} \quad , \quad (k = 2,3,4,...) \tag{7.5}$$

where:

$$\alpha = \sin^{-1}\left[(1 - \frac{\varphi_0}{\varphi_s}).\frac{\omega L_s}{V_{max}}\right] \tag{7.6}$$

$$\varphi_0 = \varphi_r - \frac{V_{max}}{\omega}.\sin(\omega.t_0) \ , \quad \omega = 2\pi f_0$$

and where φ_s stands for the saturation flux linkage, φ_r for the remanent flux, L_s for the saturated inductance, and t_0 for the switching time.

The simplified saturation characteristic, on which Equations (7.3) to (7.5) are based, is shown in Figure 7.1. It consists of two slopes, the first one with an infinitely high value and the second one with value L_s.

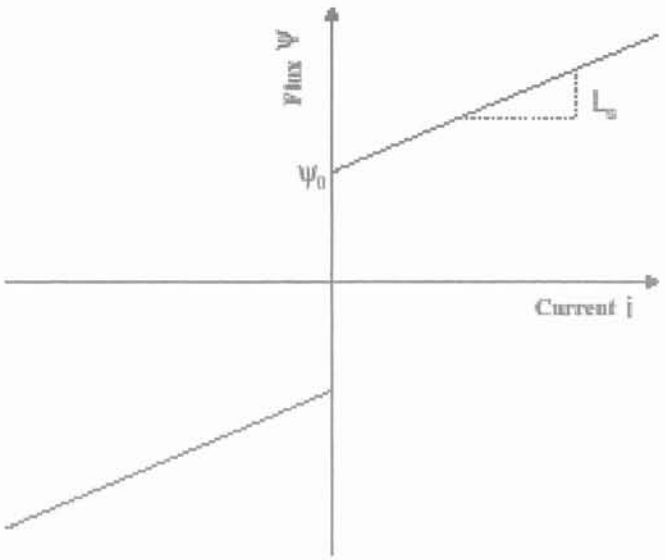

Figure 7.1: Ideal saturation characteristic

Saturation characteristics are usually given as n pairs of numbers [φ(1), i(1)] , [φ(2), i(2)],…, [φ(n), i(n)]. The magnetizing inductance and the saturation flux linkage can then be calculated from the equations

$$\overline{L}_s = \frac{\varphi(n) - \varphi(n-1)}{i(n) - i(n-1)} \tag{7.7}$$

$$\varphi_s = \varphi_n - \overline{L}_s . i(n) \tag{7.8}$$

In addition to the nonlinear magnetizing inductance, transformers have a leakage inductance $L_{leakage}$, resistances R_1 and R_2 representing the I^2R-losses, and resistance R_c representing also the core losses. For our approximation, the resistances R_1 and R_2 can be neglected since R_1, $R_2 << \omega L_{leakage}$. The core loss resistance R_c can be neglected as well since $Rc >> \omega L_s$.

We can then include the inductance $L_{leakage}$ in the magnetizing inductance L_s and obtain:

$$L_s = \overline{L}_s + L_{leakage} \tag{7.9}$$

Using this value in Equations (7.3) to (7.5), we obtain the harmonic characteristic of the transformer inrush current.

B. Example

As an example for the above method, the harmonic characteristic of the transformer that have the following parameters is determined:

$R_1 = R_2 = 0.002$ p.u. , $X_1 = X_2 = 0.08$ p.u., $L_s = 0.3$ p.u., $\varphi_s = 1.2$ p.u.

The harmonics for a transformer terminal voltage of 1.0 per unit calculated with above equations are compared to an PSB time-domain simulation of the inrush current, followed

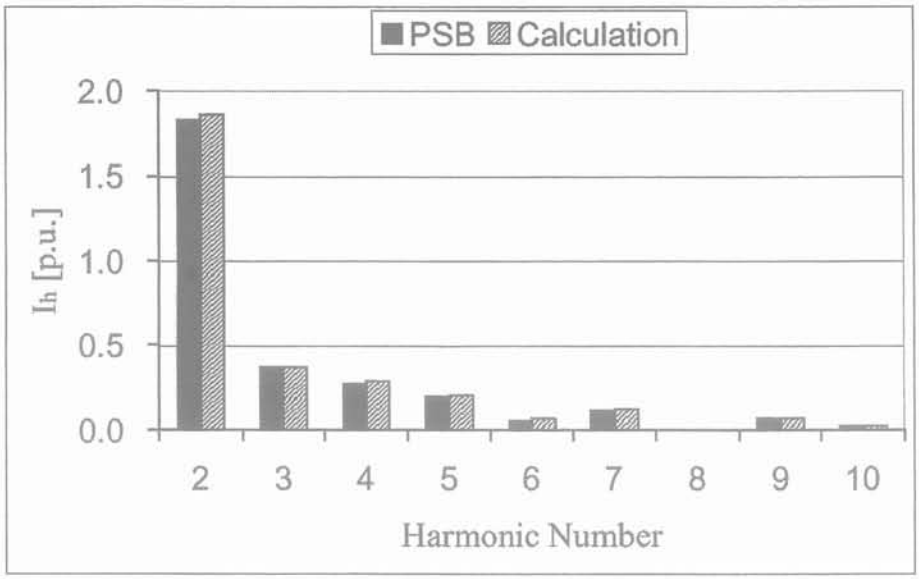

Figure 7.2: Harmonics of transformer inrush current

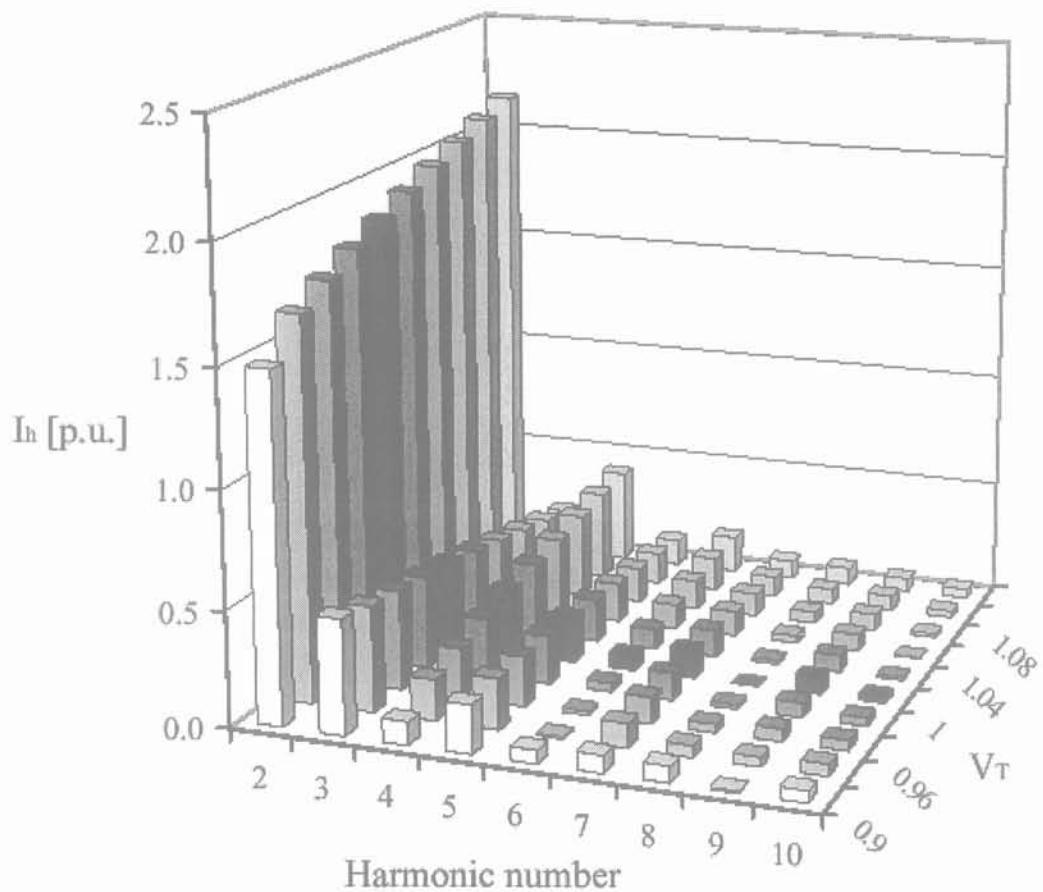

Figure 7.3: Harmonics of transformer inrush current for changes of terminal voltage

by FFT, in Figure 7.2. The results show good agreement and therefore show the validity of the approach.

Figure 7.3 shows the transformer inrush current harmonics for the terminal voltage from 0.9 (p.u.) to 1.10 (p.u.) ranges.

7.3 PROPOSED METHODS FOR HARMONIC OVERVOLTAGES STUDY

7.3.1 ASSESSMENT OF HARMONIC OVERVOLTAGES

Three different criteria for the occurrence of harmonic resonance overvoltages have to be considered: the impedance at the bus where the switching operation is performed, and the harmonic content of the transformer inrush current which is a function of the pre-switching steady-state voltage level at the switching bus and the time of switching, and the transformer saturation characteristic.

Based on the above observations we can define an index for the assessment of harmonic overvoltages for switching operations at bus j that is similar to the total harmonic distortion (THD) known from power system harmonic analysis:

$$H = \sqrt{\sum_{h=2}^{10} [Z_{jj}(h).I_j(h, V_j(t_0^-), L_{sat,j}, t_0)]^2} \tag{7.10}$$

$Z_{jj}(h)$ represents the Thevenin equivalent impedance seen from the bus j, where the transformer is switched to the bus j . I_j stands for the transformer inrush current which is a function of the frequency h, the pre-switching voltage level $V_j(t_0^-)$, the switching time t_0, and the transformer saturation characteristic $L_{sat,j}$. As criteria for overvoltages assessment H must be smaller than H_{limit}. Where the constant H_{limit} stands for the maximum allowable limit. It is defined by the system operator or restoration planner.

The above rule can only provide an approximate assessment of whether a restoration step is feasible or not with respect to the occurrence of harmonic overvoltages. It is therefore recommended to always carry out time-domain simulations when a certain level of H is exceeded. In order to keep the simulation time as short as possible in that case, a method for the reduction of the simulation time of PSB simulations is introduced in Section 7.3.3.

7.3.2 WORST SWITCHING CONDITION DETERMINATION

Normally for harmonic overvoltages analysis, worst case of the switching condition must be considered which is a function of switching time, transformer characteristics and its initial flux condition, and impedance characteristics of the switching bus [175]. Using the worst switching condition, the number of simulation for each case can be reduced significantly.

In order to determine worst case switching time, we define the following index as:

$$W = \sum_{h=2}^{10} Z_{jj}(h).I_j(h, t_0, \varphi_0) \tag{7.11}$$

Where t_0 is the switching time and φ_0 is initial transformer flux. This index can be a definition for the worst case switching condition. Using numerical algorithms we can find

the switching time for which W is maximum, i.e., harmonic overvoltages is maximum. In Section 5.A we will evaluate this index.

7.3.3 Criteria to Terminate Time-Domain Simulation

Although the methods introduced in the previous section allow for a reduction of the number of PSB time-domain simulations, it will be still necessary to perform a number of such simulations. In this chapter, we investigate the possibilities of finding appropriate criteria in order to terminate PSB transformer energization studies after a minimum amount of time, to limit the overall simulation time. The method is based on Short-Time Fourier Transform (STFT) analysis, since for one cycle the waveform damping is negligible. Sampling window is one cycle and the main (first) to 10^{th} harmonics are calculated. Then the sampling window is moved one cycle and the calculations are repeated. In each cycle the sum of the harmonic amplitudes are calculated:

$$A_{total} = A_1 + A_2 + ... + A_{10} \tag{7.12}$$

Where A_i is amplitude of i^{th} harmonic. The rate of amplitude change is given as:

$$\Delta A_{total}^{(n)} = A_{total}^{(n)} - A_{total}^{(n-1)} \tag{7.13}$$

Where $A_{total}^{(n)}$ is A_{total} in n^{th} cycle. The following heuristic rule is proposed for the algorithm:

If for 5 sequence cycles, the sign of ΔA_{total} is negative, and If the A_{total} is smaller than $A_{total,limit}$, then the simulation will be ended.

7.3.4 Remedial Action for Harmonic Overvoltages Control

There are several methods for preventing harmonic overvoltages:

I) Adding a load or a shunt element that lead to a decrease in the magnitude of the impedance, and consequently to a reduced amplification.

II) Bringing additional generators online: a higher number of generators results in a lower overall inductance, and consequently in a higher resonance frequency, according to the equation:

$$f_{resonance} = 1/2\pi\sqrt{L.C} \tag{7.14}$$

This means that if generators are added, the resonance peak is shifted to higher frequencies and if generators are omitted, it is shifted to lower frequencies.

III) Decreasing of the generators' scheduled voltage that leads to a proportional decrease of the pre-switching steady-state voltages. This effect results in a change of the transformer inrush current.

In the following section we explain the sensitivity analysis technique for selecting a suitable bus for admittance changes.

7.3.5 Sensitivity Analysis

A. Overview of the Algorithm

In cases where the power system, during a restoration procedure, has already grown to a considerable size, it is not always clear at which nodes admittance changes should be made in order to obtain an optimum impedance-frequency characteristic at the switching node. Therefore, a method is developed which determines the nodes where changes are most effective. The method is based on PSB harmonic analysis and sensitivity analysis for the harmonic frequencies. It is important to note that only those frequencies are of interest since the major components of the frequency spectrum of the voltages and currents in the system (as a result of transformer saturation) are multiples of the fundamental frequency f_0. The algorithm consists of four steps, which will be described in detail in the following sections:

1. Calculate the Thevenin equivalent circuit for the system.
2. Determine the sensitivity for each harmonic frequency.
3. Determine the weighting function for the inrush current.
4. Calculate the total sensitivity.

B. Thevenin Equivalent Circuit

In the first step of the procedure the multi-node Thevenin equivalent circuit is determined for the desired frequency range (here the frequencies up to $f = 10 f_0$ are considered to be sufficient). The terminals of this circuit consist of the bus where the next switching operation is to be performed and buses where parameters can be changed, i. e. where capacitors, reactances, generators, etc. can be switched in or out. Examples for buses with variable parameters are those where the number of generators can be varied, where loads can be changed or shunt reactances can be added.

In order to find the matrix representing the Thevenin equivalent circuit, currents of magnitude 1 p.u. are successively injected into each of the terminals. For this calculation, the voltage sources in the system are short circuited and other current sources are open circuited.

The voltages at the nodes of the Thevenin equivalent circuit then give, column by column, the matrix elements.

C. Individual Sensitivity

We define the sensitivity of an impedance as its magnitude's derivative with respect to an admittance change at each node of the Thevenin equivalent circuit. For a harmonic frequency h the sensitivity with respect to a change at node k is defined as:

$$S_{jk}(h) = \partial\left|Z_{jj}(h, \Delta Y_k)\right| \Big/ \partial\left|\Delta Y_k\right| \tag{7.15}$$

where Z_{jj} stands for the self impedance at bus j, ΔY_k for a change in admittance at bus k, and $\partial(\Delta Y_k)$ for a very small number representing an incremental perturbation. Performing the same operation for all the nodes 1 …, k,…, n of the Thevenin equivalent circuit then gives the sensitivity vector for the harmonic frequency h:

$$\boldsymbol{S}(h) = \left[S_{j1}(h) \quad \ldots \quad S_{jk}(h) \quad \ldots \quad S_{jn}(h)\right]^{\mathrm{T}} \tag{7.16}$$

If only sensitivities for single frequencies are considered, the vectors can be normalized by referring the vector S(h) to the value of its maximum element, i. e. we get

$$\overline{\boldsymbol{S}}(h) = \frac{1}{max_i(S_{ji}(h))} . \boldsymbol{S}(h) \tag{7.17}$$

Since we deal with either resistive, inductive or resistive-inductive changes depending on the available devices, two different sensitivity vectors can be defined, one for resistive ($\mathbf{S_R}$) and one for inductive ($\mathbf{S_I}$) changes. This is also reflected in the incremental change $\partial(\Delta Y_k)$, which in the case of resistive changes can be defined as a real number and in the case of inductive changes as an imaginary number. Capacitive changes can be considered as negative inductive changes.

D. Total Sensitivity

Calculating the sensitivities for each of the harmonics results in a sensitivity matrix, defined as:

$$\boldsymbol{S} = \begin{bmatrix} S_{11,2f_0} & S_{11,3f_0} & \cdots & S_{11,10f_0} \\ S_{12,2f_0} & S_{12,3f_0} & \cdots & S_{12,10f_0} \\ \vdots & \vdots & & \vdots \\ S_{1n,2f_0} & S_{1n,3f_0} & \cdots & S_{1n,10f_0} \end{bmatrix} \tag{7.18}$$

An overall sensitivity taking into account the sensitivities for all the harmonics up to a frequency of $f = 10f_0$ can then be calculated using a weighting vector

$$\boldsymbol{I}_w = \left[I_{w,2f_0} \quad I_{w,3f_0} \quad \cdots \quad I_{w,10f_0}\right]^{\mathrm{T}} \tag{7.19}$$

and the matrix multiplication

$$\boldsymbol{S}_{total} = \boldsymbol{S}.\boldsymbol{I}_w = \begin{bmatrix} \sum_{h=2}^{10} (S_{11,h}.I_{w,h}) \\ \sum_{h=2}^{10} (S_{12,h}.I_{w,h}) \\ \vdots \\ \sum_{h=2}^{10} (S_{1n,h}.I_{w,h}) \end{bmatrix} \tag{7.20}$$

where n stands for the number of buses where changes are possible.

E. Weighting Vector

The lower harmonics of transformer inrush currents are of higher magnitude than the higher ones. Therefore a resonance peak at a lower harmonic is worse with respect to resonant overvoltages conditions than one at a higher harmonic. Consequently, changes at lower harmonics are considered more important than changes at higher harmonics. This is taken into account by a weighting vector $\mathbf{I}_w$ which is based on the harmonic characteristic of the transformer inrush current. This characteristic is either given by the manufacturer or can be obtained by simulating the energization of an unloaded transformer using the PSB and taking the Fast Fourier Transform (FFT) of the inrush current. Another method is to use approximate equations such as given e.g. in [22, 175].

In order to find a suitable weighting vector $\mathbf{I}_w$, a normalized current for each transformer terminal voltage V_T is calculated as:

$$\bar{I}(h,V_T) = I(h,V_T)/max_h(I(h,V_T)) \tag{7.21}$$

where h stands for the harmonic frequency and V_T for the pre-switching steady-state transformer voltage. We then obtain the normalized average by

$$\boldsymbol{I}_w(h) = \frac{\sum_{V_T=V_{T,min}}^{V_{T,max}} \bar{I}(h)}{max_h(\sum_{V_T=V_{T,min}}^{V_{T,max}} \bar{I}(h))} \tag{7.22}$$

7.3.6 Steps of Assessment and Analysis of Harmonics Overvoltages

The steps for harmonic overvoltages assessment and analysis are listed below:

1) Determine characteristics of transformer that must be energized
2) Calculation of $Z_{ii}(h)$ at the transformer bus
3) Calculation of H index using Equation.(7.10)
4) If $H > H_{limit}$, then perform remedial action based on sensitivity analysis and go to step3
5) If $H < H_{limit}$, calculate the worst switching condition for harmonic overvoltages simulation
6) Run PSB simulation for 1 cycle
7) Calculate the criteria for terminating the simulation
8) Go to step 6 to continue the simulation
9) If there is overvoltages, then perform remedial action based on sensitivity analysis and go to step3
10) End (go to next restoration step)

Figure 7.4 shows the flow chart of harmonic overvoltages assessment and analysis.

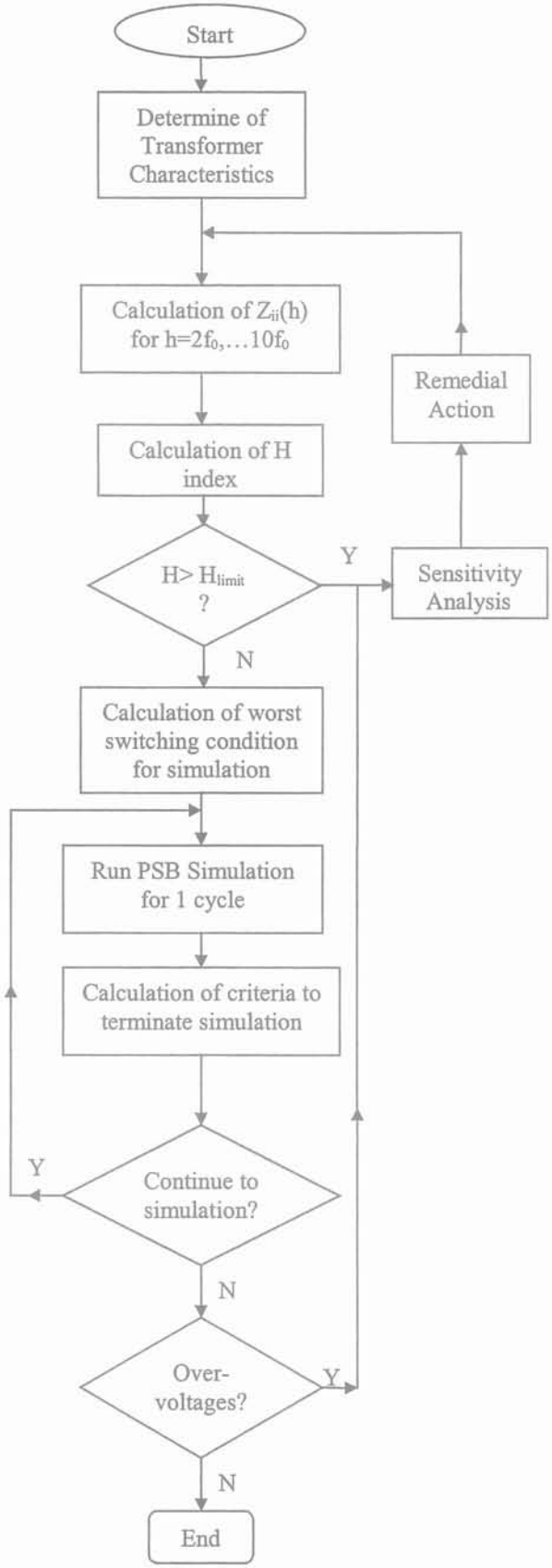

Figure 7.4: Flow chart of harmonic overvoltages assessment and analysis

7.4 CASE STUDY

In this section the proposed algorithms are tested for two case study that are a portion of 39 bus New England test system, which its parameters are listed in Appendix-A.

7.4.1 CASE 1

Figure 7.5 shows one line diagram of a portion of 39 bus New England test system which is in restorative state. Generator at bus 30 is a black-start unit and generator at bus 39 is a non-black-start unit. The load 39 presents cranking power of the later generator that must be restored by transformer of bus 39. In this condition harmonic overvoltages can be resulted because the transformer is lightly loaded.

Figure 7.6 shows the result of the PSB frequency analysis at bus 39. The magnitude of the Thevenin impedance, seen from bus 39, Z_{bus39} shows a parallel resonance peak at the 232Hz. When the transformer is energized, this resonance condition can produce overvoltages.

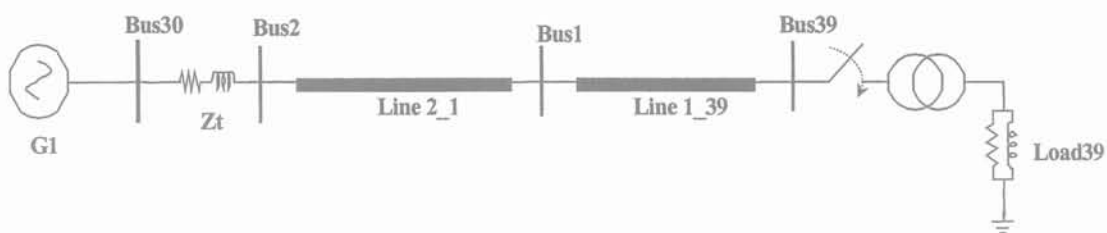

Figure 7.5: Power system at the beginning of a restoration procedure

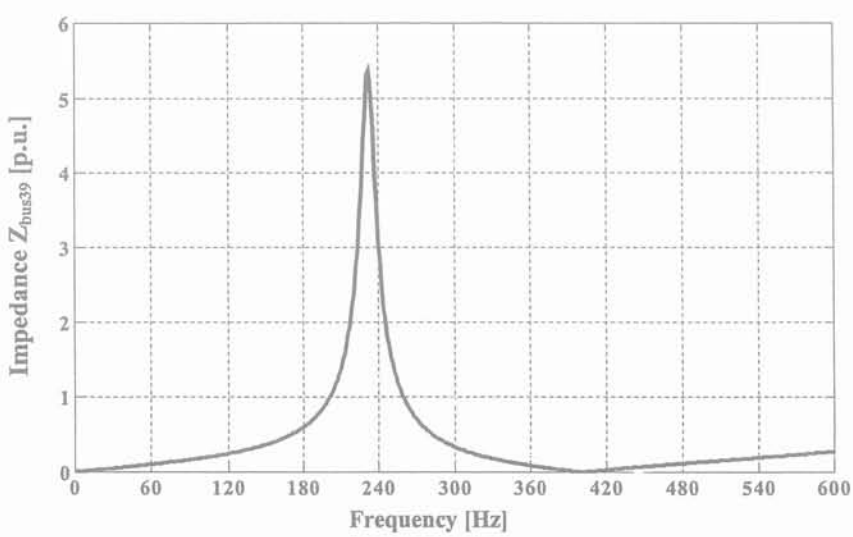

Figure 7.6: Impedance at bus 39

A. Determination of Worst Switching Condition

Figure 7.7 shows changes of harmonic currents and W index with respect to α (Equation.(7.6)).

Figure 7.8 shows voltage at bus 39 after transformer switching for the worst case condition.

Table 7.1 summarizes the results of overvoltages simulation for 3 different switching conditions that verify the effectiveness of W index. Harmonic overvoltages of bus 39 for other conditions are plotted in Figures 7.9 and 7.10

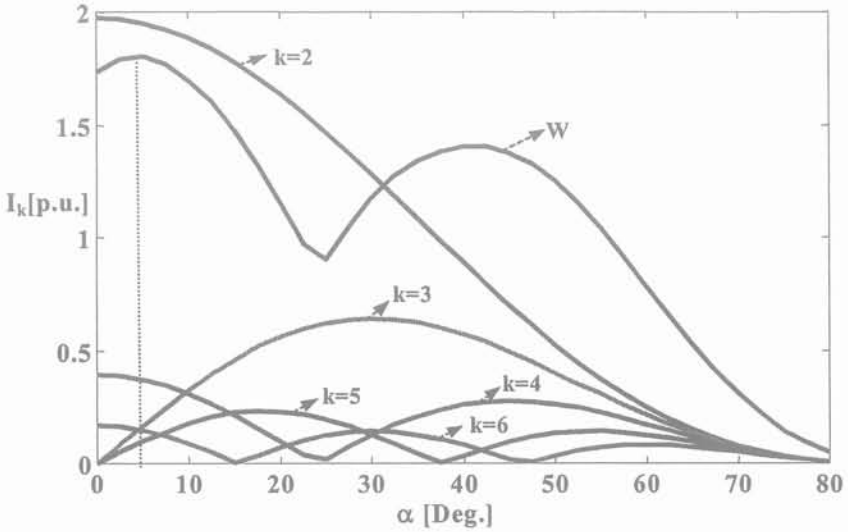

Figure 7.7: Changes of harmonic currents and W index with respect to α

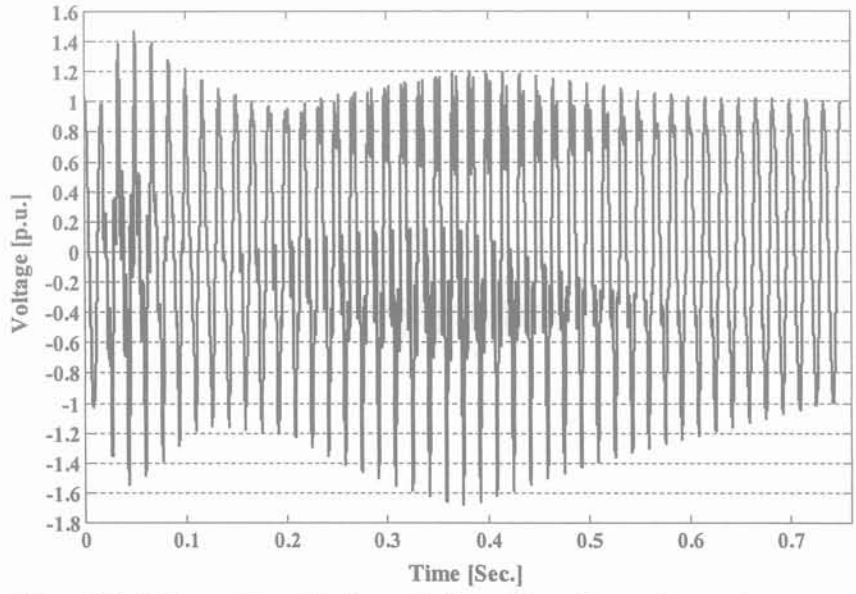

Figure 7.8: Voltage at bus 39 after switching of transformer for worst case condition

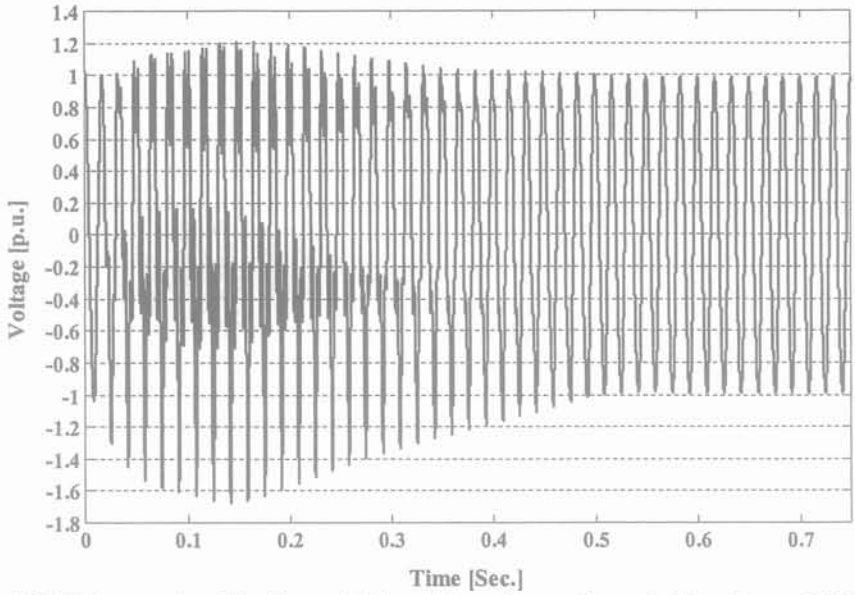

Figure 7.9: Voltage at bus 39 after switching of transformer for switching time = 0.0097976 Sec.

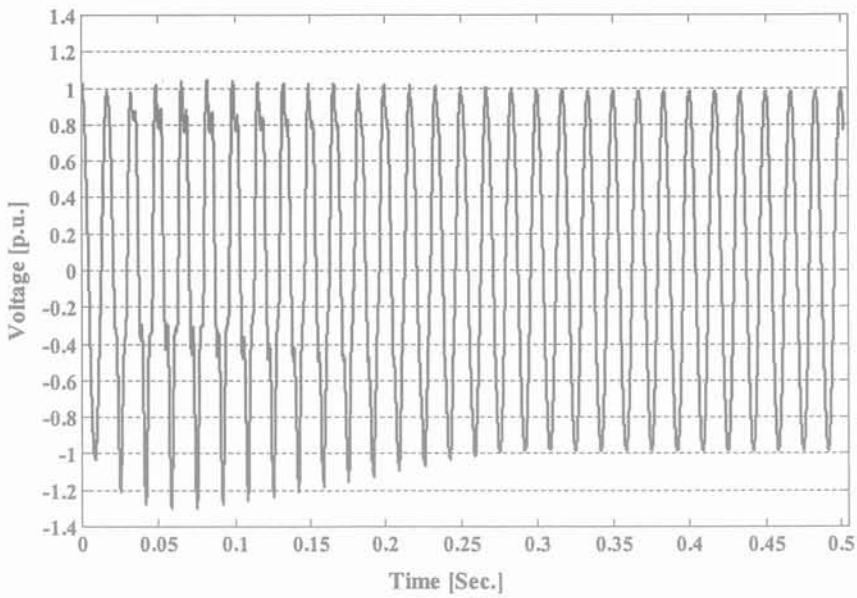

Figure 7.10: Voltage at bus 39 after switching of transformer for switching time = 0.0092366 Sec.

Table 7.1: Effect of Switching time on the Maximum of Overvoltage and Duration of V_{peak} >1.3 p.u.

Switching Time (Sec.)	α (Deg.)	V_{PEAK} (p.u.)	Duration of V_{PEAK} >(1.3 p.u.) (Sec.)
0.012018	5.0	1.67	0.385
0.0097976	42.5	1.67	0.323
0.0092366	60.0	1.29	0.000

B. Assessment of Harmonic Overvoltages

In order to control harmonic overvoltages, there are 4 different solutions:

- Adding load to bus 1,
- Adding shunt reactor to bus 1,
- Decreasing terminal voltage of generator at bus 30,
- Bringing additional generators online.

Figure 7.11 shows the impedance at bus 39 after each operation to control harmonic overvoltages. Also, Figures 7.12 to 7.15 demonstrate harmonic overvoltages at bus 39 after these operations. Table 7.2 summarizes results of simulations for these cases, where H index for each case is calculated. It can be seen from this table that suitable value for H_{limit} in this system is 1. Also note that adding reactor at bus 1 increases overvoltages which is not a suitable solution.

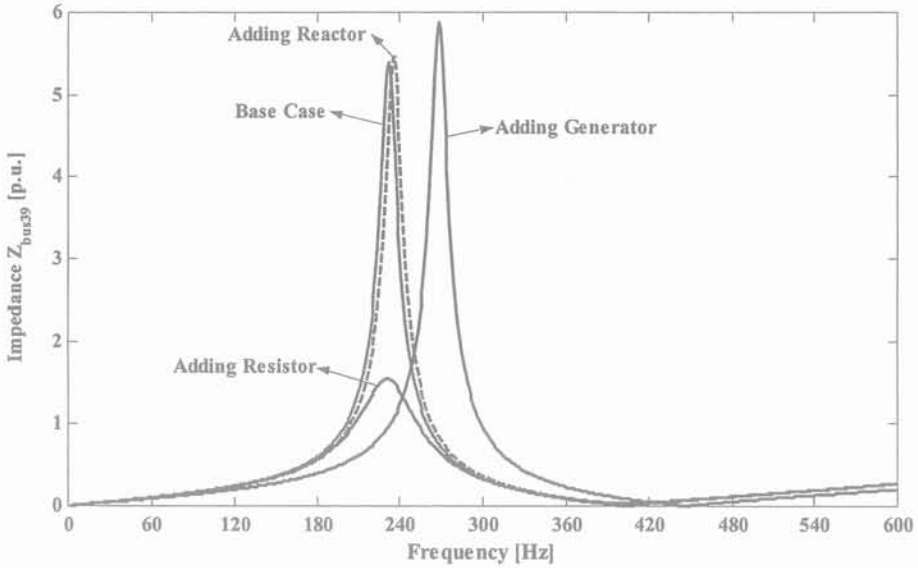

Figure 7.11: Impedance at bus 39 for different cases

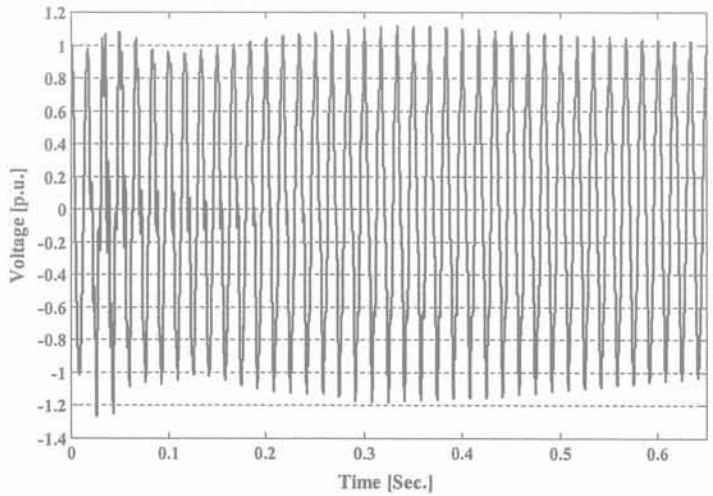

Figure 7.12: Voltage at Bus 39 after bringing additional generators online

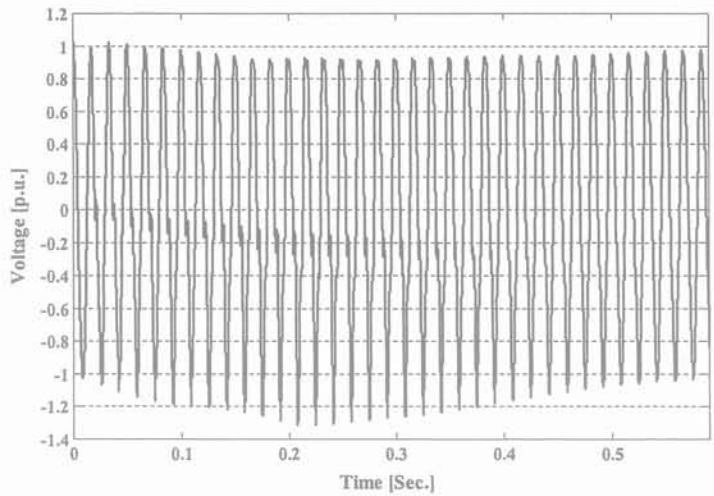

Figure 7.13: Voltage at Bus 39 after adding a resistive load at Bus 1

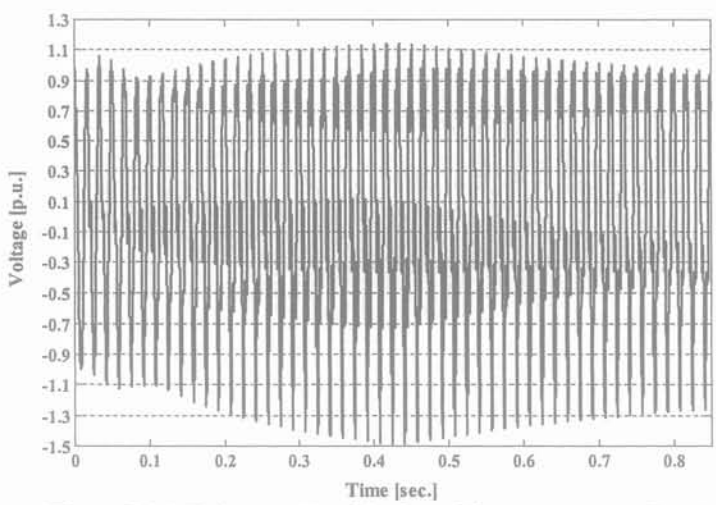

Figure 7.14: Voltage at Bus 39 after adding a reactor at Bus 1

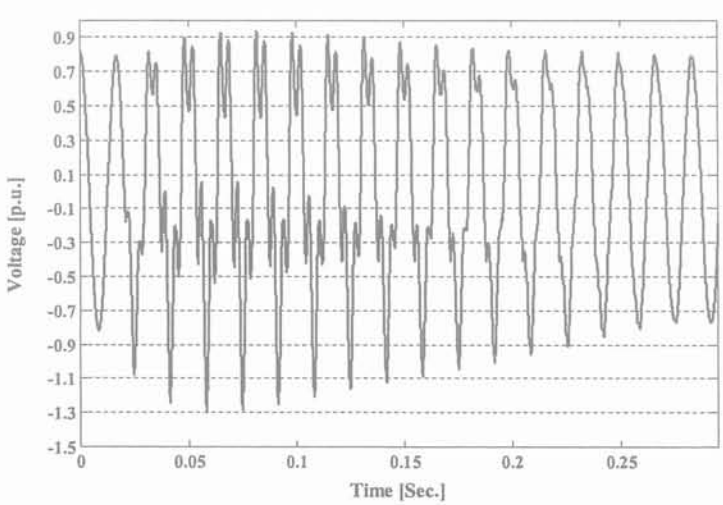

Figure 7.15: Voltage at Bus 39 with decreasing generator terminal voltage

Table 7.2: H index for different cases

CASE	H	V_{PEAK} (p.u.)	Duration of (V_{peak} >1.3 p.u.)(Sec.)
Base Case	1.6	1.67	0.385
bringing additional generators online	0.8	1.26	0
Adding Resistive Load	0.9	1.299	0
Adding Reactor	2.0	1.49	0.53
Decreasing Generator Voltage	1.0	1.298	0

7.4.2 CASE 2

As another example, the system in Figure 7.16 is examined. It represents the same system as the one in Figure 7.5, but with few restoration steps later. After starting up the black-start unit at bus 30, generators at bus 39 and 37 are restarted, respectively. In the next step, unit at bus 29 must be restarted. In order to provide cranking power for this unit, transformer at bus 29 should be energized. In this condition harmonic overvoltages can be produced because the load of the transformer is small. Figure 7.17 shows the result of the PSB frequency analysis at bus 29. The magnitude of the Thevenin impedance, seen from bus 29, Z_{bus29} shows a parallel resonance peak at the 170 Hz. Figures 7.18 and 7.19 illustrate voltage at bus 29 and current of transformer after switching, respectively.

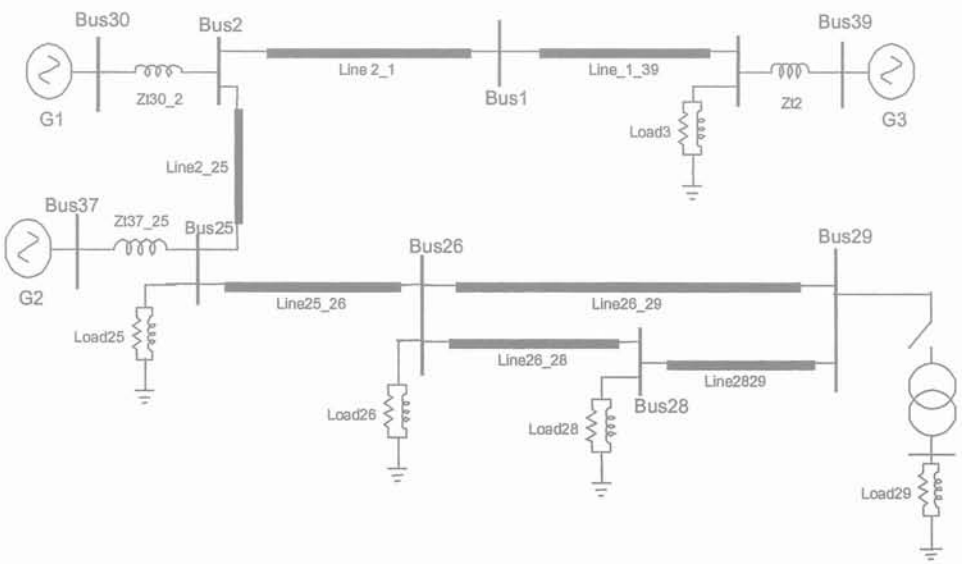

Figure 7.16: Studied system for Case 2

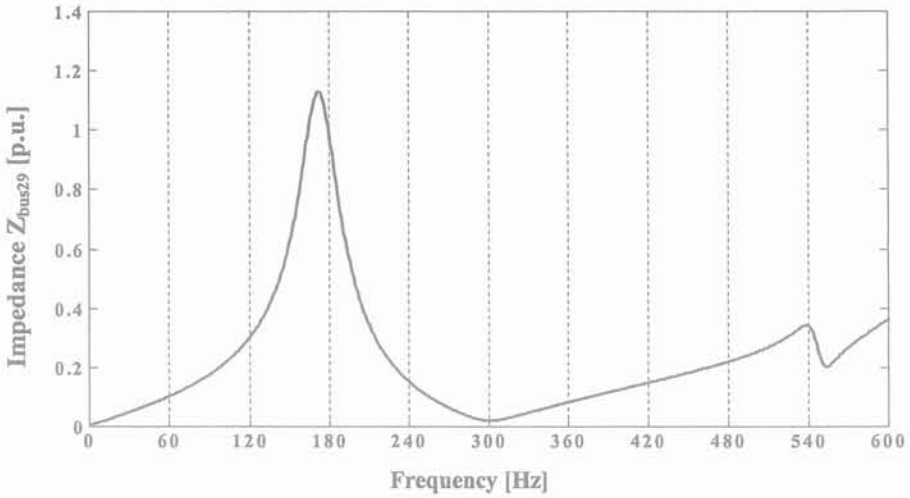

Figure 7.17: Impedance at bus 29

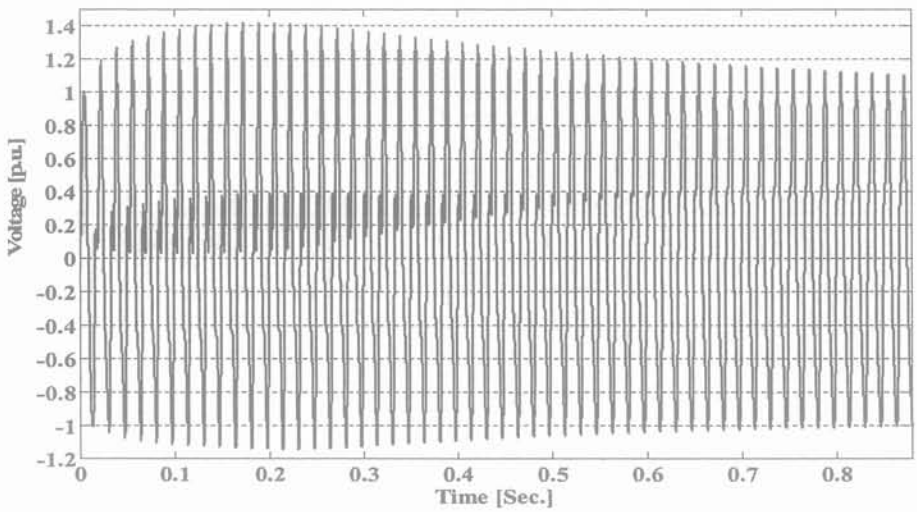

Figure 7.18: Voltage at bus 29 after switching of transformer

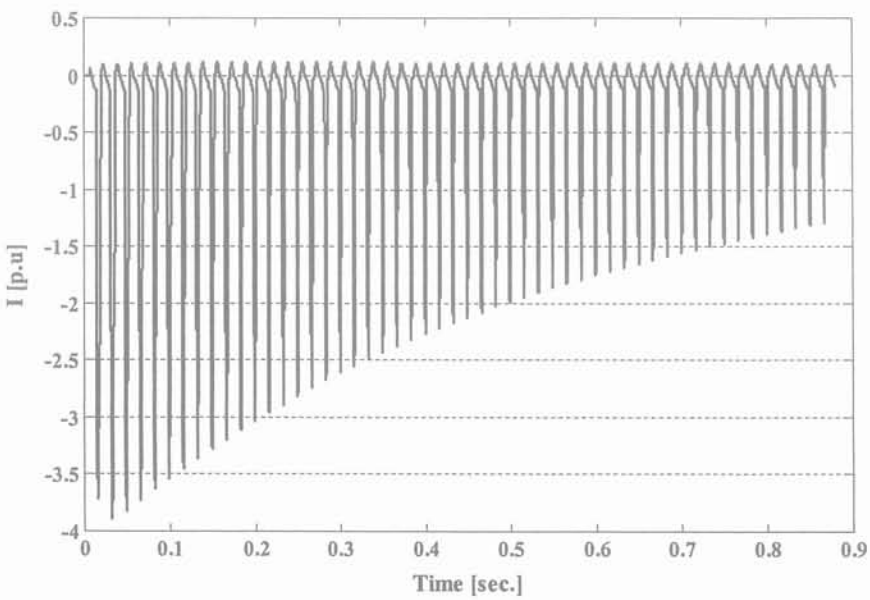

Figure 7.19: Current waveform after transformer energization

A. Harmonic Analysis

Figure 7.20 to 7.23 show the main, second, third, and fourth harmonic waveforms. The other harmonics are negligible. The amplitudes of these harmonics and sum of them are plotted in Figure 7.17. Both Figures 7.25 and 7.26 show the PSB simulation result, where the predicted signal (as sum of the first 4 harmonics) is also displayed. It is so close to the PSB simulation result that the differences are barely noticeable.

B. Criteria to Terminate Time-Domain Simulation

The proposed algorithm (in Section 7.3.3) terminates the PSB simulation after m = 30 STFT analyses (or 0.5 Sec.). Figure 7.25 illustrates harmonic overvoltages during 30 cycle that contain overvoltages pick and duration of V_{peak} greater than 1.3 p.u. This example denotes the efficiency of the proposed algorithm to terminate time domain simulation.

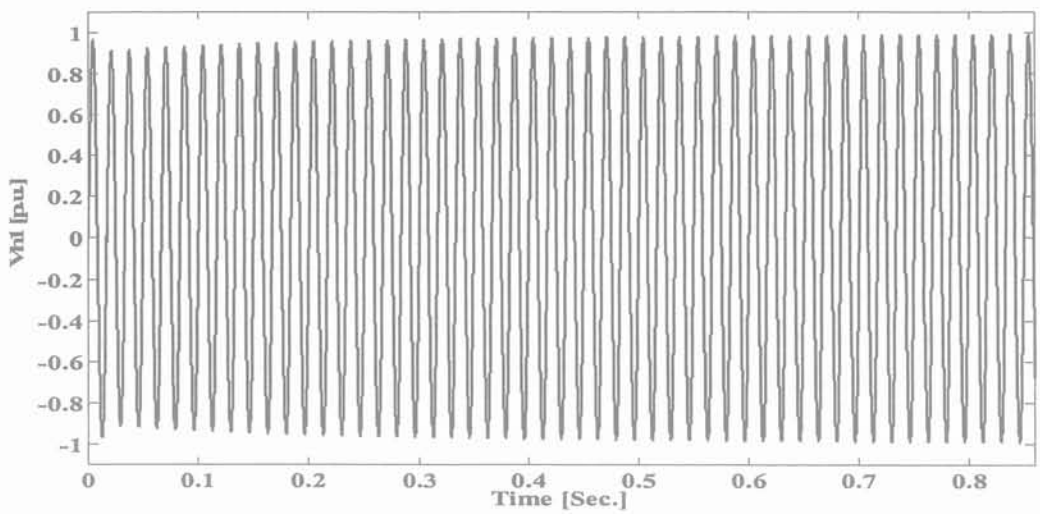

Figure 7.20: The main harmonic voltage at bus 29

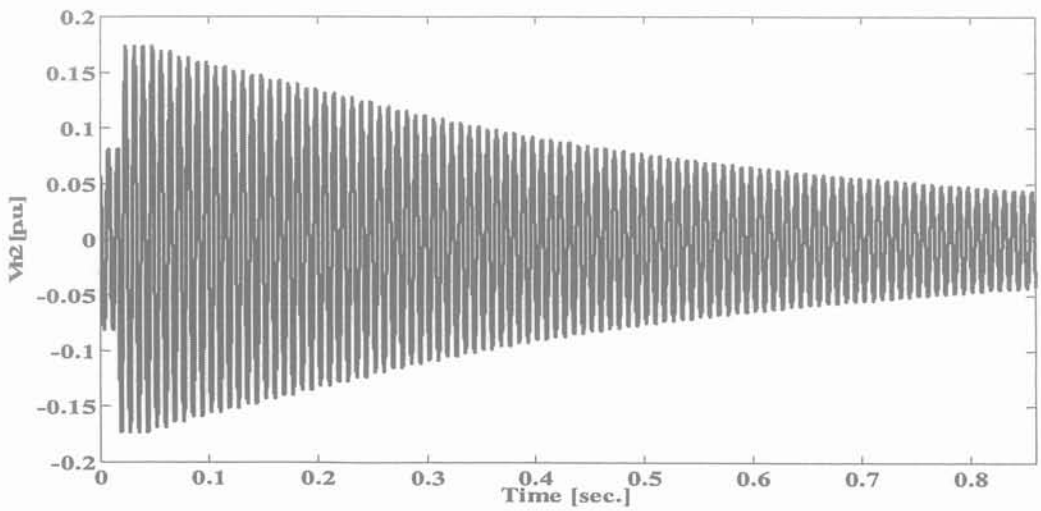

Figure 7.21: The second harmonic voltage of bus 29

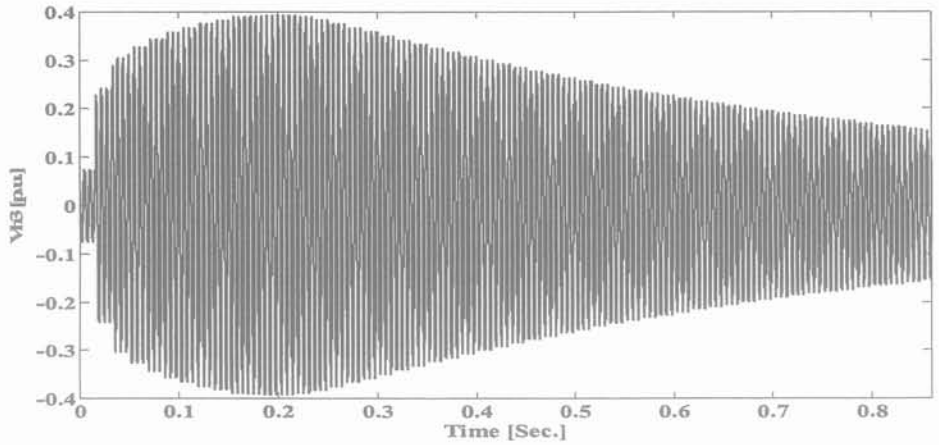

Figure 7.22: The third harmonic voltage of bus 29

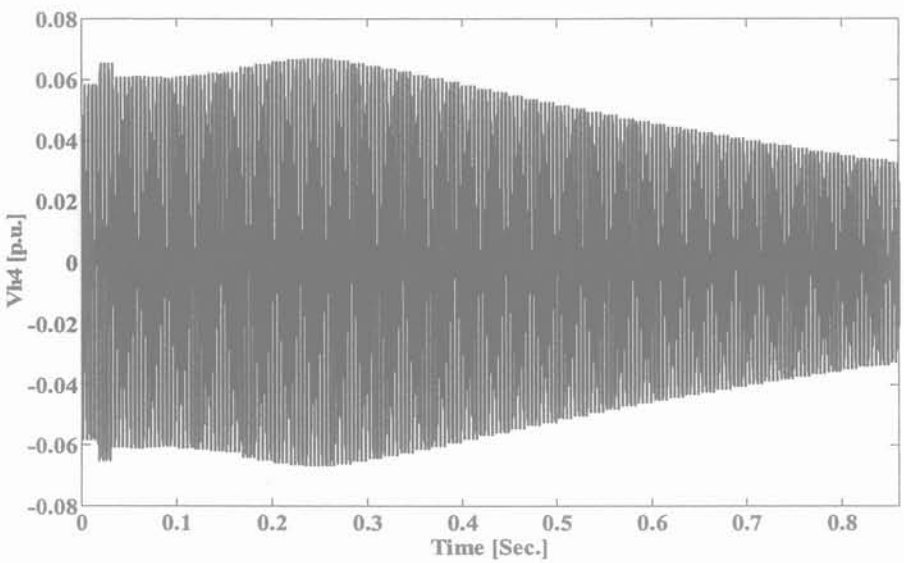

Figure 7.23: The fourth harmonic voltage of bus 29

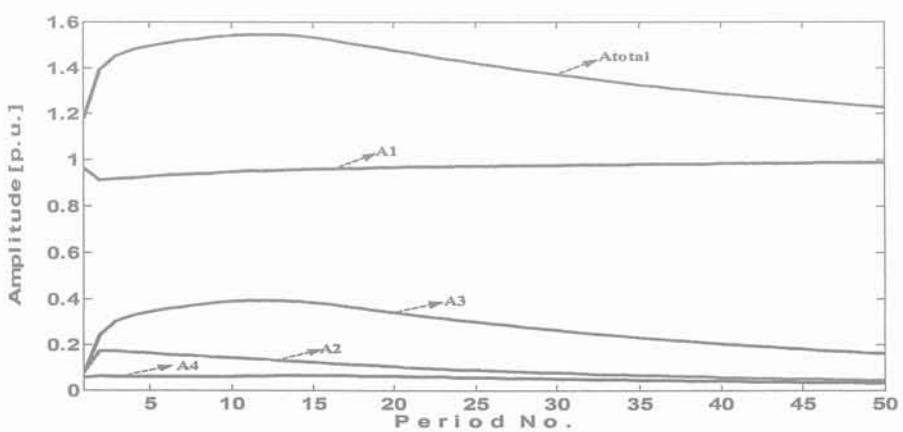

Figure 7.24: Amplitude of voltage harmonics at bus 29

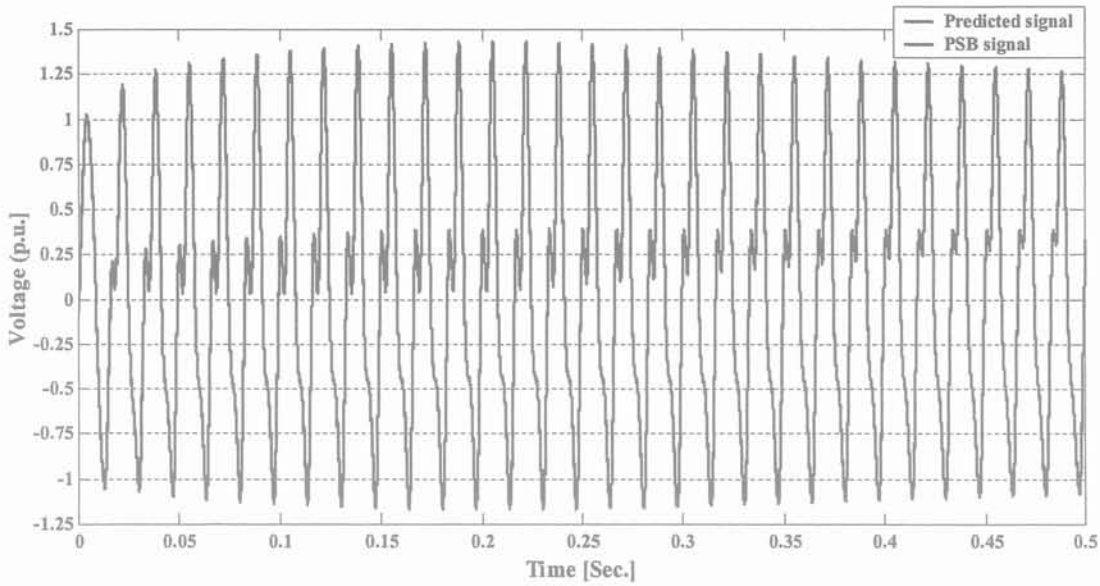

Figure 7.25: PSB signal and predicted signal

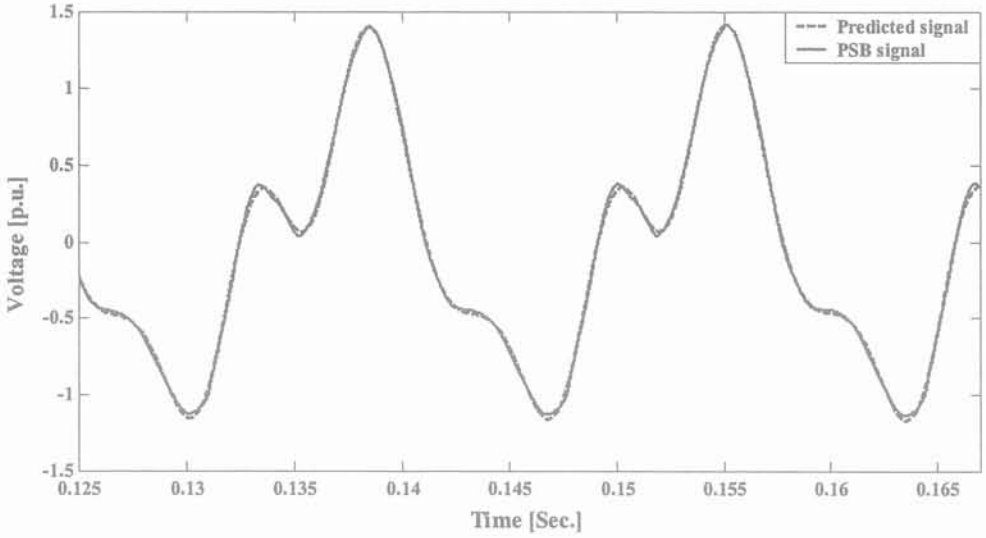

Figure 7.26: PSB signal and predicted signal near the overvoltages peak

C. Sensitivity Analysis

The impedance sensitivity at bus 29 is investigated with respect to changes at buses 28, 26, 25, and 39. The elements of the resistive sensitivity vector $\mathbf{S_R}$ and of the inductive sensitivity vector $\mathbf{S_I}$ can be found in Table 7.3 and 7.4. In order to investigate the validity of these results, the impedance at bus 29 as a function of impedance changes at the selected buses is calculated. The result of resistive changes are depicted in Figures 7.27 to 7.29 for second, third and fourth harmonics, respectively. Note that the impedance changes are not similar for different harmonics. For example the impedance at fourth harmonic will be increased while the resistive load is added to bus 26. Also, maximum of impedance changes is related to third harmonic.

Figures 7.30 to 7.32 demonstrate the impedance at bus 29 as function of inductive changes at the selected buses for second, third and fourth harmonics, respectively. Note that the impedance will be increased for third and fourth harmonics while inductive load is added to the buses. Therefore adding reactor is not suitable for control of harmonic overvoltages. The result for the weighting function is depicted in Figure 7.20. The results for the total resistive and inductive sensitivities can be found in Table 7.5. This table denote that the most effective changes in order to reach an optimum resonance condition are changes of the resistances at bus 29, 28 and 26, respectively. Inductive changes should be avoided at all buses.

Table 7.3: Sensitivity vectors for Resistive changes

Bus No.	S_R at 120 HZ	S_R at 180 HZ	S_R at 240 HZ
29	-1	-1	-1
28	-0.8989	-0.9616	-0.2883
26	-0.4678	-0.5844	0.193
25	-0.0422	-0.0442	0.0834
39	0	0	0

Table 7.4: Sensitivity vectors for inductive changes

Bus No.	S_I at 120 HZ	S_I at 180 HZ	S_I at 240 HZ
29	-1	0.6892	0.3394
28	-0.6487	1	1
26	-0.3154	0.6412	0.7901
25	-0.0221	0.0583	0.0653
39	0	0	0

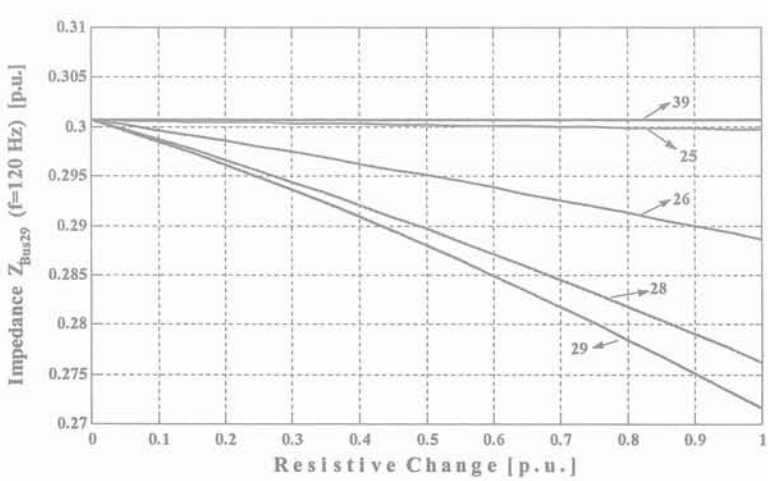

Figure 7.27: Impedance Z_{bus29}(f=120 Hz) as a function of resistive changes

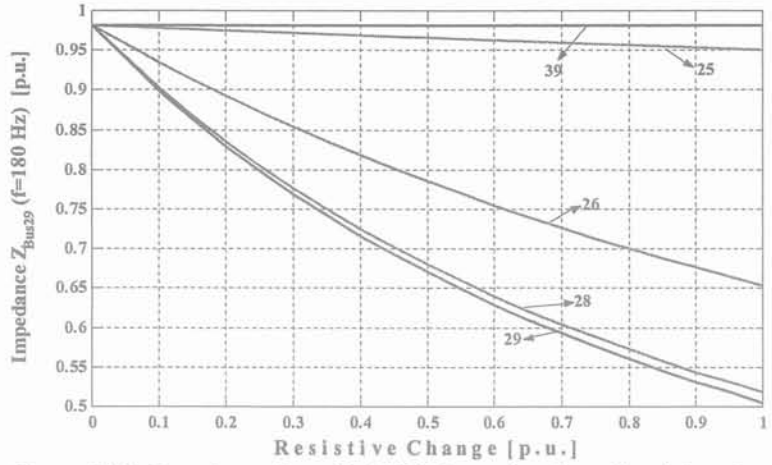

Figure 7.28: Impedance Z_{bus29}(f=180 Hz) as a function of resistive changes

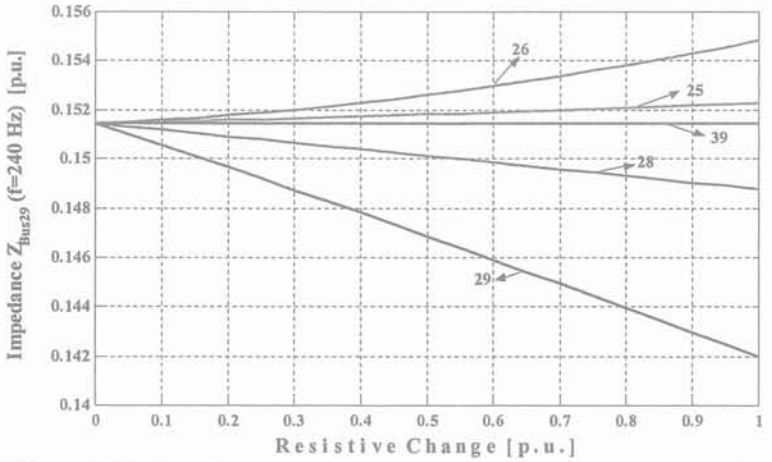

Figure 7.29: Impedance Z_{bus29}(f=240 Hz) as a function of resistive changes

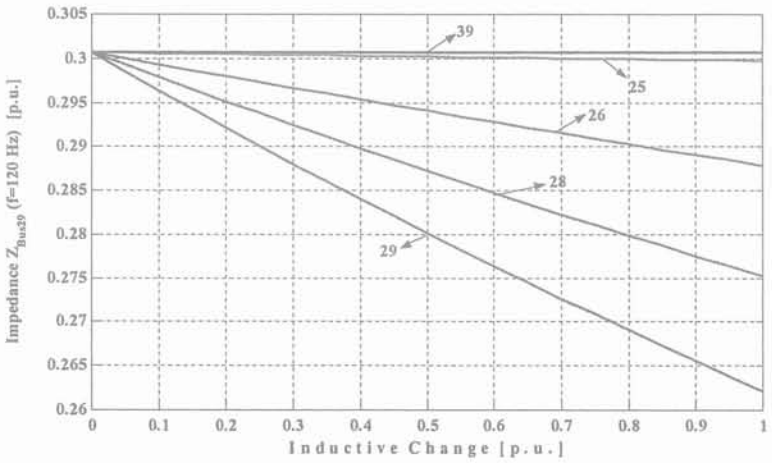

Figure 7.30: Impedance Z_{bus29}(f=120 Hz) as a function of inductive changes

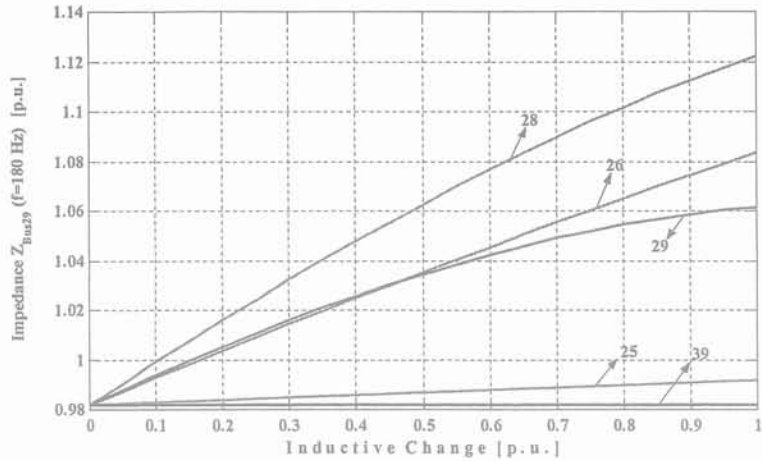

Figure 7.31: Impedance Z_{bus29}(f=180 Hz) as a function of inductive changes

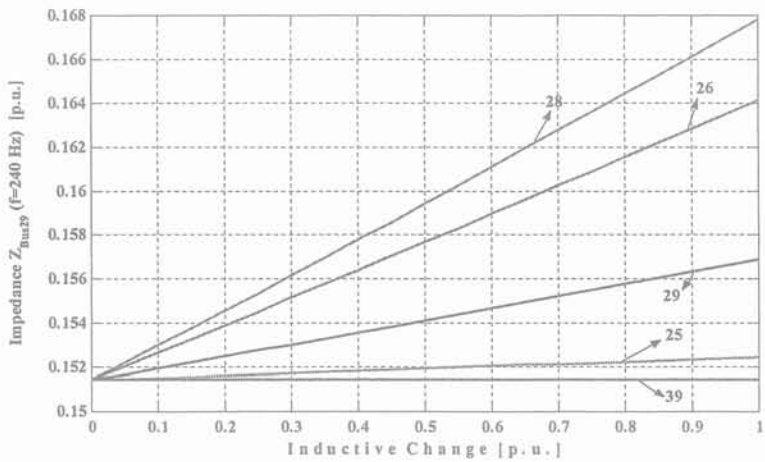

Figure 7.32: Impedance Z_{bus29}(f=240 Hz) as a function of inductive changes

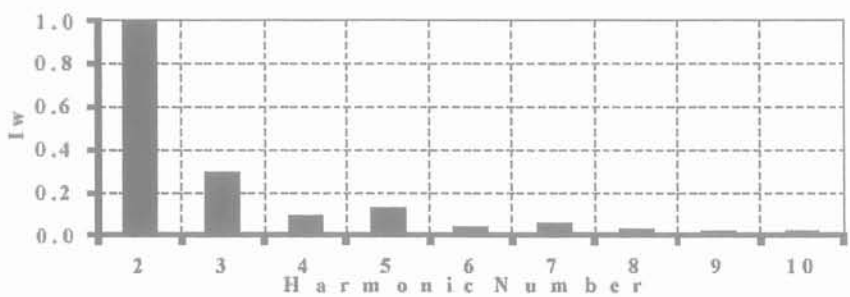

Figure 7.33: Weighting function I_w

Table 7.5: Total Sensitivity vectors

Bus No.	29	28	26	25	39
S_R_total	-1	-0.956	-0.574	-0.044	-1.93e-9
S_I_total	0.025	1	0.764	0.077	2.05e-9

7.5 SUMMARY

In this chapter, a methodology that assesses the feasibility of restoration steps with respect to harmonic overvoltages has been outlined.

The proposed method can be used to estimate whether an overvoltage occurs and whether time-domain need to be carried out. In the case of time-domain simulations, a method is introduced that allows to shorten the simulation time using a method based on Short-Time Fourier Transform.

When overvoltage problems occur, the most efficient remedial action is determined by sensitivity analysis. The simulation time could be reduced significantly, resulting in more efficient restoration planning studies with respect to harmonic resonance overvoltages.

The validity of the methods has been shown using several examples based on IEEE 39-Bus New England test system.

CHAPTER 8

CONCLUSIONS AND RECOMMENDATIONS FOR FUTURE WORK

CHAPTER 8

CONCLUSIONS AND RECOMMENDATIONS FOR FUTURE WORK

This dissertation presents new approaches for power system restoration. The results of an extensive bibliographical research showed that there is a need for a methodology that allows one to assess restoration steps quickly and efficiently, and that supports operators during on-line restoration, and system planners during restoration planning. Moreover, it revealed that models and modeling techniques that help to take into account the abnormal voltage and frequency conditions during restoration are needed.

The approach's principle is based on a subdivision of the aggregation of complex phenomena encountered during the restoration process into simpler problems that can be assessed using efficient approaches. The proposed approaches allow for fast screening of the large number of possible combinations of restoration steps, and support the selection of the most promising restoration actions.

The long term dynamics simulation program that have been developed for this thesis allow simulations of the large deviations in frequency and voltage that are of particular concern during the black or emergency start phase of a system restoration procedure. Special emphasis is thereby given to the frequency behavior after load pick-up. This simulator, also, can be used for operator training purposes.

The major conclusions and contributions of this work are:

- Description of an approach for units start-up sequence determination during system restoration. This approach is based on backtracking search method, which determines the generating starting times to maximize the MWH generated over a restoration period and guarantees optimality of the start up sequence. The dynamic characteristics of different types of units have been considered.
- Development of a method for calculating prime movers frequency response during restoration. It determines the maximum load pick-up within the allowable system frequency dip for each bus and each stage of load restoration. This method also

considers dynamics of frequency response of prime movers and loads. A suitable form is used for frequency behavior during load reconnection, which change differential equations of the system into algebraic equations to find the minimum frequency. The proposed method is suitable for on line operator guiding to select load steps, and/or to compute the minimal frequency for a given load step during system restoration.

- Development of an approach for reduction of Standing Phase Angle (SPA) difference between two buses of a power system during system restoration. SPA difference must be within specific limits before an attempt is made to close breakers to firm up the bulk power transmission network. The proposed method, offers a fast algorithm that considers all operational constraint. If SPA difference isn't reduced to a desired value by generation rescheduling, then it is reduced by load shedding.
- Description of a methodology to assess the feasibility of restoration steps with respect to harmonic overvoltages. The proposed method can be used to estimate whether an overvoltage occurs and whether time-domain need to be carried out. In the case of time-domain simulations, a method is introduced that allows to shorten the simulation time using a the Short-Time Fourier Transform. When overvoltage problems occur, the most efficient remedial action is determined by sensitivity analysis.

In summary, the new approaches give an assessment of the feasibility of restoration steps. By eliminating infeasible restoration sequences, the overall restoration time can be reduced significantly.

The following studies are suggested for future research:

- The proposed method for calculating prime movers frequency response could be used for the design of load shedding schemes that are in use, e. g. when the system disintegrates into several islands with the system frequencies below the allowable limits.
- Rules that help to assess transient switching overvoltages could be investigated.
- The possibility of replacing Short-Time Fourier Transform analysis by a method such as wavelets that is more suitable for time-frequency analysis should be explored.
- Rules that cover other parts of the restoration process, such as the integration of subsystems or the protection system, could be developed.
- Uncertainties of data during restoration and development a method to handle them can be investigated.

BIBLIOGRAPHY

BIBLIOGRAPHY

[1] M. M. Adibi, R. W. Alexander, and D.P. Milanicz, "Energizing High and Extra-High Voltage Lines during Restoration," IEEE Transactions on Power Systems, vol. 14, no. 3, pp. 1121-1126, August 1999.

[2] M. M. Adibi and L. H. Fink, "Power System Restoration Planning," IEEE Transactions on Power Systems, vol. 9, no. 1, pp. 22-28, February 1994.

[3] M. M. Adibi and R. J. Kafka, "Power System Restoration Issues," IEEE Computer Applications in Power, vol. 4, no. 2, pp. 19-24, April 1991.

[4] M.M. Adibi, "Local Load Shedding," IEEE Transactions on Power Systems, vol. 3, no. 3, August 1988.

[5] M.M. Adibi, J.N. Borkoski, R.J. Kafka, and T.L. Volkmann, "Frequency Response of Prime Movers during Restoration," IEEE Transactions on Power Systems, vol. 14, no. 2, pp. 751-756, May 1999.

[6] M.M. Adibi and D.P. Milanicz, "Reactive Capability Limitation of Synchronous Machines," IEEE Transactions on Power Systems, vol. 9, no. 1, pp. 29-40, February 1994.

[7] M.M. Adibi and D.P. Milanicz, "Estimating Restoration Duration," IEEE Transactions on Power Systems, vol. 14, no. 4, pp. 1493-1498, November 1999.

[8] M.M. Adibi, D.P. Milanicz, and T.L. Volkmann, "Simulating Transformer Taps for Remote Cranking Operations," IEEE Computer Applications in Power, vol. 9, no. 3, pp. 24-29, July 1996.

[9] M.M. Adibi, D.P. Milanicz, and T.L. Volkmann, "Asymmetry Issues in Power System Restoration," IEEE Transactions on Power Systems, vol. 14, no. 3, pp. 1085-1091, August 1999.

[10] M.M. Adibi, D.P. Milanicz, and T.L. Volkmann, "Optimizing Generator Reactive Power Resources," IEEE Transactions on Power Systems, vol. 14, no. 1, pp. 319-326, February 1999.

[11] E. Agneholm, "The Restoration Process following a Major Breakdown in a Power System," Tech. Rep., Chalmers University of Technology, Department of Electric Power Engineering, Goeteburg, Sweden, 1996, Licentiate Thesis, No.230L.

[12] E. Agneholm, Cold Load Pick-up, Ph.D. thesis, Chalmers University of Technology, Department of Electric Power Engineering, Goeteburg, Sweden, 1999.

[13] E. Agneholm and J.E. Daalder, "Shunt Reactor Behaviour during Power System Restoration," in International Symposium on Modern Electric Power Systems, Wroclaw, Poland, September 1996, pp. 154-161.

[14] O. Alsac, B. Stott, and W.F. Tinney, "Sparsity-Oriented Compensation Methods for Modified Network Solutions," IEEE Transactions on Power Apparatus and Systems, vol. 102, no. 5, pp. 1050-1060, May 1983.

[15] J.J. Ancona, "A Framework for Power System Restoration following a Major Power Failure," IEEE Transactions on Power Systems, vol. 10, no. 3, pp. 1480-1483, April 1988.

[16] P.M. Anderson and M. Mirheydar, "A Low-Order System Frequency Model," IEEE Transactions on Power Systems, vol. 5, no. 3, pp. 720-729, August 1990.

[17] P.F. Arnold, "Summary of System Restoration Plan for the Pacific Northwest Power System," in Proceedings of the IEEE/PES Winter Meeting, New York, NY, USA, 1982.

[18] M.S. Baldwin and J.S. Schenkel, "Determination of Frequency Decay Rates during Periods of Reduced Generation," IEEE Transactions on Power Apparatus and Systems, vol. PAS-95, no. 1, pp. 26-36, January/February 1976.

[19] M.H. El Banhawy, A.T. Johns, and M.M. Elkateb, "Planning of Frequency-Constrained Generation Margins," in First Symposium on Electrical Engergy in the United Arab Emirates, April 1988.

[20] L.R. Blessing, C.K. Bush, and S.J. Yak, "Automated Power System Restoration Planning incorporating Expert System Techniques," in Proceedings of the Second Symposium on Expert System Applications to Power Systems, Seattle, WA, USA, July 1989, pp. 133-139.

[21] P.G. Bollaris, J.M. Prousalidis, N.D. Hatziargyriou, and B.C. Papadias, "Simulation of Long Transmission Lines Energization for Black Start Studies," in Proceedings of the 7th Mediterranean Electrotechnical Conference, Antalya, Turkey, 1994.

[22] O. Bourgault and G. Morin, "Analysis of Harmonic Overvoltage due to Transformer Saturation following Load Shedding on Hydro-Quebec - NYPA 765 kV Interconnection," IEEE Transactions on Power Delivery, vol. 5, no. 1, pp. 397-405, January 1990.

[23] British Electricity International, *Modern Power Station Practice*, vol. C, D, G. Pergamom, 1991.

[24] A.M. Bruning, "Cold Load Pickup," IEEE Transactions on Power Apparatus and Systems, vol. PAS-98, no. 4, pp. 1384-1386, July/August 1979.

[25] E. G. Cate, K. Hemmaplardh, J. W. Manke and D. P. Gelopulos, "Time Frame Notion and Time Response of the Models in Transient, Midterm and Long term Stability Programs," IEEE Trans. on PAS, pp. 143-151, January 1984.

[26] M.L. Chan, R.D. Dunlop, and F.C. Schweppe, "Dynamic Equivalents for Average System Frequency Behavior following Major Disturbances," in Proceedings of the IEEE/PES Winter Meeting, New York, USA, January/February 1972.

[27] E. Cheres, "Small and medium size Drum Boiler Models Suitable for Long Term Dynamic Response," *IEEE Transaction on Energy Conversion,* vol.*5, no.*4, 1990,pp. 686-692.

[28] C.-Y. Chong and R.P. Malhami, "Statistical Synthesis of Physically Based Load. Models with Application to Cold Load Pickup," IEEE Transactions on Power Apparatus and Systems, vol. PAS-103, no. 7, pp. 1621-1628, 1984.

[29] N. Chowdhury and B. Zhou, "Intelligent Training Agent for Power System Restoration," in Proceedings of the 1998 11th Canadian Conference on Electrical and Computer Engineering, 1998, pp. 786-789.

[30] R.F. Chu, E.J. Dobrowolski, E.J. Barr, J. McGeehan, D. Scheurer, and K. Nodehi, "The Uses of an Operator Training Simulator for System Restoration," in Proceedings of the 1991 IEEE Power Industry Computer Applications Conference, Baltimore, MD, USA, 1992, pp. 171-177.

[31] R.F. Chu et al., "Restoration Simulator prepares Operators for Major Blackouts," IEEE Computer Applications in Power, vol. 4, no. 4, pp. 1126-1132, August 1993.

[32] CIGRE Study Committee 38.02.02, "Modeling and Simulation of Black Start and Restoration of an Electric Power System. Results of a Questionnaire," Electra, , no. 131, pp. 157-169, July 1990.

[33] CIGRE Study Committee 38.02.02, "Modeling and Simulation of Black Start and Restoration of Electric Power Systems," Electra, , no. 147, pp. 21-41, April 1993.

[34] CIGRE Task Force 38.06.04, "A Survey of Expert Systems for Power System Restoration," Electra, , no. 150, pp. 87-105, October 1993.

[35] CIGRE Working Group 13-02 Switching Surge Phenomena in EHV Systems, "Switching Overvoltages in EHV and UHV Systems with Special Reference to Closing and Reclosing Transmission Lines," Electra, ,no. 30, pp. 70-122, 1973.

[36] C. Concordia, L. H. Fink, and G. Poullikkas, "Load Shedding on an Isolated System," IEEE Transactions on Power Systems, vol. 10, no. 3, pp. 1467-1472, August 1997.

[37] C. Counan et al., "Major Incidents on the French Electric System: Potentiality and Curative Measures Studies," IEEE Transactions on Power Systems, vol. 8, no. 3, pp. 879-886, August 1993.

[38] P.H. Darnault et al., "An Expert System as a Guide for Information Synthesis and Decision Making in the Restoration of a Power System after a Blackout," in Proceedings of the Second Symposium on Expert System Applications to Power Systems, Seattle, WA, USA, July 1989.

[39] F.P. de Mello and J.C. Westcott, "Steam Plant Startup and Control in System Restoration," IEEE Transactions on Power Systems, vol. 9, no. 1, pp. 93-101, February 1994.

[40] B. Delfino, G.B. Denegri, E. C. Bonini, R. Marconato, and P. Scarpellini, "Black Start and Restoration of a Part of the Italian HV Network: Modeling and Simulation of a Field Test," IEEE Transactions on Power Systems, vol. 11, no. 3, pp. 1371-1379, July 1996.

[41] B. Delfino, G.B. Denegri, M. Invernezzi, and A. Morini, "Enhancing Flexibility of Restoration Guides through an integrated Simulator-KB Approach," in Proceedings of the Stockholm Powertech Conference, Stockholm, Sweden, June 1995.

[42] B. Delfino, M. Invernizzi, and A. Morini, "Knowledge-Based Restoration Guidelines," IEEE Computer Applications in Power, vol. 5, no. 3, pp. 54-59, July 1992.

[42] K. Dickers and D. Rumpel, "Modelling for Grid Restoration Studies," Electric Power and Energy Systems, pp. 45-55, 1987.

[43] H.E. Dijk et al., "An Expert System for Power System Restoration Strategies," in Proceedings of the Symposium on Expert System Applications to Power Systems, Stockholm, Sweden - Helsinki, Finland, August 1988, pp. 8.9-8.16.

[44] M.A. Di lascio, R. Moret and M. Poloujadoff, "Long term Power Simulation for Real -Time Training with a Reduced Size Program," IEEE Transactions on Power Systems, vol. 2, no. 1, pp. 113-118, Feb. 1987.

[45] M.B. Djukanovic, D.P. Popovic, D.J. Sobajic, and Y.-H. Pao, "Prediction of Power System Frequency Response after Generator Outages using Neural Nets," IEE Proceedings-C, vol. 140, no. 5, pp. 389-398, September 1993.

[46] E. Barr et al., "The Use of an Operator Training Simulator for Power System Restoration," in Proceedings of the IEEE Power Industry Computer Applications Conference, Baltimore, MD, USA, May 1991.

[47] A. Ebert, M. Eppel, S. Genthe, H. Schwarzjirg, J. Stark, and W. Werner, "System Restoration of a Transmission Network," in Proceedings of the 1995 International Conference on Energy Management and Power Delivery, Singapore, 1995, pp. 91-95.

[48] I.M. Elders, "The Application of an Intelligent System to Power Network Operation and Control," in Proceedings of the International Conference on Intelligent Systems Applications to Power Systems, Orlando, FL, USA, 1996, pp. 170-174.

[49] EPRI REPORT, "Long-term System Dynamics Simulation Methods," EPRI, EL-3894, PROJECT 1469-1,Final Report, 1985.

[50] O. Faucon and L. Dousset, "Coordinated Defense Plan protects against Transient Instabilities," IEEE Computer Applications in Power, pp. 22-26, June 1997.

[51] L.H. Fink, K.-L. Liou, and C.-C. Liu, "From Generic Restoration Actions to Specific Restoration Strategies," IEEE Transactions on Power Systems, vol. 10, no. 2, pp. 745-752, May 1995.

[52] N. A. Fountas and N. D. Hatziargyriou, "Hierarchical Time-extended Petri Nets as a generic Tool for Power System Restoration," in IEEE/PES 1996 SM, Denver, Colorado, August 1996.

[53] N.A. Fountas, N.D. Hatziargyriou, C. Orfanogiannis, and A. Tasoulis, "Interactive Long-Term Simulation for Power System Restoration Planning," IEEE Transactions on Power Systems, vol. 12, no. 1, pp. 1825-1832, February 1997.

[54] S. Fukui, "A Knowledge-Based Method for Making Restoration Plan of Bulk Power System," IEEE Transactions on Power Systems, vol. 7, no. 2, May 1992.

[55] Z.L. Gaing, C.N. Lu, B.S. Chang, and C.L. Cheng, "Object-oriented Approach for Implementing Power Restoration Package," IEEE Transactions on Power Systems, vol. 11, no. 1, pp. 483-489, February 1996.

[56] Z.L. Gaing, C.N. Lu, B.S. Chang, and K.K. Cheng, "Implementation of a Power System Restoration Simulator," Proceedings of the National Science Council, Republic of China, Part A, vol. 20, no. 5, pp. 564-572, September 1996.

[57] J. Gutierrez, M. Starpolsky, and M. Garcia, "Policies for Restoration of a Power System," IEEE Transactions on Power Systems, vol. PWRS-2, no. 2, pp. 436-442, May 1987.

[58] L.N. Hannett, F.P. de Mello, G.H. Tylinski, and W.H. Becker, "Validation of Nuclear Plant Auxiliary Power Plant Supply by Test," IEEE Transactions on Power Apparatus and Systems, vol. PAS-101, no. 9, pp. 3068-3074, September 1982.

[59] C.W. Hansen et al., "EPRI Restore Evaluation: Phase I Final Report (#4TS3038)," Tech. Rep., Decision Systems International, Atlanta, Georgia, February 1997.

[60] I.D. Hassan, R. Weronick, and R.M. Bucci, "Evaluating the Transient Performance of Standby Diesel-generator units by simulation," IEEE Transactions on Energy Conversion, vol. 7, no. 3, pp. 470-477, June 1992.

[61] N.D. Hatziargyriou, N.A. Fountas, and K.P. Valavanis, "Systematic Petri Net-based Methodology for Power System Restoration," International Journal of Engineering Intelligent Systems for Electrical Engineering and Communications, vol. 5, no. 3, pp. 167-176, September 1997.

[62] M.C. Hayden and J.G. Kennedy, "Use of Soft Energisation in Power System Restoration," in Proceedings of the Universities Power Engineering Conference, London, UK, 1995.

[63] E. Horowitz, S. Sahni, *Fundamental of Computer Algorithms*, Galgotia Publication, 1996.

[64] D. Hazarika and A.K. Sinha, "Standing Phase Angle Reduction for Power System Restoration," IEE Proceedings: Generation, Transmission and Distribution, vol. 145, no. 1, pp. 82-88, January 1998.

[65] K. Hemmaplardh, J.W. Lamont, J.W. Manke, W.R. Pauly, "Considerations for a Long Term Dynamics Simulation Program," IEEE Transactions on Power Systems, vol. 1, no. 1, pp. 129-136, Feb. 1986.

[66] K. Hotta, H. Nomura, H. Takemoto, K. Suzuki, S. Nakamura, and S. Fukui, "Implementation of a Real-Time Expert System for a Restoration Guide in a Dispatching Center," IEEE Transactions on Power Systems, vol. 5, no. 3, pp. 1032-1038, April 1990.

[67] J. Huang, F.D. Galiana, and G.T. Vuong, "Power System Restoration incorporating Interactive Graphics and Optimization," in Proceedings of the 1991 IEEE Power Industry Computer Application Conference, Baltimore, MD, USA, November 1992, pp. 216-222.

[68] J.A. Huang, L.Audette, and S. Harrison, "A Systematic Method for Power System Restoration Planning," IEEE Transactions on Power Systems, vol. 10, no. 2, pp. 869-875, May 1995.

[69] IEEE Committee Report, "Power System Restoration - A Task Force Report," IEEE Transactions on Power Systems, vol. PWRS-2, no. 2, pp. 271-277, May 1987.

[70] IEEE Committee Report, "Power System Restoration - The Second Task Force Report," IEEE Transactions on Power Systems, vol. PWRS-2, no. 4, pp. 927-933, November 1987.

[71] IEEE Committee Report, "System Operation Challenges," IEEE Transactions on Power Systems, vol. 3, no. 1, pp. 118-126, February 1988.

[72] IEEE Committee Report, "Dispatcher Training Simulators: Lessons Learned," IEEE Transactions on Power Systems, vol. 6, no. 2, pp. 594-604, May 1991.

[73] IEEE Committee Report, "New Approaches in Power System Restoration," IEEE Transactions on Power Systems, vol. 7, no. 4, pp. 1428-1433, November 1992.

[74] IEEE Committee Report, "Overvoltage Control during Restoration," IEEE Transactions on Power Systems, vol. 7, no. 4, pp. 1464-1470, November 1992.

[75] IEEE Committee Report, "Special Considerations in Power System Restoration," IEEE Transactions on Power Systems, vol. 7, no. 4, pp. 1419-1427, 1992.

[76] IEEE Committee Report, "Bulk Power System Restoration Training Techniques," IEEE Transactions on Power Systems, vol. 8, no. 1, pp. 191-197, February 1993.

[77] IEEE Committee Report, "Analytical Tool Requirements for Power System Restoration," IEEE Transactions on Power Systems, vol. 9, no. 3, pp. 1582-1591, August 1994.

[78] IEEE Committee Report, "Expert System Requirements for Power System Restoration," IEEE Computer Applications in Power, vol. 9, no. 3, pp. 1592-1600, April 1994.

[79] IEEE Committee Report, "Nuclear Plant Requirements during Power System Restoration," IEEE Transactions on Power Systems, vol. 10, no. 3, pp. 1486-1491, August 1995.

[80] IEEE Committee Report, "Bibliography on load models for power flow and dynamic performance simulation," IEEE Transactions on Power Systems, vol.10, no.1, pp. 523 –538, Feb. 1995.

[81] IEEE Committee Report, "Protective System Issues during Restoration," IEEE Transactions on Power Systems, vol. 10, no. 3, pp. 1492-1497, August 1995.

[82] IEEE Committee Report, "Remote Cranking of Steam Electric Stations," IEEE Transactions on Power Systems, vol. 11, no. 3, pp. 1613-1618, August 1996.

[83] IEEE Standard, "IEEE recommended practice for excitation system models for power system stability studies," IEEE Std 421.5-1992 , Aug. 1992.

[84] IEEE Task Force, "Excitation System Models for Power System Stability Studies," *IEEE Transaction on Power Apparatus and Systems , vol.PAS-100, no.*1, 1981, pp.494-509.

[85] IEEE Task Force, "Load Representation for Dynamic Performance Analysis," *IEEE Transaction on Power Systems,* vol.*8*, no.2, 1993, pp.472-482.

[86] IEEE Task Force, "Dynamic models for fossil fueled steam units in power system studies," IEEE Transactions on Power Systems, vol. 6, no.2, pp. 753 -761, May 1991.

[87] S. Ihara and F.C. Schweppe, "Physically Based Modeling of Cold Load Pickup," in Proceedings of the IEEE/PES Winter Meeting, Atlanta, USA, February 1981.

[88] W. Jiang and C.Y. Teo, "Knowledge-based Approach for Bulk Power System Restoration," in Proceedings of the International Conference on Energy Management and Power Delivery, Singapore, 1995, pp. 108-111.

[89] K. Ju, G. Krost, and D. Rumpel, "Expert System for Interlocking and Sequence- Switching," in Proceedings of the International Conference on Intelligent Systems Applications to Power Systems, Orlando, FL, USA, 1996, pp. 385-389.

[90] P. Kádár, "New Solutions in the Control of the Hungarian Power System," in Proceedings of the 1996 4th IEEE AFRICON Conference, Stellenbosch, South Africa, 1996, pp. 816-821.

[91] P. Kádár and A.K. Mergl, "CORES - The Continuous Restoration Expert System," in Proceedings of the 1996 International Conference on Intelligent Systems Applications to Power Systems, Orlando, FL, USA, 1996, pp. 390-393.

[92] R.J. Kafka, D.R. Penders, S.H. Bouchey, and M.M. Adibi, "System Restoration Plan Development for a Metropolitan Electric System," IEEE Transactions on Power Systems, vol. PAS-100, no. 8, August 1981.

[93] R.J. Kafka, D.R. Penders, S.H. Bouchey, and M.M. Adibi, "Role of Interactive and Control Computers in the Development of a System Restoration Plan," IEEE Transactions on Power Apparatus and Systems, vol. PAS-101, no. 1, pp. 43-52, January 1982.

[94] N. Kakimoto, , M. Emoto, and M. Hayashi, "Expert System for Restoring Trunk Power Systems from Complete System Collapse," Mem. Fac. Eng. Kyoto University, vol. 51, no. 1, pp. 39-58, January 1989.

[95] N. Kakimoto, , S. Ezure, and M. Hayashi, "Development of Simulator with Artificial Intelligence on Secondary Power System Operation," Mem. Fac. Eng. Kyoto University, vol. 50, no. 3, pp. 129-153, July 1988.

[96] N. Kakimoto, B. Lin, and H. Sugihara, "Expert System for Voltage Control in Restoration of EHV Power System Following Complete Blackout," Electrical Engineering in Japan, vol. 115, no. 1, pp. 35-50, February 1995.

[97] N. Kakimoto et al., "An Application of Artificial Intelligence to Restoration of Bulk Power Systems," in Proceedings of the Symposium on Expert System Applications to Power Systems, Stockholm, Sweden-Helsinki, Finland, August 1988, pp. 8.24-8.31.

[98] T. Kasuya, H. Oda, H. Inoue, and S. Iizuka, "Development of Automatic Restorative Operation Applicable to Power System Local Area Dispatching," Electrical Engineering Japan, vol. 110, no. 3, pp. 37-49, October 1990.

[99] M. Kato et al., "The Development of Power System Restoration Method for a Bulk Power System by Applying Knowledge Engineering Technique," IEEE Transactions on Systems, vol. 7, no. 2, May 1992.

[100] R. Kearsley, "Restoration in Sweden and Experience gained from the Blackstart of 1983," IEEE Transactions on Power Systems, vol. PWRS-2, no. 2, pp. 422-428, May 1987.

[101] S.A. Khaparde and S. Jadid, "Expert System for Fault Diagnosis and Restoration of Iran's 400 KV Network," International Journal of Engineering Intelligent Systems for Electrical Engineering and Communications, vol. 5, no. 2, pp. 107-114, June 1997.

[102] A.G. King, J.R. McDonald, J. Spiller, D. Brooke, and R. Samwell, "Power System Restoration Using Expert Systems," in Proceedings of the 29th Universities Power Engineering Conference, 1994, pp. 224-227.

[103] D. S. Kirschen and T. L. Volkmann, "Guiding a Power System Restoration with an Expert System," IEEE Transactions on Power Systems, vol. 6, no. 2, pp. 558-566, May 1991.

[104] T. Kobayashi, D. Moridera, S. Fukui, and K. Komai, "Verification of an Advanced Power System Restoration Support System using an Operator Training Simulator," IEEE Transactions on Power Systems, vol. 9, no. 2, pp. 707-713, May 1994.

[105] H. Kodoma and H. Suzuki, "Interactive Restoration Control of Electric Power Systems," in Proceedings of the IFAC Symposium on Control Applications for Power System Security, Florence, Italy, September 1983.

[106] S. Koenig, L. Mohr, G. Krost, D. Rumpel, and U. Spanel, "Expert System in Training Power System Restoration at the Stadtwerke Duisbergag," International Journal of Engineering Intelligent Systems for Electrical Engineering and Communications, vol. 3, no. 3, pp. 175-183, September 1995.

[107] Y. Kojima, S. Warashina, M. Kato, and H. Watanabe, "Application of Knowledge Engineering Techniques to Electric Power System Restoration," in Proceedings of the International Workshop on Artificial Intelligence for Industry Applications, Hitachi, Japan, 1988, pp. 320-325.

[108] Y. Kojima, S. Warashina, M. Kato, and H. Watanabe, "The Development of Power System Restoration Method for a Bulk Power System by Applying Knowledge Engineering Techniques," IEEE Transactions on Power Systems, vol. 4, no. 3, pp. 1228- 1235, August 1989.

[109] Y. Kojima, S. Warashina, S. Nakamura, and K. Matsumoto, "Knowledge-Based Guidance System for Trunk Power Transmission System Restoration," in Proceedings of the International Workshop on Artificial Intelligence for Industry Applications, Hitachi, Japan, 1988, pp. 315-319.

[110] Y. Kojima, S. Warashina, S. Nakamura, and K. Matsumoto, "Development of a Guidance Method for Power System Restoration," IEEE Transactions on Power Systems, vol. 4, no. 3, pp. 1219-1225, August 1989.

[111] K. Komai, K. Matsumoto, and T. Sakaguchi, "Analysis and Evaluation of Expert's Knowledge for Power System Restoration by Mathematical Programming Method," in Proceedings of the IEEE International Symposium on Circuits and Systems, June 1988, pp. 1895-1898.

[112] T. Kostic, R. Cherkaoui, A.J. Germond, and P. Pruvot, "Decision Aid Function for Restoration of Transmission Power Systems: Conceptual Design and Considerations," IEEE Transactions on Power Systems, vol. 13, no. 3, pp. 923-929, August 1998.

[113] T. Kostic, A.J. Germond, and J.J. Alba, "Optimization and Learning of Load Restoration Strategies," International Journal of Electrical Power & Energy Systems, vol. 20, no. 2, pp. 131-140, February 1998.

[114] D. Kottick, M. Blau, and Y. Halevi, "Evaluation of an Underfrequency Load Shedding Optimization Algorithm," in Proceedings of the 11th Power Systems Computation Conference, Avignon, France, 1993, pp. 437-441.

[115] A. Kovàcs and A.K. Mergl, "Generating Switching Sequences - A Genetic Algorithm Approach," in Proceedings of the International Conference on Intelligent Systems Applications to Power Systems, Orlando, FL, USA, 1996, pp. 380-384.

[116] G. Krost and D. Rumpel, "Network Restoration Expert System," in Proceedings of the IFAC Symposium, Seoul, Korea, 1989.

[117] G. Krost, D. Rumpel, and E. N'Guessan, "Design of a Network Restoration Expert System with Training Facilities," in Proceedings of the Second Symposium on Expert System Applications to Power Systems, Seattle, WA, USA, July 1989.

[118] G. Krost, U. Spanel, " Heuristic Power Set-point Assignment for Restoration," in Proceedings of the International Conference on Intelligent Systems Applications to Power Systems (ISAP'97), 1997, pp.536-540.

[119] G. Krost et al., "Network Restoration Expert System," in Proceedings of the Second Symposium on Expert System Applications to Power Systems, Seattle, WA, USA, July 1989.

[120] P. Kundur, Power System Stability and Control, McGraw-Hill, Inc., 1994.

[121] P. Kundur, L. Wang, and S. Yirga, "Dynamic Equivalents for Power System Stability Studies," in Proceedings of the Fifth Symposium of Specialists in Electric Operation and Expansion Planning, Recife, Brazil, May 1996.

[122] A. Kuppurajulu, "Analytical Tools to Aid Power System Restoration," International Journal of Power and Energy Systems, vol. 16, no. 1, pp. 36-39, 1996.

[123] K. Kuroda, Y. Takegoshi, M. Ito, and S. Fukui, "Verification of a Knowledge-based Restoration Guidance System in a Local Dispatching Centre," International Journal of Electrical Power and Energy Systems, vol. 15, no. 3, pp. 185-192, June 1993.

[124] D. Lindenmeyer, H.W. Dommel, A. Moshref, and P. Kundur, "A Framework for Black Start and Power System Restoration," in Proceedings of the Canadian Conference on Electrical and Computer Engineering, Halifax, Canada, May 2000.

[125] R.R. Lindstrom, "Simulation and Field Test of the Black Start of a Large Coal-Fired Generating Station Utilizing Small Remote Hydro Generation," IEEE Transactions on Power Systems, vol. 5, no. 1, pp. 162-168, February 1990.

[126] K.L. Liou, A Knowledge-Based System for Generation Capability Dispatch during Bulk Power System Restoration, Ph.D. thesis, University of Washington, WA, USA, 1993.

[127] K.L. Liou, C.C. Liu, and R.F. Chu, "Tie Line Utilization during Power System Restoration," IEEE Transactions on Power Systems, vol. 10, no. 1, pp. 192-199, February 1995.

[128] C.-C. Liu and R.F. Chu, "Tie Line Utilization during Power System Restoration," IEEE Transactions on Power Systems, vol. 8, no. 1, pp. 192-199, February 1995.

[129] C.-C. Liu, Seung Jae Lee, and S. S. Venkata, "An Expert System Operational Aid for Restoration and Loss Reduction of Distribution Systems," IEEE Transactions on Power Systems, vol. 3, no. 2, pp. 619-625, May 1988.

[130] C.-C. Liu, K.-L. Liou, R.F. Chu, and A.T. Holen, "Generation Capability Dispatch for Bulk Power System Restoration: A Knowledge-based Approach," IEEE Transactions on Power Systems, vol. 8, no. 1, pp. 316-323, February 1993.

[131] C.-C. Liu et al., "Operational Experience and Maintenance of an On-Line Expert System for Customer Restoration and Fault Testing," IEEE Transactions on Power Systems, vol. 7, no. 2, pp. 835-842, May 1992.

[132] T.-K. Ma, C.-C. Liu, M.-S. Tsai, R. Rogers, S.L. Muchlinski, and J. Dodge, "Operational Experience and Maintence of an On-Line Expert System for Customer Restoration and Fault Testing," IEEE Transactions on Power Systems, vol. 7, no. 2, pp. 835-842, May 1992.

[133] E. Mariani, F. Mastroianni, and V. Romano, "Field Experiences in Re-energization of Electrical Networks from Thermal and Hydro Plants," IEEE Transactions on Power Apparatus and Systems, vol. PAS-103, no. 7, pp. 1707-1713, July 1984.

[134] The Mathworks Inc., Natick, MA, USA, Matlab: The Language of Technical Computing-Function Reference Version 3, January 1999.

[135] The Mathworks Inc., Natick, MA, USA, Simulink: Dynamic System Simulation for Matlab-
163 Using Simulink Version 3, January 1999.

[136] K. Matsumoto and R. J. Kafka, "Knowledge-based Systems as Operational Aids in Power System Restoration," Proceedings of the IEEE, vol. 80, no. 5, pp. 689-696, May 1992.

[137] K. Matsumoto et al., "Heuristic Management of Complex and Large Scale Power Systems in

Restorative States," in Proceedings of the CIGRE/IFAC Symposium 39- 83, 1983.

[138] A. Mayland, "Operator Assistance using Knowledge-Based Technology for Power Systems Restoration," in Proceedings of the Symposium on Expert System Applications to Power Systems, Tokyo-Kobe, Japan, April 1991, pp. 250-255.

[139] Miller et al., "Experience using the Dispatcher Training Simulator as a Training Tool," IEEE Transactions on Systems, vol. 8, no. 3, pp. 1126-1132, August 1993.

[140] K. Miura and et al., "An Expert System for Procedure Generation of Power System Restoration in Regional Control Centre," IEEE Transactions on Industry Applications, vol. 27, no. 1, pp. 167-172, January/February 1991.

[141] E. Mondon, P. Erhard, J.N. Marquet, J.C. Grand, and L. Pierrat, "Morgat: A Tool for Electric Transient Simulation. An Application to the Restoration of a Power System after a Major Failure," in Third International Conference on Power System Monitoring and Control, London, UK, 1991, pp. 44-49.

[142] E. Mondon et al., "MARS - An Aid for Network Restoration after a Local Disturbance of a Power System after a major Failure," in Proceedings of the 1991 IEEE Power Industry Computer Application Conference, 1991, pp. 344-349.

[143] G. Morin, "Service Restoration following a Major Failure on the Hydro-Quebec Power System," IEEE Transactions on Power Delivery, vol. PWRD-2, no. 2, pp. 454-462, April 1987.

[144] R. Nadira, T.E. Dy Liacco, and K.A. Loparo, "A Hierarchical Interactive Approach to Electric Power System Restoration," IEEE Transactions on Power Systems, vol. 7, no. 3, pp. 1125-1131, August 1992.

[145] T. Nagata, H.Sasaki, and R. Yokoyama, "Power System Restoration by Joint Usage of Expert System and Mathematical Programming Approach," IEEE Transactions on Power Systems, vol. 10, no. 3, pp. 1473-1479, August 1995.

[146] S. Nishida et al., "Analysis of Overvoltages caused by Self-Excitation in a Separated Power System with Heavy Load and Large Shunt Capacitance," IEEE Transactions on Power Apparatus and Systems, vol. PAS-102, no. 7, pp. 1970-1978, July 1983.

[147] P. Omahen and F. Gubina, "Simulations and Field Tests of a Reactor Coolant Pump Emergency Start-Up by Means of Remote Gas Units," IEEE Transactions on Energy Conversion, vol. 7, no. 4, pp. 691-697, December 1992.

[148] Working Group on Prime Mover and Energy Supply Models for System Dynamic Performance Studies, "Hydraulic Turbine and Turbine Control Models for System Dynamic Studies," IEEE Transactions on Power Systems, vol. 7, no. 1, pp. 167-179, February 1992.

[149] T. Oyama, "Restoration Planning of Power System Using Genetic Algorithm with Branch Exchange Method," in Proceedings of the International Conference on Intelligent Systems Applications to Power Systems, Orlando, FL, USA, 1996, pp. 175-179.

[150] Y.-M. Park and K.-H. Lee, "Application of Expert System to Power System Restoration in Local Control Center," International Journal of Electrical Power and Energy System, vol. 17, no. 6, pp. 407-415, December 1995.

[151] Y.-M. Park and K.-H. Lee, "Application of Expert System to Power System Restoration in Sub-control Center," IEEE Transactions on Power Systems, vol. 12, no. 2, pp. 629-635, May 1997.

[152] F.S. Prabhakara et al., "System Restoration - Deploying the Plan," IEEE Transactions on Power Apparatus and Systems, vol. PAS-101, no. 11, pp. 4263-4271, November 1982.

[153] K.L. Praprost and K.A. Loparo, "Power System Transient Stability Analysis for Random Initial Conditions and Parameters," in Proceedings of the IEEE International Conference on Systems, Man and Cybernetics, October 1992.

[154] X. Qiu, H. Tang, X. Li, G. Wang, J. Liu, and W. Liu, "Power System Restoration based on Expert System and Numerical Computation," Proceedings of the Chinese Society of Electrical Engineering, vol. 16, no. 6, pp. 413-416, November 1996.

[155] M. Rafian, P. Sigari, D. Kirschen, S. Silverman, R. Hamlin, and R. Bednarik, "Evaluating a Restoration Tool using Consolidated Edison's Training Simulator," IEEE Transactions on Power Systems, vol. 11, no. 3, pp. 1636-1642, August 1996.

[156] R. Ramanathan, H. Ramchandani, S. A. Sackett," Dynamic Load Flow Technique for Power System Simulation," IEEE Transactions on Power Systems, vol.1, no.3, pp. 25-30, August 1986.

[157] H. B. Ross et al., "An AGC Implementation for System Islanding and Restoration Conditions," IEEE Transactions on Power Systems, vol. 9, no. 3, pp. 1399-1410, August 1994.

[158] L. Roytelman & S.M. Shahidehpour, "A Comprehensive Long Term Dynamic Simulation for Power System Recovery," *IEEE Transaction on Power Systems , vol.9, no.*3, 1994, pp.1427-1433.

[159] D. Rumpel, G. Krost, and T. Ader, "Training Simulator with an Advising Expert System for Power System Restoration," in Proceedings of the IFAC Symposium on Control of Power Plants and Power Systems, Munich, Germany, 1992, pp. 451-456.

[160] M.M. Saha, W. Jianping, and E.O. Werner, "Challenges for Emergency Control and System Restoration in Power Systems," in Proceedings of the 1996 6th International Conference on AC and DC Power Transmission, London, UK, 1996, pp. 226-232.

[161] T. Sakaguchi and K. Matsumoto, "Development of a Knowledge Based for Power System Restoration," IEEE Transactions on Power System Apparatus and Systems, vol. PAS-102, no. 2, pp. 320-329, February 1983.

[162] J.L. Sancha, B. Meyer & W.W. Price, "Application of Long – Term Simulation Program for Analysis of System Islanding," *IEEE Transaction on Power Systems* , vol. *12,* no 1, 1997, pp. 189-197.

[163] D. Scheurer, "System Restoration at Philadelphia Electric Company," in IEEE 8th Biennial Workshop on Real-Time Monitoring and Control of Power Systems, Montreal, Canada, October 1985.

[164] R. P. Schulte, S. L. Larson, G. B. Sheble, and J. N. Wrubel, "Artificial Intelligence Solutions to Power System Operating Problems," IEEE Transactions on Power Systems, vol. PWRS-2, no. 4, pp. 920-926, November 1987.

[165] S. Shah and S.M. Shahidepur, "A Heuristic Approach to Load Shedding Scheme," IEEE Transactions on Power Systems, vol. 4, no. 4, pp. 1421-1429, October 1989.

[166] K. Shimakura, J. Imagaki, Y. Matsunoki, M. Ito, S. Fukui, and S. Hori, "A Knowledge- based Method for making Restoration Plan of Bulk Power System," IEEE Transactions on Power Systems, vol. 7, no. 2, pp. 914-920, May 1992.

[167] J.I. Shinohara, I. Kozakai, M. Kunugi, J.I. Nagata, and H. Saito, "Knowledge-based Behavior Interface: its Application to Power Network Restoration Support System," IEEE Transactions on Power Systems, vol. 11, no. 1, pp. 383-389, February 1996.

[168] J.I. Shinohara, J.I. Nagata, H. Saito, I. Kozakai, and A. Ohuchi, "Development of Restoration System Based on Human Performance Model," Electrical Engineering in Japan, vol. 117, no.

4, pp. 34-45, October 1996.

[169] G. Shu and D. Zhen-guo, "An Expert System for Failure Analysis and Restoration Operation of Local Power Networks," in IEE International Conference on Advances in Power System Control, Operation and Management, Hongkong, November 1991.

[170] R.D. Shultz and G.A. Mason, "Blackstart Utilization of Remote Combustion Turbines: analytical Analysis and Field Test," IEEE Transactions on Power Apparatus and Systems, vol. PAS-103, no. 8, pp. 2186-2191, August 1984.

[171] E.J. Simburger and F.J. Hubert, "Low Voltage Bulk Power System Restoration Simulation," IEEE Transactions on Power Apparatus and Systems, vol. PAS-100, no. 11, pp. 4479-4484, November 1981.

[172] V. Singh and N.D. Rao, "An Expert System for Cold Load Pickup," in Proceedings of the 1994 Canadian Conference on Electrical and Computer Engineering, Halifax, Canada, 1994.

[173] I. Susumago, M. Suzuki, T. Tsuji, and K. Dan, "Development of Real-time Simulation Method for Power System Restoration after Major Disturbances," in International Conference on Large High Voltage Electric Systems, Paris, France, 1986, pp. 38.03.1- 38.03.8.

[174] I. Susumago et al., "Development of a Large-Scale Dispatcher Training Simulator and Training Results," IEEE Transactions on Power Systems, vol. 1, no. 2, pp. 167-175, 1986.

[175] G. Sybille, M.M Gavrilovic, J. Belanger, and V.Q. Do, "Transformer Saturation Effects on EHV System Overvoltages," IEEE Transactions on Power Apparatus and Systems, vol. PAS-104, no. 3, pp. 671-680, March 1985.

[176] G Sybille, P. Brunelle, Le-Huy Hoang, L.A.Dessaint, K. Al-Haddad, " Theory and applications of power system blockset, a MATLAB/ Simulink-based simulation tool for power systems," Power Engineering Society Winter Meeting, 2000. IEEE, Vol.1, 2000, pp.: 774-779.

[177] I. Takeyasu et al., "An Expert System for Fault Analysis and Restoration of Trunk Line Power Systems," in Proceedings of the Symposium on Expert System Applications to Power Systems, Stockholm, Sweden - Helsinki, Finland, August 1988, pp. 8.24-8.31.

[178] S. L. Tanimoto, *The elements of Artificial Intelligence: An Introduction Using LISP*, computer Science Press, 1987.

[179] C.Y. Teo and W. Jiang, "Adaptive Real-time Knowledge Based Approach for Bulk Power System Restoration," Electric Machines and Power Systems, vol. 25, no. 10, pp. 1079-1088, December 1997.

[180] C.Y. Teo, W. Jiang, and H.B. Gooi, "Review of Restoration Strategies and a Real-time Knowledge Based Approach for Bulk Power System Restoration," Knowledge-Based Systems, vol. 9, no. 1, pp. 15-21, February 1996.

[181] D.J. Trodnowski, "Order Reduction of Large-Scale Linear Oscillatory System Models," IEEE Transactions on Power Systems, vol. 9, no. 1, pp. 451-458, February 1994.

[182] A. Vorbach, H. Schwingshandl, D. Rumpel, and M Brockmann, "Power System Restorations. Methods and Model-simulations," in Power Systems Modelling and Control Applications - Selected Papers from the IFAC Symposium, Brussels, Belgium, 1989, pp. 281-285.

[183] J. Waight et al., "An Advanced Transportable Operator Training Simulator," in Proceedings of the IEEE Power Industry Computer Applications Conference, Baltimore, MD, USA, May 1991.

[184] S.-M. Wang, "An Expert System for Bulk Power System Restoration," in Proceedings of the Second Symposium on Expert System Applications to Power Systems, Seattle, WA, USA, July 1989.

[185] S.-M. Wang, Z. Dong, Q. Sun, and D. Xia, "Decision-support Expert System for Bulk Power System Restoration," Proceedings of the Chinese Society of Electrical Engineering, vol. 11, no. Suppl, pp. 92-98, 1991.

[186] J.D. Willson, "System Restoration Guidelines: How to Set-Up, Conduct, and Evaluate a Drill," IEEE Transactions on Power Systems, vol. 11, no. 3, pp. 1619-1629, August 1996.

[187] J.D. Willson, "System Restoration Training Questionnaire Results," IEEE Transactions on Power Systems, vol. 11, no. 3, pp. 1630-1635, August 1996.

[188] K.P. Wong and B.S.Lau, "An Algorithm for Load Shedding and Restoration During Reduced Generation Periods," in IEE International Conference on Advances in Power System Control, Operation and Management, Hong Kong, November 1991.

[189] F. Wu and A. Monticelli, "Analytical Tools for Power System Restoration – Conceptual Design," IEEE Transactions on Power Systems, vol. 3, no. 1, pp. 10-16, February 1988.

[190] J.S. Wu, C.-C. Liu, K.L. Liou, and R.F. Chu, "Petri Net Algorithm for Scheduling of Generic Restoration Actions," IEEE Transactions on Power Systems, vol. 12, no. 1, pp. 69-76, February 1997.

[191] *F.F Wu,* "Theoretical Study of the Convergence of the Fast Decoupled Load Flow," IEEE Trans. on Power Appar. a. Syst. PAS-96 (1977), pp.268-271

[192] S. Wunderlich, M.M. Adibi, R. Fischl, and C.O.D. Nwankpa, "An Approach to Standing Phase Angle Reduction," IEEE Transactions on Power Systems, vol. 9, no. 1, pp. 470-478, February 1994.

[193] K.E. Yeager and J.R. Willis, "Modeling of Emergency Diesel Generators in an 800 Megawatt Nuclear Power Plant," IEEE Transactions on Energy Conversion, vol. 8, no. 3, pp. 433-441, September 1993.

[194] M.H. Yolu, "Adaption of the Simplex Algorithm to Modeling of Cold Load Pickup of a Large Secondary Network Distribution System," IEEE Transactions on Power Apparatus and Systems, vol. 103, no. 7, pp. 1621-1628, 1984.

[195] J. Zaborszky, G. Huang, P.J. Clelland, and D.A. Fagnan, "Optimal Partnership of Operator and Computer for Power System Restoration," in Proceedings of the 11th Triennial World Congress of the International Federation of Automatic Control, 1991, pp. 73-78.

[196] Z.Z. Zhang, G.S. Hope, and O.P. Malik, "Expert Systems in Electric Power Systems - a Bibliographical Survey," IEEE Transactions on Power Systems, vol. 4, no. 4, pp. 1355-1362, October 1989.

[197] B. Zhou, N.A. Chowdhury, and D. Slade, "Case-based Intelligent Agent for Power System Restoration," in Proceedings of the 1996 Canadian Conference on Electrical and Computer Engineering, Calgary, Canada, 1996, pp. 369-372.

[198] N. Zhu, S. Vadari, D. Hwang, "Analysis of a static VAR compensator using the dispatcher training simulator," IEEE Transactions on Power Systems, vol.10, no.3 , pp.1234 –1242, Aug. 1995.

[199] Y. Zhu, Investigation of Practical Application of AI Technology in Power System Operation and Analysis, Ph.D. thesis, University of New South Wales, Australia, 1994.

APPENDIX

Appendix A

IEEE 39 bus (New England) Test System Data

a) Bus data

BUS NO.	VOLTAGE		GENERATION		LOAD	
	(p.u.)	(Deg.)	(MW)	(MVAR)	(MW)	(MVAR)
1	1.048	-9.37	0	0	0	0
2	1.049	-6.80	0	0	0	0
3	1.030	-9.65	0	0	322.0	2.4
4	1.004	-10.47	0	0	500.0	184.0
5	1.005	-9.31	0	0	0	0
6	1.007	-8.62	0	0	0	0
7	0.997	-10.81	0	0	233.8	84.0
8	0.996	-11.32	0	0	522.0	176.0
9	1.028	-11.12	0	0	0	0
10	1.017	-6.21	0	0	0	0
11	1.013	-7.03	0	0	0	0
12	1.000	-7.04	0	0	8.5	88.0
13	1.014	-6.92	0	0	0	0
14	1.012	-8.58	0	0	0	0
15	1.016	-8.97	0	0	320.0	153.0
16	1.023	-7.55	0	0	329.0	0.323
17	1.034	-8.55	0	0	0	0
18	1.031	-9.40	0	0	158.0	30.0
19	1.050	-2.92	0	0	0	0
20	0.991	-4.34	0	0	628.0	103.0
21	1.032	-5.14	0	0	274.0	115.0
22	1.050	-0.69	0	0	0	0
23	1.045	-0.89	0	0	247.5	84.6
24	1.038	-7.43	0	0	308.6	-92.0
25	1.058	-5.43	0	0	224.0	47.2
26	1.052	-6.68	0	0	139.0	17.0
27	1.038	-8.7	0	0	281.0	75.5
28	1.050	-3.17	0	0	206.0	27.6
29	1.050	-0.41	0	0	283.5	26.9
30	1.048	-4.38	250.0	145.1	0	0
31	0.982	0.0	563.3	205.5	9.2	4.6
32	0.983	1.79	650.0	205.7	0	0
33	0.997	2.29	632.0	109.1	0	0
34	1.012	0.85	508.0	167.0	0	0
35	1.049	4.27	650.0	211.3	0	0

Bus data (continue)						
36	1.064	6.96	560.0	100.5	0	0
37	1.028	1.35	540.0	0.7	0	0
38	1.027	6.65	830.0	22.8	0	0
39	1.030	-10.92	1000.0	88.0	1104.0	250.0

b) Line data

LINE		ELECTRICAL PARAMETERS			TRANSFORMER TAP CHANGER	
From bus	To bus	R (p.u.)	X (p.u.)	Charging (p.u.)	tap ratio (p.u.)	phase shift (deg.)
1	2	0.0035	0.0411	0.6978	1	0
1	39	0.001	0.025	0.75	1	0
2	3	0.0013	0.0151	0.2572	1	0
2	25	0.007	0.0086	0.146	1	0
3	4	0.0013	0.0213	0.2214	1	0
3	18	0.0011	0.0133	0.2138	1	0
4	5	0.0008	0.0128	0.1342	1	0
4	14	0.0008	0.0129	0.1382	1	0
5	6	0.0002	0.0026	0.0434	1	0
5	8	0.0008	0.0112	0.1476	1	0
6	7	0.0006	0.0092	0.113	1	0
6	11	0.0007	0.0082	0.1389	1	0
7	8	0.0004	0.0046	0.078	1	0
8	9	0.0023	0.0363	0.3804	1	0
9	39	0.001	0.025	1.2	1	0
10	11	0.0004	0.0043	0.0729	1	0
10	13	0.0004	0.0043	0.0729	1	0
13	14	0.0009	0.0101	0.1723	1	0
14	15	0.0018	0.0217	0.366	1	0
15	16	0.0009	0.0094	0.171	1	0
16	17	0.0007	0.0089	0.1342	1	0
16	19	0.0016	0.0195	0.304	1	0
16	21	0.0008	0.0135	0.2548	1	0
16	24	0.0003	0.0059	0.068	1	0
17	18	0.0007	0.0082	0.1319	1	0
17	27	0.0013	0.0173	0.3216	1	0
21	22	0.0008	0.014	0.2565	1	0
22	23	0.0006	0.0096	0.1846	1	0
23	24	0.0022	0.035	0.361	1	0
25	26	0.0032	0.0323	0.513	1	0
26	27	0.0014	0.0147	0.2396	1	0

Line data (continue)						
26	28	0.0043	0.0474	0.7802	1	0
26	29	0.0057	0.0625	1.029	1	0
28	29	0.0014	0.0151	0.249	1	0
1	27	0.0032	0.0323	0.513	1	0
23	36	0.0005	0.0272	0	1	0
12	11	0.0016	0.0435	0	1.006	0
12	13	0.0016	0.0435	0	1.006	0
6	31	0	0.025	0	1.07	0
10	32	0	0.02	0	1.07	0
19	33	0.0007	0.0142	0	1.07	0
20	34	0.0009	0.018	0	1.009	0
22	35	0	0.0143	0	1.025	0
25	37	0.0006	0.0232	0	1.025	0
2	30	0	0.0181	0	1.025	0
29	38	0.0008	0.0156	0	1.025	0
19	20	0.0007	0.0138	0	1.06	0

c) Generator data

BUS NO.	Ra (p.u.)	Xl (p.u.)	H (sec.)	Q_{max} (MVAR)	Q_{min} (MVAR)
30	0	0.028	24.3	400	-200
31	0	0.035	30.3	380	-220
32	0	0.0304	35.8	560	-400
33	0	0.0295	28.6	560	-400
34	0	0.054	26	480	-220
35	0	0.0224	34.8	560	-400
36	0	0.0322	26.4	480	-220
37	0	0.003	40	480	-220
38	0	0.0298	34.5	800	-600
39	0	0.0125	42	1000	-800

d) Excitation system data

BUS NO.	K_A	T_A	K_E	T_E	K_F	T_F	V_{RMAX}	V_{RMIN}	C_1	C_2
30	5	0.05	-0.01	0.5	0.04	0.5	1.0	-1.0	0.6	0.8
31	20	0.05	-0.0198	0.5	0.08	1	4.0	-4.0	0.07	0.91
32	5	0.06	-0.0198	0.5	0.08	1	1.0	-1.0	0.15	0.35
33	5	0.06	-0.0125	0.5	0.08	1	1.0	-1.0	0.1	0.3
34	20	0.02	1	0.785	0.03	1	4.0	-4.0	0.08	0.31
35	5	0.02	-0.0419	0.471	0.0754	1.246	1.0	-1.0	0.064	0.251
36	20	0.02	1	0.73	0.03	1	4.0	-4.0	0.08	0.28
37	5	0.05	-0.047	0.528	0.0854	1.26	1.0	-1.0	0.072	0.282
38	20	0.02	1	1.4	0.03	1	4.0	-4.0	0.6	0.8
39	5	0.06	-0.0485	0.25	0.04	1	1.0	-1.0	0.08	0.26

e) Start-up characteristics (used in chapter 4)

Unit No.	Bus No.	Unit Type	MW Cap. (MW)	Min. load (MW)	Start-Up Req. (MW)	Crank to paral. Time in hot state (min)	Paral. to Min. load time in hot state (min)	Min. to full load time in hot state (min)
1	30	CT	40	10	0	6	3	6
2	31	Drum	650	200	23	50	35	50
3	32	Drum	750	250	28	100	40	70
4	33	CT	200	50	4	20	10	20
5	34	Drum	840	300	30	75	40	60
6	35	CT	50	12	0	7	8	15
7	36	Drum	560	180	20	42	30	45
8	37	Drum	540	110	18	70	30	80
9	38	SCOT	830	280	26	80	40	85
10	39	Drum	1000	350	30	100	50	95

Unit No.	Shot down time for change hot to warm state (min)	Ccrank to paral. time in warm state (min)	Paral. To Min. Load time In warm state (min)	Min. To Full Load time in warm state (min)	Shot down time for change warm to cold state (min)	Crit. Min. int. (min)	Crit. Max. Int. (min)
1	20	9	5	10	40	N/A	N/A
2	60	100	55	75	90	N/A	90
3	120	150	55	90	120	N/A	120
4	60	28	14	25	60	N/A	60
5	90	90	60	100	150	N/A	150
6	10	10	12	20	30	N/A	N/A
7	50	80	60	80	100	N/A	100
8	70	120	40	95	140	N/A	140
9	80	200	50	100	180	200	N/A
10	80	220	60	110	240	N/A	240

Appendix B

IEEE 118 bus Test System Data

a) Bus Data

BUS NO.	VOLTAGE		GENERATION		LOAD	
	(p.u.)	(Deg.)	(MW)	(MVAR)	(MW)	(MVAR)
1	1.051	0	116.976	-25.34	51	27
2	1.064	-1.941	0	0	20	9
3	1.058	-0.947	0	0	39	10
4	1.1	-0.386	100	331.027	39	12
5	1.078	-0.118	0	0	0	0
6	1.085	-2.224	5	59.466	52	22
7	1.082	-2.468	0	0	19	2
8	1.055	1.947	100	-212.4	28.000	0
9	1.097	3.282	0	0	0	0
10	1.1	4.807	100	-71.174	0	0
11	1.076	-2.277	0	0	70	23
12	1.08	-2.554	30	93.438	47	10
13	1.061	-3.311	0	0	34	16
14	1.075	-3.06	0	0	14	1
15	1.063	-3.019	-6	32.708	90	30
16	1.074	-2.408	0	0	25	10
17	1.081	-0.009	0	0	11	3
18	1.068	-2.259	5	38.029	60	34
19	1.06	-3.098	5	13.666	45	25
20	1.052	-1.406	0	0	18	3
21	1.051	0.623	0	0	14	8
22	1.059	3.568	0	0	10	5
23	1.085	9.016	0	0	7	3
24	1.08	10.403	100	101.447	13	0
25	1.1	12.397	100	222.911	0	0
26	0.976	13.615	300	-326.02	0.000	0
27	1.095	6.602	100	12.904	71	13
28	1.092	5.242	0	0	17	7
29	1.096	4.457	0	0	24	4
30	1.034	1.639	0	0	0	0
31	1.1	4.54	100	46.499	43	27
32	1.089	5.3	5	7.566	59	23
33	1.036	-5.032	0	0	23	9
34	1.049	-6.627	5	332.38	59	26

Bus data (continue)						
BUS NO.	VOLTAGE		GENERATION		LOAD	
	(p.u.)	(deg.)	(MW)	(MVAR)	(MW)	(MVAR)
35	1.037	-6.856	0	0	33	9
36	1.041	-6.902	5	37.245	31	17
37	1.024	-5.785	0	0	0	0
38	1.011	-3.064	0	0	0	0
39	0.98	-6.388	0	0	27	11
40	0.965	-5.861	101.7	-76.827	66	23
41	0.968	-7.012	0	0	37	10
42	1.005	-7.332	106.6	12.865	96	23
43	1.046	-9.262	0	0	18	7
44	1.058	-10.833	0	0	16	8
45	1.059	-10.576	0	0	53	22
46	1.077	-7.609	111.1	-1.852	28	10
47	1.058	-8.775	0	0	34	0
48	1.078	-9.435	0	0	20	11
49	1.077	-9.343	100	132.189	87	30
50	1.078	-11.162	0	0	17	4
51	1.071	-13.256	0	0	17	8
52	1.07	-14.028	0	0	18	5
53	1.079	-14.688	0	0	23	11
54	1.1	-13.884	109.4	155.935	113	32
55	1.091	-14.093	15	2.22	63	22
56	1.093	-13.998	7.2	-25.104	84	18
57	1.091	-13.273	0	0	12	3
58	1.079	-13.816	0	0	12	3
59	1.09	-11.561	120.1	258.778	277	113
60	1.004	-7.772	0	0	78	3
61	0.998	-6.78	205	-344	0.000	0
62	1.006	-7.845	10	-0.537	77	14
63	1.034	-8.551	0	0	0	0
64	1.029	-6.793	0	0	0	0
65	1.068	-4.447	100	479.753	0	0
66	1.064	-6.369	100	-211.53	39.000	18
67	1.032	-7.824	0	0	28	7
68	1.046	-3.098	0	0	0	0
69	0.95	-3.093	0	-495.52	0.000	0
70	0.915	0.918	10	7.308	66	20
71	0.906	5.228	0	0	0	0
72	0.9	14.768	100	-103.57	12.000	0
73	0.9	8.394	100	-27.745	6	0
74	0.9	-4.392	5	5.092	68	27
75	0.91	-4.328	0	0	47	11
76	0.9	-6.258	0	11.766	68	36
77	0.978	-1.621	30.7	32.891	61	28

Bus data (continue)						
BUS NO.	VOLTAGE		GENERATION		LOAD	
	(p.u.)	(deg.)	(MW)	(MVAR)	(MW)	(MVAR)
78	0.976	-2.081	0	0	71	26
79	0.984	-2.023	0	0	39	32
80	1.021	-0.402	100	40.714	130	26
81	1.016	-2.03	0	0	0	0
82	0.983	4.843	0	0	54	27
83	0.983	8.357	0	0	20	10
84	0.996	14.454	0	0	11	7
85	1.013	17.635	10	-13.588	24	15
86	1.035	24.396	0	0	21	10
87	1.1	37.022	124.2	27.985	0	0
88	1.032	20.027	0	0	48	10
89	1.059	23.363	400	-6.267	0	0
90	1.074	23.499	150.7	60.789	163	42
91	1.074	24.499	125.6	-11.934	10	0
92	1.049	18.394	10	-18.964	65	10
93	1.034	13.893	0	0	12	7
94	1.032	10.359	0	0	30	16
95	1.006	7.76	0	0	42	31
96	0.998	5.401	0	0	38	15
97	1.004	2.192	0	0	15	9
98	1.037	3.261	0	0	34	8
99	1.071	11.149	124.9	-23.946	42	0
100	1.1	11.902	100	286.837	37	18
101	1.065	13.85	0	0	22	15
102	1.053	16.772	0	0	5	3
103	1.091	13.632	18.7	8.068	23	16
104	1.079	13.798	20	5.554	38	25
105	1.079	14.472	20	-14.957	31	26
106	1.079	13.898	0	0	43	16
107	1.1	17.196	120.1	5.815	50	12
108	1.079	16.093	0	0	2	1
109	1.079	16.786	0	0	8	3
110	1.083	18.894	0	-13.552	39	30
111	1.1	22.54	100	-2.387	0	0
112	1.1	20.312	118.1	19.703	68	13
113	1.1	1.68	100	45.445	6	0
114	1.087	5.407	0	0	8	3
115	1.087	5.463	0	0	22	7
116	1.062	-3.029	250	420.312	184	0
117	1.066	-3.85	0	0	20	8
118	0.898	-5.746	0	0	33	15

b) Line Data

From bus	To bus	R (Ohm)	X (Ohm)	Charg-ing	Rating (MVA)
1	2	3.03	9.99	2.52	144
1	3	1.29	4.24	1.08	144
2	12	1.87	6.16	1.56	144
3	5	2.41	10.8	2.84	350
3	12	4.84	16	4.06	144
4	5	0.18	0.8	0.2	310
4	11	2.09	6.88	1.74	144
5	6	1.19	5.4	1.42	175
8	5	0	2.67	0	9999
5	11	2.03	6.82	1.74	144
6	7	0.45	2.08	0.54	175
7	12	0.86	3.4	0.86	160
8	9	0.24	3.05	116.2	1550
8	30	0.43	5.04	51.4	776
9	10	0.26	3.22	123	1550
11	12	0.59	1.96	0.5	144
11	13	2.22	7.31	1.88	144
12	14	2.15	7.07	1.82	144
12	16	2.12	8.34	2.14	160
12	117	3.29	14	3.58	160
13	15	7.44	24.44	6.26	144
14	15	5.95	19.5	5.02	144
15	17	1.32	4.37	4.44	288
15	19	1.2	3.94	1	144
15	33	3.8	12.44	3.2	144
16	17	4.54	18.01	4.66	160
17	18	1.23	5.05	1.28	350
30	17	0	3.88	0	9999
17	31	4.74	15.63	4	144
17	113	0.91	3.01	0.76	311
18	19	1.11	4.93	1.14	292
19	20	2.52	11.7	2.98	175
19	34	7.52	24.7	6.32	144
20	21	1.83	8.49	2.16	175
21	22	2.09	9.7	2.46	175
22	23	3.42	15.9	4.04	175
23	24	1.35	4.92	4.98	320
23	25	1.56	8	8.64	187
23	32	3.17	11.53	11.72	288
24	70	10.22	41.15	10.2	160
24	72	4.88	19.6	4.88	160
26	25	0	3.82	0	9999
25	27	3.18	16.3	17.64	374

From bus	To bus	R (Ohm)	X (Ohm)	Charg-ing	Rating (MVA)
27	28	1.91	8.55	2.16	175
27	32	2.29	7.55	1.92	144
27	115	1.66	7.41	1.9	144
28	29	2.37	9.43	2.34	175
29	31	1.08	3.31	0.82	166
30	38	0.46	5.4	42.2	717
31	32	2.98	9.85	2.5	311
32	113	6.15	20.3	5.18	311
32	114	1.35	6.12	1.62	175
33	37	4.15	14.2	3.66	144
34	36	0.87	2.68	0.56	175
34	37	0.26	0.94	0.98	316
34	43	4.13	16.81	4.22	160
35	36	0.22	1.02	0.26	160
35	37	1.1	4.97	1.32	175
38	37	0	3.75	0	9999
37	39	3.21	10.6	2.7	144
37	40	5.93	16.8	4.2	316
38	65	0.9	9.86	104.6	717
39	40	1.84	4.05	1.54	144
40	41	1.45	4.87	1.22	144
40	42	5.55	18.3	4.66	144
41	42	4.1	13.5	3.44	144
42	49	3.58	16.1	17.2	330
43	44	6.08	24.54	6.06	160
44	45	2.24	9.01	2.24	160
45	46	4	13.56	3.32	144
45	49	6.84	18.6	4.44	175
46	47	3.8	12.7	3.16	144
46	48	6.01	18.9	4.72	144
47	49	1.91	6.25	1.6	144
47	69	8.44	27.78	7.1	144
48	49	1.79	5.05	1.26	144
49	50	2.67	7.53	1.86	316
49	51	4.86	13.7	3.42	316
49	54	3.98	14.5	14.68	320
49	66	0.9	4.59	4.96	932
49	69	5.85	22.4	6.28	144
50	57	4.74	13.4	3.32	316
51	52	2.03	5.89	1.4	316
51	58	2.55	7.19	1.78	316
52	53	4.05	16.35	4.04	160
53	54	2.63	12.2	3.1	175

Line Data (continue)					
From bus	To bus	R (Ohm)	X (Ohm)	Charg-ing	Rating (MVA)
26	30	0.79	8.6	90.8	717
54	56	0.27	0.95	0.72	260
54	59	5.03	22.93	5.88	514
55	56	0.48	1.51	0.38	144
55	59	4.73	21.58	5.66	175
56	57	3.43	9.66	2.42	316
56	58	3.43	9.66	2.42	316
56	59	4.07	12	11.04	230
59	60	1.17	14.5	3.76	175
59	61	3.28	15	3.68	175
63	59	0	3.86	0	9999
60	61	0.26	1.35	1.46	187
60	62	1.23	5.61	1.46	175
61	62	0.82	3.76	0.98	175
64	61	0	2.68	0	776
62	66	4.82	21.8	3.78	776
62	67	2.58	11.7	3.1	9999
63	64	0.17	2	21.6	1493
64	65	0.27	3.02	38	175
65	66	0	3.7	0	9999
65	68	0.14	1.6	63.8	717
66	67	2.24	10.15	2.68	776
68	69	0	3.7	0	160
68	81	0.17	2.02	80.8	144
68	116	0.03	0.4	16.5	144
69	70	3	12.7	12.2	160
69	75	4.05	12.2	12.4	144
69	77	3	10.1	10.38	144
70	71	0.68	3.55	0.86	160
70	74	4.01	13.23	3.36	144
70	75	4.28	14.1	3.6	144
71	72	4.46	18	4.44	160
71	73	0.87	4.54	1.18	187
74	75	1.23	4.06	1.02	144
75	77	6.01	19.99	4.98	144
75	118	1.45	4.81	1.18	144
76	77	4.44	14.8	3.68	144
76	118	1.64	5.44	1.36	144
77	78	0.37	1.24	1.26	144
77	80	1.08	3.31	7	254
77	82	2.98	8.53	8.18	127
78	79	0.54	2.44	0.64	175
79	80	1.56	7.04	1.86	175
81	80	0	3.7	0	9999
80	96	3.56	18.2	4.96	187
80	97	1.83	9.34	2.64	187

From bus	To bus	R (Ohm)	X (Ohm)	Charg-ing	Rating (MVA)
114	115	0.23	1.06	0.28	175
54	55	1.69	7.07	2.02	350
80	98	2.38	10.8	2.86	175
80	99	4.54	20.6	5.46	175
82	83	1.12	3.66	3.8	288
82	96	1.62	5.3	5.44	144
83	84	6.25	13.2	2.58	203
83	85	4.3	14.8	3.48	144
84	85	3.02	6.41	1.22	187
85	86	3.5	12.3	2.76	144
85	88	2	10.2	2.76	187
85	89	2.39	17.3	4.7	187
86	87	2.82	20.74	4.44	201
88	89	1.39	7.12	1.92	187
89	90	1.63	6.52	15.88	748
89	92	0.79	3.8	9.62	374
90	91	2.54	0.36	2.14	144
91	92	3.87	12.72	3.26	144
92	93	2.58	8.48	2.18	144
92	94	4.81	15.8	4.06	144
92	100	6.65	29.5	7.72	175
92	102	1.23	5.59	1.66	175
93	94	2.23	7.32	1.88	144
94	95	1.32	4.34	1.1	144
94	96	2.69	6.69	2.3	144
94	100	1.78	5.6	6.04	288
95	96	1.71	5.67	1.48	144
96	97	1.73	8.85	2.4	187
98	100	3.97	17.9	4.76	175
99	100	1.8	8.13	2.16	175
100	101	2.77	12.62	3.28	175
100	103	1.6	5.25	5.36	144
100	104	4.51	20.4	5.4	175
100	106	6.05	22.9	6.2	175
101	102	2.46	11.2	2.94	175
103	104	4.66	15.84	4.06	144
103	105	5.35	16.25	4.08	144
103	110	3.91	18.13	4.6	175
104	105	0.99	3.78	0.98	144
105	106	1.4	5.47	1.44	144
105	107	5.3	18.3	4.72	144
105	108	2.61	7.03	1.84	127
106	107	5.3	18.3	4.72	144
108	109	1.05	2.86	0.76	127
109	110	2.78	7.62	2.02	127
110	111	2.2	7.55	2	144
110	112	2.47	6.4	6.2	127

Published or Proposed Papers

Published or Proposed Papers

[1] A. Ketabi and A.M. Ranjbar, "New Approach to Standing Phase Angle Reduction for Power System Restoration," *Proceedings of IEEE Budapest Power Tech'99 conference, Budapest-Hungary, Aug.– Sept. 1999, pp. 78-83.*

[2] A. Ketabi, A.M. Ranjbar and R. Feuillet, " Long –Term Dynamics Evaluation in Restoring Customer Loads," *Proceedings of the American Power Conference (APC'00), 62st Annual Meeting, Chicago Marriott Downtown USA, April 10-12 2000, pp. 275-281.*

[3] **A. Ketabi, A.M. Ranjbar and R. Feuillet, "New Approach to Standing Phase Angle Reduction for Power System Restoration,"** ***Accepted paper for publishing in "European Transaction on Electrical Power (ETEP)" journal, March 2001, Paper No. ET1681.***

[4] Ketabi, A.M. Ranjbar and R. Feuillet, "A New Method for Dynamic Calculation of Load Steps during Power System Restoration," *Proceedings of CCECE' 2000, Halifax N.S Canada, 7-10 May 2000, pp.*158 –162.

[5] **A. Ketabi, A.M. Ranjbar and R. Feuillet, " A New Method for Load Steps Calculation during Power System Restoration,"** ***Paper accepted for publishing in the Scientia Iranica, international journal of Science and Technology, July 2001, Paper No. 25.163.000929.***

[6] A. Ketabi, A.M. Ranjbar and R. Feuillet, "Application of Finite State Machines Concepts for Scheduling of Generic Restoration Actions," *Proceedings of 35th University Power Engineering Conference (UPEC'2000), Belfast UK, Sep. 6-8, 2000.*

[7] A. Ketabi, A.M. Ranjbar and R. Feuillet, " An Approach for Optimal Units Start-up during Bulk Power System Restoration," *Proceedings of LESCOPE'01* (2001 Large Engineering Systems Conference on Power Engineering), Halifax, Nova Scotia, Canada, July 11-13, 2001.

[8] A. Ketabi, A.M. Ranjbar and R. Feuillet, " Analysis of Temporary Overvoltages due to Transformer Energization during System Restoration," Accepted for IEEE/PES T&D 2002 Latin Aamerica Conference, Sao Paulo Brazil, 18-22 March 2002

[9] **A. Ketabi, A.M. Ranjbar and R. Feuillet, " Analysis and Control of Temporary Overvoltages for Automated Restoration Planning,"** ***Under reviewing by the technical committee of the IEEE Transactions on Power Delivery, Paper No. 2001TR529.***

FRENCH EXTENDED SUMMARY

SOMMAIRES

Remerciements

Je tiens à remercier:

- Monsieur **J.P. Rognon**, Directeur du Laboratoire d'Electrotechnique de Grenoble (LEG) pour m'avoir accueilli au LEG,
- Monsieur **R. Feuillet**, professeur du LEG pour m'avoir accepte dans l'équipe réseaux électriques du LEG et pour avoir été mon directeur de thèse (côté français),
- Monsieur **A.M. Ranjbar**, professeur du Sharif Université de Technologie d'Iran pour avoir propose le sujet de thèse, pour avoir été mon directeur de thèse (côté iranien) et pour m'avoir accueilli au Centre de recherche de NIROO (NRI),
- Monsieur **M. Baribuad,** professeur de l'INPG pour avoir accepte d'être président du jury de ma thèse,
- Monsieur **N. Hadj-said**, professeur du LEG pour avoir su me consacrer le temps qu'il fallait pour la lecture de ce rapport et pour avoir accepte d'être examinateur de ma thèse,
- Madame **Z.A. Do VALE**, professeur de l'Institut Polytechnique de Porto, de Portugal pour avoir accepte d'être rapporteur de mon travail,
- Monsieur **M. Abedi**, professeur de l'Amir-Kabir Université de Technologie, d'Iran pour avoir accepte d'être rapporteur de ce travail,
- Monsieur **M. Vakilian**, Maître de Conférence du Sharif Université de Technologie, d'Iran pour avoir accepte d'être examinateur de ma thèse,
- Monsieur **F. Farzaneh**, Maître de Conférence du Sharif Université de Technologie, d'Iran pour avoir accepte d'être examinateur de ma thèse et aussi pour avoir traduit mon expose à la langue française.

Je remercie les gens du LEG avec qui j'ai eu l'occasion de travailler dans la bonne humeur.
Je remercie le Ministère d'Education Supérieur d'Iran qui a finance mes recherches en Iran et le Président de Centre de Relation International de Sharif Université de Technologie.
Je tiens à remercier également le Ministère des Affaires Etrangers Français et les gens du Centre Culturel Français en Iran qui ont finance mes recherches en France.

CHAPITRE 1: INTRODUCTION

INTRODUCTION

Le fonctionnement d'un réseau électrique peut être classé en cinq états différents: l'état normal, l'état d'alerte, l'état critique, l'état catastrophique, et l'état de remise en charge (cf. Figure 1.1) [57, 120].

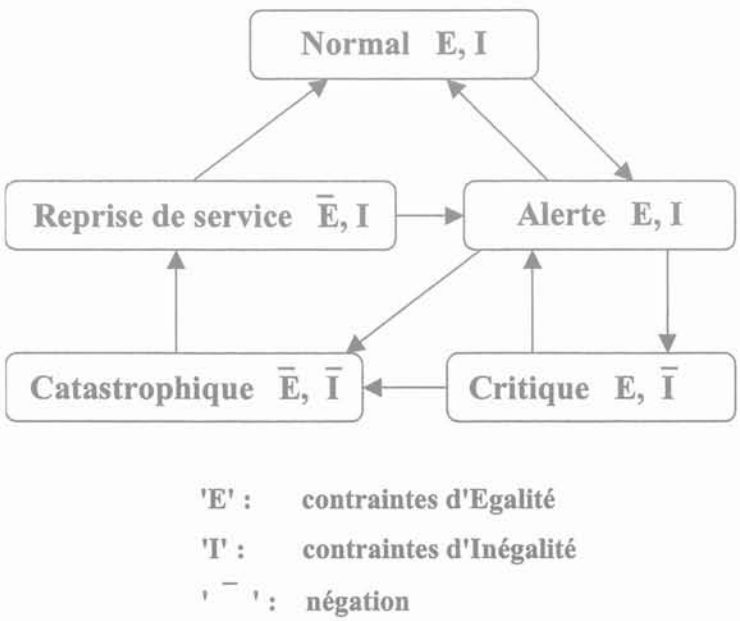

Figure 1.1: états de fonctionnement d'un réseau électrique

Dans l'état normal, toutes les variables du système sont dans la gamme des valeurs normales; aucun équipement n'est surchargé et le système satisfait la demande de tous les consommateurs. Dans cet état même, le système peut subir une contingence sans que cela réduise le niveau de sa sécurité et l'ensemble des contraintes d'égalité (ou la répartition de charge du réseau) et d'inégalité (ou limites) sont satisfaites.

Dans l'état d'alerte, le niveau de sécurité du système est réduit mais les contraintes d'égalité et d'inégalité demeurent toujours satisfaites. Même dans le cas du fonctionnement d'un système dans ses limites admissibles, une contingence peut provoquer un état critique, voire même l'état catastrophique si cette contingence est sévère.

Le système se trouve dans un état critique soit dans le cas où les contraintes d'inégalité ne sont pas respectées (c'est à dire que la fréquence du système et les tensions ne sont plus comprises dans l'intervalle des valeurs admissibles), soit lorsqu'une partie des équipements est surchargée.

Un système supposé être dans un état critique peut être ramené à un état d'alerte si les actions d'urgence sont activées. Si ces mesures ne sont pas appliquées avec succès, le réseau commence à s'écrouler et entre dans l'état catastrophique (violation des contraintes

d'égalités et d'inégalités). Dans le cas d'une série de panne, des parties plus ou moins étendues du réseau peuvent se trouver sans tension [120].

On dit qu'un système est dans l'état de remise en charge quand des manœuvres sont prises et reprises pour reconnecter tous les équipements, ré-alimenter les charges et finalement amener le système à son état normal. Dans cet état, les contraintes d'inégalité sont satisfaites mais l'équation de répartition de charge n'est pas complètement satisfaite.

La reprise de service du réseau électrique est le processus de reconstitution des centrales électriques, la mise sous tension du réseau de transmission et la ré-alimentation des consommateurs. Cette phase doit s'achever le plus rapidement possible sans causer d'autres pannes ou de dommages matériels.

En raison de la dérégulation et des changements actuels des structures industrielles, les réseaux électriques fonctionnent de plus en plus près de leurs limites. Depuis quelques années, les réseaux électriques sont devenus de plus en plus complexes et leurs dimensions sont de plus en plus importantes ; par conséquent le nombre d'incidents a augmenté. Nous pouvons citer l'exemple de trois incidents généralisés (black-out) intervenant en 1996 sur la Côte Ouest de l'Amérique du Nord, en 1999 au Brésil et en 2001 en Iran.

De tels incidents peuvent être causés par plusieurs perturbations, entre autres: les catastrophes naturelles, la surcharge des lignes, les instabilités du système...etc. Par ailleurs, les défauts temporaires dus par exemple à la foudre, même s'ils disparaissent immédiatement, peuvent donner lieu au phénomène 'château de cartes' ou de cascade. Ce phénomène est suffisant pour causer des pannes partielles qui causent à leur tour la séparation du réseau en plusieurs sous-systèmes et le délestage des charges (load shedding). Après une panne quelconque, il est plus intéressant de restaurer le réseau que de chercher les causes initiales de la panne [2].

La restauration d'un réseau électrique est un processus très complexe qui implique typiquement tous les composants du système à savoir la production, le transport et la distribution. Cependant, il est plus pratique, dans les entreprises d'énergie électrique, de développer des stratégies distinctes pour la restauration des systèmes de transport et de distribution. Cette thèse se focalise sur les systèmes de production et de transport.

L'effet des pannes de puissance sur le public et sur l'économie, ainsi que la probabilité de destruction du matériel peuvent être réduits considérablement en utilisant un processus rapide, efficace et ordonné de la reprise de service [2]. Il y a donc une demande croissante en procédures systématiques, en outils pour la planification et pour la restauration en ligne.

1.1 Objectifs et Etapes de la Reprise de Service

Bien que chaque incident de puissance et scénario de reprise de service soit un événement particulier, certains objectifs et étapes de restauration sont communs pour toutes les

procédures de la reprise de service. La Figure 1.2 présente les objectifs de la reprise de service tels qu'ils sont définis dans [59, 128, 130].

Ils impliquent presque tous les aspects de fonctionnement et de planification du réseau électrique. Chaque procédure de reprise de service d'un réseau électrique peut être subdivisée en quatre étapes [2, 33]:

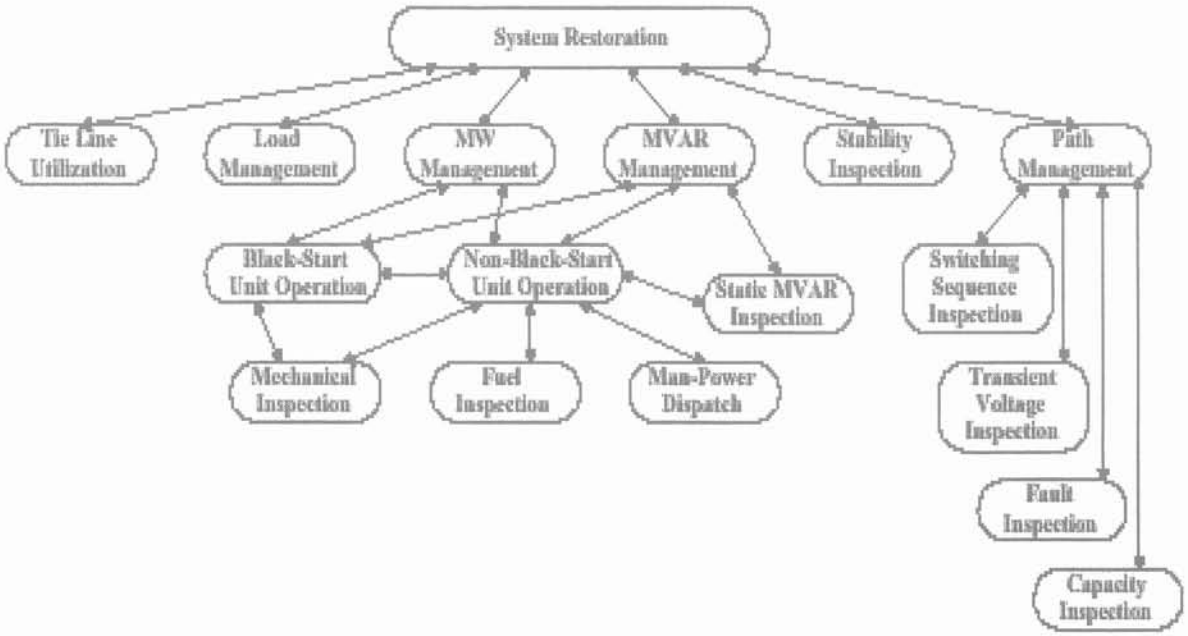

Figure 1.2: Les objectifs de la reprise de service

1. *Détermination de l'état du système.* Dans cette étape, les frontières des zones alimentées sont identifiées afin que leurs fréquences et tensions soient évaluées. Par ailleurs, s'il n'y a pas de connexion avec les systèmes voisins, les sources de réalimentation 'black-start or cranking' et les charges critiques de chaque sous-système sont respectivement identifiées et localisées.

2. *Redémarrage des Grands Groupes Thermiques.* Les grandes centrales thermiques doivent être redémarrées au cours d'une certaine période. Par exemple, le démarrage a chaud des chaudières de type tambour est possible en trente minutes seulement. S'il n'est pas accompli pendant cette durée, la chaudière ne peut pas être opérationnelle dans une durée de quatre a six heures. Dans ces conditions, un démarrage a froid peut être exécute.

   Les centrales thermiques peuvent être démarrées au moyen des petits groupes de capacité 'black-start'; elles peuvent donc être démarrées sans aide extérieure pendant une courte durée. Les centrales électriques de capacités 'black-start' sont soit des centrales hydrauliques, soit des centrales à gaz ou bien des centrales diesel.

Lorsque ces dernières en sont à leur phase finale de fonctionnement, un chemin haute tension s'établit avec les grandes centrales thermiques et les auxiliaires des centrales thermiques entraînées par les grands moteurs d'induction sont démarrés.

Tout au long de ce chemin, des charges sont connectées. Elles servent d'une part à maintenir la tension dans des limites acceptables et d'autre part à préparer une base de charges pour les centrales thermiques connectées ultérieurement.

Des petits groupes supplémentaires peuvent aussi être connectés (mise en ligne) à travers ce chemin pour améliorer la stabilité du système [40].

3. *Mise sous tension de sous-systèmes.* En cas d'un grand incident de puissance, il est plus pratique de subdiviser le système en plusieurs sous-systèmes pour réaliser une mise en service parallèle, ce qui réduit le temps total de la procédure.

   Dans chaque sous-système, il faut d'abord démarrer la grande centrale thermique et mettre ensuite sous tension le squelette du réseau électrique.

   A ce stade, les chemins des centrales électriques et des grands centres de charge sont rétablis. Ces charges sont ré-alimentées pour raffermir le réseau de transport.

   A la fin de cette étape, le réseau dispose suffisamment de puissance et de stabilité, ce qui lui permet de supporter les transitoires dans le cas où des charges supplémentaires sont ré-alimentées.

4. *Interconnexion des Sous-systèmes.* A cette phase du processus de remise en service d'un réseau électrique, les sous-systèmes sont interconnectes. Finalement, le système passe soit a un état d'alerte, soit a un état normal lorsque toutes les charges sont re-alimentées.

   Parmi les quatre étapes générales du processus de remise en service, les deuxième et troisième étapes sont les plus critiques.

Une erreur pendant ces deux étapes peut mener à la déconnexion des générateurs et au délestage de charges, à la suite de déviation de la fréquence et de la tension ou delà des limites et ....

1.2 Problèmes Pendant la Reprise de Service

Plusieurs phénomènes et états anormaux peuvent se produire pendant la reprise de service d'un réseau électrique. Les problèmes rencontrés pendant la reprise de service peuvent être subdivisés en trois parties principales [2, 33, 69, 70, 75]:

1. *Equilibre de la puissance active et réponse fréquentielle.* La fréquence est l'expression électrique de la vitesse de rotation des alternateurs. En régime établi, les alternateurs rendus solidaires par le couple synchronisant, tournent tous à la même vitesse électrique. Pour chaque alternateur, il y a alors égalité entre le couple moteur, fourni par

la turbine et le couple résistant, couple électrique opposé par le réseau; autrement dit, il y a égalité entre la production et la consommation de puissance active. Tout déséquilibre de ce bilan entraînera une variation de vitesse, donc de fréquence.

Pendant le processus de la remise en service, deux aspects différents de ce problème peuvent être identifiés.

Le premier est le redémarrage des grandes centrales thermiques. Pendant ce temps, une grande partie des moteurs auxiliaires est ré-alimentée soit par des petits générateurs hydrauliques soit par des centrales à gaz/diesel .

Ceci peut résulter en une forte décroissance de la fréquence et par conséquent le relais fréquencemétrique est activé. Dans le pire des cas, les charges déjà restaurées sont déconnectées ce qui mène à une répétition du black-out [33].

Comme ce problème (défini comme une partie de la problématique de reprise de service d'un réseau électrique) est important, nous le traiterons plus en détails plus tard.

Le deuxième est la ré-alimentation des charges froides. Dans un réseau, des centrales électriques sont rajoutées et les charges sont ré-alimentées tout en conservant l'équilibre entre la production et la consommation.

Toute perturbation de cet équilibre conduit à une diminution de la fréquence du système. Comme pour le premier problème, les même opérations sont effectuées en cas de fortes perturbations à la seule différence qu'il y a déconnexion des groupes générateurs par des relais de protection fréquencemétrique dans le cas où la fréquence continu a baisser. Ceci est dû au fait que la fréquence de fonctionnement des turbines à vapeurs est limitée à 58.8 Hz (pour 60Hz système) [120].

Ainsi, les valeurs des charges réalimentées ne doivent pas dépasser certaines grandeurs afin de garder la variation de la fréquence dans les limites admissibles. Cependant, toute augmentation faible de la charge entraîne une prolongation inutile de la durée de reprise de service [5, 40, 69].

Le Tableau 1.1 montre, pour le réseau électrique de Chypre (de fréquence 50Hz) [33], les valeurs limites du délestage de charge (load shedding) correspondant aux valeurs décroissantes de la fréquence du système. On note sur ce tableau que pour une diminution de 3Hz de la fréquence, 80% de la charge est déconnectée.

Tableau 1.1: Les valeurs limites du délestage de charge pour le réseau électrique de Chypre

Fréquence (Hz)	49.0	48.8	48.4	47.8	47.0
Délestage de charge (%)	15	20	25	10	10
Délai (Retard) (s)	0.2	0.2	0.35	0.35	0.35
Délestage cumulé (%)	15	35	60	70	80

2. Equilibre *de puissance réactive et réponse en tension.* Comme pour l'équilibre de puissance active, il est nécessaire de maintenir l'équilibre de la puissance réactive. Les forts courants réactifs, issus des lignes de transport à faibles charges, peuvent induire des surtensions permanentes dans le cas où les générateurs ne peuvent pas absorber la totalité de la puissance réactive. Ce phénomène peut causer la sous-excitation, l'auto-excitation et l'instabilité du réseau. La saturations des transformateurs est également l'une des conséquences des surtensions permanentes. Dans cet état, des harmoniques de distorsion sont produits.

   Les surtensions transitoires sont rencontrées lors des opérations d'aiguillage des lignes de transport longes et des dispositifs capacitifs. Elles peuvent aussi provoquer la destruction des parafoudres.

   Les surtensions causés par la résonance harmonique sont le résultat des fréquences de résonance proches des fréquences multiples de la fréquence fondamentale du système et essentiellement des courants harmoniques injectés suite aux aiguillages des transformateurs. Les surtensions de ce type, à longues durées, peuvent entraîner la détérioration des parafoudres et des défauts du système.

   Au début d'un processus de reprise de service, les oscillations de la tensions sont importantes car les charges ont de faibles valeurs (une faible atténuation de ces oscillations). Ces oscillations sont plus importantes encore dans le cas de saturation des transformateurs ou dans le cas de la présence des dispositifs d'électronique de puissance dans les réseaux [69].

   Le Tableau 1.2 [143] présente la gamme des valeurs acceptables des tensions pendant la remise en service pour le réseau électrique de Hydro Québec. Ce tableau montre que dans le cas des surtensions harmoniques, il faut prendre en compte à la fois les durées et les amplitudes des surtensions.

Tableau 1.2: La gamme des valeurs acceptables des tensions pendant la remise en service pour le réseau électrique de Hydro Québec

Surtensions permanentes (p.u.)	$0.9 \leq V \leq 1.05$
Surtensions transitoires (p.u.)	$V \leq 1.8$
Surtensions harmoniques (p.u.)	$V \leq 1.5$ (8 cycles)

3. *La Réduction de l'Angle de la Phase Stationnaire (SPA).* Au cours de la réalimentation d'un réseau électrique, les opérateurs rencontrent parfois une grande différence de SPA à travers une ligne.

   La fermeture du disjoncteur de puissance lors d'une grande différence SPA peut déstabiliser le système et endommager le matériel suite aux pannes répétitives survenant sur le système. Afin d'éviter la fermeture des disjoncteurs pour une grande

différence de l'angle de phase, ces derniers sont équipés d'un relais synchronisateur. Ces relais empêchent la fermeture des disjoncteurs pour une valeur d'angle plus élevée que celles des valeurs initialement introduites.

Dans ce cas même, il est possible pour les opérateurs du système de réduire la différence de SPA par un changement de la puissance active des centrales électriques en se servant de la méthode 'essais et erreurs'. Cette technique exige une longue durée et par conséquent prolonge la durée de reprise de service [6].

1.3 Motifs et Objectif de la Thèse

A partir des sections précédents, nous pouvons conclure que plusieurs problèmes complexes et importants ont besoin d'être résolus pendant la remise en service du réseau électrique.

Il est donc nécessaire d'effectuer, durant les phases de planification et de mise en ligne de la remise en service du réseau, une analyse détaillée.

Comme il le sera montré dans l'étude bibliographique du chapitre 2, une grande partie des travaux de recherche dans le domaine des réseaux électriques s'est focalisée sur l'application des techniques de l'intelligence artificielle pour le développement des procédures de la remise en service d'un réseau après un incident généralisé.

Cependant, les systèmes experts ou bien les approches similaires ne représentent pas des méthodes générales applicables à toutes les entreprises d'énergie électriques puisque la philosophie et les objectifs de la remise en service sont différents.

L'évaluation de la faisabilité des étapes de reprise de service a été, principalement, établie par une analyse en régime établi sans prendre en compte les effets dynamiques.

Cependant, il est important de prendre en compte les effets dynamiques dans la planification de la reprise de service du réseau électrique.

Afin de pouvoir prendre en considération ces effets, il est nécessaire

- D'utiliser des outils analytiques supplémentaires comme par exemple : les programmes de la stabilité dynamique à long terme et les programmes d'analyse des transitoires rapides de type électromagnétique. ;
- De développer de nouveaux modèles permettant la simulation dans les conditions extrêmes en dehors de l'état nominal de la tension et de la fréquence[32, 33].

Au cours de la reprise de service, plusieurs phénomènes et conditions anormales sont observés et les résoudre tous en même temps est une tâche assez difficile.

L'utilisation des outils de simulations évoqués précédemment exige beaucoup de temps pour déterminer les séquences convenables à la restauration, ce qui exclut leurs utilisations pour une restauration en ligne à cause du temps disponible limité (une opération de restauration limitée dans le temps).

L'objectif de cette thèse est de proposer, dans un premier temps, des approches permettant l'évaluation de la faisabilité des étapes de reprise de service et de développer, dans un deuxième temps, des techniques de modélisation pour la simulation des états anormaux de la fréquence et de la tension.

Ces approches fournissent aux opérateurs des outils à la fois simples et rapides pour la restauration en ligne, car elles réduisent considérablement le temps de simulation de la planification de la restauration basée sur la méthode 'essais et erreurs'.

Le chapitre 2 présente l'état de l'art de la reprise de service et ce pour les travaux réalisés pendant les deux dernières décennies.

Des travaux de simulation en dynamique à long terme effectués dans le cadre de cette thèse feront l'objet du chapitre 3.

Nous proposerons dans le chapitre 4 une méthode permettant la détermination de la séquence optimale du démarrage des groupes pendant le redémarrage des centrales électriques.

Dans le chapitre suivant nous décrivons une méthode pour l'estimation de la réponse fréquentielle des régulations de vitesses après la ré-alimentation des charges.

La méthode de réduction de l'angle de la phase stationnaire sera expliquée et présentée dans le chapitre 6.

Le chapitre 7 décrit les méthodes d'estimation et de contrôle des surtensions harmoniques. Nous verrons qu'elles réduisent le temps de simulation.

Enfin et pour conclure, nous ferons le point dans le dernier chapitre sur les principaux sujets abordés au cours de ce travail et nous évoquerons les travaux de perspective qui pourraient être entrepris.

CHAPITRE 3

CHAPITRE 3

LA SIMULATION DYNAMIQUE A LONG TERME PENDANT LA REPRISE DE SERVICE DU RESEAU ELECTRIQUE

L'instabilité dans un réseau électrique peut se manifester de plusieurs façons, qui dépendent de la configuration et du mode du fonctionnement du système. La stabilité d'un réseau électrique peut être définie comme l'état de fonctionnement équilibré sous les conditions de fonctionnement normal ou bien comme son aptitude à revenir vers son état d'équilibre après avoir subi une perturbation.

On peut classer la stabilité du réseau électrique comme suit [120]:

a) **la stabilité de l'angle de puissance**

   i- **la stabilité dynamique :** Il arrive que de petites oscillations apparaissent sur les signaux, à cause de changements dans la structure du réseau, des conditions d'exploitation, des systèmes d'excitation ou des charges. Ces oscillations peuvent augmenter et finalement venir déstabiliser une machine, une partie du réseau ou tout le réseau.

   ii- **la stabilité transitoire :** On appelle stabilité transitoire la capacité de maintenir le synchronisme des machines d'un réseau électrique en dépit de grandes perturbations. Cette stabilité concerne les quelques mili secondes qui suivent l'arrivée d'une grande perturbation sur le réseau électrique.

b) **la stabilité de tension :** L'instabilité peut aussi être rencontrée sans perte de synchronisme. L'écroulement de la tension en certains nœuds peut causer l'instabilité du système. Le réseau électrique analysé devrait être capable de maintenir, à une valeur constante et acceptable, la tension en tous point du système, qu'il soit dans les conditions de fonctionnement normales ou bien soumis à des perturbations. L'incapacité du réseau à satisfaire la demande en terme de puissance réactive représente le facteur principal de l'instabilité.

c) **la stabilité à long terme :** La stabilité à long terme suppose que les oscillations de puissance inter- machine sont amorties, ce qui résulte en une fréquence uniforme pour toutes les machines du système. L'intérêt de la dynamique à long terme est l'analyse

des effets des importantes variations de la tension et de la fréquence sur un réseau électrique pour une longue durée. Au cours de cette analyse nous nous intéressons à la modélisation des séquences des évènements apparaissant après une forte perturbation, alors que pour l'analyse de la stabilité transitoire on se consacre particulièrement à l'étude des effets des oscillations inter-machines sur les machines synchrones sous d'autres contraintes (après une forte perturbation également). Les études analytiques de la stabilité à long terme se focalisent sur les performances d'un système sous les fortes perturbations menant à l'apparition des processus lents et l'activation des système de protection et de contrôle. Ces phénomènes ne sont pas prévus dans les programmes de stabilité transitoire. En plus des modèles utilisés dans les outils de simulations de la stabilité transitoire, les logiciels de simulation dynamique à long terme devraient disposer d'une représentation adéquate de la régulation primaire de vitesse et les systèmes d'alimentation d'énergie. Ils devraient également inclure des modèles appropriés pour une large gamme de fonctionnement des systèmes de protection et de contrôle invoquée dans le cas d'un état critique ou catastrophique du réseau.

Parallèlement à la progression de la thèse, nous avons créé un logiciel de simulation de la dynamique à long terme. Ce logiciel peut être utilisé pour étudier la réponse de la fréquence et de la tension due au déséquilibre entre la charge et la production afin d'analyser les scénarios de la reprise de service du réseau électrique. Il peut également être employé pour étudier la réponse de la fréquence de système pendant des réalimentations de charges (consommateur). Ce logiciel a été développé dans l'environnement MATLAB/SIMULINK doté d'une interface graphique permettant une utilisation facile et convivial. Au cours de ce chapitre, nous avons présentés des modèles appropriés des composants du système dédiés aux calcul dynamique de la répartition de charge lors d'une simulation dynamique à long terme.

CHAPITRE 4

CHAPITRE 4

DETERMINATION DES SEQUENCES DE DEMARRAGE DES CENTRALES ELECTRIQUES

La reprise de service d'un système électrique après un incident généralisé nécessite la remise en route des groupes générateurs selon une certaine séquence. Celle-ci doit être choisie de la façon la plus appropriée, en fonction de la disponibilité des groupes et de leur temps de démarrage.

Pour le redémarrage des groupes générateurs, une coordination entre les groupes générateurs, les charge caractéristiques et le réseau de transport est exigée.

Afin de pouvoir restaurer un système avec succès, il est indispensable de connaître les caractéristiques de ses composants ainsi que la structure détaillée du réseau. Ajoutons à cela les différentes contraintes imposées par les groupes de production qu'il faut prendre en considération. Ces dernières peuvent être classées en trois catégories: les contraintes physiques, les contraintes de planification (ou programmation) et les contraintes politiques.

Les contraintes physiques sont les durées maximales et minimales nécessaires pour le redémarrage des groupes générateurs. Dans cette catégorie de contraintes, la puissance active et la pente d'augmentation de la puissance des groupes sont des facteurs dont il faut tenir compte.

Les contraintes de la planification (ou programmation) font référence à la disponibilité du personnel dans une centrale électrique. Nous donnons l'exemple d'un cas d'insuffisance de personnel pour un redémarrage simultané de plusieurs groupes d'une centrale électrique.

Plusieurs chercheurs avaient déjà proposé la technique de détermination des séquences de démarrage des générateurs [107, 126]. Cependant, ces méthodes heuristiques n'assurent pas des séquences de démarrage optimales.

Nous présentons donc au cours de ce chapitre une nouvelle approche permettant la détermination des séquences de démarrage optimales des groupes pendant la reprise de service du système.

Cette technique utilise le même principe que la méthode 'backtracking search' à savoir la détermination des temps de démarrage des générateurs afin de maximiser l'énergie produite sur une période correspondant à la remise en service des générateurs. Les caractéristiques dynamiques des différents types de groupes ainsi que les contraintes du système sont pris en compte par cette méthode.

Dans la mesure du possible, le chemin sélectionné est celui nécessitant le minimum de d'actions d'aiguillage entre les centrales électriques et le groupe de charges.

La méthode proposée est testée et validée par des simulations sur le réseau New - England.

CHAPITRE 5

CHAPITRE 5

CALCUL DE LA VALEUR DE L'AUGMENTATION DE LA CHARGE PENDANT LA REALIMENTATION DES CONSOMMATEURS

Pendant la reprise de service d'un réseau électrique, il est souhaitable d'alimenter les charges aussi rapidement que possible et ce, de façon fiable. Au début de la reprise de service,

- les grands moteurs asynchrones utilisés pour les auxiliaires des centrales thermiques, et
- les charges servant d'une part à maintenir la tension dans des limites acceptables et d'autre part à améliorer la stabilité du système,

sont réalimentées. Lors de la prise d'une charge, les groupes participant aux réglages de la fréquence augmentent leurs consignes de puissance par leur régulation de vitesse. Les centrales électriques fonctionnant durant cette phase sont des petits groupes générateurs de capacité 'black-start'. Le réseau est donc faible et la prise de charges peut causer une forte décroissance de la fréquence .

En général, les opérateurs cherchent, pendant cette phase, à déterminer la valeur de l'augmentation (incrément) de la charge que l'on peut réalimenter sans risque [3, 5, 82, 124].

D'une part, la réalimentation avec de grandes augmentations de charges peut résulter en une forte décroissance de la fréquence et par conséquent les relais fréquence-métriques sont activés. Les charges déjà restaurées sont alors déconnectées et dans le cas où la fréquence continue a baisser, les groupes générateurs sont déconnectés par des relais de protection à manque de fréquence, ce qui mène à une répétition du black-out [3, 5, 82].

D'autre part, toute faible augmentation de la charge entraîne une prolongation inutile de la durée de reprise de service.

Ainsi, un des critères qui pourrait servir aux opérateurs pendant la reprise de service est la détermination de la valeur des blocs de charge à réalimenter.

La détermination de la valeur des charges à réalimenter réduit le temps de calcul pendant la planification de la restauration et la restauration en ligne [2].

Dans les travaux précédents [5, 124], les charges dynamiques et les limitations de la régulation de vitesse n'ont pas été prises en compte et par conséquent l'évaluation du

comportement de la fréquence ne peut être complète et exacte, surtout quand il s'agit de déterminer la fréquence minimale pendant l'alimentation de la charge.

Le fonctionnement des relais du délestage de charge et des relais de protection à manque de fréquence des générateurs dépend de la fréquence minimale.

Une nouvelle méthode pour le calcul des valeurs de l'augmentation de charge est présentée dans ce chapitre. Elle consiste en la détermination de la valeur maximale de charges pouvant être réalimentées en fonction de la diminution admissible de la fréquence du système; cela peut être fait pour chaque nœud et pendant chaque phase d'alimentation de la charge.

Cette méthode tient compte à la fois de la dynamique des charges et de la réponse fréquentielle des régulations de vitesses. Nous avons employé une forme appropriée du comportement fréquentiel du système durant l'alimentation de la charge. Cette forme permet de transformer les équations différentielles du système en équations algébriques utilisées pour la détermination de la fréquence minimale.

La méthode proposée est efficace et sert de guide en ligne pour les opérateurs qui l'utilisent pour sélectionner les valeurs de charge.

La méthode développée a été testée par des simulations de réseau test IEEE (39-bus New England test system) et les résultats sont comparés avec ceux obtenus par un logiciel de simulation à long terme qui a été décrit dans le chapitre 3.

Puisqu'un rejet de la charge peut être considéré comme une réalimentation de charge négative, il est tout à fait possible, avec notre méthode, d'estimer les oscillations de la fréquence lors d'un délestage de charge. Cette estimation est d'une grande importance pendant la phase de remise en service qui s'accompagne de situations appelées îlotage du système (c'est à dire déconnexion d'un sous système faisant partie d'un système global).

CHAPITRE 6

CHAPITRE 6

REDUCTION DE L'ANGLE DE PHASE STATIONNAIRE

Au cours de la réalimentation i d'un réseau électrique, les opérateurs rencontrent parfois une grande différence d'angle de phase stationnaire SPA (Standing Phase Angle Reduction) entre deux nœuds d'une ligne de transmission (Figure 6.1).

Figure 6.1: Différence SPA à travers une ligne avant la fermeture du disjoncteur($|\theta_i-\theta_j|$)

La fermeture du disjoncteur de puissance lors d'une grande différence SPA peut déstabiliser le système et endommager le matériel à la suite de pannes répétitives survenant sur le système. Afin d'éviter la fermeture des disjoncteurs lors d'une grande différence de l'angle de la phase, ces derniers sont équipés de relais synchronisateur. Ces relais empêchent la fermeture des disjoncteurs pour une valeur d'angle plus élevée que les valeurs pré-déterminées.

Les gammes de différences SPA qu'un système peut supporter dépendent du niveau de la tension, des conditions de manœuvre et de l'emplacement de ses disjoncteurs.

En pratique, les réglages typiques de l'angle pour un relais du synchronisateur (synchrocheck) sont [192] :

- 20° pour des lignes THT de tension supérieure ou égale à 400KV,
- de 30° à 40° pour des lignes de tension égale à 230KV,
- de 50° à 60° pour des lignes de tension inférieure à 132KV.

A la reprise de service d'un réseau électrique, l'angle de phase devrait être réduit à une valeur inférieure ou égale à dix degrés avant de réaliser l'interconnexion.

Dans de telles conditions, les opérateurs du système ont la possibilité de réduire la différence SPA par un changement de la production de la puissance active de quelques centrales électriques en se servant de la méthode 'essais et erreurs'. Cette technique exige une longue durée et par conséquent prolonge la durée de reprise de service [77].

Plusieurs chercheurs avaient déjà étudié la réduction de l'angle de phase stationnaire. Dans ce travail, la technique de répartition de charge basée sur le modèle a courant continu [192] est utilisée, ce qui n'est pas exact dans certains cas et ne prend pas en considération le délestage de charge pour la réduction du SPA. Puisque le réseau électrique est faible pendant les phases initiales de la reprise de service, les puissances active et réactive ne sont pas découplées et la technique de répartition de charge DC ne peux pas s'appliquer. Ceci nous a incité à utiliser un modèle exact de répartition de charge au lieu du modèle DC.

Au cours de ce chapitre, nous présentons une nouvelle méthode pour la réduction du SPA. L'algorithme développé propose la réduction de la différence SPA entre deux nœuds via un changement (re-scheduling) de la production de la puissance active de quelques centrales électriques, de façon à ce que les variations des puissances actives et le nombre de centrales qui participent à ce processus soient minimales. Ces deux contraintes sont rappelées ci dessous:

- Limitation de la production de puissances active et réactive des centrales électriques,
- Limitation des lignes de transmission.

La différence SPA entre deux nœuds spécifiés est exprimée (formulée) lors d'un changement de la production de la puissance active. La série optimale des centrales électriques est sélectionnée à partir de la sensibilité des centrales pour la réduction du SPA. Dans le cas où tous les groupes atteignent leurs limites, un réglage de la puissance active des nœuds de charge par du délestage de charge est autorisé, de façon à ce que les valeurs du délestage et les nombres de nœuds de charge soient minimum.

La validité et l'efficacité de la méthode proposée sont montrées par plusieurs études sur le réseau de 'IEEE 118 bus system'.

CHAPITRE 7

CHAPITRE 7

ANALYSE ET CONTRÔLE DES SURTENSIONS HARMONIQUES

GENERALITES SUR LES SURTENSIONS

L'une des préoccupations majeures pendant la remise en service des réseaux électriques est le problème des surtensions dues aux procédures de renvoi de tension [77]. Celles-ci peuvent être classées en quatre catégories à savoir, les surtensions transitoires, les surtensions permanentes, les surtensions de la résonance harmonique et les surtensions résultant de la ferro- résonance [74].

Les surtensions permanentes proviennent de la puissance réactive fournie par les lignes de transmission à faibles charges. Les fortes surtensions permanentes peuvent causer des dommages aux transformateurs ainsi qu'à d'autres équipements du réseau électrique.

Les surtensions transitoires apparaissent soit pendant les opérations de renvoi de tension sur les lignes de longues transport, soit pendant de renvoi de tension des dispositifs capacitifs. Celles-ci peuvent causer la destruction des parafoudres.

Les surtensions harmoniques sont dues aux fréquences de résonance du système proche des fréquences multiples du fondamental. Si elles sont de longue durée, elles entraînent des pannes de parafoudres et des défauts dans le réseau.

Les surtensions de la ferro- résonance sont le résultat d'une résonance non – harmonique. Les courbes de ce type de surtensions sont déformées ce qui peut causer des dégradations du matériel [74].

LES SURTENSIONS HARMONIQUES

Au début d'une phase de remise en service d'un réseau électrique, les fréquences de résonance de système sont différentes de celles en fonctionnement normal puisque le système est peu chargé. De fortes surtensions de longues durées peuvent se produire si la caractéristique fréquentielle montre des pics de résonance autour des fréquences multiples du fondamental du système et aussi si le réseau est excité par une perturbation harmonique. Une telle perturbation peut être à l'origine de la saturation des transformateurs et des dispositifs de l'électronique de puissance, etc.

Les surtensions de la résonance harmonique sont principalement causées par de renvoi de tension sur les transformateurs à faibles charges à l'extrémité des lignes de transmission. Par ce moyen, un courant d'appel est produit. Ce courant contient un nombre considérable de composantes harmoniques jusqu'à des fréquences autour de $f = 10f_0$.

Ce courant peut être représenté par une source de courant harmonique I(h) connecté au nœud du transformateur [143]. La relation entre les tensions nodales, la matrice du réseau et les courants injectés peuvent être exprimés par la relation:

$$V(h) = Z(h).\ I(h) \qquad (7.1)$$

où h représente la fréquence harmonique $h = 2f_0, 3f_0, \ldots$. Les composantes harmoniques du courant qui sont à la même fréquence que les harmoniques résonants du système sont amplifiés, ce qui se traduit par de fortes valeurs de tensions aux bornes des transformateurs. Ceci s'accompagne par un niveau plus élevé de la saturation conduisant ainsi à des composantes harmoniques du courant d'appel de plus en plus importantes et par conséquent à des tensions plus élevées.

Ce phénomène peut se manifester dans un système à faible atténuation. Celle-ci peut être particulièrement présente au début d'un processus de reprise de service, où un chemin s'établit d'une source 'black-start' avec une grande centrale électrique et que seulement quelques charges sont déjà ré-alimentées [74, 143].

Bien que l'analyse des surtensions permanentes peut être réalisée par des programmes conventionnels (à base de répartition de charge), une méthode systématique n'a pas été encore développée pour l'analyse des surtensions harmoniques. Donc, nous nous sommes intéressés dans cette partie à l'analyse et au contrôle des surtensions pendant la remise en service des réseaux électriques.

Ce phénomène (les surtensions harmoniques) est habituellement étudié par les programmes d'analyse des transitoires électromagnétiques [74, 176]. Afin d'étudier un grand nombre de configurations possibles du système, il est nécessaire d'effectuer beaucoup de simulations dont les durées sont trop longes. Pour limiter la durée de simulation, le nombre de configurations du système est réduit par l'application des règles analytiques permettant d'abandonner ces configurations avant l'exécution de la simulation.

Ce chapitre décrit une approche pour l'estimation et le contrôle des surtensions harmoniques pendant le processus de remise en service du réseau électrique. Cette méthode, en plus des calculs analytiques, utilise le module PSB (Power System Blockset) de l'outil de simulation MATLAB/Simulink [176].

Les surtensions harmoniques dans le domaine fréquentiel sont évaluées. Grâce à une analyse de la sensibilité, nous pouvons efficacement déterminer le changement permettant de limiter des surtensions harmoniques. Au cas où des simulations sont indispensables,

nous proposons également une méthode basée sur la transformée de Fourier à courte durée qui permet de réduire considérablement le temps de simulation.
Il est important de souligner ici que les approches développées ont été testées et validées par des simulations sur des réseaux test IEEE (IEEE 39-Bus New England test system).

CONCLUSION GENERALE

CHAPITRE 8

CONCLUSION GÉNÉRALE

L'objectif du travail présenté dans cette thèse est d'étudier le problème de la de reprise de service des réseaux électriques à la suite d'un incident généralisé et bien sûr de proposer de nouvelles méthodes pour résoudre les différents problèmes liés à la reprise de service.
Cette thèse, structuré en huit chapitres, présente les résultats du travail comme suit :

- Le premier chapitre est consacré à la définition du problème et à l'explication des objectifs de cette thèse.
- Parallèlement à la progression de cette thèse, nous avons créé un logiciel de simulation de dynamique à long terme. Ce logiciel peut être utilisé pour étudier la réponse de la fréquence et de la tension due au déséquilibre entre la charge et la production afin d'analyser des scénarios de la reprise de service du réseau électrique. Il peut également être employé pour étudier la réponse de la fréquence de système pendant des ré alimentations de charges (consommateur). Ce logiciel a été développé dans l'environnement MATLAB/SIMULINK doté d'une interface graphique qui permet d'utiliser facilement ce logiciel.
- Une nouvelle approche permettant la détermination des séquences de démarrage optimales des groupes pendant la reprise de service du système a été également proposée. Cette technique utilise le principe de la détermination des temps de démarrage des générateurs afin de maximiser l'énergie produite sur une période correspondant à la remise en service des générateurs. Les caractéristiques dynamiques des différents types de groupes ainsi que les contraintes du système sont prises en compte par cette méthode.
- Une nouvelle méthode pour le calcul des valeurs de l'augmentation (incréments) de charge est présentée dans le cinquième chapitre. Elle consiste en la détermination de la valeur maximale des charges pouvant être réalimentées en fonction de la diminution admissible de la fréquence du système ; cela peut être fait pour chaque nœud et pendant chaque phase d'alimentation de la charge. Cette méthode tient compte à la fois de la dynamique des charges et de la réponse fréquentielle des régulations de vitesses. Nous avons employé une forme appropriée du comportement fréquentiel du système durant l'alimentation de la charge. Cette forme permet de transformer les équations différentielles du système en équations algébriques utilisées pour la détermination de la fréquence minimale. La méthode proposée est efficace et sert de guide en ligne pour les opérateurs qui pourront l'utiliser pour la sélection des valeurs de charge.

- Dans le cinquième chapitre, une nouvelle méthode pour la réduction du SPA a été présentée. L'algorithme développé propose la réduction de la différence SPA entre deux nœuds via un changement (re- scheduling) de la production de la puissance active de quelques centrales électriques, de façon à ce que les variations des puissances actives et le nombre de centrales participant à ce processus soient minimales. Ces deux contraintes sont rappelées ci dessous:

  1. Limitation de la production de puissances active et réactive des centrales électriques,
  2. Limitation des lignes de transmission.

  La différence SPA entre deux nœuds spécifiés est exprimée (formulée) lors d'un changement de la production de la puissance active. La série optimale des centrales électriques est sélectionnée à partir de la sensibilité des centrales pour la réduction du SPA. Dans le cas où tous les groupes atteignent leurs limites, un réglage de la puissance active des nœuds de charge par un délestage de charge est autorisé, de façon à ce que les valeurs de délestage de charge et le nombre de nœuds de charge soient minimum.
- Le septième chapitre décrit une approche pour l'estimation et le contrôle des surtensions harmoniques pendant la processus de la remise en service du réseau électrique. Cette méthode, en plus des calculs analytiques, utilise le module PSB (Power System Blockset) de l'outil de simulation MATLAB/Simulink.

  Les surtensions harmoniques dans le domaine fréquentiel sont évaluées. Grâce à une analyse de la sensibilité, nous pouvons efficacement déterminer le changement permettant de limiter les surtensions harmoniques. Au cas où des simulation sont nécessaires à faire, nous proposons également une méthode basée sur la transformée de Fourier à courte durée (Short-Time Fourier Transform) qui permet de réduire considérablement le temps de simulation.